

Effects of drought and elevated CO₂ on growth and mortality of pine trees

Zur Erlangung des akademischen Grades einer
DOKTORIN DER NATURWISSENSCHAFTEN (Dr. rer. nat.)

von der KIT Fakultät für
Bauingenieur-, Geo- und Umweltwissenschaften
des Karlsruher Instituts für Technologie (KIT)

genehmigte
DISSERTATION

von

M.Sc. Marielle Gattmann
aus Osnabrück

Tag der mündlichen Prüfung: 19. Februar 2025

Referentin: Prof. Dr. Nadine K. Rühr
Korreferentin: Prof. Dr. Christiane Werner

Karlsruhe (2025)



This document is licensed under a Creative Commons
Attribution-ShareAlike 4.0 International License (CC BY-SA 4.0):
<https://creativecommons.org/licenses/by-sa/4.0/deed.en>

Surrounded

**Sunk deep in the dense embrace of the forest
I imagine this is the polar opposite of suffocation
My lungs seem to gain extra capacity here
And I feel like an empty inbox
As I contemplate the ultimate assault course
The roots, the stumps, the branches
I squint into eternity
As I try to get to grips with the fact that we have
No idea what we're dealing with
My lungs fill with air
I feel supercharged now
I'm hyper-aware
I shiver and short-circuit
At the depth of the universe
We are the dust on the stained-glass windows
Trying to comprehend the cathedral**

Shinrin-yoku by Enter Shikari

Table of contents

Summary.....	V
Zusammenfassung.....	VII
List of Publications	IX
Abbreviations	XI
List of Figures.....	XV
List of Tables	XVII
1 Introduction	1
Forests and climate change	1
Tree mortality due to soil drought.....	1
Rising atmospheric CO ₂ and VPD – stress mitigation and amplification.....	2
Water management of pine trees	3
Objectives of the thesis.....	3
Approach	4
Outline of the thesis	5
2 Dying by drying: timing of physiological stress thresholds related to tree death is not significantly altered by highly elevated CO ₂	7
2.1 Introduction	7
2.2 Material and Methods	10
2.2.1 Plant material.....	10
2.2.2 Experimental setup	10
2.2.3 Gas exchange measurements	12
2.2.4 Sampling procedure and needle water status	13
2.2.5 Non-structural carbohydrate quantification.....	13
2.2.6 Statistical data analyses.....	14
2.3 Results	15
2.3.1 [CO ₂] effect under favorable conditions	15
2.3.2 Gas exchange response to drought	16
2.3.3 [CO ₂] effect on tree C balance during drought.....	17
2.3.4 Needle water potential and non-structural carbohydrates.....	18

Table of contents

2.3.5	[CO ₂] effect on risk thresholds during lethal drought.....	20
2.4	Discussion.....	22
2.4.1	Pre-drought [CO ₂] effect.....	22
2.4.2	[CO ₂] effect under mild to moderate drought conditions	23
2.4.3	[CO ₂] effect on tipping points and drought-induced mortality	24
2.5	Supplement	27
3	Anatomical adjustments of the tree hydraulic pathway decrease canopy conductance under long-term elevated CO ₂	33
3.1	Introduction	33
3.2	Materials and Methods	36
3.2.1	Plant Material.....	36
3.2.2	Experimental setup and growth conditions	37
3.2.3	Gas exchange measurements	37
3.2.4	Tissue sampling for anatomy and hormone analysis	38
3.2.5	Quantification of foliage ABA levels	39
3.2.6	Epidermal and leaf cross-sectional anatomy	39
3.2.7	Hydraulic conductivity, xylem vulnerability curves, and wood anatomy.....	39
3.2.8	Statistical analyses	40
3.3	Results	41
3.3.1	Long-term acclimation to eCO ₂ affects gas exchange	41
3.3.2	Stomata control and characteristics under eCO ₂	43
3.3.3	[CO ₂] effect on wood anatomy and hydraulic parameters.....	45
3.4	Discussion.....	47
3.4.1	Stomatal responses to eCO ₂	47
3.4.2	Hydraulic conductance in leaves and branches under eCO ₂	48
3.4.3	Implications for drought and VPD responses under eCO ₂	50
3.5	Supplement	52
4	High vapor pressure deficit and soil drought impair aboveground growth before photosynthesis while shifting C allocation to roots in Scots pine.....	59
4.1	Introduction	60
4.2	Material and methods	62
4.2.1	Plant material.....	62
4.2.2	Experimental setup	63
4.2.3	Radial growth, sampling procedure and needle water status	65
4.2.4	Non-structural carbohydrate quantification	66
4.2.5	Sample preparation and isotope ratio mass spectrometry	67
4.2.6	Statistical data analyses.....	67

Table of contents

4.3	Results	67
4.3.1	Responses of gas exchange and non-structural carbohydrates to drought progression	67
4.3.2	Needle water status, carbon uptake and growth parameters.....	69
4.3.3	Dynamics of the ¹³ C label.....	71
4.4	Discussion.....	74
4.4.1	Responses of canopy conductance and C uptake to VPD and soil drought	74
4.4.2	Tree growth affected by water availability and VPD.....	75
4.4.3	Sink activity drives C allocation under drought stress.....	76
4.5	Conclusion	78
4.6	Supplement	79
5	Synthesis.....	83
6	References.....	89
	Acknowledgements	121

Summary

Effects of drought and elevated CO₂ on growth and mortality of pine trees

In the global carbon cycle, forests represent an immense carbon stock that evolves following the growth and death of trees. Predicting the evolution of forest carbon stocks under climate change is a major challenge, as rising atmospheric CO₂ concentrations favor tree growth, while the increasing frequency and severity of extreme weather events such as droughts favor tree mortality. A promising approach to improve accuracy and reliability of the predictions is to directly link key climatic factors to tree growth and mortality risk. In the present work, this approach was followed for soil water availability considering the influence of either highly elevated atmospheric CO₂ concentration (eCO₂, c. 900 ppm) or high atmospheric vapor pressure deficit (VPD, c. 2.9 kPa) on pine seedlings.

To this end, four experiments were carried out in a greenhouse facility with specially designed tree chambers in which all relevant environmental factors could be monitored and individually regulated. At the same time, the setup allowed continuous measurements of gas exchange. Depending on the objective of the respective experiment, these measurements were complemented by analyses of biomass, non-structural carbohydrates (NSC), growth and hydraulic parameters, stomatal properties, wood anatomy and carbon allocation. The latter was based on changes in carbon isotope signatures in biomass and respiration resulting from continuous ¹³CO₂ labeling.

Long-term exposure of Aleppo pine (*Pinus halepensis* Mill.) seedlings to eCO₂ resulted in anatomical adjustments of leaves and the branch xylem, such as increased vein-to-epidermis distance (+65 %) and reduced conduit lumen fraction (-11 %), causing a significant, irreversible reduction in leaf-level canopy conductance (g_{canopy} , -55 %). However, due to eCO₂-induced increases in leaf area, there were no apparent overall water savings. Furthermore, stomatal sensitivity to drought and xylem safety thresholds remained unaffected. Despite larger NSC pools in needles, there was no eCO₂ benefit on tree survival or timing of death, as cause of death was hydraulic failure rather than carbon deficiency. This was the case for both rapid (41 days) and slow (82 days) simulated soil drought.

Under soil drought and high VPD, Scots pine (*Pinus sylvestris* L.) seedlings maintained a positive C balance (assimilation minus total respiration) because photosynthesis proved to be less water sensitive than g_{canopy} , total respiration (sum of shoot night and root respiration) decreased in parallel with photosynthesis, and starch remobilization presumably supported respiration. An early decline in aboveground growth was observed despite a positive C balance, indicating a high sensitivity of growth to soil and atmospheric drought. In contrast to aboveground biomass, allocation of recently assimilated C to belowground biomass was detectable during water stress, suggesting that belowground sink activity and thus belowground growth were partially maintained.

The results presented in this thesis indicate that the potential benefits of eCO₂ for tree growth and survival are unlikely to offset the detrimental impact of impending drought events on forests. This could lead to a reduction in the positive effect of forests on the climate, which would accelerate climate change. It is therefore vital that we continue to improve our understanding of the processes and interactions associated with climate impacts on tree vitality.

Zusammenfassung

Auswirkungen von Trockenheit und erhöhtem CO₂ auf Wachstum und Sterblichkeit von Kiefern

Im globalen Kohlenstoffkreislauf stellen Wälder einen immensen Kohlenstoffspeicher dar, der sich durch das Wachstum und Absterben von Bäumen verändert. Die Entwicklung der Kohlenstoffvorräte in Wäldern im Zuge des Klimawandels vorherzusagen, ist eine große Herausforderung, da steigende CO₂-Konzentrationen in der Atmosphäre das Wachstum von Bäumen fördern, während die zunehmende Häufigkeit und Schwere extremer Wetterereignisse, wie zum Beispiel Dürren, das Absterben von Bäumen begünstigen. Ein vielversprechender Ansatz zur Verbesserung der Genauigkeit und Zuverlässigkeit von Vorhersagen besteht darin, die wichtigsten Klimafaktoren direkt mit dem Baumwachstum und dem Mortalitätsrisiko zu verknüpfen. In der vorliegenden Arbeit wurde dieser Ansatz für die Wasserverfügbarkeit im Boden unter Berücksichtigung des Einflusses von entweder stark erhöhter atmosphärischer CO₂ Konzentration (eCO₂, ca. 900 ppm) oder hohem atmosphärischem Dampfdruckdefizit (VPD, ca. 2,9 kPa) auf Kiefernkeimlinge verfolgt.

Zu diesem Zweck wurden vier Versuche in einer Gewächshausanlage mit speziell konzipierten Baumkammern durchgeführt, in denen alle relevanten Umweltfaktoren überwacht und individuell reguliert werden konnten. Gleichzeitig ermöglichte der Aufbau kontinuierliche Messungen des Gasaustausches. Je nach Zielsetzung des jeweiligen Experimentes wurden diese Messungen ergänzt durch Analysen von Biomasse, Nicht-Struktur-Kohlenhydraten (NSC), Wachstums- und hydraulischen Parametern, stomatären Eigenschaften, Holzanatomie und Kohlenstoffallokation ergänzt. Letztere basierte auf Veränderungen der Kohlenstoffisotopensignaturen in Biomasse und Atmung, die sich aus der kontinuierlichen ¹³CO₂-Markierung ergaben.

Infolge des langfristigen Wachstums unter eCO₂ kam es bei den jungen Aleppokiefern (*Pinus halepensis* Mill.) zu anatomischen Anpassungen der Nadeln und des Xylems der Äste, wie zum Beispiel einer Vergrößerung des Abstandes zwischen Ader und Epidermis (+65 %) und einer Verringerung des Anteils des Leitungslumens (-11 %), was zu einer signifikanten, irreversiblen Verringerung der Leitfähigkeit auf Blattebene führte (g_{canopy} , -55 %). Aufgrund der eCO₂-induzierten Vergrößerung der Blattfläche gab es jedoch keine offensichtlichen Wassereinsparungen. Außerdem blieben die stomatäre Empfindlichkeit gegenüber Trockenheit und die Xylem-Sicherheitsschwellen unbeeinflusst. Trotz größerer NSC-Pools in den Nadeln wirkte sich eCO₂ nicht positiv auf das Überleben der Bäume oder den Zeitpunkt ihres Absterbens aus, da es eher zu einem hydraulischen Versagen als zu einem Kohlenstoffmangel kam. Dies war sowohl bei schneller (41 Tage) als auch bei langsamer (82 Tage) simulierter Bodentrockenheit der Fall.

Bei Bodentrockenheit und hoher VPD bewahrten die jungen Waldkiefern (*Pinus sylvestris* L.) eine positive C-Bilanz (Assimilation minus Gesamtatmung), da sich die Photosynthese als weniger wasserempfindlich erwies als g_{canopy} , die Gesamtatmung (Summe aus Wurzel- und nächtlicher Sprossatmung) parallel zur Photosynthese abnahm und die Remobilisierung von Stärke vermutlich die Atmung unterstützte. Trotz einer positiven C-Bilanz wurde ein früher Rückgang des oberirdischen Wachstums beobachtet, was auf eine hohe Empfindlichkeit von Wachstumsprozessen gegenüber Boden- und Lufttrockenheit hindeutet. Im Gegensatz zur oberirdischen Biomasse war während des Wasserstressses eine Allokation von kürzlich assimiliertem C in der unterirdischen Biomasse nachweisbar, was darauf hindeutet, dass die unterirdische Senkenaktivität und damit das unterirdische Wachstum teilweise aufrechterhalten wurde.

Die in dieser Arbeit vorgestellten Ergebnisse deuten darauf hin, dass die potenziellen Vorteile von $e\text{CO}_2$ für das Wachstum und Überleben von Bäumen die nachteiligen Auswirkungen drohender Dürreereignisse auf die Wälder wahrscheinlich nicht ausgleichen können. Dies könnte zu einer Verringerung der positiven Auswirkungen der Wälder auf das Klima führen, was den Klimawandel beschleunigen würde. Daher ist es von entscheidender Bedeutung, dass wir unser Verständnis der Prozesse und Wechselwirkungen im Zusammenhang mit den Klimaauswirkungen auf die Vitalität von Bäumen weiter verbessern.

List of Publications

The content and structure of the publications included have been retained in the form of the original publication or manuscript submitted for publication. 1. and 2. are included as chapters in the state after peer review but before journal typesetting. 3. is presented as it will be submitted to a journal/preprint server.

1. Gattmann, M., Birami, B., Nadal Sala, D., and Ruehr, N. K. 2021. "Dying by Drying: Timing of Physiological Stress Thresholds Related to Tree Death Is Not Significantly Altered by Highly Elevated CO₂". *Plant, Cell & Environment* 44(2): 356-370.
2. Gattmann, M., McAdam, S. A. M., Birami, B., Link, R., Nadal-Sala, D., Schuldt, B., Yakir, D., and Ruehr, N. K. 2023. "Anatomical Adjustments of the Tree Hydraulic Pathway Decrease Canopy Conductance under Long-Term Elevated CO₂". *Plant Physiology* 191(1): 252-264.
3. Gattmann, M. and Ruehr, N. K. "High Vapor Pressure Deficit and Soil Drought Impair Aboveground Growth Before Photosynthesis while Shifting C Allocation to Roots in Scots Pine.

Since the papers (or the manuscript in preparation) include the work of co-authors, I list my contribution to 1.-3. as follows:

1. I contributed to the conceptualization of the study, conducted the experiments, performed the chemical analyses, analyzed the data, and led the writing of the paper.
2. I contributed to the conceptualization of the study, conducted the experiment with N.K.R. and B.B., analyzed the data with contributions of R.L., D.N.S., S.A.M.M. and B.S., and wrote the manuscript with N.K.R. and contributions from all authors.
3. I was involved in the design of the study, conducted the experiment, carried out the physical measurements and some of the chemical analyses, analyzed the data, and led the writing of the paper.

During my PhD project I had the opportunity to co-author the following publications. These papers were not included as separate chapters in this thesis, but were used to interpret the results.

- Birami, B., Gattmann, M., Heyer, A. G., Grote, R., Arneth, A., and Ruehr, N. K. 2018. "Heat Waves Alter Carbon Allocation and Increase Mortality of Aleppo Pine Under Dry Conditions". *Frontiers in Forests and Global Change* 1: 1285.
- Birami, B., Nägele, T., Gattmann, M., Preisler, Y., Gast, A., Arneth, A. and Ruehr, N. K. 2020. "Hot drought reduces the effects of elevated CO₂ on tree water-use efficiency and carbon metabolism". *New Phytologist* 226: 1607-1621.

Abbreviations

$\%E_{\max}$	percentage of maximum water loss through transpiration
$\delta^{13}\text{C}$	isotopic ratio relative to the international standard VPDB
$\delta^{13}\text{C}_\text{N}$	isotope composition of needle biomass
$\delta^{13}\text{C}_\text{R}$	isotope composition of fine root biomass
$\delta^{13}\text{C}_\text{RC}$	isotope composition of fine root cellulose
$\delta^{13}\text{C}_\text{S}$	nighttime shoot respiration
$\delta^{13}\text{C}_\text{sample}$	isotopic ratio in the sample air stream
$\delta^{13}\text{C}_\text{supply}$	isotopic ratio in the supply air stream
$^{13}\text{C}_\text{IN}$	^{13}C of the supply air stream
$^{13}\text{C}_\text{R}$	^{13}C of the root respiration
$^{13}\text{C}_\text{S}$	^{13}C of the shoot night respiration
$\delta^{13}\text{C}_\text{XC}$	isotope composition of xylem cellulose
ΣC	sum of net assimilation, shoot dark and root respiration
ΣE	sum of shoot day and night transpiration
Ψ	water potential
$\Psi_{\text{gc-close}}$	Ψ_{leaf} at stomatal closure
Ψ_{leaf}	leaf water potential
Ψ_{md}	midday needle water potential
Ψ_{xylem}	xylem water potential
$\pm\text{SD}$	standard deviation
$\pm\text{SE}$	standard error
$[\text{CO}_2]$	CO_2 concentration
$[\text{H}_2\text{O}]$	water concentration
ABA	abscisic acid
$a\text{CO}_2$	ambient atmospheric CO_2 concentration
$A_i:A_s$	leaf-to-sapwood area ratio
A_{leaf}	leaf area
A_{lumen}	lumen fraction
A_{net}	net assimilation

$A_{\text{net canopy}}$	net canopy assimilation
A_{xylem}	sapwood area
C	carbon
^{13}C	natural, stable isotope of carbon
C_a	atmospheric CO_2 concentration
C_i	leaf internal CO_2 concentration
CD	conduit density
CI	credible interval
Cntrl	control
CO_2	carbon dioxide
C_{sample}	$[\text{CO}_2]$ in sample air stream
C_{supply}	$[\text{CO}_2]$ in supply air stream
CUE	carbon-use efficiency
D	conduit diameter
D_h	hydraulically weighted conduit diameter
dH_2O	distilled water
D_m	vein-to-epidermis distance
dS	soil drought
dSA	combined air and soil drought
DW	dry weight
E	transpiration rate
eCO_2	elevated atmospheric CO_2 concentration
ED	epidermal cell density
F_m	molar flow
$g_{\text{canopy max,}}$ g_{cmax}	maximum canopy conductance under control conditions
$g_{\text{canopy,}}$ g_c	canopy conductance; sum of stomatal and cuticular conductance
$g_{\text{c-ref}}$	reference canopy conductance at VPD = 1 kPa
$g_{\text{c-rel}}$	relative canopy conductance
g_s	stomatal conductance
H_2O	water
K_h	hydraulic conductivity
K_l	leaf specific conductivity
K_{leaf}	leaf hydraulic conductivity
K_p	potential conductivity
K_s	specific conductivity

LA	needle leaf area
lme	linear mixed effects model
LW	leaf width
NSC	non-structural carbohydrates
NSC ₅₀	50 % loss of needle starch
P_{12} , P_{50} , P_{88}	12 %, 50 %, 88 % hydraulic conductivity loss
PAR	photosynthetic active radiation
PLC	percentage loss of hydraulic conductivity
PLC ₅₀	50 % potential loss of xylem conductivity
PLC ₈₀	80 % potential loss of xylem conductivity
RH	relative humidity
RLWC	relative leaf water content
R_{root}	root respiration
R_{sample}	isotope ratio of the sample
$R_{\text{shoot night}}$	shoot dark respiration
R_{standard}	isotope ratio of the standard
R_{total} , R_{sum}	sum of shoot night and root respiration
RWC	relative soil water content
SD	stomatal density
SI	stomatal index
SL	stomata length
SLA	specific leaf area
SS _N	needle soluble sugar concentration
SS _R	fine root soluble sugar concentration
St _N	needle starch concentration
St _R	fine root starch concentration
T_{Air}	air temperature
TLP	turgor loss point
T_{Soil}	soil temperature
UV	ultraviolet
VPD	vapor pressure deficit
VPDB	Vienna Pee Dee Belemnite
W_{leaf}	leaf saturated vapor pressure
W_{sample}	[H ₂ O] in sample air stream
W_{supply}	[H ₂ O] in supply air stream
WUE	water-use efficiency

List of Figures

Figure 2.1: Environmental drivers during the lethal drought in the ambient ($a\text{CO}_2$, c. 413 ppm) and elevated ($e\text{CO}_2$, c. 914 ppm) atmospheric CO_2 concentration treatment.

Figure 2.2: Gas exchange parameters during the course of the lethal drought experiment.

Figure 2.3: $[\text{CO}_2]$ effect on tree carbon balance (ΣC) and tree water loss from transpiration (ΣE) as well as leaf internal $[\text{CO}_2]$ / atmospheric $[\text{CO}_2]$ ratios (C_i/C_a) (for day-time measurements, photosynthetic active radiation (PAR) $>100 \mu\text{mol m}^{-2}\text{s}^{-1}$) over the course of stomatal closure.

Figure 2.4: Needle soluble sugar (SS_N , a), needle starch (St_N , b) concentrations, midday needle water potential (Ψ_{md} , a) and relative needle water content (RLWC , b) over the course of the experiment.

Figure 2.5: Needle soluble sugar (SS_N) to starch (St_N) ratios over midday needle water potential (Ψ_{md}).

Figure 2.6: Logistic regressions to determine the $[\text{CO}_2]$ effect on risk thresholds of Aleppo pine seedlings during a lethal drought ($n = 9$ per treatment).

Figure 3.1: Timeline of cultivation of *P. halepensis* seedlings under ambient ($a[\text{CO}_2]$, c. 400 ppm) or elevated ($e[\text{CO}_2]$, c. 860 ppm) atmospheric $[\text{CO}_2]$.

Figure 3.2: Treatment-specific relationships of canopy conductance (g_c) with vapor pressure deficit (VPD) for 40-month-old *P. halepensis* seedlings grown under ambient ($a\text{CO}_2$) or elevated ($e\text{CO}_2$) atmospheric CO_2 concentration.

Figure 3.3: Canopy conductance (g_c) measured at three different CO_2 concentrations of Aleppo pine seedlings grown for 40 months under elevated atmospheric CO_2 concentration (c. 870 ppm).

Figure 3.4: Hydraulic responses to increasing drought in Aleppo pine seedlings grown under ambient ($a\text{CO}_2$) or elevated ($e\text{CO}_2$) atmospheric CO_2 concentration.

Figure 3.5: Wood anatomy parameters in relation to branch cross-sectional area in Aleppo pine seedlings grown for 40 months under ambient ($a\text{CO}_2$) or elevated ($e\text{CO}_2$) atmospheric CO_2 concentration.

Figure 3.6: Responses of hydraulic conductivity and leaf-to-sapwood area in 40-month-old Aleppo pine seedlings grown under ambient ($a\text{CO}_2$) or elevated ($e\text{CO}_2$) atmospheric CO_2 concentration.

Figure 4.1: Progression of environmental drivers over the course of the experiment in Scots pine seedlings.

Figure 4.2: Progression of gas exchange over the course of the experiment in Scots pine seedlings.

Figure 4.3: Responses of non-structural carbohydrates in Scots pine seedlings to experimental drought at the end of the experiment.

Figure 4.4: Progression of midday needle water potential and growth over the course of the experiment in Scots pine seedlings.

Figure 4.5: Dynamics of the isotopic signatures of nighttime shoot and root respiration before and during the $^{13}\text{CO}_2$ -labeling as well as the ^{13}C respired and retained in Scots pine seedlings.

Figure 4.6: Isotopic signature of biomass and cellulose in Scots pine seedlings following six days of constant $^{13}\text{CO}_2$ -labeling ($\delta^{13}\text{CO}_2$ of 500 ‰).

Figure 5.1: The multifaceted mortality process of pine trees during soil drought.

List of Tables

Table 2.1: Irrigation modulation during the seven experimental steps (I-VII) of the lethal drought simulation in relation to the pre-determined maximum of transpiration per [CO₂] treatment.

Table 2.2: Biomass (*P. halepensis*, $n = 9$ per treatment, \pm SD) of needles, shoot woody tissue, roots and shoot/root ratio was measured at tree death.

Table 3.1: Treatment responses of leaf morphology, stomatal characteristics, reference stomatal conductance at VPD = 1 kPa (g_{c-ref}), and hydraulic vulnerability parameters for Aleppo pine seedlings grown for 40 months under ambient (aCO₂) or elevated (eCO₂) atmospheric CO₂ concentration.

1 Introduction

Forests and climate change

The future climate will be characterized by a rise in atmospheric CO₂ concentrations and an increase in the frequency and severity of extreme events such as droughts (Dai 2013; Huang et al. 2016; IPCC 2021; Reichstein et al. 2013; Seneviratne et al. 2021), which will affect forest ecosystems by affecting tree growth and survival (Fuhrer et al. 2006). In the context of climate change, the impacts on forests are of particular interest because forests not only play a vital role in the global water and energy cycles, but are also a critical regulating component of the global carbon cycle (Ballantyne et al. 2012; Beer et al. 2010; Cole, Hararuk, and Solomon 2021; Friedlingstein et al. 2022; Hui et al. 2017; Lal et al. 2018; Lindquist 2012; Pan et al. 2011, 2024; Reichstein et al. 2013; Trumbore, Brando, and Hartmann 2015; Zhao and Running 2010). By fixing atmospheric carbon into organic compounds through photosynthesis, trees help to absorb anthropogenic CO₂ emissions and potentially slow the progression of climate change. Furthermore, due to their large carbon pools and fluxes and the long recovery time to regain previous carbon stocks after disturbance, forests are also likely to have the largest net effect of drought extremes. It is therefore of paramount importance to understand if and how tree carbon assimilation, growth and carbon stocks are affected by elevated atmospheric CO₂ concentration (eCO₂) and drought, and to translate this understanding into mechanistic vegetation models. Recently, there has been mounting evidence that the potential increase in carbon uptake by forests due to higher CO₂ availability and longer growing seasons (Novick et al. 2024) may be offset by drought-related losses in forest carbon stocks. Particularly in water-scarce environments, the predicted greater variability in precipitation with more frequent and intense drought extremes is expected to lead to more widespread forest dieback, threatening the long-term viability of tree species in the drier parts of their range (Allen et al. 2010; Williams et al. 2020). Characterizing the responses of key species to extreme climate events can therefore provide important information for assessing and predicting tree and forest functioning under increasing climate variability.

Tree mortality due to soil drought

In contrast to mild and moderate droughts, where drought-induced stress may be short-term and can potentially be mitigated or restored by rainfall, prolonged and severe droughts can cause trees to exceed certain internal biological thresholds, leading to growth cessation (Castellaneta et al. 2022; Zhao et al. 2018), anomalies in primary productivity (Ciais et al. 2005; Du et al. 2018), or even large-scale forest dieback (Allen et al. 2010; Liu et al. 2013). As drought-induced tree mortality is considered a non-linear change in tree vigor and growth, determining growth responses to climatic stressors is a useful tool to assess vegetation

dynamics, especially during forest dieback when tree vulnerability is amplified (Hereş et al. 2014). To date, there is ongoing debate about how climatic factors control vegetation growth, and it remains difficult to determine the cause-effect relationship of water and carbon relations at the point where drought conditions become lethal, as the underlying mechanisms are closely interlinked (McDowell et al. 2022; Sevanto et al. 2014). Taking into account the interdependencies, hydraulic failure and carbon starvation are currently the leading hypotheses for the mechanisms of tree mortality. While hydraulic failure refers to the collapse of the water flow through the tree (McDowell et al. 2008; Sperry et al. 1998), carbon starvation refers to the depletion of carbon reserves when the carbon supply via photosynthesis is insufficient (McDowell et al. 2008). To improve model predictions of the impact of future droughts on forests, a deeper understanding of the mechanisms that determine a tree's response to drought is crucial (Fatichi et al. 2019). In this context, it is essential to consider individual acclimatization processes, including the coordination of fast physiological and slower structural adjustments. In addition, recent plant science studies on drought have addressed the challenge of defining mortality thresholds beyond which tree death is inevitable (Choat et al. 2018; Hammond et al. 2019). Such stress thresholds can provide important information on tree performance and survival under increasing drought (Knipfer et al. 2020), but they appear to be species-specific and show how different tree species cope with drought stress (Adams et al. 2017).

Rising atmospheric CO₂ and VPD – stress mitigation and amplification

The effects of meteorological drought caused by precipitation deficits on vegetation growth and mortality are influenced by multiple factors that may interact in ways that either mitigate or exacerbate the effects of drought. eCO₂ is generally associated with carbon assimilation at lower water cost due to reduced stomatal opening, which may be beneficial for maintaining tree function during drought (Ainsworth and Rogers 2007; Brodribb et al. 2020; Dusenge, Duarte, and Way 2019). However, the interaction between CO₂ and drought is not straightforward due to the complex nature of the tree drought response (Chaves, Maroco, and Pereira 2003; Choat et al. 2018; Vicente-Serrano et al. 2022) and the numerous feedbacks that occur at increasing temporal and spatial scales (Field, Jackson, and Mooney 1995).

In contrast to the potential stress reduction from eCO₂, high vapor pressure deficit (VPD) is usually associated with stress amplification. Low atmospheric humidity and high temperatures elevate VPD, an important proxy for atmospheric water demand, which is a driving force for water loss from leaves by transpiration and from the soil by evaporation (Grossiord et al. 2020; Novick et al. 2016). To minimize hydraulic losses, trees reduce stomatal conductance (Berg et al. 2016; Lange et al. 1971; McAdam and Brodribb 2015; Rigden and Salvucci 2017), which affects the synergistic regulation of photosynthesis and transpiration. Recently, increases in VPD have been found to significantly contribute to drought-induced tree mortality (Adams et al. 2009; Breshears et al. 2013; Hammond et al. 2022; Park Williams et al. 2013). However, whether soil moisture or VPD has the greatest effect on plant function during drought remains controversial (Fu et al. 2022; L. Liu et al. 2020; Novick et al. 2016; Sulman et al. 2016), as empirical research on their relative contribution to the development of plant drought stress and the resulting effects on tree morphology, physiology and molecular structure is still sparse (Mendonca et al. 2023; Novick et al. 2024; Wang et al. 2024; Yu et al. 2024; Zhang et al. 2024).

Altogether, this raises the question of whether and to what extent a potential benefit from eCO₂ can offset the effects of high VPD and drought on tree vitality and survival. A better understanding of the multidimensionality of plant drought stress is needed to answer this question, and subsequently to improve predictions of ecosystem functioning under the influence of climate change.

Water management of pine trees

The movement of water from the soil through the tree to the atmosphere follows a tension gradient, with the internal gradient in trees from roots to stem to leaves being maintained by transpiration at the leaf surface through stomata. Regulation of stomatal aperture, and ultimately stomatal conductance, is a way for trees to actively influence the otherwise passive water flow and maintain an optimal trade-off between carbon uptake for photosynthesis and transpirational water loss. Drought stress generally occurs when either soil water supply is low, atmospheric water demand (expressed as VPD) is high, or a combination of both (Passioura 1982; Torres-Ruiz et al. 2024). Following an isohydric water management strategy, pine trees strictly regulate stomatal conductance to maintain a constant midday leaf water potential under both water-abundant and drought conditions (Tardieu and Davies 1993; Tardieu and Simonneau 1998). Such conservative water balance management is associated with the avoidance of drought-induced hydraulic failure, a reduced risk of cavitation (Creek et al. 2020) and thus relative drought resistance. However, drought-induced growth reductions and tree mortality have now been reported in many pine species (Allen et al. 2010; Hereş et al. 2013; Linton, Sperry, and Williams 1998; Piñol and Sala 2000), particularly in environments where water availability was already a dominant limiting factor. As soil drought and VPD are expected to increase as a consequence of climate change in many regions within the wide distribution of pines, studying their vulnerability to environmental stressors and disturbances such as drought holds great promise for improving model predictions of ecosystem carbon-water coupling.

Objectives of the thesis

In the context of the research projects "Climate feedbacks and benefits of semi-arid forests (CLiFF, YA 274/1-1; SCHM 2736/2-1)" and "Forests out of balance" (DFG RU 1657/2-1), this thesis aims to improve the understanding of the response of pine seedlings to soil drought by considering the influence of eCO₂ and high VPD on the underlying physiological and metabolic processes from pre-drought characteristics to tree death.

The research objectives can be specified as follows:

1. To determine the effect of eCO₂ on carbon and water relations of pine seedlings prior to soil drought and to determine the cause of the reduction in canopy conductance (g_{canopy}) under eCO₂.
2. To determine how eCO₂ and high VPD affect the response of pine seedlings to soil drought, particularly in terms of carbon balance, carbon allocation and growth.

3. To identify critical thresholds beyond which tree mortality is inevitable in severe drought and to determine the effect of eCO₂ on these thresholds and hence on the mortality risk of pine seedlings.

Approach

The objectives of this thesis were addressed in four separate experiments using a specially designed tree chamber setup (see 2.2.2, 3.2.2, 4.2.2) in a greenhouse facility at the Institute of Meteorology and Climate Research in Garmisch-Partenkirchen (KIT-IMK/IFU), Germany (708 m a.s.l., 47°28932.999N, 11°3944.299E). The experiments were carried out with either two-year-old Aleppo pine (*Pinus halepensis* Mill) seedlings, with a focus on soil drought and highly eCO₂ (Experiments 1, 2, 4), or with three-year-old Scots pine (*Pinus sylvestris* L.) seedlings, with a focus on soil drought and high VPD (Experiment 3).

Experiment 1 (2017) and Experiment 2 (2018):

Aleppo pine seedlings grown for two years under eCO₂ (c. 900 ppm) or ambient atmospheric CO₂ concentration (aCO₂, c. 400 ppm) were subjected to either a rapid (41 days, Experiment 1, 2017) or a slow (82 days, Experiment 2, 2018) lethal drought while continuously measuring gas exchange, needle water status and non-structural carbohydrate (NSC) concentrations. As these two experiments mapped the entire mortality process, they were relevant to all three objectives, with a focus on Objective 3 and thus the effect of eCO₂ on critical thresholds and time to mortality.

Experiment 3 (2018):

To address Objective 2, Scots pine seedlings were exposed to either moderate soil drought or moderate soil drought combined with increasing VPD. Gas exchange, carbon isotope signatures of shoot night and root respiration, leaf water potential, needle length and stem radial growth were continuously monitored throughout the experiment. The application of a continuous canopy ¹³CO₂ label towards the end of the experiment allowed the identification of carbon partitioning and growth priorities. In addition, NSC concentrations in and carbon isotope signatures of biomass samples were determined before and at the end of labeling.

Experiment 4 (2019):

Experiment 4 (2019) consisted of four parts and mainly addressed Objectives 1 and 2, but also had implications for Objective 3. First, Aleppo pine seedlings grown under eCO₂ (c. 900 ppm) were exposed to decreasing atmospheric [CO₂] (c. 400 ppm and c. 200 ppm). Second, eCO₂ and aCO₂ (c. 400 ppm) seedlings were exposed to increasing VPD (from 0.5 to 2 kPa). Gas exchange was measured continuously throughout both parts of the experiment. Third, needle samples collected from both aCO₂ and eCO₂ seedlings during Experiment 2 were sent to the Department of Botany and Plant Pathology, Purdue Center for Plant Biology, Purdue University, West Lafayette, Indiana, USA, for quantification of leaf abscisic acid (ABA) levels and analysis of epidermal and leaf cross-sectional leaf anatomy. Fourth, branch samples from control Aleppo pine seedlings in aCO₂ and eCO₂ were sent to the Julius-von-Sachs-Institute of Biological Science at the University of Würzburg, Würzburg, Germany, for analysis of hydraulic conductivity, xylem vulnerability and wood anatomy.

Outline of the thesis

This thesis is organized as follows. In Chapter 2, the effect of eCO₂ on the mortality process of Aleppo pine seedlings during soil drought is presented based on critical thresholds. Chapter 1 deals with morphological changes and metabolic and hydrological responses to soil and atmospheric drought of Aleppo pine seedlings grown under eCO₂, answering the question of the cause of the reduction in g_{canopy} . Chapter 4 presents the effect of high VPD on the response of Scots pine seedlings to moderate soil drought, focusing on carbon balance, carbon allocation and growth. Chapter 5 summarizes the main findings of this thesis and their implications, looking at the different phases of soil drought from pre-drought to death.

2 Dying by drying: timing of physiological stress thresholds related to tree death is not significantly altered by highly elevated CO₂

This chapter was published as:

Gattmann, M., Birami, B., Nadal Sala, D., and Ruehr, N. K. 2021. "Dying by Drying: Timing of Physiological Stress Thresholds Related to Tree Death Is Not Significantly Altered by Highly Elevated CO₂". *Plant, Cell & Environment* 44(2): 356-370.

Abstract

Drought-induced tree mortality is expected to occur more frequently under predicted climate change. However, the extent of a possibly mitigating effect of simultaneously rising atmospheric [CO₂] on stress thresholds leading to tree death is not fully understood, yet. Here, we studied the drought response, the time until critical stress thresholds were reached and mortality occurrence of *Pinus halepensis* (Miller). In order to observe a large potential benefit from highly elevated atmospheric [CO₂] (eCO₂, c. 936 ppm), the seedlings were grown with ample of water and nutrient supply under either eCO₂ or ambient atmospheric [CO₂] (aCO₂, c. 407 ppm) during 2 years. The subsequent exposure to a fast or a slow lethal drought was monitored using whole-tree gas exchange chambers, measured leaf water potential and non-structural carbohydrates (NSC). Using logistic regressions to derive probabilities for physiological parameters to reach critical drought stress thresholds indicated a longer period for halving the starch storage under eCO₂ than aCO₂. Stomatal closure, turgor loss, the duration until the daily tree C balance turned negative, leaf water potential at thresholds and time-of-death were unaffected by eCO₂. Overall, our study provides for the first-time insights into the chronological interplay of physiological drought thresholds under long-term acclimation to eCO₂.

2.1 Introduction

Rising temperatures, changing precipitation patterns, more frequent as well as more severe extreme weather events are well-known projections of global climate change (Dai 2013; Huang et al. 2016; IPCC 2014; Reichstein et al. 2013). In the last two decades, many experimental as well as modeling approaches have been broaching the issue of how climate affects forest ecosystems (Hlásny et al. 2017; Hui et al. 2017) as this research topic significantly gained in importance and acuteness (Liu et al. 2017; Nabuurs et al. 2010; Sáenz-Romero et al. 2017)

due to an increase in reports of drought-induced tree mortality events in forest ecosystems around the globe (Allen et al. 2010; Allen, Breshears, and McDowell 2015; Anderegg et al. 2019; Bréda et al. 2006; Fensham and Holman 1999; Phillips et al. 2010). In light of these observations and the regulatory function of forests within the global carbon and water cycle, the ability to assess and attribute tree death is of great interest (Adams et al. 2010). In this context, increasing atmospheric [CO₂] (C_a), a main driver of global climate change is considered as a possible antagonistic factor that may mitigate some of the adverse impacts of climate alterations on tree mortality to a certain extent (Brodribb et al. 2020).

During drought events, stomatal closure reduces water loss and simultaneously impairs CO₂ diffusion (Hsiao 1973; Niu et al. 2014; Rennenberg et al. 2006; Sperlich et al. 2015). As a result, photosynthesis is reduced. Numerous studies on a variety of tree species found rising C_a to mitigate restrictions on C assimilation under declining water availability due to increased leaf internal CO₂ concentrations (C_i) and suppressed photorespiration (Ainsworth and Rogers 2007; Birami et al. 2020; Dusenge et al. 2019; Pushnik et al. 1995). CO₂ enrichment generally triggers decreases in stomatal conductance (g_s) and increases in water-use efficiency (WUE) often going along with reduced transpiration rates (E) (Birami et al. 2020; Dusenge et al. 2019; Haworth, Heath, and McElwain 2010). As a possible outcome of this, soil water may be preserved, potentially slowing water stress development. However, if a decrease in leaf-level E is accompanied by growth stimulation and hence increases in leaf area, these two [CO₂] effects could most likely counterbalance each other (Jin et al. 2018; Knauer et al. 2017; Torgern et al. 2015).

While there is some knowledge on eCO₂ impacts on tree drought responses, little is known about possible effects of eCO₂ on stress thresholds and time-to-mortality during a lethal drought (but see Bartlett et al. 2016 for an in-depth overview of hydraulic drought tolerance thresholds). (Duan et al. 2014) suggested that eCO₂ (+240 $\mu\text{l l}^{-1}$) has no effect on time-to-mortality during drought in either *Pinus radiata* or *Callitris rhomboidea* seedlings and that air temperature is more influential than [CO₂] on drought responses (Duan et al. 2015). However, these studies monitored leaf gas exchange only on a weekly basis. In order to get a more detailed impression on mortality risk and the chronological sequence of events leading to mortality, continuous gas exchange measurements at the whole tree level along with a closely timed monitoring of the hydraulic status could be of particular importance (Hartmann et al. 2018; Ryan 2011).

In connection with tree mortality, carbon starvation and hydraulic failure have been identified and discussed as the two main processes causing tree death. Carbon starvation is defined to occur when C requirements for respiration exceed C assimilation during stomatal closure (Adams et al. 2010; Hartmann 2015). Under such conditions, C reserves namely NSC gain enormous importance for osmoregulation and maintaining physiological functioning (Hartmann 2015). The ability to access and mobilize these reserves has been shown to support tree survival (Mitchell et al. 2013; Sevanto 2018; Sevanto et al. 2014). As NSCs have been found to increase under eCO₂ (Ainsworth and Long 2004), trees may benefit from this during drought conditions. Moreover, the longer the drought the more critical are NSC reserves to sustain respiration rates (Mitchell et al. 2013), which might further enhance any potential benefit from eCO₂.

The process of hydraulic failure in drought mortality has been recently identified as the most prominent cause of tree death (Brodribb et al. 2020). It is mainly associated with turgor loss

and decreases in xylem conductivity ultimately leading to tissue dehydration (Hsiao 1973) and xylem embolisms (Brodribb and Cochard 2009). Values between 50 and 80 % loss in xylem hydraulic conductivity have been related to tree death in conifers (Brodribb and Cochard 2009; Hammond et al. 2019). Although C starvation and hydraulic failure were at first considered as separate causes (McDowell et al. 2008) such a distinction has proven to be difficult. Carbon and water processes in trees are tightly interconnected as the transport of assimilates for example depends on phloem velocity and NSCs, as osmolytes, are crucial for maintaining turgor pressure (Adams et al. 2017; Duan et al. 2018; Hartmann et al. 2018).

In the attempt to attribute a cause of tree mortality, the identification of general critical thresholds or tipping points beyond that death is inevitable, has been a much sought objective (Brodribb and Cochard 2009; Hammond and Adams 2019; O'Brien et al. 2017; Resco et al. 2009). However, defining such tipping points is associated with enormous difficulties as there is no general consensus on when a tree can be declared dead (see Hartmann et al. 2018). This leaves the question whether a specific threshold marks a tree in the process of dying or a tree that is already dead (Hammond et al. 2019). Regardless of this uncertainty, recent studies have suggested drought-related thresholds that may critically impair tree functioning (Bartlett et al. 2016; Ruehr et al. 2019), including a tree's C balance turning negative, stomatal closure, leaf turgor loss point and substantial loss of xylem conductivity. However, it has yet to be investigated if eCO₂ may affect these thresholds during drought.

While in a previous study we could show that eCO₂ can modestly impact heat and hot-drought stress responses in Aleppo pine seedlings (Birami et al. 2020), we followed here the assumption that tree survival under prolonged drought stress might benefit from greater NSC reserves (e.g. Mitchell et al. 2013) stimulated by eCO₂. Hence, we assessed the time-to-mortality during a fast and a slow lethal drought to identify the importance of NSC for survival. In addition, we assessed if critical physiological drought thresholds and mortality risk of *P. halepensis* seedlings are altered by eCO₂.

In contrast to the majority of previous studies, we designed our eCO₂ treatment according to CO₂ concentrations prescribed for the RCP8.5 at the end of this century (range 794 to 1,142 ppm) (Collins et al. 2013) and are therefore much higher than in most studies. Although some voices are currently critical of the scenario (Hausfather and Peters 2020), our treatment design (C_i of about 630 ppm) is close to the value given for CO₂-saturated photosynthesis of 600 and 800 ppm for C_i (Benner, Sabel, and Wild 1988; Greer 2019; Maruyama et al. 2005; Roberntz and Stockfors 1998), we should be able to observe a maximum benefit of eCO₂ in our study. Hence, our seedlings were grown either under aCO₂ (c. 407 ppm) or highly eCO₂ (c. 936 ppm) under controlled conditions for 2 years from seeds originating from the Yatir forest in Israel. The Yatir forest is dominated by *P. halepensis* and has been planted c. 1965 at the northern edge of the Negev desert (Grünzweig et al. 2003).

As current climate conditions in the Yatir forest are already highly stressful and contrasting with natural sites of *P. halepensis* in Israel, the question is under consideration whether the forest is particularly at risk under predicted climate change. In light of this, our hypotheses were a) larger net C uptake and enhanced water-use-efficiency as long-term acclimation to highly eCO₂ benefit the survival of *P. halepensis* seedlings during drought, b) the [CO₂] advantage is more pronounced during a slow lethal drought compared with a fast lethal drought as NSC reserves are more crucial when carbon starvation becomes the main mortality risk, c) the [CO₂]

benefit is apparent in the change of critical thresholds of mortality risk factors resulting in the prolonging of the time-to-mortality in *P. halepensis* seedlings.

2.2 Material and Methods

2.2.1 Plant material

Pinus halepensis (Miller) seedlings - seeds originating from trees in the vicinity of the flux tower in the Yatir forest, Israel (31°20'49.2"N, 35°3'7.2"E) - were grown either under aCO₂ (407±23 ppm) or eCO₂ (936±9 ppm) (Supplemental Figure S2.1b) in a greenhouse facility in Garmisch-Partenkirchen, Germany (732 m a.s.l., 47°28'32.87"N, 11°3'44.03"E). The seedlings were cultivated for 24 months and repotted twice in a mixture of C-free potting substrate. After germination in vermiculite, seedlings were transferred to 0.25-L pots containing a C-free potting substrate (1:1:0.5 quartz sand (0.7 mm and 1-2 mm), vermiculite (c. 3 mm) and quartz sand (Dorsolit 4-6 mm) and expanded clay (8-16 mm)) enriched with 2 g of slow-release fertilizer (Osmocote® Exact + TE 3-4 month fertilizer 16-9-12+2MgO+TE, ICL Specialty Fertilizers, Geldermalsen, The Netherlands) and liquid fertilizer (Manna® Wuxal Super, Wilhelm Haug GmbH & Co. KG, Ammerbuch, Germany), and were finally placed into 4.5-L pots holding substrate (1:1:2 vermiculite (3-6 mm), coarse (4-6 mm) and fine quartz sand (2-3 mm) with expanded clay (8-16 mm)) enriched with 5 g of slow-release fertilizer (Osmocote® Exact Standard 5-6M fertilizer 15-9-12+2MgO+TE, ICL Specialty Fertilizers, Geldermalsen, The Netherlands), liquid fertilizer and phosphate-magnesium addition once. Throughout, environmental conditions were maintained constant between the two treatments (aCO₂ and eCO₂) with no significant differences in daily air temperatures (T_{Air}) (daytime: 21.5±2.9 °C, nighttime: 15.5±2.1 °C, CS215, Campbell Scientific, Logan, UT, USA), relative humidity (RH, 74.6±15.7 %) (Supplemental Figure S2.1c), relative soil water content (RWC, watered to full saturation) and photosynthetic active radiation (PAR) (on average 662±286 $\mu\text{mol m}^{-2}\text{s}^{-1}$, PQS 1 Kipp & Zonen, Delft, The Netherlands) (Supplemental Figure S2.1d). During the winter month (December to February), seedlings were kept at reduced T_{Air} and RWC, which afterwards was reversed to previous control conditions (Supplemental Figure S2.1a, e). Additionally, seedlings were subjected to a drought period of approximately 30 days with RWC of <20 % 9 months prior to the main experiment to mimic natural summer drought conditions in the Yatir forest (Preisler et al. 2019). The placement of the CO₂ treatments within the two greenhouse compartments was iterated in 1 to 2 monthly intervals.

2.2.2 Experimental setup

In order to monitor gas exchange throughout the lethal drought experiment, nine seedlings per CO₂ treatment were randomly selected and each of these seedlings was placed into its own tree chamber within the greenhouse to measure above- and belowground gas exchange separately (Birami et al. 2020) (Supplemental Figure S2.2). The tree chambers consisted of a light transmitting aboveground compartment separated gas tight from the opaque belowground compartment. Chambers were constantly supplied with an air stream of pre-defined [H₂O] and [CO₂] depending on the respective treatment (aCO₂: 413.67±57.49 ppm; eCO₂: 914.36±31.35 ppm).

Conditions in the tree chambers were kept at daytime mean T_{Air} (5SC-TT1-36-2M, Newport Electronics GmbH, Deckenpfronn, Germany) of 24 °C (Figure 2.1a) (night temperatures of

about 20 °C) and PAR (PQS 1, Kipp & Zonen, Delft, the Netherlands) was on average 476 $\mu\text{mol m}^{-2}\text{s}^{-1}$ for 16 hr during daytime (Figure 2.1f) by supplementing outside light with plant growth lamps (T-agro 400 W; Philips, Hamburg, Germany). Lower levels of PAR are not untypical at the forest floor and we found that our seedlings reached 77 % (aCO₂)/67 % (eCO₂) of their maximum photosynthesis as derived from light response curves at a PAR of 500 $\mu\text{mol m}^{-2}\text{s}^{-1}$ (Supplemental Figure S2.3). Since we omitted from increasing the supply of water vapor to the aboveground tree chambers during drought progression, vapor pressure deficit (VPD) increased similar to observations at the Yatir site (Tatarinov et al. 2016). Hence, decreasing E gradually decreased RH from 50 % to 20 % with increasing soil drought (Figure 2.1d). Accordingly, VPD increased from 1-2 kPa to values near 3 kPa (Figure 2.1c). Since soil temperature (T_{Soil}) (T107, Campbell Scientific Inc., Logan, UT, USA) was not actively controlled, temperatures ranged between 20 and 27 °C but were similar in all chambers (Figure 2.1b).

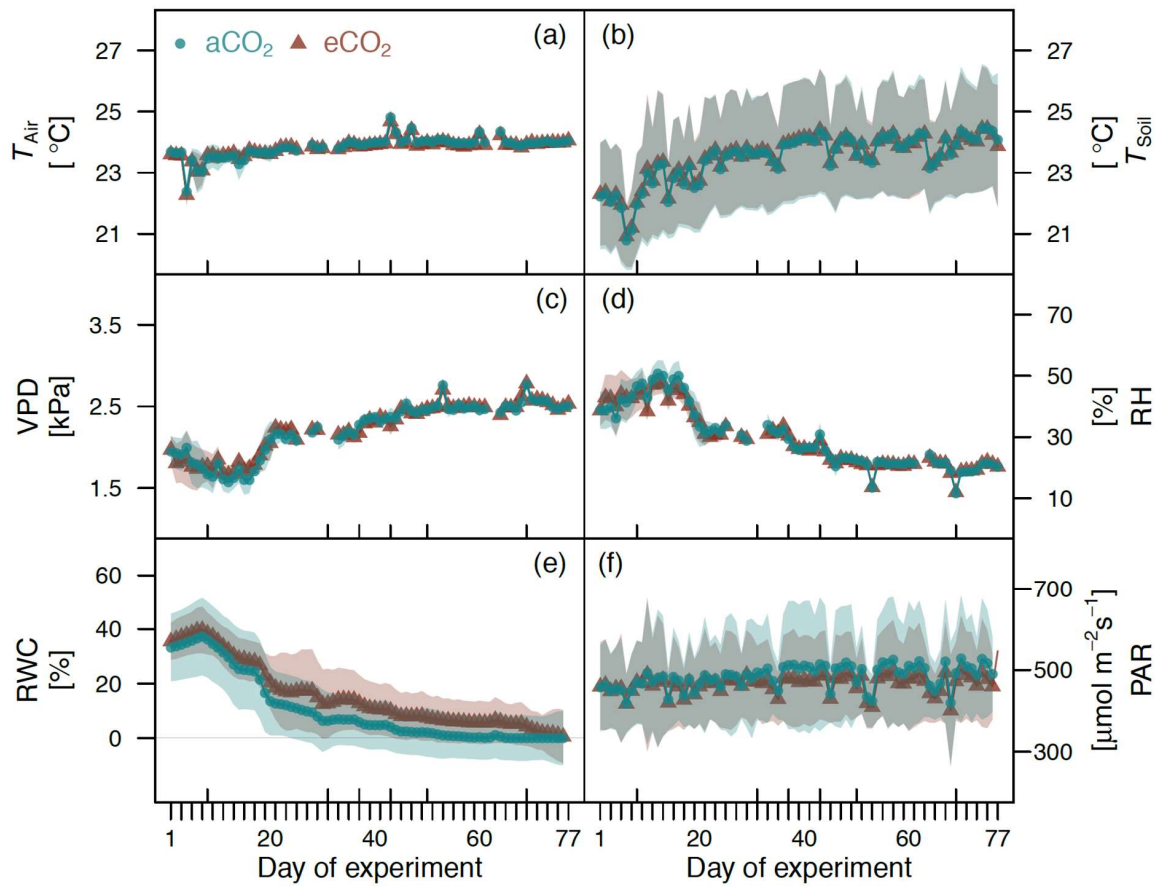


Figure 2.1: Environmental drivers during the lethal drought in the ambient (aCO₂, c. 413 ppm) and elevated (eCO₂, c. 914 ppm) atmospheric CO₂ concentration treatment.

Air temperature (T_{Air} , a), soil temperature (T_{Soil} , b), vapor pressure deficit (VPD, c), relative humidity (RH, d), relative soil water content (RWC, e) and photosynthetic active radiation (PAR, f) are shown. Lines and symbols mark daily treatment averages during daytime (PAR >100 $\mu\text{mol m}^{-2}\text{s}^{-1}$) and the shaded areas are \pm SD ($n = 9$). aCO₂ is shown in turquoise, solid points, eCO₂ in dark red, solid triangles.

RWC (10HS, Decagon Devices, Inc., WA, USA) under control conditions was maintained at about 50 % (Figure 2.1e). Before stopping irrigation completely, water availability was progressively reduced in five steps simulating a slow lethal drought (Table 2.1). Slightly higher

Dying by drying: timing of physiological stress thresholds related to tree death is not significantly altered by highly elevated CO₂

RWC under eCO₂ resulted from lower E , which also explains higher percentage of maximum water loss through transpiration (% E_{max}) values.

Table 2.1: Irrigation modulation during the seven experimental steps (I-VII) of the lethal drought simulation in relation to the pre-determined maximum of transpiration per [CO₂] treatment.
Shown are length of each irrigation step in days and irrigation amount in ml per day as well as in percentage of the maximum water loss through transpiration (% E_{max}) for the ambient (aCO₂) and elevated (eCO₂) atmospheric CO₂ concentration treatment.

step		I	II	III	IV	V	VI	VII
days		7	21	8	6	7	19	9
irrigation [ml d ⁻¹]		300	100	50	37.5	30	16.7	0
irrigation % E_{max} [%]	aCO ₂	500	83	42	31	21	14	0
	eCO ₂	582	97	49	36	24	16	0

With the experimental setup just described and also nine Aleppo pine seedlings per [CO₂] treatment (not the same seedlings as in the slow drought experiment) we previously conducted an experiment mimicking a fast, lethal drought by only reducing irrigation twice before stopping it all together after 2 weeks. Air temperature and relative humidity of the tree chambers and the initial RWC did not differ between the two experiments (Supplemental Figure S2.4).

2.2.3 Gas exchange measurements

Above- and belowground CO₂ and H₂O gas exchange ($n = 9$ per [CO₂] treatment) was quantified using two gas analyzers connected in series. First, absolute [CO₂] and [H₂O] of the supply air stream (LI-840, Li-cor, Lincoln, NE, USA) and secondly, differences between supply and sample air stream (Li-7000, Li-cor, Lincoln, NE, USA) were measured. While automatically switching between chambers every 120 s, the data was logged to a computer at 10 s intervals. CO₂ fluxes from the belowground compartments were treated as root respiration signal because all belowground C was planted related as C-free substrate has been used as potting material (see above). Two empty chambers containing the same C-free potting substrate, but without seedlings, were used as blanks to constantly monitor the system and to correct gas exchange estimates for any fluctuations in [CO₂] and [H₂O] not caused by changes in plant activity (3.09±2.36 ppm CO₂ and -0.05±0.05 ppt H₂O in the above- and 4.74±2.77 ppm CO₂ in the belowground compartment). For each chamber measurement, only the last 40 s were used to calculate gas exchange fluxes according to the following equations.

Tree E in [mol s⁻¹] was calculated as

$$E = \frac{F_m(W_{supply} - W_{sample})}{(1 - W_{sample})} \quad (1)$$

with W_{supply} [mol mol⁻¹] as [H₂O] in supply air stream, W_{sample} [mol mol⁻¹] as [H₂O] in sample air stream and F_m [mol s⁻¹] as molar flow.

Tree net assimilation ($A_{net, canopy}$) as well as root and night-time shoot respiration in [mol s⁻¹] were calculated using the equation for CO₂ fluxes

$$CO_2 \text{ flux} = -F_m(C_{supply} - C_{sample}) - EC_{sample} \quad (2)$$

with C_{supply} [mol mol⁻¹] as [CO₂] in supply air stream, C_{sample} [mol mol⁻¹] as [CO₂] in sample air stream, F_m [mol s⁻¹] as molar flow and E [mol s⁻¹]. Total daily respiration rates (R_{total}) were then calculated from the sum of nighttime shoot and day-and nighttime root respiration.

Canopy conductance (g_{canopy}) [mol H₂O s⁻¹] was determined from daytime gas exchange data as follows

$$g_{\text{canopy}} = \frac{E \left(1000 - \frac{W_{\text{leaf}} + W_{\text{sample}}}{2} \right)}{W_{\text{leaf}} - W_{\text{sample}}} \quad (3)$$

with W_{leaf} as leaf saturated vapor pressure, W_{sample} [mol mol⁻¹] as [H₂O] in sample air stream and E [mol s⁻¹]. This approach neglects boundary layer conductance, which should be negligible under high mixing conditions inside the chamber (Birami et al. 2020).

C_i [μmol mol⁻¹] was calculated using the following equation

$$C_i = \frac{\left(\frac{g_{\text{canopy}}}{1.6} - \frac{E}{2} \right) C_{\text{sample}} - A_{\text{net canopy}}}{\frac{g_{\text{canopy}}}{1.6} + \frac{E}{2}} \quad (4)$$

with C_{sample} [μmol s⁻¹] as [CO₂] in sample air stream, g_{canopy} [mol s⁻¹], $A_{\text{net canopy}}$ [μmol s⁻¹] and E [mol s⁻¹].

2.2.4 Sampling procedure and needle water status

Throughout the experiment we sampled needle material for non-structural carbohydrates analysis and tree water status. The sampling was conducted between 12 p.m. and 2 p.m. Midday needle water potential (Ψ_{md}) was measured using a pressure bomb (Modell 1000, PMS Instrument Company, Albany, OR, USA) on one needle fascicle per tree. Additionally, in order to determine relative needle water content (RLWC) needle mass was determined a) from the same fresh needles used for water potential analysis, b) after being submerged in distilled water for 48 hr and c) post drying at 60 °C. We defined a sudden sharp drop in RLWC and Ψ_{md} as indication that the turgor loss point has been reached. Needle samples for non-structural carbohydrate analysis were immediately frozen in liquid nitrogen and stored at -80 °C until further analysis. Tree biomass was harvested at the last day of the experiment when seedlings appeared dead and divided into needle, woody and root tissue and dried at 60 °C for 48 hr prior dry mass was measured.

2.2.5 Non-structural carbohydrate quantification

2.2.5.1 Soluble sugar

The determination of soluble sugar was conducted as described by Landhäusser et al. (2018) with minor modifications. For the extraction, 15 mg of frozen plant powder was added to 0.5 ml 80 % ethanol. After shaking, 10 min incubation at 80 °C and centrifugation (13,000 g for 3 min), the supernatant was taken and the extraction process repeated twice. While the remaining pellet swelled in 1 ml distilled water (dH₂O) at 95 °C for 2 hr before being stored at -80 °C for subsequent starch analysis (see below), the supernatants were mixed and the fluids were vaporized in a vacuum concentrator. The pellet was then dissolved in 1 ml dH₂O. For sugar quantification, 200 μl aliquots of extract (1:10 diluted in dH₂O) were mixed with 100 μl invertase

solution (300 U ml⁻¹, Sigma-Aldrich I4504-250 mg, Merck, Darmstadt, Germany) diluted in 10 mM sodium acetate buffer (pH 4.5) and incubated for 35 min at 55 °C. Afterwards 200 µl (5 mM MgCl, 95 mM Tris-HCL, 1.7 mM ATP, 4.5 mM NAD⁺, 1.1 U ml⁻¹ G6PDH (Sigma-Aldrich G8404-2KU, Merck, Darmstadt, Germany), 10 U ml⁻¹ HK (Roche 1,142,632,001, Roche, Mannheim, Germany), 1.6 U ml⁻¹ phosphoglucose isomerase (Sigma-Aldrich P5381-1KU, Merck, Darmstadt, Germany) were added to 50 µl aliquots of sugar extract in 96-well microtest plates (Brand, Wertheim, Baden-Württemberg, Germany). After 20 min of incubation at room temperature, absorbance was determined at 340 nm with a microplate absorbance reader (Epoch2, BioTek, Winooski, VT, USA).

2.2.5.2 Starch

After thawing and shaking, 80 µl aliquots of water diluted starch samples (see above) were mixed with 20 µl α-amylase (30 U ml⁻¹, Megazyme E-BLAAM-10 ml) and boiled at 85 °C for 1 hr. Following a quick cooling, 100 µl amyloglucosidase (20 U ml⁻¹ amyloglucosidase (Sigma-Aldrich 10115-1G-F, Merck, Darmstadt, Germany) dissolved in 25 mM potassium acetate buffer) were added and samples boiled at 55 °C for another hour. In preparation for the analysis, samples were cooled again and centrifuged (13,000 g for 3 min) before 50 µl aliquots were mixed with 200 µl buffer (5 mM MgCl, 95 mM Tris-HCL 1.7 mM ATP, 4.5 mM NAD⁺, 1.1 U ml⁻¹ G6PDH (Sigma-Aldrich G8404-2KU), 10 U ml⁻¹ HK (Roche 1,142,632,001, Roche, Mannheim, Germany), 10 U ml⁻¹ HK) in 96-well microtest plates (Brand, Wertheim, Baden-Württemberg, Germany). Absorbance at 340 nm was measured using a microplate absorbance reader (Epoch2, BioTek, Winooski, VT, USA).

2.2.6 Statistical data analyses

Gas exchange data of each chamber were quality controlled. Day and nighttime measurements outside 1.5 times the interquartile range above the upper quartile or below the lower quartile, which were adjusted for each experimental phase, were considered outliers and therefore not included in the analysis. This removed on average 5.2 % and 8.4 % of the CO₂ and H₂O gas exchange data, respectively.

All statistical analyses were performed using R 3.5.2 (R Core Team 2016). Differences were considered significant at $p \leq 0.05$. Treatment and drought effects were assessed by fitting linear mixed effects models (lme) (package lme4: Bates et al. 2015 and package lmerTest: Kuznetsova, Brockhoff, and Christensen 2017) with time and treatment as fixed effects and tree as random factor. Additionally, *post-hoc* Tukey multiple comparisons test of means (package emmeans: Lenth et al. 2019) was performed to assess daily differences. Differences in biomass were tested using *t*-test for two independent samples. The correlation between needle soluble sugar (SS_N) to starch (St_N) ratios and needle water potential Ψ_{md} was fitted using a Michaelis-Menten kinetics function ($y = ax/[b+x]^{-1}$). A logarithmic function ($y = \log[x]$) was used to simulate the tree C balance response to stomatal closure.

To assess possible [CO₂] effects on tree mortality risk factors during the lethal drought we first identified core parameters associated with tree survival such as tree C balance, stomatal closure and hydraulic integrity. We then defined critical thresholds for these parameters (see 2.3) and determined the probability for seedlings to match these threshold criteria per day. Aiming to assess the tree mortality risk, we combined the separate parameter observations by quantifying the probability for seedlings to reach all three critical thresholds per day. All these evaluations were made for aCO₂ and eCO₂ separately. We used logistic regression to analyze

the [CO₂] effect on risk threshold probability per day, and accounted for temporal autocorrelation by bootstrap sampling. We assessed model performance using a pseudo R² metric (package sigr, Mount and Zumel 2019). Significant differences between treatments were assessed via a non-parametric Mann-Whitney U test comparing the average number of days required to reach the threshold per treatment.

As indicators of tree death, we used foliar browning, cessation of shoot respiration and Ψ_{md} below -5 MPa, which is associated with 50 % potential loss of xylem conductivity (PLC₅₀) in *P. halepensis*.

2.3 Results

2.3.1 [CO₂] effect under favorable conditions

Atmospheric [CO₂] had a clear effect on the biomass of Aleppo pine seedlings resulting in significantly higher shoot and root biomass under eCO₂ (needle +27 %; woody tissue +30 %; root +27 %) (Table 2.2). However, root/shoot ratios were similar to aCO₂.

Table 2.2: Biomass (*P. halepensis*, $n = 9$ per treatment, \pm SD) of needles, shoot woody tissue, roots and shoot/root ratio was measured at tree death.

Values are given in dry weight (DW) for the ambient (aCO₂, c. 413 ppm) and elevated (eCO₂, c. 914 ppm) atmospheric CO₂ concentration treatment. Using *t*-test for two independent samples tested for potential treatment effects. Statistical significance (*t*-Test, $p < 0.05$) is indicated by different lower-case letters.

	biomass [gDW]			
	aCO ₂		eCO ₂	
needle	41.38 \pm 8.88	(a)	52.56 \pm 6.15	(b)
woody tissue	26.96 \pm 5.81	(a)	34.97 \pm 5.03	(b)
root	80.72 \pm 12.57	(a)	102.59 \pm 13.28	(b)
root/shoot	1.11 \pm 0.21		1.16 \pm 0.21	

During 12 days of acclimation to the tree chambers under sufficient water supply, tree *E* and $A_{net, canopy}$ steadily increased. $A_{net, canopy}$ rates were twice as high in eCO₂ than in aCO₂ (TukeyHSD: $p = 0.014$, $t = -5.15$) on the tree level reaching maximum rates of 1.24 \pm 0.17 (aCO₂)/ 1.98 \pm 0.71 (eCO₂) [mol hr⁻¹tree⁻¹] (Figure 2.2b). Simultaneously, tree *E* was not significantly lower in eCO₂ than aCO₂ (Figure 2.2a) on the tree level, reaching maximum rates of 0.40 \pm 0.06 (aCO₂)/ 0.31 \pm 0.11 (eCO₂) [mol hr⁻¹tree⁻¹]. On a leaf area basis, the [CO₂] effect on $A_{net, canopy}$ vanished suggesting the increase in leaf area as the main reason for higher $A_{net, canopy}$ in eCO₂ (Supplemental Figure S2.5b). In contrast, treatment differences in *E* were significantly amplified on a leaf area basis (TukeyHSD: $p = 0.021$, $t = 5.113$) (Supplemental Figure S2.5a), which can be explained by lower canopy conductance (g_{canopy} , sum of stomatal and cuticular conductance) in eCO₂ of 22 % at the tree level and 33 % at the leaf level (leaf area) (data not shown). Respiration rates (sum of shoot nighttime, root day- and nighttime R_{total}) were not significantly higher under eCO₂ compared to aCO₂, despite a significantly larger tree biomass (+27 %) under eCO₂.

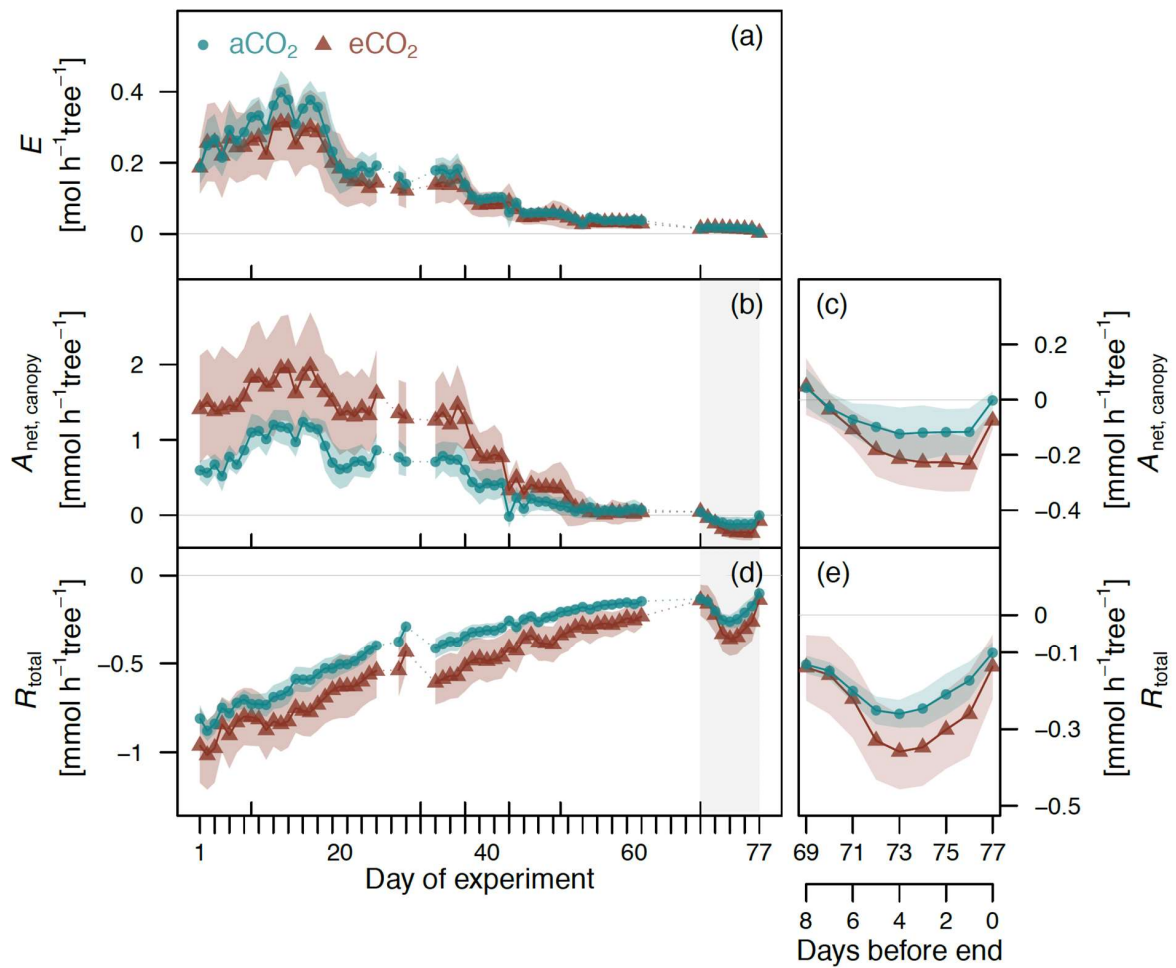


Figure 2.2: Gas exchange parameters during the course of the lethal drought experiment.

Shown are transpiration rate (E) (a), net assimilation ($A_{\text{net, canopy}}$) (b) and respiration (R_{total} , sum of shoot dark and root respiration) (d) rates as hourly means per day and tree for the ambient (aCO₂, c. 413 ppm) and the elevated (eCO₂, c. 914 ppm) atmospheric CO₂ concentration treatment. The shaded areas depict \pm SD. Data gaps are bridged by thin dotted lines. For $A_{\text{net, canopy}}$ and R_{total} , the light grey colored areas mark the final phase of the experiment, which is additionally shown on a finer scale (c, e) highlighting the respiration burst just before death of the seedlings occurred. Longer tick marks on the x-axis mark days of irrigation reductions. aCO₂ is shown in turquoise, solid points, eCO₂ in dark red, solid triangles.

2.3.2 Gas exchange response to drought

In the course of step-wise reductions in irrigation, E and $A_{\text{net, canopy}}$ declined gradually and reached new stable rates during each drought phase. Simultaneously, treatment differences in $A_{\text{net, canopy}}$ and E diminished with progressing drought. In contrast, the [CO₂] effect on R_{total} apparent in 1.5 times higher rates in eCO₂ compared to aCO₂ (not statistically significant) was largely sustained by concurrently decreasing R_{total} in both treatments with increasing soil drought (Figure 2.2d). Interestingly, ceasing irrigation completely triggered a sudden respiration burst notable in $A_{\text{net, canopy}}$ as well as R_{total} (Figure 2.2c, e). Contrary to the transition from assimilation to respiration in $A_{\text{net, canopy}}$, the renewed rise in R_{total} was significant (TukeyHSD: aCO₂ $p < 0.01$, $t = 6.99$; eCO₂ $p < 0.01$, $t = 9.72$) due to a doubling of respiration rates measured during the burst. This phenomenon had also been observed during the prior, fast lethal drought experiment (Supplemental Figure S2.4a, c). Since occurring at times when trees started dying, the burst in respiration may indicate drought-induced lethal cell damage.

2.3.3 [CO₂] effect on tree C balance during drought

We further assessed the [CO₂] effects on the tree C balance ($\Sigma C = A_{\text{net, canopy}} - R_{\text{total}}$, see also Supplemental Figure S2.6b) and water loss (ΣE , see also Supplemental Figure S2.6a) in relation to g_{canopy} . To overcome the differences in g_{canopy} from [CO₂], g_{canopy} was expressed in relation to maximum g_{canopy} ($g_{\text{canopy max}}$) per treatment (Figure 2.3). Based on changes in C_i/C_a ratios, which remained unaffected by [CO₂], we have separated drought effects on assimilation into four phases (see Figure 2.3, dashed vertical lines). Following this structuring, we analyzed the [CO₂] effect on ΣC in the course of declining g_{canopy} .

During non-stressful conditions, indicated by C_i/C_a ratios of about 0.7 (phase I), assimilation was not limited by water availability (irrigation step one and the beginning of step two) and ΣC in eCO₂ was with 0.17 gC day⁻¹ about 300 % higher than in aCO₂ (TukeyHSD: $p = 0.012$, $t = -4.90$). With developing drought stress (during irrigation steps two and three), as stomatal restriction on assimilation increased causing C_i/C_a ratios to decline (at 40-60 % $g_{\text{canopy max}}$), the stimulation of eCO₂ on ΣC also declined. In phase III, when C_i/C_a is nearly stagnant again at about 0.6 (at around 35 % $g_{\text{canopy max}}$), the restriction on assimilation is slowly transitioning from stomatal to non-stomatal accompanied by again increasing relative difference in ΣC between aCO₂ and eCO₂. However, high variances of drought stress development within the treatments prevented these differences from being statistically significant. Sharply increasing C_i/C_a ratios mark the reaching of the C_i inflexion point and simultaneously the beginning of phase IV. During this last phase (irrigation steps 4 to 7) characterized by dominating and further increasing non-stomatal restriction on assimilation, the [CO₂] effect transitioned from a benefit to a detriment at 15 % of $g_{\text{canopy max}}$ (Ψ_{md} of -2.3 MPa). This goes along with the transition from assimilation to respiration during the last week of the experiment ($C_i/C_a > 1$) and higher respiration rates in eCO₂ (Figure 2.2b, c). In contrast to the [CO₂] effect on ΣC , the difference in ΣE between treatments (on average -12±5 %) was not significant at the tree level, as variances were high and the larger biomass under eCO₂ almost annulled the effect of reduced E per unit leaf area.

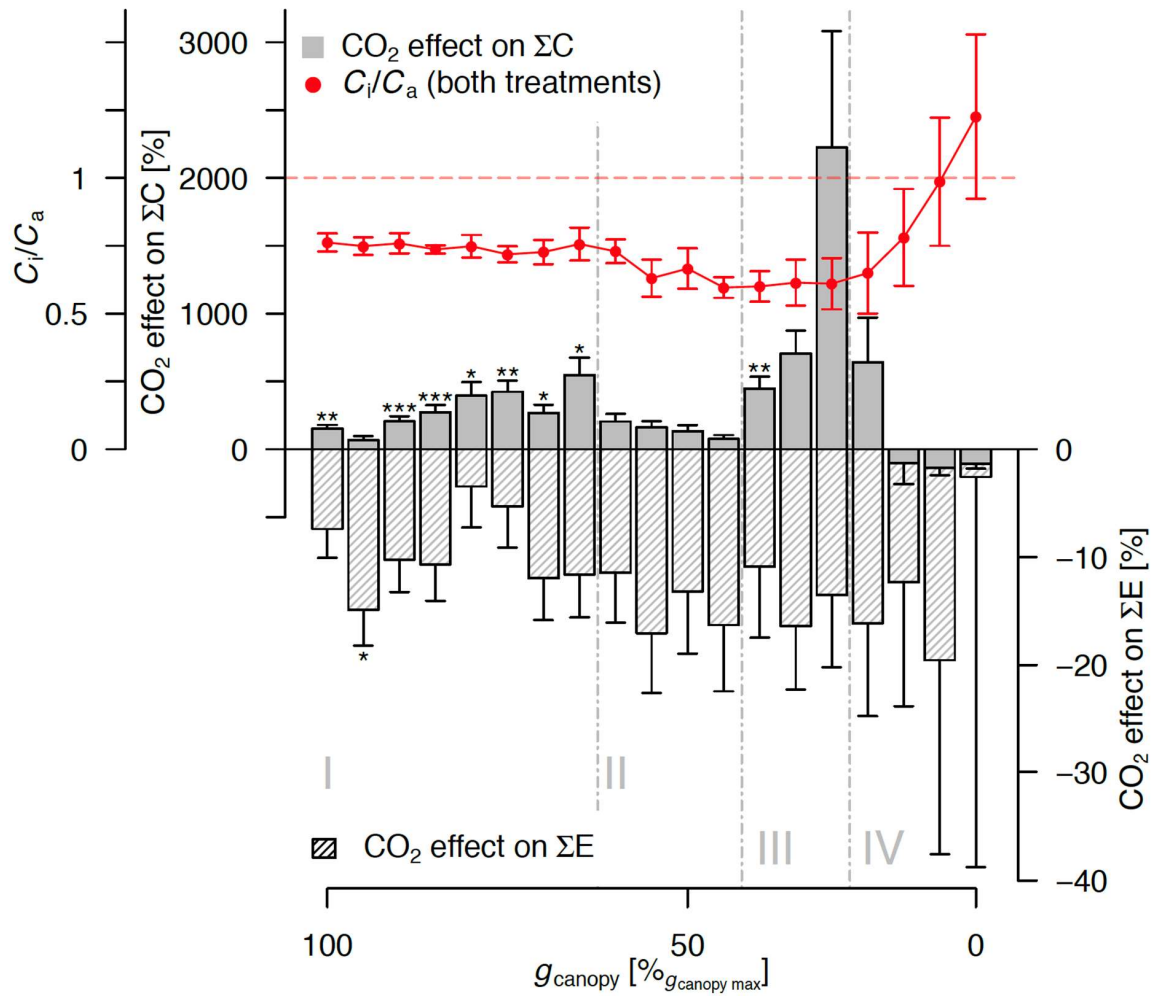


Figure 2.3: [CO₂] effect on tree carbon balance (ΣC) and tree water loss from transpiration (ΣE) as well as leaf internal [CO₂]/atmospheric [CO₂] ratios (C_i/C_a) (for day-time measurements, photosynthetic active radiation (PAR) >100 μmol m⁻²s⁻¹) over the course of stomatal closure.

ΣC (sum of net assimilation, shoot dark and root respiration, grey bars) and ΣE (sum of shoot day and night transpiration, shaded bars) are shown as differences between the ambient (aCO₂) and the elevated (eCO₂) atmospheric [CO₂] treatment in percentage of aCO₂ values (%=[(eCO₂-aCO₂)/aCO₂]*100). The degree of stomatal closure was calculated by expressing canopy conductance (g_{canopy} , sum of stomatal and cuticular conductance) as percentage of maximum g_{canopy} under control conditions for each treatment. Bars show averages over 5 % bins of g_{canopy} expressed as percentage of maximum g_{canopy} with error bars depicting ±SD. C_i/C_a values (red solid points) are also shown as means over 5 % bins of g_{canopy} ±SD for both treatments. Asterisks above bars represent statistical significance (linear mixed effects model with post-hoc Tukey; $p < 0.05^*$, $p < 0.01^{**}$, $p < 0.001^{***}$) of the [CO₂] effect derived from absolute values. Grey dashed lines and roman numerals mark the four phases of assimilation restriction differentiated by changes in C_i/C_a ratios in the course of declining g_{canopy} .

2.3.4 Needle water potential and non-structural carbohydrates

Despite treatment differences in tree water fluxes (g_{canopy} , E) on the leaf level, Ψ_{md} and RLWC measurements revealed no [CO₂] effect (Figure 2.4). Following a slow but steady decrease during mild to moderate drought stress, Ψ_{md} fluctuated around the turgor loss point identified at -2.2 MPa as water availability was further reduced (Table 2.1, 16.7 ml day⁻¹). While the decline in Ψ_{md} responded to increasing drought, RLWC was maintained at values between 70 and 80 %. However, once the turgor loss point was reached, Ψ_{md} and RLWC steeply declined

reaching values of about -7 MPa and 31±16 %, respectively, within eight days after irrigation had been stopped.

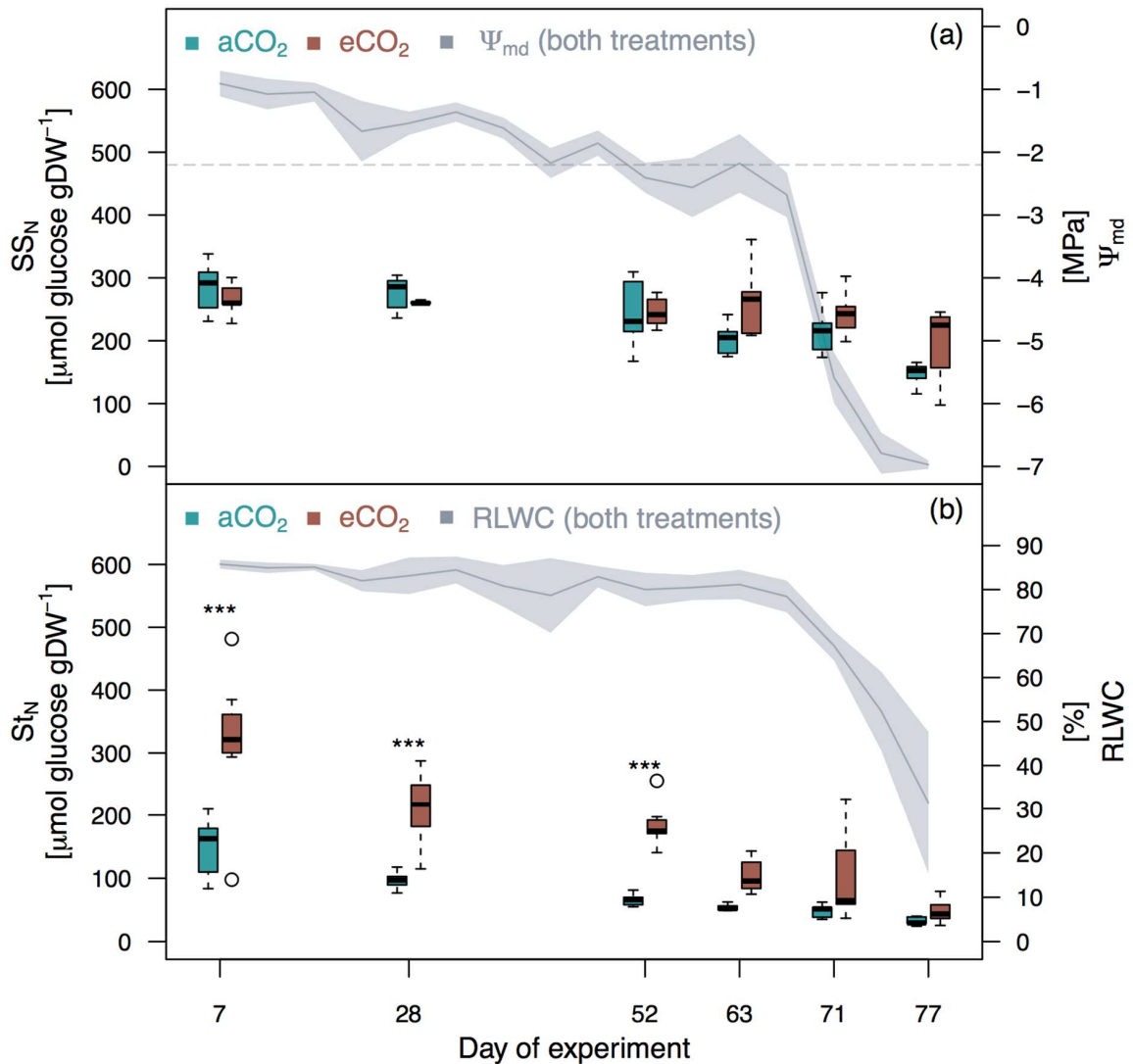


Figure 2.4: Needle soluble sugar (SSN, a), needle starch (StN, b) concentrations, midday needle water potential (Ψ_{md} , a) and relative needle water content (RLWC, b) over the course of the experiment. Ψ_{md} and RLWC are shown as average over both treatments (ambient (aCO₂) and elevated (eCO₂) atmospheric [CO₂]) \pm SD depicted as shaded area. The turgor loss point at -2.2 MPa is marked as grey dashed line. SSN and StN are shown as boxplots with measurements outside 1.5 times the interquartile range above the upper quartile or below the lower quartile considered outliers. Asterisks above boxes represent statistical significance between treatments (linear mixed effects model with *post-hoc* Tukey; $p < 0.05^*$, $p < 0.01^{**}$, $p < 0.001^{***}$). aCO₂ is shown in turquoise, eCO₂ in dark red.

Similar to Ψ_{md} , SSN content was not affected by eCO₂ (Figure 2.4a). In addition, SSN showed no drought effect, as concentrations were maintained relatively stable. The observed slight decrease in SSN at the final harvest could be due to metabolic processes triggered by tree death (Figure 2.4a). As a consequence of these SSN results, steadily rising SSN to StN ratios (Figure 2.5) were mainly attributed to decreasing StN concentrations (Figure 2.4b). In the course of the experiment, StN reserves were depleted by about 80 and 85 % in aCO₂ and eCO₂, respectively. Accordingly, the distinct [CO₂] effect on SSN/StN ratios under mild and

moderate drought ($\Psi_{md} > -2.2$ MPa) resulted from St_N concentrations being twice as high in eCO_2 than in aCO_2 (TukeyHSD: $p < 0.001$, $t = -6.27$). However, this treatment effect diminished with amplifying drought due to stronger decreasing St_N concentrations in eCO_2 compared to aCO_2 , while the overall St_N concentration remained higher under eCO_2 . The course of SS_N/St_N ratios indicates the use of St_N to maintain SS_N levels and respiration during drought. Furthermore, it would explain the increased reduction of St_N in eCO_2 , as assimilation per leaf dry weight in eCO_2 was lower than in aCO_2 after reaching the turgor loss point. Similar developments of SS_N/St_N ratios in relation to Ψ_{md} could be observed during a prior fast lethal drought experiment (Figure 2.5, Supplemental Figure S2.4).

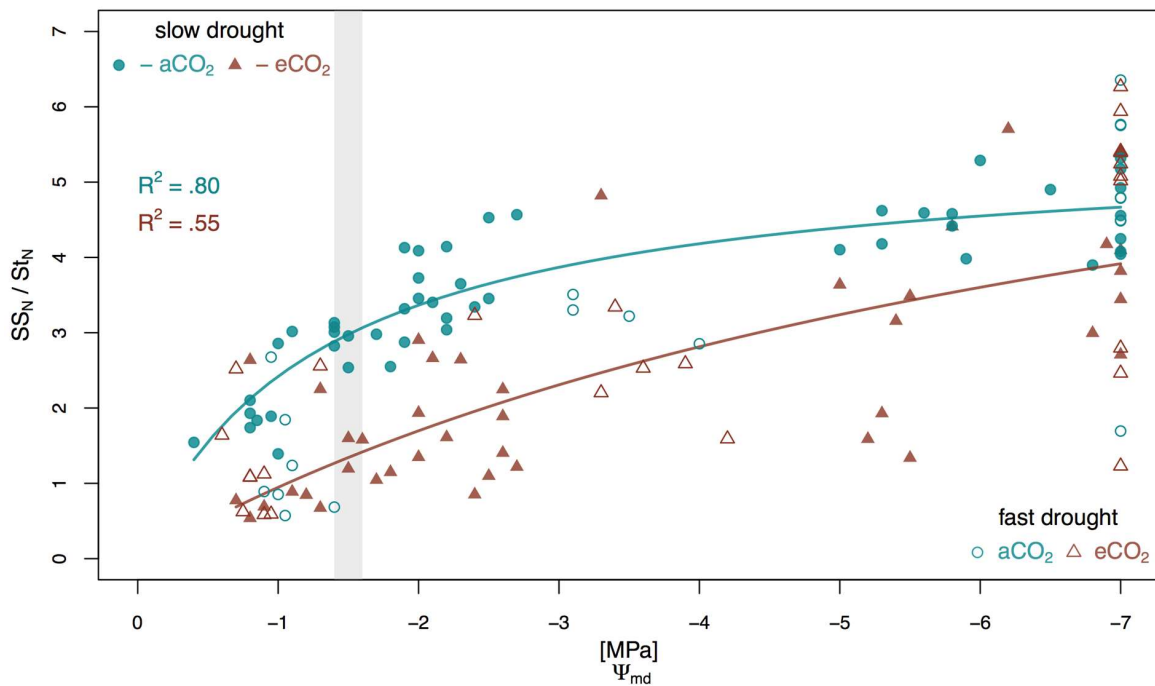


Figure 2.5: Needle soluble sugar (SS_N) to starch (St_N) ratios over midday needle water potential (Ψ_{md}). The carbon safety margin between -1.4 and -1.6 MPa is marked as light grey area. SS_N to St_N ratios are shown as individual measurements for the 2018 slow drought (ambient atmospheric [CO_2] (aCO_2): solid points, elevated atmospheric [CO_2] (eCO_2): solid triangles) and for the 2017 fast drought (aCO_2 : points, eCO_2 : triangles). Lines (aCO_2 : turquoise, eCO_2 : dark red) show regressions using non-linear least squares. aCO_2 is shown in turquoise, eCO_2 in dark red.

2.3.5 [CO_2] effect on risk thresholds during lethal drought

We used critical values to assess differences in the probabilities of reaching critical thresholds between the CO_2 treatments (see 2.2.6). The threshold criteria we assigned were: negative ΣC , daytime $g_{canopy} \leq 5\% g_{canopy\ max}$ and Ψ_{md} below the turgor loss point (-2.2 MPa). We preferred turgor loss to PLC_{50} , as we did not directly assess PLC in our seedlings. To test if eCO_2 might affect drought-induced carbon starvation, we introduced a 50 % threshold for St_N (relative to the initial values) (NSC_{50}), although there is no consensus on critical NSC values (Adams et al. 2017).

The treatment difference was only significant in St_N (Figure 2.6d); here aCO_2 seedlings reached the NSC_{50} threshold earlier and faster (Mann-Whitney U test: $p = 0.019$). Furthermore, declines in St_N followed shortly after ΣC turned negative in aCO_2 (Figure 2.6a),

whereas a time lag of about 10 days between these two events was observed in eCO₂ suggesting a positive [CO₂] effect on the carbon safety margin. While for ΣC and Ψ_{md} (Figure 2.6c) the probability of reaching the respective threshold increased slowly, the transition in g_{canopy} (Figure 2.6b) indicating stomatal closure was rather sudden, changing the probability from zero to one within 2 days irrespective of [CO₂]. Interestingly, these 2 days were the same in both treatments indicating that the relative response of g_{canopy} to severe drought was identical in aCO₂ and eCO₂.

When we assessed the overall risk factor by combining the results for ΣC , Ψ_{md} and g_{canopy} (Figure 2.6e), it became apparent that [CO₂] did not affect the probability of reaching the threshold, nor the timing of mortality. Ψ_{md} declining below the turgor loss point clearly marked the time at which survival in both treatments became critical. In summary, this clearly indicates that the mortality risk under severe drought stress was not reduced by eCO₂. Furthermore, our results show that this applies to both fast and slow (data not shown) lethal droughts.

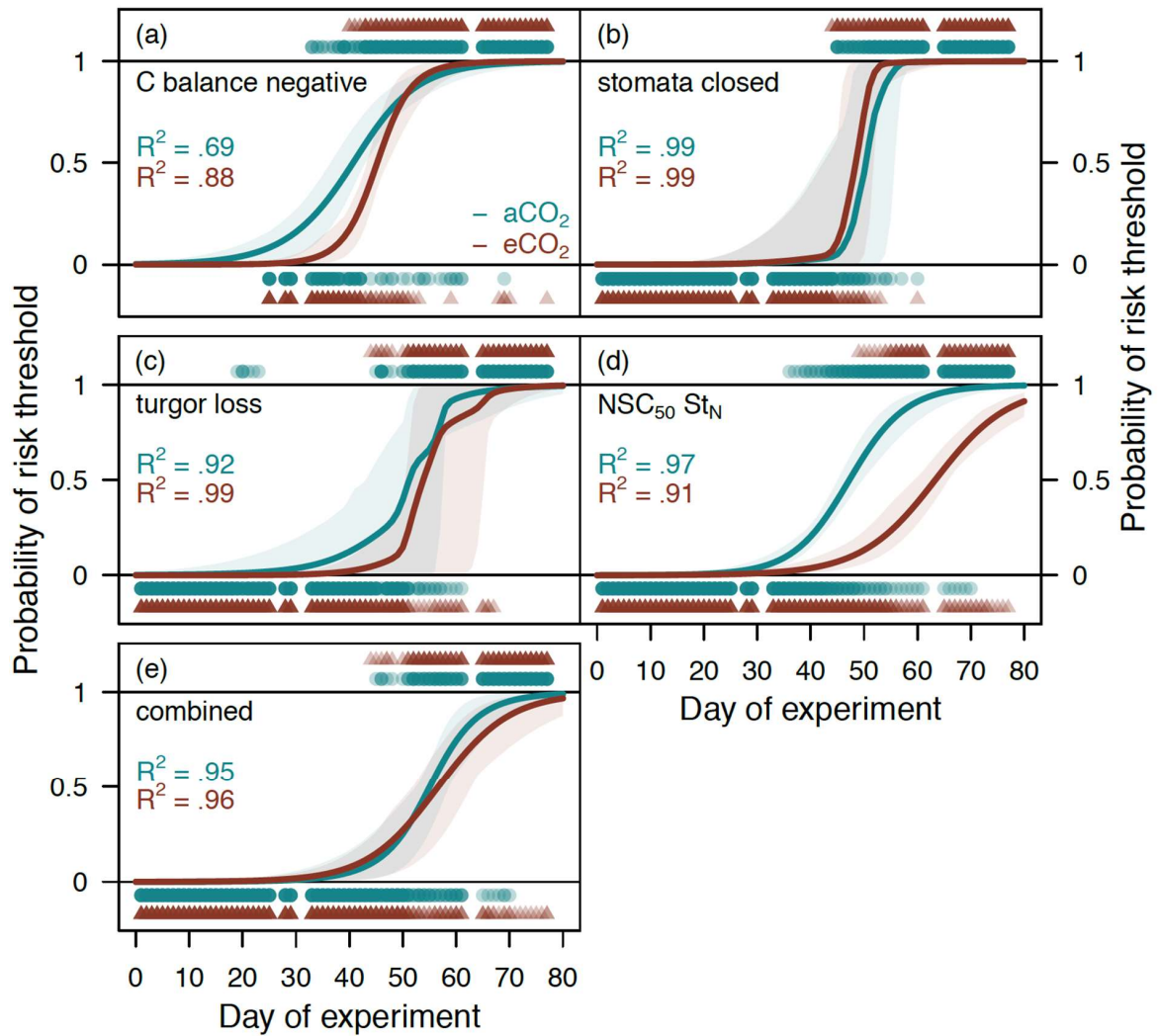


Figure 2.6: Logistic regressions to determine the [CO₂] effect on risk thresholds of Aleppo pine seedlings during a lethal drought ($n = 9$ per treatment).

For carbon balance (a), canopy conductance (g_{canopy}) (b), point of leaf turgor loss (c) and needle starch concentration (St_N) (d). In panel (e) mortality risk for each treatment and day is computed as the combined probability for a tree to present values above risk thresholds for carbon balance, canopy conductance and leaf turgor loss. The critical values were defined as C balance turning negative, g_{canopy} declining below minimum g_{canopy} , Ψ_{md} falling under the turgor loss point ($\Psi_{md} < -2.2$ MPa) and a 50 % loss of St_N (NSC_{50}). The quality of the fitted logistic regressions is shown by 95 % confidence intervals depicted as shaded areas and pseudo- R^2 values are given. Additionally, the transition of seedlings from 'not meeting the critical threshold' to 'meeting the critical threshold' is shown below and above each regression plot, respectively, with coloring becoming more transparent as number of seedlings decrease. Shown are the results for the ambient atmospheric [CO₂] (aCO₂: turquoise) and the elevated atmospheric [CO₂] (eCO₂: dark red) treatment.

2.4 Discussion

2.4.1 Pre-drought [CO₂] effect

We found eCO₂ to stimulate plant growth, equally reflected in increasing root and shoot biomass and therefore not affecting root/shoot ratios of the *P. halepensis* seedlings in our study (Table 2.2). In addition, larger needle starch storage and net C uptake at eCO₂ suggests that

excess C was stored as starch in leaves (Eguchi et al. 2004; Poorter et al. 1997; Pritchard et al. 1999) (Figure 2.4b). Frequently, increases in $A_{\text{net, canopy}}$ are accompanied by decreasing E and g_{canopy} under eCO₂ (Ainsworth and Rogers 2007; Birami et al. 2020; Gamage et al. 2018), as was the case at the leaf level in our study (Supplemental Figure S2.5). An optimization of the stomatal density (SD) to stomatal index (SI) (stomata to epidermal cells ratio) ratio would account for such an enhanced WUE (Haworth et al. 2010). However, we did not find a significant [CO₂] effect on SD ($p > 0.1$, $n = 17$) (data not shown). The lack of changes in SD and SI supports the hypothesis that trees more likely respond to eCO₂ by adjusting needle function, which is most prominently done by controlling stomatal aperture (Apple et al. 2000; Bettarini, Vaccari, and Miglietta 1998; Pritchard et al. 1999). As has been documented in several studies, eCO₂ stimulates stomatal closure (Ainsworth and Rogers 2007; Birami et al. 2020; Gamage et al. 2018; Xu et al. 2016). This together with biochemical adjustments most likely resulted in constant C_i/C_a in *P. halepensis* leaves under eCO₂ (Figure 2.3), which is concordant with a previous study (Birami et al. 2020) and suggested scenarios regarding WUE and rising C_a (Lavergne et al. 2019; Saurer, Siegwolf, and Schweingruber 2004). As a possible underlying mechanism, Tor-ngern et al. (2015) introduced the idea of long-term reductions in E and g_{canopy} being rather indirect, than direct effects of eCO₂. After extensive experiments in a temperate forest (FACE, +200 $\mu\text{mol mol}^{-1}$ for 17 years), they concluded that reductions of g_{canopy} were not a direct stomatal response to increasing [CO₂], but were considered to be attributable to decreases in leaf hydraulic capacity as well as reductions of hydraulic conductance from the xylem to the stomata as long-term acclimation to eCO₂ (Domec et al. 2009; Domec, Palmroth, and Oren 2016). As our seedlings were grown from seeds under eCO₂ for 2-years such a CO₂ acclimation response might be a likely scenario.

2.4.2 [CO₂] effect under mild to moderate drought conditions

Initial responses to drought are typically characterized by a gradual closure of stomata (Blackman et al. 2016; Mackay et al. 2015; Taïbi et al. 2017). During this phase, *P. halepensis* seedlings seemed to be able to offset restrictions on C assimilation under eCO₂ as $A_{\text{net, canopy}}$ was maintained at higher rates in spite of lower g_{canopy} compared to aCO₂ (Table 2.2), in agreement to previous observations (Birami et al. 2020). This indicates a potential ameliorating effect of eCO₂ (Ainsworth and Rogers 2007; Je et al. 2018; Robredo et al. 2010), supported by a delay in the C_i inflexion point, which marks the transition from stomatal to non-stomatal limitation as dominant restriction on $A_{\text{net, canopy}}$ (Flexas and Medrano 2002). In our study we did not observe such an effect on the C_i inflexion point as C_i/C_a in *P. halepensis* seedlings were unaffected by [CO₂].

One consideration in connection with reduced g_{canopy} resulting in lower E on the leaf level was a possible preservation of soil moisture and a resulting slowing down of the development of drought stress under eCO₂. However, such a phenomenon of ‘water saving’ is debatable due to the trade-off between the reduced water loss through transpiration and the simultaneous increase of leaf area under eCO₂ (Dusenge et al. 2019; Tor-ngern et al. 2015; Wullschleger, Tschaplinski, and Norby 2002), which was also apparent in our study. In addition, we observed no significant eCO₂ effect on Ψ_{md} or RLWC since *P. halepensis* seedlings in both treatments maintained Ψ_{md} above the turgor loss point (TLP) (-2.2 MPa) and RLWC at around 82 % for the longer part of the drought period (63 days) (Figure 2.4). The seemingly stable leaf water status along with no apparent up-regulation of SS_N (Figure 2.4a) suggest a lack of osmotic adjustment with decreasing water availability, controversial to the general drought response of plants (Adams et al. 2017; Li et al. 2018). However, decreasing St_N concentrations indicate the

remobilization of starch reserves in *P. halepensis* seedlings in order to meet C requirements when drought response reduces C assimilation (Martínez-Vilalta et al. 2016). A more detailed look at the primary metabolome, but excluding starch, of *P. halepensis* seedlings subjected to heat and hot drought stress revealed that eCO₂ enhanced root protein stability at high temperatures, but did not alter the general stress response (Birami et al. 2020). Contrary to our expectations, eCO₂ trees did apparently not benefit from enhanced NSC reserves. NSC patterns were rather similar between a slow and a fast drought as relations between SS_N/St_N ratios and Ψ_{md} show (Figure 2.5), emphasizing the complex as well as versatile use of NSC in response to drought.

2.4.3 [CO₂] effect on tipping points and drought-induced mortality

In response to severe drought, *P. halepensis* seedlings kept stomata closed but still lost water through cuticular conductance and stomatal leakiness (Blackman et al. 2016). During such conditions, survival depends on both C accessibility, required for instance for metabolic processes such as respiration, and the integrity of the plants hydraulic functions ensuring the maintenance of capacitance and conservation of water storage (Adams et al. 2017; Blackman et al. 2019; Choat et al. 2018; Nardini, Battistuzzo, and Savi 2013; Sevanto 2018; Sevanto et al. 2014; Zhu et al. 2018). Regarding C availability under severe drought, NSC have been identified as a key C source (Galiano, Martínez-Vilalta, and Lloret 2011; Garcia-Forner et al. 2016; O'Brien et al. 2014).

However, because of their various functions in plant C metabolism it has been proven to be extremely difficult to specify a particular NSC threshold below which death is more likely than survival (Adams et al. 2017; McDowell et al. 2013; Meir, Mencuccini, and Dewar 2015). In a global synthesis, Martínez-Vilalta et al. (2016) found a 54 % NSC loss as an overall estimate for minimum NSC in dying relative to control trees. Applied to our SS_N and St_N measurements, the NSC₅₀ threshold underlines the mitigating effect of eCO₂ on St_N depletion (Figure 2.6d). However, due to the uncertainty regarding this threshold we also considered the transition from positive to negative C balance (after growth ceases) as a critical threshold. Since we estimated the C balance as $A_{net, canopy}$ minus R_{total} , a negative C balance means that reductions in $A_{net, canopy}$ exceed decreases in R_{total} under declining water availability (Figure 2.2) further suggesting the requirement for alternative C sources namely NSC. Mitchell et al. (2014) attributed importance to Ψ_{md} values between -1.4 and -1.5 MPa by proposing the phase between the cessation of growth and assimilation as a carbon safety margin for isohydric tree species. Since this attempt at defining a carbon safety margin is very rare due to the complex and diverse functions of NSC, the applicability of this approach remains questionable. However, in our study a similar Ψ_{md} range (between -1.4 and -1.6 MPa) delimited the crucial period beyond which growth must have ceased (net C uptake zero), shortly before the C balance turned negative and stress turned from mild to severe. We found eCO₂ to not affect this carbon safety margin.

In order to assess the risk of dehydration and hydraulic failure under drought, leaf turgor and xylem conductivity are considered as crucial traits (Körner 2019). Losses in conductivity are strongly linked to xylem cavitation and embolisms indicating a rising possibility of hydraulic dysfunction and ultimately tree mortality (Breshears et al. 2018; Cochard 2006; T Klein et al. 2016; Klein, Cohen, and Yakir 2011). Irrespective of [CO₂], the TLP of *P. halepensis* seedlings was reached at 80 % RLWC and a Ψ_{md} of -2.2 MPa, which is in line with findings by Villar-Salvador et al. (1999) and Royo, Gil, and Pardos (2001). Beyond the TLP, seedlings dehydrated at a fast rate and RLWC was as low as 30 % at mortality. Substantial xylem

embolism must have occurred alongside dehydration and PLC₅₀ was reached at Ψ_{md} of about -5 MPa (Gleason et al. 2016) concordant with other PLC₅₀ results for *P. halepensis* (Martin-StPaul, Delzon, and Cochard 2017).

In previous studies, PLC₅₀ to 80 % PLC (PLC₈₀) was suggested as the likely critical threshold between survival and death in gymnosperms (Brodribb and Cochard 2009; Choat et al. 2018; Hammond et al. 2019). All of our seedlings were well beyond a Ψ_{md} related to PLC₅₀, when mortality was reached, indicating that PLC₈₀ might be a more meaningful threshold for mortality in Aleppo pine. In addition, our findings indicate that eCO₂ altered neither the hydraulic thresholds directly nor the time to reach the lethal hydraulic thresholds (Ψ_{md} did not differ between treatments). This corroborates the surmise that the detected water savings on leaf level are counterbalanced by the leaf area increase in *P. halepensis* seedlings under eCO₂. A similar lack of a [CO₂] effect on whole tree water relations and drought-induced mortality was reported by Duan et al. (2014) on *Eucalyptus radiata* and *Pinus radiata* as well as *Callitris rhomboidea* (Duan et al. 2015). As critical hydraulic thresholds were reached earlier than NSC thresholds, our results indicate that the water status is more meaningful than the C status for predicting mortality risks of *P. halepensis* seedlings under severe drought conditions. This in turn is consistent with findings by Duan et al. (2018) suggesting that predicting time-to-mortality for *Eucalyptus sideroxylon* is better based on leaf water potential than C status. In summary our results further support dehydration as the main cause of death in our seedlings and that eCO₂ did not alter dehydration rates.

Since our study was conducted on potted seedlings in a controlled greenhouse how meaningful are our results for the future of Aleppo pines in the Yatir forest? [CO₂]-stimulated root growth may expand the root zone, which may open up new water sources for the trees. This could be advantageous as our study shows that trees under eCO₂, despite a larger leaf area, transpire the same amount of water on the whole tree level due to reduced stomatal conductance. Together with larger C reserves, this in turn could influence the fate of the trees during drought conditions in favor of their survival. However, predicted reductions in precipitation for the Mediterranean region (Giorgi and Lionello 2008) alongside new evidence finding allocation changes under eCO₂ to increase leaf area compared to water supplying sapwood area (Trugman et al. 2019), calls into question the potential advantage just described. In combination with an overall absence of [CO₂] interacting with three critical drought thresholds, we conclude that eCO₂ will not improve survival of Aleppo pine seedlings under severe drought. Moreover, a larger non-structural carbohydrate buffer under eCO₂ seemed of no advantage neither during fast nor slow terminal drought, which clearly challenges the carbon starvation hypothesis.

Conflict of interest

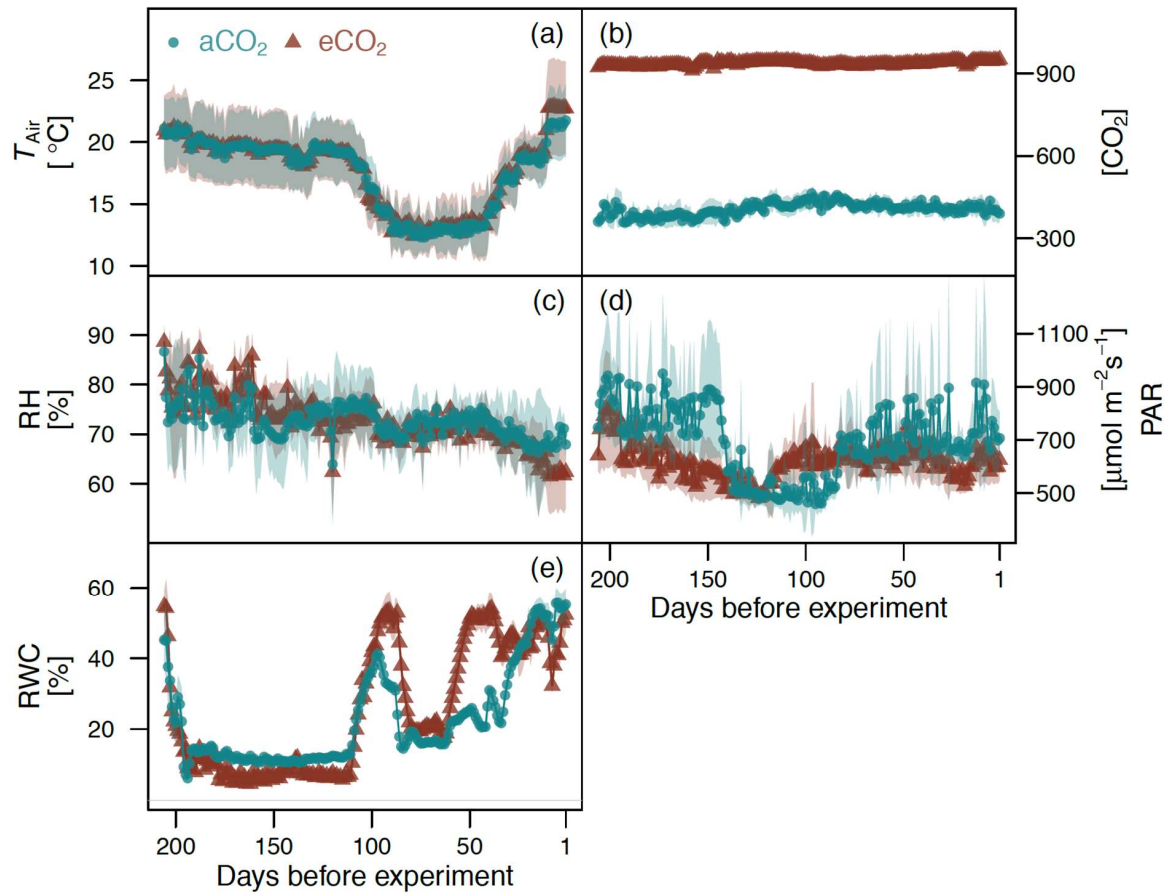
The authors declare no conflict of interest.

Acknowledgements

We would like to thank especially Andreas Gast, Andrea-Livia Jakab and Johanna Schnurr for assistance with the experimental set-up and lab work and we want to thank all colleagues who helped on sampling days.

This study was supported by the German Research Foundation through its Emmy Noether Program (RU 1657/2-1). We further acknowledge funding from the German Research Foundation through its German-Israeli project cooperation program (CSCHM 2736/2-1) and by the German Federal Ministry of Education and Research (BMBF), through the Helmholtz Association and its research program ATMO.

2.5 Supplement

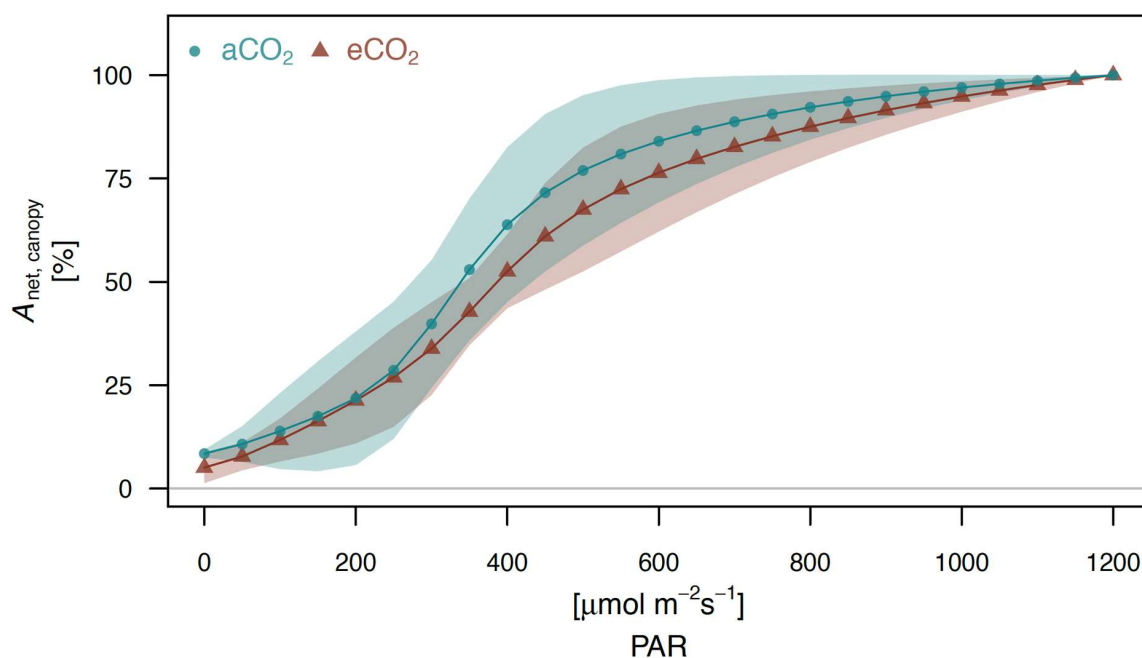


Supplemental Figure S2.1: Environmental drivers during cultivation (200 days prior to the experiment) of seedlings in the ambient (aCO₂) and elevated (eCO₂) atmospheric [CO₂] treatment. Air temperature (T_{Air} , a), [CO₂] of supply air stream ([CO₂], b), relative humidity (RH, c), photosynthetic active radiation (PAR, d) and relative soil water content (RWC, e) are shown. Lines and symbols mark treatment averages during daytime (PAR > 100 μmol m⁻² s⁻¹) and the shaded areas are ±SD. aCO₂ is shown in turquoise, solid points, eCO₂ in dark red, dark red triangles.

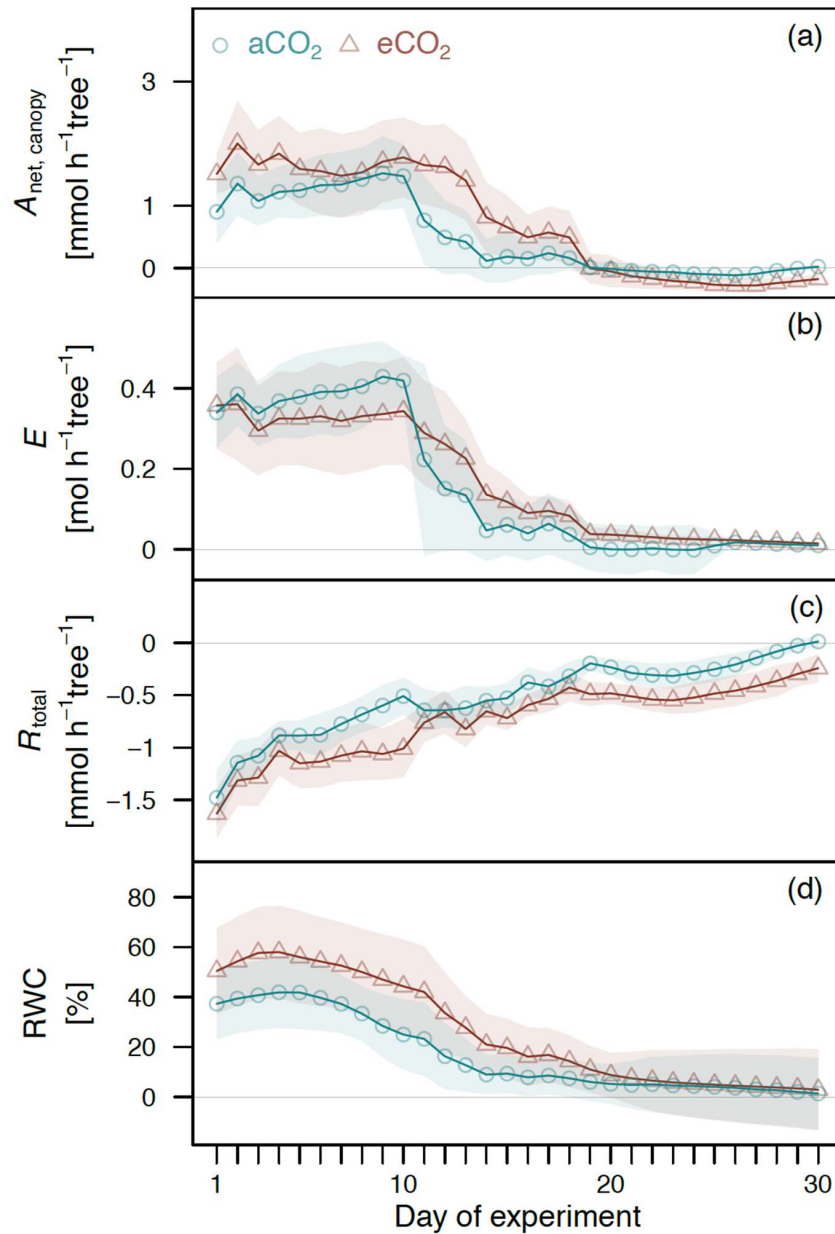


Supplemental Figure S2.2: Overview of the experimental setup in the greenhouse facility in Garmisch-Partenkirchen.

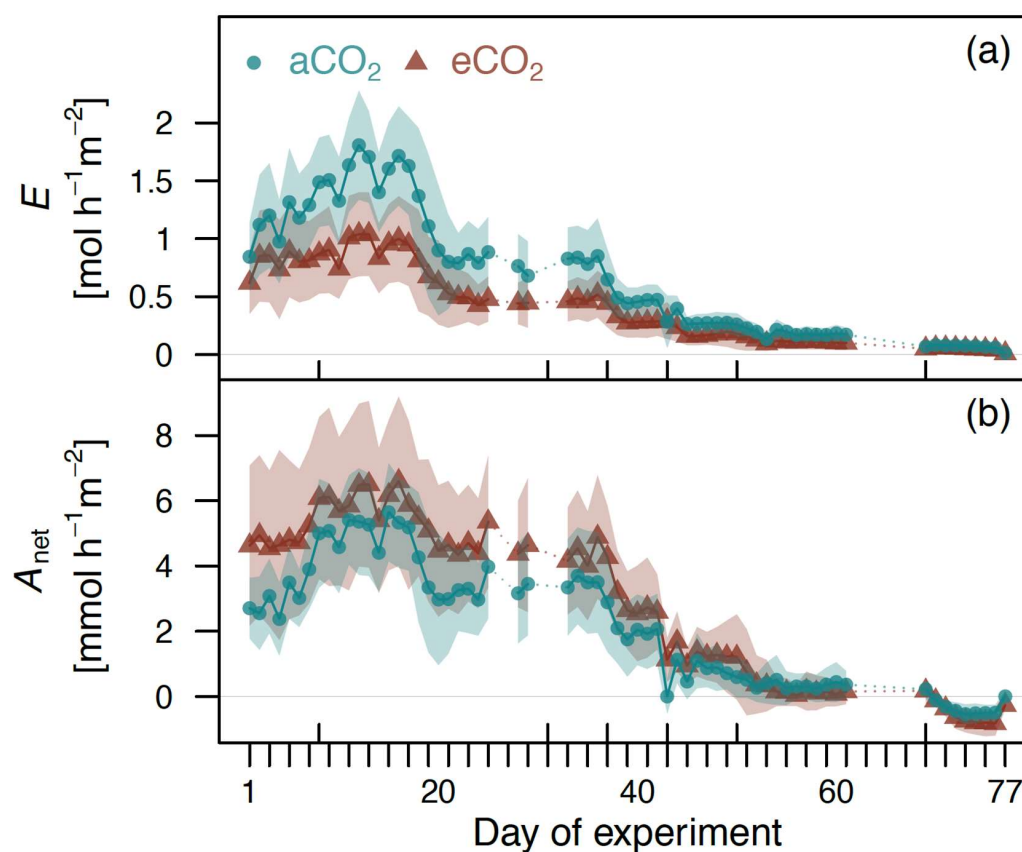
The picture shows the 20 tree chambers and their position in the greenhouse compartment.



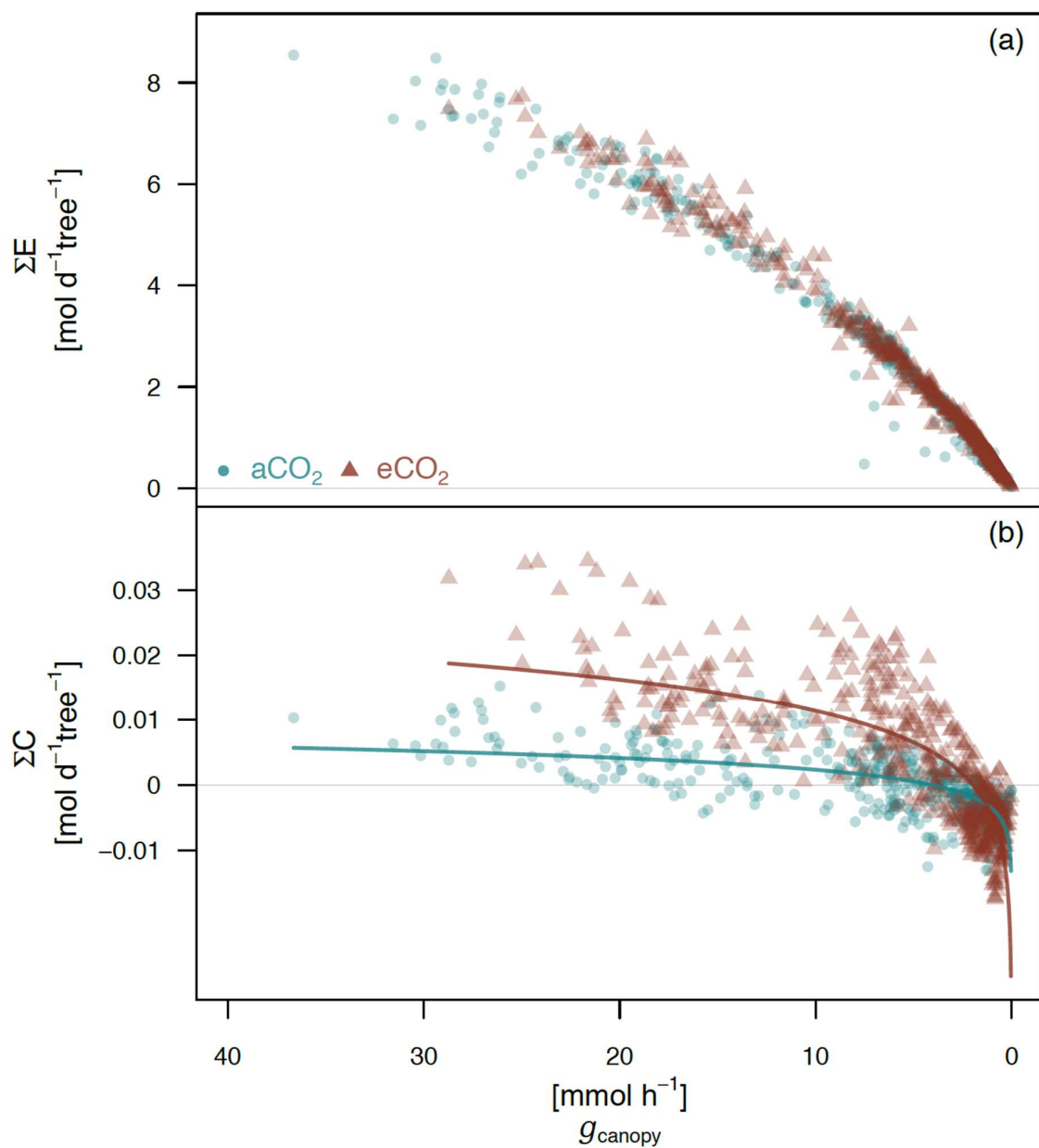
Supplemental Figure S2.3: Net canopy assimilation ($A_{\text{net, canopy}}$), expressed as % of maximum $A_{\text{net, canopy}}$ at photosynthetic active radiation (PAR) 1200 $\mu\text{mol m}^{-2}\text{s}^{-1}$, over a PAR range of 0 to 1200 $\mu\text{mol m}^{-2}\text{s}^{-1}$. Data is shown as treatment (ambient atmospheric [CO₂] (aCO₂): solid, turquoise points, elevated atmospheric [CO₂] (eCO₂): solid, dark red triangles) means \pm SD (shaded areas).



Supplemental Figure S2.4: Gas exchange parameters during a fast lethal drought experiment in 2017. Shown are net assimilation ($A_{\text{net, canopy}}$, a), transpiration (E , b), respiration (R_{total} , sum of shoot dark and root respiration, c) and relative soil water content (RWC, d) as hourly treatment (ambient atmospheric [CO₂] (aCO₂): turquoise points, elevated atmospheric [CO₂] (eCO₂): dark red triangles) means per day \pm SD depicted as shaded area.



Supplemental Figure S2.5: Gas exchange parameters during the slow lethal drought experiment in 2018. Shown are transpiration (E , a) and net assimilation (A_{net} , b) on the leaf level, as hourly treatment (ambient atmospheric [CO₂] ($a\text{CO}_2$): solid, turquoise points, elevated atmospheric [CO₂] ($e\text{CO}_2$): solid, dark red triangles) means per day \pm SD depicted as shaded area.



Supplemental Figure S2.6: ΣC (sum of net assimilation, shoot dark and root respiration, b) and ΣE (sum of shoot day and night transpiration, a) over the course of stomatal closure, expressed as canopy conductance (g_{canopy}).

Data is shown as daily values per tree (ambient atmospheric [CO₂] ($a\text{CO}_2$): solid, turquoise points, elevated atmospheric [CO₂] ($e\text{CO}_2$): solid, dark red triangles).

3 Anatomical adjustments of the tree hydraulic pathway decrease canopy conductance under long-term elevated CO₂

This chapter was published as:

Gattmann, M., McAdam, S. A. M., Birami, B., Link, R., Nadal-Sala, D., Schuldt, B., Yakir, D., and Ruehr, N. K. 2023. "Anatomical Adjustments of the Tree Hydraulic Pathway Decrease Canopy Conductance under Long-Term Elevated CO₂". *Plant Physiology* 191(1): 252-264.

Abstract

The cause of reduced leaf-level transpiration under elevated atmospheric CO₂ concentrations (eCO₂) remains largely elusive. Here, we assessed stomatal, hydraulic and morphological adjustments in a long-term experiment on Aleppo pine (*Pinus halepensis* Miller) seedlings germinated and grown for 22–40 months under eCO₂ (c. 860 ppm) or ambient atmospheric CO₂ concentrations (aCO₂; c. 410 ppm). We assessed if eCO₂-triggered reductions in canopy conductance (g_c) alter the response to soil or atmospheric drought and are reversible or lasting due to anatomical adjustments by exposing eCO₂ seedlings to decreasing [CO₂]. To quantify underlying mechanisms, we analyzed leaf abscisic acid (ABA) level, stomatal and leaf morphology, xylem structure, hydraulic efficiency, and xylem safety. Effects of eCO₂ manifested in a strong reduction in leaf-level g_c (-55 %) not caused by ABA and not reversible under low [CO₂] (c. 200 ppm). Stomatal development and size were unchanged, while stomatal density increased (+18 %). An increased vein-to-epidermis distance (+65 %) suggested a larger leaf resistance to water flow. This was supported by anatomical adjustments of branch xylem having smaller conduits (-8 %) and lower conduit lumen fraction (-11 %), which resulted in a lower specific conductivity (-19 %) and leaf-specific conductivity (-34 %). These adaptations to CO₂ did not change stomatal sensitivity to soil or atmospheric drought, consistent with similar xylem safety thresholds. In summary, we found reductions of g_c under elevated CO₂ to be reflected in anatomical adjustments and decreases in hydraulic conductivity. As these water savings were largely annulled by increases in leaf biomass, we do not expect alleviation of drought stress in a high CO₂ atmosphere.

3.1 Introduction

Decreases in transpiration and stomatal conductance are among the most widely documented effects of eCO₂ on plants (Ainsworth and Rogers 2007; Birami et al. 2020; Domec, Smith, and

McCulloh 2017; Drake, González-Meler, and Long 1997; Dusenge et al. 2019; Medlyn et al. 2001; Poorter et al. 2022). Given that drought spells and extreme weather events are increasing with climate change (Seneviratne et al. 2021), quantifying the extent to which increased CO₂ reduces plant water loss has been the objective of numerous studies over the past two decades. Results indicate that eCO₂ could potentially mitigate the negative effects of drought and heat in many plant species, although the extent varies depending on the type, severity, and duration of the stress (Brodribb et al. 2020; Huang and Xu 2015). Contrastingly, it has also been observed that leaf-level responses – most prominently water savings from reduced stomatal conductance under eCO₂ – could be counterbalanced at the plant level due to enhanced leaf growth at higher [CO₂] (Gatmann et al. 2021; Jin et al. 2018; Knauer et al. 2017; Tor-ngern et al. 2015). While the body of literature on plant responses to eCO₂ is growing, major knowledge gaps persist (De Kauwe, Medlyn, and Tissue 2021), particularly, in terms of understanding the mechanisms driving the [CO₂] effect on stomatal conductance (Poorter et al. 2022).

Addressing the processes that limit stomatal conductance under eCO₂ is of utmost importance in a rapidly changing climate (Ainsworth and Rogers 2007; Bonan 2008; Jasechko et al. 2013; Klein and Ramon 2019). In angiosperms, there is a well-described instantaneous stomatal response to changes in atmospheric CO₂ concentration (Morison 1985, 1987; Mott, Sibbernsen, and Shope 2008). Stomata in most angiosperm species will open when exposed to [CO₂] lower than ambient, and close when exposed to [CO₂] higher than ambient. The mechanism driving these responses remains relatively elusive, although recent molecular work in *Arabidopsis* (*Arabidopsis thaliana*) suggests that a network of core and peripheral guard cell signaling pathways drive stomatal responses to eCO₂ (Dubeaux et al. 2021). Nothing is known about the molecular signaling pathway for stomatal responses to [CO₂] outside of angiosperms and there appears to be a considerable evolutionary transition in stomatal responsiveness to [CO₂] across the land plant phylogeny, with angiosperm species generally having a much greater stomatal sensitivity to instantaneous changes in [CO₂] in comparison to other stomata-bearing land plants (Brodribb and Cochard 2009; Brodribb and McAdam 2013; Doi and Shimazaki 2008; Franks and Britton-Harper 2016; Haworth, Elliott-Kingston, and McElwain 2013; Kubásek et al. 2021). In angiosperms, the magnitude and speed of stomatal responses to an instantaneous change in [CO₂] are regulated by ABA levels, with enhanced responses occurring in leaves with high ABA levels (Chater et al. 2015; Dubbe, Farquhar, and Raschke 1978; McAdam et al. 2011; Raschke 1975). This augmentation of stomatal sensitivity to instantaneous changes in [CO₂] does not occur in conifers (McAdam et al. 2011), but it has never been examined whether ABA might play a role in regulating stomatal sensitivity to long-term increases in [CO₂] in conifers.

The regulation of stomatal aperture and water loss is not restricted to physiological responses but could be altered by leaf anatomical adjustments after long-term exposure to high CO₂. As widely observed, growth under eCO₂ may result in reduced development of stomatal complexes in the epidermis, reducing both stomatal density (SD; number of stomata per unit leaf area) and stomatal index (SI; the proportion of epidermal cells that are stomata) (Woodward and Kelly 1995). This anatomical adjustment reduces overall stomatal conductance and increases water-use efficiency (WUE) without a change in stomatal aperture. To date, results are far from conclusive, and often no effect, and in some cases, even an increase in SD in response to eCO₂ has been observed (Domec et al. 2017; Luomala et al. 2005; Pritchard et al. 1999). Hence, the magnitude of the SD response seems to be affected by the experimental setup and duration, species, and other environmental factors (Haworth et

al. 2013; Xu et al. 2016). Contributing to lower SD under eCO₂ could be a promotion of leaf size, as observed in grasses (Xu et al. 2014; Xu and Zhou 2008), or an increase in needle thickness or width as observed in Scots pine (*Pinus sylvestris*) (Lin, Jach, and Ceulemans 2001). These changes are often related to alterations in cell division and/or cell expansion driven mainly by increased carbon availability combined with a reduction in water demand (Pritchard et al. 1999; Xu et al. 2016).

In agreement, a growing number of studies suggest that anatomical adjustments from long-term exposure to eCO₂ are not restricted to stomata but may affect leaf hydraulic conductance (Domec et al. 2009; Phillips et al. 2010). Increases in needle thickness and/or mesophyll tissue (Lin et al. 2001), which affect the path length water has to travel from the vein to the stomata, have been attributed to lower leaf hydraulic conductivity (K_{leaf}) (Domec et al. 2016), and could be related to lower stomatal conductance as well as an enhanced WUE (Trueba et al. 2022). Moreover, a few studies have observed adjustments in xylem structure in response to eCO₂ (Domec et al. 2017). In conifers, structural changes were mixed and seem to vary among species, showing no responses (Maherali and DeLucia 2000), increases in cell wall thickness (Atwell, Henery, and Whitehead 2003; Conroy et al. 1990; Domec et al. 2016; Kilpelainen et al. 2007), wood density (Atwell et al. 2003; Telewski et al. 1999), or tracheid diameter (Ceulemans et al. 2002). A recent literature review summarizes the impacts of some of these findings on tree hydraulics but no clear picture for conifers emerged. It appears that specific conductivity (K_s), i.e. hydraulic conductivity normalized by xylem cross-sectional area, might slightly increase while plant hydraulic conductance and leaf water potential remain largely unchanged under eCO₂ (Domec et al. 2017). As the tree water transport system from roots to leaves is tightly coordinated (Bartlett et al. 2016; Meinzer and Grantz 1990; Santiago et al. 2004), stomatal conductance could be indirectly affected by anatomical adjustments of xylem porosity, leaf thickness or vein-to-stomata distance. The linking element here is the water status at the site of stomatal evaporation, which is influenced in part by the hydraulic conductivity of branches and leaves, and by stomatal aperture (Bartlett et al. 2016). Furthermore, changes in whole-plant water transport capacities become likely if growth under eCO₂ alters xylem anatomy. These might ultimately affect the vulnerability of trees to hydraulic failure (Domec et al. 2010).

Trees growing in seasonal dry environments could be particularly affected by CO₂-induced changes that affect water demand and transport. In two previous studies, we have investigated the effect of eCO₂ to heat, hot-drought and lethal drought in Aleppo pine (*Pinus halepensis*) seedlings (Birami et al. 2020; Gattmann et al. 2021) grown from seeds either under ambient atmospheric [CO₂] (aCO₂ c. 410 ppm) or highly eCO₂ (c. 870 ppm) for 18 to 22 months. Seeds originated from the Yatir forest, an Aleppo pine dominated forest plantation at the northern edge of the Negev desert in Israel (Grünzweig et al. 2003). The experimental CO₂ concentrations were within the range of the RCP8.5 scenarios (794 – 1,142 ppm for 2,100) and hence close to CO₂ saturation for photosynthesis, providing a strong CO₂ response. Results of these two previous studies showed that eCO₂ enhanced whole-tree C uptake (c. +100 %), WUE, and overall tree biomass (+35 %). Pronounced reductions in leaf-level g_c largely counterbalanced the increase in leaf area resulting in comparatively small water savings at the tree level (c. -10 % at 25 °C). Exposing the seedlings to heat or hot drought spells revealed little effect of eCO₂ on the stress response, albeit maintaining a higher WUE until respiration rates exceed photosynthesis (Birami et al. 2020). Further, eCO₂ did not improve the overall tree vulnerability to a lethal soil drought and the decline in leaf water potential, as well as thresholds for stomatal closure and turgor loss point, appeared unaffected

(Gattmann et al. 2021). This raises the question of the underlying mechanisms that reduced g_c under eCO₂ and why the physiological drought response remained largely unaltered.

Here, we take advantage of this long-term eCO₂ experiment and assessed the coordination between anatomical and physiological adjustments of Aleppo pine seedlings from the same population grown for 22–40 months under eCO₂ averaging c. 860 ppm over the entire period. We studied leaf-level g_c responses to [CO₂] and increasing soil or atmospheric drought and assessed if those are coordinated by morphological changes in the hydraulic system (Figure 3.1). We addressed the following hypotheses: (i) stomatal closure under eCO₂ is reversible upon exposure to low CO₂ if a direct stomatal response, possibly mediated by the phytohormone ABA; (ii) stomatal closure under eCO₂ is not reversible as hydraulic conductance is modified by anatomical adjustments of leaves and wood, specifically reductions in xylem tracheid diameter and stomatal density; and (iii) stomatal responses to drought and increasing vapor pressure deficit are unaffected by eCO₂ and hence hydraulic vulnerability is unchanged.

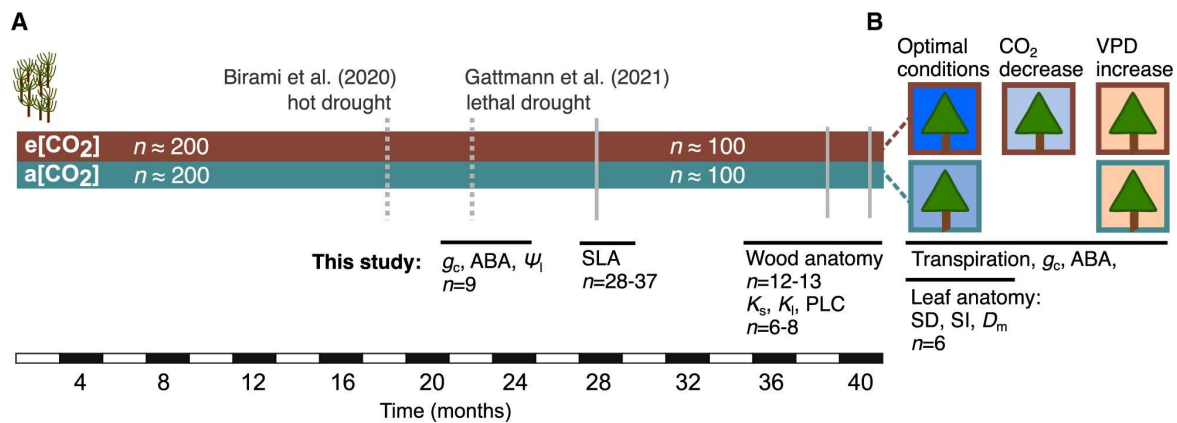


Figure 3.1: Timeline of cultivation of *P. halepensis* seedlings under ambient (a[CO₂], c. 400 ppm) or elevated (e[CO₂], c. 860 ppm) atmospheric [CO₂].

(A) The number of seedlings cultivated after germination, the conducted experiments and references, as well as measurements related to this study are shown. (B) After 40 months cultivation, randomly selected seedlings ($n = 6$ per treatment) were placed into automated gas exchange chambers enclosing the canopy of one seedling each and transpiration and canopy conductance (g_c) were measured during optimal conditions, decreasing CO₂ (in e[CO₂] seedlings only) and increasing vapor pressure deficit (VPD) over several days alongside which leaf samples were taken to analyze for abscisic acid (ABA) content (B). This chamber system was also used to measure responses in the same population of seedlings during a dry-down experiment on 22-month-old seedlings when also leaf water potential (Ψ_i) was measured as published in Gattmann et al. (2021). Changes in leaf morphology were assessed via analyses of specific leaf area (SLA), stomatal density (SD), stomatal index (SI) and vein-to-epidermis distance (D_m). Measurements of wood anatomy included conduit diameter, lumen fraction, and potential hydraulic conductivity. Changes in xylem hydraulic properties were assessed via measurements of specific conductivity (K_s), leaf-specific conductivity (K_l) and percent loss of hydraulic conductivity (PLC).

3.2 Materials and Methods

3.2.1 Plant Material

Aleppo pine (*Pinus halepensis* (Miller)) seedlings were cultivated from seed either under aCO₂ (on average 410±23 ppm) or eCO₂ (on average 860±15 ppm) for 40 months in a greenhouse facility in Garmisch-Partenkirchen, Germany (732 m a.s.l., 47°28'49.2"N, 35°3'7.2"E). Other

environmental drivers such as air temperature (daytime c. 22 ± 2.5 °C, nighttime 15 ± 2 °C), relative humidity (75 ± 15 %), photosynthetically active radiation (PAR; 480 ± 180 $\mu\text{mol m}^{-2}\text{s}^{-1}$), and water availability (watered daily to full saturation) were maintained at similar levels in both CO₂ treatments, and the mean difference between daily mean air temperature was typically <1 °C. Winter periods (months December to February) were mimicked in the greenhouse by reducing daily air temperature to 12 °C on average. The placement of the seedlings was repeatedly changed between and within the greenhouse compartments. During the initial 24 months of cultivation, the seedlings were placed in pots and repotted twice (last into 4.5-L pots). The potting substrate, a mixture of quartz sand, vermiculite, and expanded clay, was repeatedly enriched with slow-release fertilizer (Osmocote® Exact Standard 5-6M 15-9-12+2MgO+TE; ICL Specialty Fertilizers) and supplemented by liquid fertilizer during the growing period. Initially about 200 seedlings were grown under aCO₂ or eCO₂ to ensure a large enough population from which to randomly select seedlings for stress experiments involving destructive sampling. More details on seedling cultivation and experiments can be found in the two previously published studies, which used seedlings from the same population (Birami et al. 2020; Gattmann et al. 2021).

3.2.2 Experimental setup and growth conditions

We assessed stomatal responses in eCO₂- and aCO₂-grown seedlings to drought, VPD, and decreasing [CO₂] using custom-made gas exchange chambers (Birami et al. 2020; Gattmann et al. 2021; Rehschuh et al. 2022) consisting of a tightly sealed shoot compartment separated from the root compartment. In brief, each of the shoot compartments was made of a light-transmitting cylinder and was individually temperature-controlled and equipped with temperature sensors (5SC-TTII-36-2 M, Newport Electronics GmbH, Deckenpfronn, Germany). The drought experiment was conducted in early 2018 when the seedlings ($n = 9$ per treatment) were approximately 22-month-old (see Figure 3.1) as described in detail by Gattmann et al. (2021). The VPD and decreasing [CO₂] experiments (Figure 3.1) were conducted later on 40-month-old seedlings in September 2019. Prior to experiments, we randomly selected six seedlings per treatment (each about 50 cm tall). We conducted the experiments in a sequence starting with the eCO₂ seedlings followed by aCO₂ seedlings. Each seedling was placed into one of the six individual gas exchange chambers with the shoot compartment tightly sealed from the belowground part of the plant. Ambient sunlight was supplemented by plant growth lamps (T-agro 400 W; Philips, Hamburg, Germany), ensuring a relatively constant average photosynthetically active radiation (PAR; PQS 1, Kipp & Zonen, Delft, the Netherlands) of 450 ± 50 $\mu\text{mol m}^{-2}\text{s}^{-1}$ over each 16-h day measurement period (Supplemental Figure S3.1c, d). All seedlings were automatically drip irrigated daily to field capacity.

3.2.3 Gas exchange measurements

To test for reversibility in the restriction on g_c in eCO₂ plants, [CO₂] was reduced as follows. After the shoot of each seedling was placed into an individual gas exchange chamber, eCO₂ was maintained for three days at 854 ± 29 ppm, then [CO₂] was reduced close to ambient concentrations (382 ± 19 ppm) and then to 199 ± 9 ppm, maintaining each [CO₂] change for two days. All other chamber conditions were kept constant with the day-time VPD at 1.34 ± 0.22 kPa and day-time air temperature at 24.2 ± 0.49 °C (min/max: 21.9/25.9 °C). Nighttime temperature was maintained at 19.70 ± 0.58 °C. Temperature variations between chambers were small (<2 °C).

We evaluated the responses of g_c in eCO₂ seedlings to changes in VPD during three days under eCO₂ (841±23 ppm). VPD was allowed to vary diurnally from 0.9 kPa to 2.1 kPa while air-temperature was maintained almost constant (min/max: 23.0/24.7 °C). Following the removal of the eCO₂ seedlings from the chambers, the aCO₂ seedlings were installed, and g_c responses to VPD were assessed over three consecutive days at aCO₂ (432±17 ppm) with VPD ranging from 0.8 to 2.0 kPa, while air-temperature was maintained relatively constant (min/max: 22.0/25.8 °C).

Canopy H₂O gas exchange ($n = 6$ per treatment) was derived by directly measuring absolute [CO₂] and [H₂O] of the 10 L min⁻¹ supply air stream (LI-840, Li-cor, Lincoln, NE) and the concentration differences between supply and sample air stream (Li-7000, Li-cor, Lincoln, NE). Data were recorded every 10 s while the system automatically switched between chambers every 120 s so that each chamber was measured at least half-hourly. The last 40 s of each measurement was used to calculate net photosynthesis, transpiration, and g_c . Two empty chambers were additionally integrated into the measurement cycle to continuously monitor the system and correct the data for any fluctuations in [H₂O] that were not due to plant activity and these were typically small (0.03±0.20 ppt H₂O).

To quantify g_c to water vapor we derived leaf-level transpiration rate (E) in [mol m⁻²s⁻¹] as follows:

$$E = \frac{F_m(W_{\text{supply}} - W_{\text{sample}})}{A_{\text{leaf}}(1 - W_{\text{sample}})} \quad (1)$$

where W_{supply} [mol mol⁻¹] is [H₂O] in supply air stream, W_{sample} [mol mol⁻¹] is [H₂O] in sample air stream, F_m [mol s⁻¹] is molar flow and A_{leaf} [m²] is the two-dimensional leaf surface area of the shoot.

g_c [mol H₂O m⁻²s⁻¹] was then calculated from leaf-level transpiration and water vapor concentration using the following equation:

$$g_c = \frac{E \left(1 - \frac{W_{\text{leaf}} + W_{\text{sample}}}{2} \right)}{W_{\text{leaf}} - W_{\text{sample}}} \quad (2)$$

where W_{leaf} is leaf saturated vapor pressure, derived from saturation vapor pressure (kPa) at a given air temperature (°C) and atmospheric pressure. Boundary layer conductance was neglected due to high mixing conditions generated from fans and high flow rates inside the chambers (Birami et al. 2020).

To determine leaf area at the end of the gas exchange measurements, all leaves were harvested, dried at 60 °C for 48 h and weighed. Leaf biomass was then multiplied by specific leaf area, previously determined from a subsample of needles.

3.2.4 Tissue sampling for anatomy and hormone analysis

Leaves for ABA quantification and epidermal anatomy were sampled randomly from each of the seedlings in the gas exchange chambers ($n = 6$ per treatment). The sampling was conducted between 12 p.m. and 2 p.m., and leaf samples (4–6 fascicles each) were weighed and placed either in 80 % methanol in water (v/v) (for ABA analysis) or ethanol (for anatomical

analysis). In addition, leaves were sampled for ABA analysis during the course of a previously conducted drought experiment (Gattmann et al. 2021). These leaf samples ($n = 18$ per treatment), initially snap frozen in liquid nitrogen and stored at -80°C , were then transferred to 80 % methanol in water (v/v) while still frozen for ABA analysis. During this previous drought experiment, midday leaf water potential (Ψ_{leaf}) was intensively measured during the dry-down.

3.2.5 Quantification of foliage ABA levels

Foliage ABA levels were quantified by physicochemical methods with an added internal standard. Samples were homogenized and 15 ng of [$^2\text{H}_6$]ABA was added to each sample as an internal standard. Endogenous ABA was extracted from homogenized tissue overnight at 4°C . An aliquot was taken and dried under vacuum until completeness. Samples were resuspended in 200 μl of 2 % acetic acid in water (v/v), and hormone levels were quantified using liquid chromatography-mass spectrometry (Agilent 6400 series triple quadrupole LC/MS, USA) (McAdam and Brodribb 2015).

3.2.6 Epidermal and leaf cross-sectional anatomy

To assess changes in stomatal development, cuticle morphology of the sampled leaves was studied. Briefly, leaf cuticles of the central 1 cm of a needle were prepared by making a longitudinal section through one corner of the leaf and then macerating the sample in aqueous chromium trioxide. Cuticles were mounted in glycerine jelly and imaged under 10x magnification for epidermal and stomatal cell density determination with care taken to avoid leaf margins, and 40x magnification for stomatal size measurements (AxiolmagerA2, Zeiss, Germany). Stomatal size was determined as the length of the stomatal complex. The mean stomatal and epidermal cell density of the whole leaf was quantified as the number of cells per square millimeter from five images per cuticle. Stomatal index (SI), i.e., the ratio of stomatal density (SD) to epidermal cell density (ED) was calculated for each image as follows:

$$\text{SI (\%)} = 100 \cdot \frac{\text{SD}}{\text{SD} + \text{ED}} \quad (3)$$

Leaf width (LW) was measured on the same leaves using high precision calipers (± 0.01 mm). These leaves were also cross-sectioned to measure the shortest distance between the vein-to-the-stomata-bearing epidermis using a freezing stage microtome, stained with dilute aqueous toluidine blue, and mounted in glycerine jelly for imaging as above.

3.2.7 Hydraulic conductivity, xylem vulnerability curves, and wood anatomy

Branches for hydraulic analysis were taken in August and October 2019 from seedlings of the same population but were not part of the gas exchange measurements. These branch samples were immediately wrapped in foil and kept moist until analysis was conducted 2-3 days later. Maximal hydraulic conductivity (K_h , $\text{kg m MPa}^{-1}\text{s}^{-1}$) was measured in six stem segments (mean diameter \pm SE: 7.33 ± 0.18 mm) per treatment after vacuum infiltration for 24 h at 30 mbar in the degassed solution of 10-mM KCl and 1-mM CaCl_2 in demineralized water filtered to a particle size of 0.2 μm . Then segments were recut underwater to a length of 73.91 ± 1.31 mm (mean \pm SE) with a sharp razor blade, connected to a Xyl'em Plus device (Bronkhorst France, Montigny les Cormeilles, France), and K_h was measured in the measurement solution described above. K_h was recorded at a pressure head of 4 kPa with the XylWin 3.0 software (Bronkhorst France, Montigny les Cormeilles, France). Subsequently, we estimated specific

conductivity (K_s , kg m⁻¹MPa⁻¹s⁻¹) from K_h divided by the cross-sectional area, and leaf-specific conductivity (K_l , kg m⁻¹MPa⁻¹s⁻¹) from K_h divided by the leaf area supported by the corresponding branch. The needle area of each branch was estimated from needle dry weight and treatment-averaged specific leaf area.

Xylem vulnerability curves were constructed for stem segments (aCO₂: $n = 5$; eCO₂: $n = 6$) with the flow-centrifuge technique (Cavitrone; Cochard et al. 2005). Stem segments (mean basipetal diameter \pm SE: 7.25 \pm 0.33 mm) were shorted to 27.5 cm under water and inserted in a custom-made rotor attached to an ultra-centrifuge (Sorvall RC-5C, Thermo Fisher Scientific, Waltham, MA, USA). Conductivity measurements started at -0.84 MPa and were repeated under increasingly negative water potentials until percentage loss of hydraulic conductivity (PLC, %) reached at least 90 %. We fitted Weibull functions to describe the relationship between PLC and xylem pressure (Nadal-Sala et al. 2021).

From all segments used for xylem hydraulic measurements (aCO₂: $n = 12$; eCO₂: $n = 13$), semi-thin transverse sections were cut with a sliding microtome (G.S.L.1, Schenkung Dapples, Zurich, Switzerland), stained with safranin, and the complete cross-section digitalized at 100x magnification using a light microscope (Observer Z1, Carl Zeiss MicroImaging GmbH, Jena, Germany) equipped with an automated stage. Per segment, 51,242 \pm 5,978 conduits (mean \pm SE) were analyzed on average. Image processing was performed with the open-source software Gimp (<https://www.gimp.org>) and ImageJ (Schneider, Rasband, and Eliceiri 2012) using the particle analysis function. Measured parameters included the conduit lumen-to-sapwood area ratio (A_{lumen} , %), conduit density (CD, n mm⁻²), and conduit diameter (D , μ m) from major (a) and minor (b) conduit radii according to $D = ((32 \times (a \times b)^3)/(a^2 + b^2))^{1/4}$, the hydraulically-weighted diameter (D_h , μ m) as $D_h = \Sigma D^5 / \Sigma D^4$ (Sperry and Saliendra 1994) and potential hydraulic conductivity (K_p , kg m⁻¹MPa⁻¹s⁻¹) was calculated with the Hagen-Poiseuille equation as $K_p = (\pi \times \rho \times \Sigma D^4) / (128 \eta \times A_{\text{xylem}})$, where η is the viscosity (1.002 10⁻⁹ MPa s) and ρ the density of water (998.2 kg m⁻³), both at 20 °C, and A_{xylem} (m²) the sapwood area.

3.2.8 Statistical analyses

Statistical analyses were conducted using R 4.04 (R Core Team 2021). Differences in hydraulic parameters (K_s , K_l , $A_l:A_s$), needle and stomatal morphology were tested using non-parametric Mann-Whitney U tests. Wood anatomy parameters were assessed via generalized least squares models (GLS; package nlme; Pinheiro et al. 2007). As wood anatomical traits closely covaried with branch thickness, their centered, natural log-transformed cross-sectional area was included as a covariate. Further, the residual variance was allowed to differ between treatments to account for inhomogeneous variances. We tested differences in the response of g_c to step-wise changes in CO₂ concentrations (c. 900, 400, or 200 ppm) using linear mixed effect models (package lme4; Bates et al. 2015) with tree as random factor. The most parsimonious model was selected based on the Akaike information criterion.

We applied Bayesian statistics to address treatment differences of non-linear relationships (BayesianTools package; Hartig et al. 2019). This included hydraulic vulnerability curves, responses of g_c with VPD and Ψ_{leaf} and of ABA with Ψ_{leaf} (for model details see Supplemental Methods S1). We started with broad uniform but biologically meaningful priors (Supplemental Table S3.1) assuming a Gaussian likelihood and used a Differential-Evolution Markov Monte-Carlo Chain with memory and a snooker update following the approach by Ter Braak and Vrugt (2008). The posterior was obtained for each calibration (30,000 iterations) with a burn-in of

10,000 samples. We assessed between-chain convergence via Gelman-Rubin diagnostic at $\hat{R} \leq 1.1$ (Gelman and Rubin 1992). In the case where we derived individual posteriors per tree seedling, these were later merged into a combined posterior distribution per treatment. Posterior predictive uncertainty was addressed by sampling 5,000 times the combined posterior. For each parameter, we report the median and 95 % credible intervals (CI). We considered differences between treatments to be meaningful if the CI between treatments did not overlap (see Supplemental Table S3.2 for model coefficients).

3.3 Results

3.3.1 Long-term acclimation to eCO₂ affects gas exchange

Highly eCO₂ strongly reduced leaf-level gas exchange rates in Aleppo pine seedlings compared to seedlings under aCO₂ (Supplemental Figure S3.1). These reductions were noticeable both during day-time and nighttime and g_{c-ref} (g_c at a VPD of 1 kPa) was 55 % lower in eCO₂ compared to aCO₂ seedlings (Table 3.1). But the dynamics of the diurnal cycle were not altered by the CO₂ treatment, suggesting that on a relative scale, E and g_c were affected similarly by short-term changes. This assumption was reinforced by the lack of a treatment effect in the slope of g_c responding to increasing VPD (Figure 3.2). In addition, reducing atmospheric [CO₂] from c. 900 to 400 and 200 ppm did not result in higher g_c in eCO₂ seedlings (Figure 3.3).

Table 3.1: Treatment responses of leaf morphology, stomatal characteristics, reference stomatal conductance at VPD = 1 kPa (g_{c-ref}), and hydraulic vulnerability parameters for Aleppo pine seedlings grown for 40 months under ambient (aCO₂) or elevated (eCO₂) atmospheric CO₂ concentration. Stomata length (SL), stomata density (SD), number of epidermal pavement cell density (ED), stomatal index (SI), vein-to-epidermis distance (D_m) and leaf width (LW), abscisic acid (ABA), needle leaf area (LA) and specific leaf area (SLA) are mean±SD ($n = 6$ per treatment if not noted otherwise). Statistical significance was tested with nonparametric Mann-Whitney U tests ($p < 0.05$). For g_{c-ref} , Ψ_{leaf} at stomatal closure ($\Psi_{gc-close}$) and the hydraulic vulnerability parameters (P_{12} , P_{50} , P_{88}), the treatment median with the 95 % credible intervals of the Bayesian model fit is given. Parameters with significant differences between treatments are highlighted in bold and indicated by different letters. ^aaCO₂: $n = 28$, ^eeCO₂: $n = 37$ measured in 28-month-old seedlings

parameter	unit	aCO ₂	eCO ₂
SL	[μm]	51.87±5.89 (a)	55.70±8.53 (a)
SD	[n mm ⁻²]	28.92±3.81 (a)	35.46±4.75 (b)
ED	[n mm ⁻²]	133.20±15.20 (a)	166.67±20.13 (b)
SI	[%]	17.87±1.71 (a)	17.51±1.29 (a)
D_m	[μm]	150.97±9.65 (a)	252.82±6.67 (b)
LW	[mm]	0.85±0.05 (a)	1.19±0.05 (b)
ABA	[ng g ⁻¹ FW]	305±93 (a)	169±149 (a)
LA	[cm ²]	0.74±0.21 ^a (a)	0.87±0.22 ^e (b)
SLA	[cm ² g ⁻¹]	55.48±6.01 ^a (a)	51.04±8.84 ^e (b)
g_{c-ref}	[mol m ⁻² s ⁻¹]	0.2 [0.17-0.41] (a)	0.09 [0.07-0.11] (b)
$\Psi_{gc-close}$	[-MPa]	2.1 [2.20-2.00] (a)	2.15 [2.25-2.00] (a)
P_{12}	[-MPa]	3.92 [4.24-2.92] (a)	3.33 [4.13-2.35] (a)
P_{50}	[-MPa]	5.17 [5.88-4.66] (a)	4.91 [5.96-4.19] (a)
P_{88}	[-MPa]	6.11 [7.79-5.97] (a)	6.66 [7.79-5.37] (a)

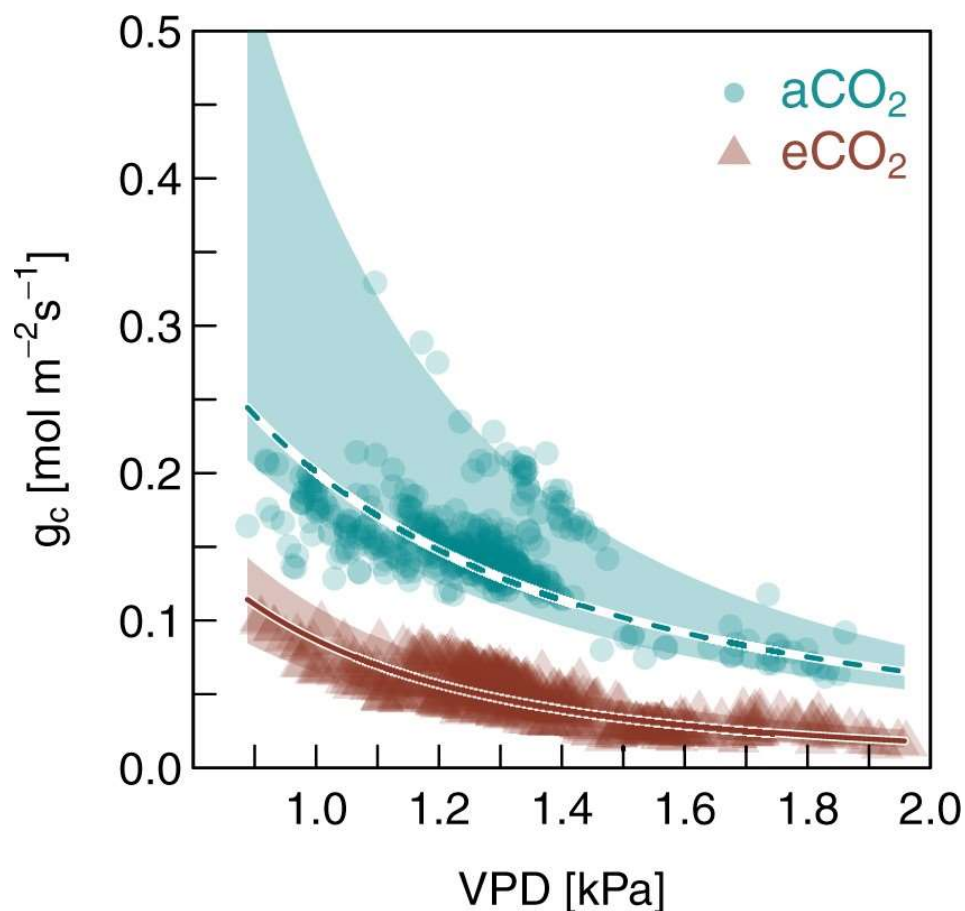


Figure 3.2: Treatment-specific relationships of canopy conductance (g_c) with vapor pressure deficit (VPD) for 40-month-old *P. halepensis* seedlings grown under ambient (aCO₂) or elevated (eCO₂) atmospheric CO₂ concentration.

Shown are single measurements for six trees per treatment (aCO₂: turquoise points; eCO₂: dark red triangles) over the course of three days for PAR >200 $\mu\text{mol m}^{-2}\text{s}^{-1}$. The trend line gives the median value of the model fit and the shaded areas represent the 95 % credible intervals per treatment (see Supplemental Table S3.2 for model coefficients).

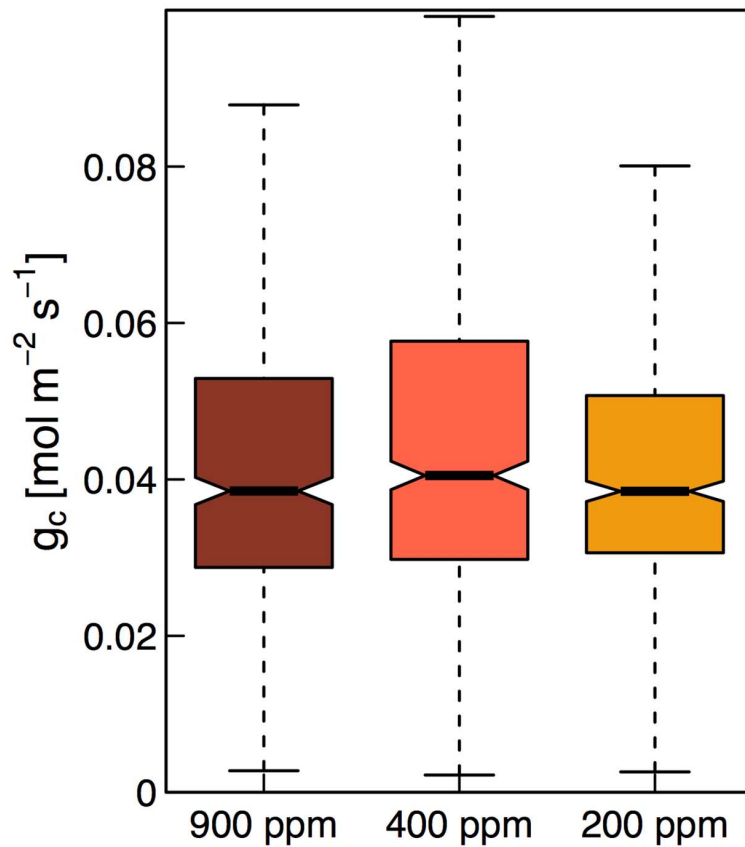


Figure 3.3: Canopy conductance (g_c) measured at three different CO₂ concentrations of Aleppo pine seedlings grown for 40 months under elevated atmospheric CO₂ concentration (c. 870 ppm). In order to test whether reduced [CO₂] can trigger stomatal opening, the CO₂ seedlings ($n = 6$) were steadily exposed to decreasing atmospheric [CO₂] from c. 900, to 400 and 200 ppm and each CO₂-level was kept for two days. Shown are boxplots of the automated gas exchange measurements for six seedlings at photosynthetic active radiation (PAR) >200 $\mu\text{mol m}^{-2}\text{s}^{-1}$. The box represents the interquartile range (IQR) of the data, the horizontal line at the notch is the median and the whiskers are 1.5 times the IQR. The number of measurements included were $n = 481$, $n = 584$, and $n = 592$ at c. 900, 400, and 200 ppm, respectively. Differences between CO₂ levels tested with linear mixed effect models were not significant ($p > 0.05$).

3.3.2 Stomata control and characteristics under eCO₂

eCO₂-induced reductions in g_c were not driven by higher leaf ABA levels (Table 3.1). Moreover, the lack of a CO₂ effect on ABA levels was further confirmed as ABA levels increased with decreasing Ψ_{leaf} in both eCO₂ and aCO₂ seedlings at the same rate (Figure 3.4A). In addition, stomatal aperture was tightly regulated by leaf water status, independent of the CO₂ treatment, as shown by the similar steep decline of relative g_c with Ψ_{leaf} in both treatments (Figure 3.4B, see also Supplemental Figure S3.3 for Ψ_{leaf} during dry-down). The decline in g_c with decreasing Ψ_{leaf} and the water potential at stomatal closure was comparable in both treatments (c. -2.1 MPa; Figure 3.4B, C; and Table 3.1).

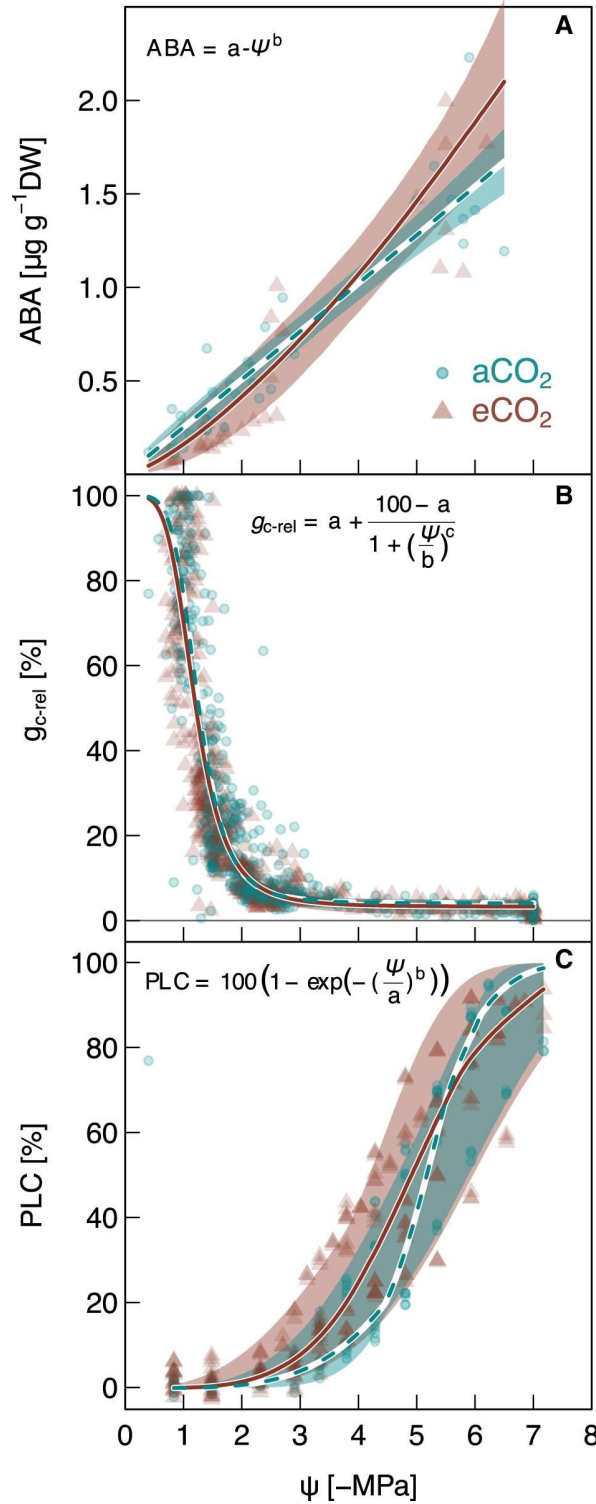


Figure 3.4: Hydraulic responses to increasing drought in Aleppo pine seedlings grown under ambient ($a\text{CO}_2$) or elevated ($e\text{CO}_2$) atmospheric CO_2 concentration.

Treatment-specific relationships of (A) leaf-level abscisic acid (ABA) concentration given per dry weight (DW) needle tissue and (B) relative canopy conductance ($g_{c\text{-rel}}$) with leaf water potential (Ψ) during a dry-down experiment are shown for the 22-month-old seedlings ($n = 6$ per treatment), and (C) percent loss of hydraulic conductivity (PLC) in branches versus xylem water potential (Ψ) is given for 40-months-old seedlings ($a\text{CO}_2$: $n = 6$, $e\text{CO}_2$: $n = 8$). Data points of individual measurements ($a\text{CO}_2$: solid, turquoise points, $e\text{CO}_2$: solid, dark red triangles) are shown. The median of each model is indicated by solid ($e\text{CO}_2$) or dashed ($a\text{CO}_2$) lines and the shaded areas represent the 95 % credible intervals per treatment (see Supplemental Table S3.2 for model coefficients). For values of P_{12} , P_{50} and P_{88} , see Table 3.1.

To assess possible morphological adjustments in response to eCO₂ that could account for the reduced g_c in eCO₂ plants, we analyzed leaf and stomata morphology (Table 3.1). We found that growth under eCO₂ resulted in a significant increase in SD and ED (Table 3.1). As these increases in SD (+23 %) and ED (+25 %) were similar, there was no significant change in SI induced by eCO₂. We also analyzed needle width and vein-to-epidermis distance and found both to be significantly larger in leaves adapted to eCO₂ (Table 3.1). These increases in needle width corresponded to increases in individual leaf area (Table 3.1).

3.3.3 [CO₂] effect on wood anatomy and hydraulic parameters

eCO₂ altered the woody anatomy of branches. As cross-sectional area had a substantial influence on all wood anatomical parameters and the samples from the different treatments differed systematically in average diameter, it was included as a covariate in the evaluation of the CO₂ effects (Figure 3.5). Comparing hydraulic parameters between CO₂ treatments including cross-sectional area revealed significant reductions in conduit lumen fraction (A_{lumen} , -11 %; Figure 3.5A), average conduit diameter (D , -8 %; Figure 3.5B), and potential conductivity (K_p , -17 %; Figure 3.5C) of eCO₂ seedlings (GLS, $p < 0.05$). Conduit density (CD; Figure 3.5E) tended to be on average about 5 % ($p = 0.057$) higher in eCO₂ than aCO₂, while the hydraulically-weighted conduit diameter (D_h , Figure 3.5D) was not affected by growth CO₂.

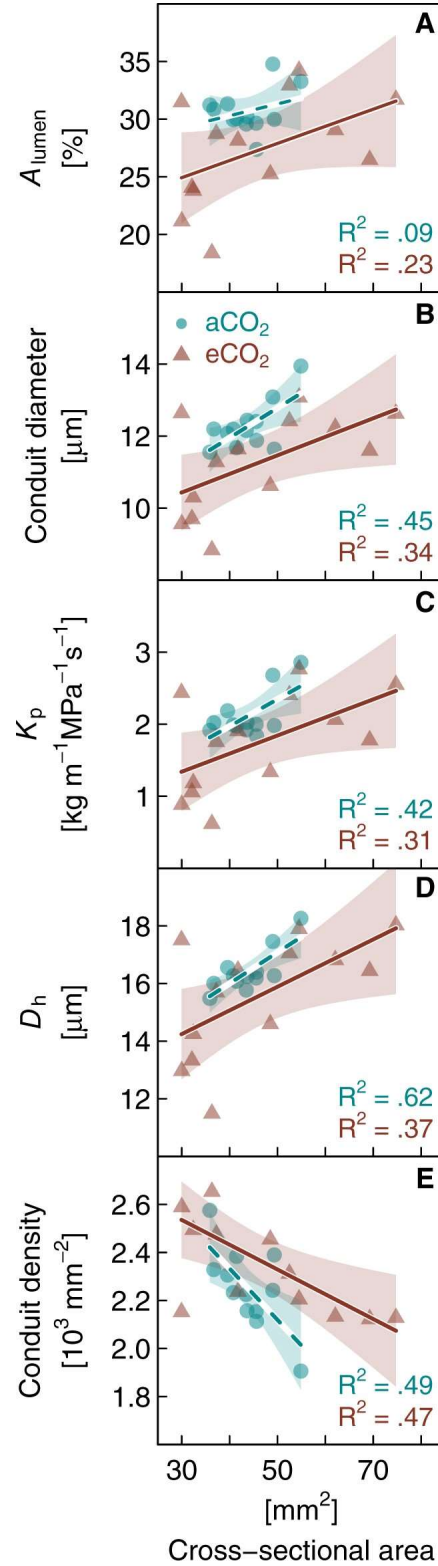


Figure 3.5: Wood anatomy parameters in relation to branch cross-sectional area in Aleppo pine seedlings grown for 40 months under ambient (aCO₂) or elevated (eCO₂) atmospheric CO₂ concentration. (A) Lumen fraction (A_{lumen}), (B) average conduit diameter, (C) potential conductivity (K_p), (D) hydraulically weighted conduit diameter (D_h) and (E) conduit density are given. Data are measurements of individual branch samples ($n = 12-13$ per treatment). Linear regressions (aCO₂: dashed lines, eCO₂: solid lines) and the 95 % confidence intervals of the fit are given (shaded areas). Note that differences between treatments were significant for A_{lumen} , conduit diameter and K_p (generalized least squares test, $p < 0.05$). aCO₂ is shown in turquoise, solid points, eCO₂ in dark red, solid triangles.

The distinct signal of morphological changes under eCO₂ was also captured in specific (K_s) and leaf-specific (K_l) conductivity. Both were significantly reduced in eCO₂ plants (K_s : -19 %; K_l : -34 %; Mann-Whitney U test, $p < 0.05$; Figure 3.6A–B). The leaf-to-sapwood area ratio ($A_l:A_s$, Figure 3.6C) tended to be larger (+24 %, $p = 0.090$) in eCO₂ compared to aCO₂ seedlings.

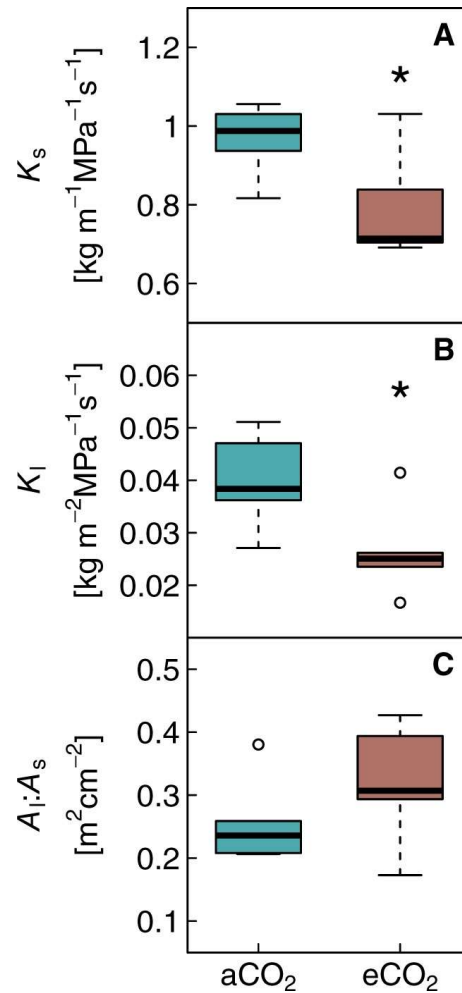


Figure 3.6: Responses of hydraulic conductivity and leaf-to-sapwood area in 40-month-old Aleppo pine seedlings grown under ambient (aCO₂) or elevated (eCO₂) atmospheric CO₂ concentration.

(A) Specific conductivity (K_s), (B) leaf specific conductivity (K_l), and (C) leaf-to-sapwood area ratio ($A_l:A_s$) are shown as boxplots per treatment ($n = 6$). The box represents the interquartile range (IQR) of the data, the horizontal line inside the box is the median, the whiskers cover 1.5 times the IQR. Data points are outliers beyond the extremes of the whiskers. Significant treatment differences are indicated by asterisks (Mann-Whitney U test $p < 0.05$). aCO₂ is shown in turquoise, eCO₂ in dark red.

3.4 Discussion

3.4.1 Stomatal responses to eCO₂

Aleppo pine seedlings grown from seeds for 40 months under highly eCO₂ had a 55 % lower leaf-level g_c than aCO₂ seedlings (Table 3.1). This reduction was 15 % larger when compared to results from our previous study (Birami et al. 2020), possibly affected by the duration of CO₂ fumigation or seasonal timing of the experiment. Overall, the observed reductions in g_c exceed

the average decrease of about 20 % reported in many other tree species grown under eCO₂ (Ainsworth and Rogers 2007; Medlyn et al. 2001; Purcell et al. 2018). These differences could be due to the high CO₂ levels of c. 860 ppm in our study, compared to the average of c. 570 ppm in previous studies (Ainsworth and Rogers 2007). To further investigate the mechanism driving this considerable reduction in leaf-level g_c in Aleppo pine seedlings, we first conducted an experiment to test whether the reduced g_c was driven by a direct stomata response (Ainsworth and Rogers 2007; Birami et al. 2020; Gamage et al. 2018; Xu et al. 2016). We found that stomata in eCO₂-adapted plants did not respond to [CO₂] reductions from c. 900 to 400 and 200 ppm with each level kept for two days (Figure 3.3). This suggests that stomata were not actively closed by the high CO₂ level; rather, the stomata were likely operating at an optimal level that was physiologically and anatomically determined. A similar result has been observed after 17 years of CO₂ enrichment (c. +200 ppm) at the DUKE FACE site, in which [CO₂] was decreased step wise, without any indications of g_c to respond in a Loblolly pine (*Pinus taeda*) dominated stand (Tor-ngern et al. 2015). In our study, we further showed that ABA levels were not causing a direct decline of g_c under eCO₂, or augmenting this response as observed in angiosperms (Dubbe et al. 1978). This reinforces the assumption that the g_c reduction might be indirect (via developmental changes) rather than direct (via active stomatal aperture adjustment) and hence rejects our first hypothesis. While this contrasts observations in most angiosperm species (Chater et al. 2015; Giday et al. 2014), it is in line with previous studies which have found that conifers lack considerable instantaneous stomatal closing responses to eCO₂ (Brodribb et al. 2009; Brodribb and McAdam 2013; Haworth et al. 2013).

As our 40-month-old Aleppo pine seedlings had grown their entire life under eCO₂, indirect responses via anatomical adjustments might be the most prominent explanation on apparent declines in g_c . We found epidermal developmental adjustments to eCO₂, particularly an increased SD and ED (Table 3.1). This increase in SD at eCO₂ has rarely been documented (Ferris 1996; Reid 2003; Zhou et al. 2013) and is contrary to our expectation of SD reductions (Haworth, Elliott-Kingston, and McElwain 2011; Kouwenberg et al. 2003; Lin et al. 2001) or no changes in SD (Apple et al. 2000; Kurepin et al. 2018). While SD and ED increased, we found SI to remain unaffected (Table 3.1), rejecting our hypothesis that – as in many angiosperms – a reduced initiation of stomata occurred in response to eCO₂ in Aleppo pine seedlings. As SD did not change independently of epidermal cell density, we suggest that the observed increase in SD was mediated by a decrease in epidermal cell expansion that led to a smaller final size of epidermal cells. Decreased epidermal cell size has been reported previously in *Phaseolus vulgaris* exposed to eCO₂ due to changes in both cell division and expansion (Ranasinghe and Taylor 1996). So far, the underlying mechanisms of increased leaf cell production under eCO₂ are not fully resolved, but could potentially be triggered by a surplus of carbohydrates and may be linked to the increase in individual leaf size we observed in eCO₂-adapted plants.

3.4.2 Hydraulic conductance in leaves and branches under eCO₂

We found needles of eCO₂ seedlings to increase in width and cross-sectional area consequently having a longer distance for water to traverse from the vein to the substomatal cavity. Increasing the radial path length for water transport effectively limits K_{leaf} (Brodribb, Feild, and Sack 2010). A larger distance from the vein-to-the-epidermis has been shown to be linearly related to K_{leaf} in a range of species (Brodribb, Feild, and Jordan 2007). This supports that K_{leaf} , although not measured directly in our study, must have been lower in eCO₂ seedlings. Moreover, an increased vein-to-epidermis distance has also been reported after long-term exposure to eCO₂ in Loblolly pine (*Pinus taeda*), which was directly related to reduced K_{leaf} and

further attributed to increased resistance of outside xylem water transport (Domec et al. 2016). Similar to our study, stomata did not open when CO₂ was reduced (Tor-ngern et al. 2015). In addition, eCO₂ increased the needle cross-sectional area and mesophyll surface area in Scots pine (*Pinus sylvestris*) (Lin et al. 2001), and recently it has been shown that a lower stomata-to-mesophyll volume ratio relates to lower stomatal conductance in conifers (Trueba et al. 2022). In Aleppo pine we found the increase in vein-to-epidermis distance (+65 %) to be proportionally larger than the increase in SD (+23 %), eventually contributing to a reduced g_c under eCO₂. Conifer leaves are not fully vascularized and as consequence exhibit a larger difference in water potentials between veins, mesophyll, and epidermis, which may result in stomata closure even when xylem water potential is relatively high (Zwieniecki, Brodribb, and Holbrook 2007). Albeit leaf water potential did not differ between CO₂ treatments (Supplemental Figure S3.2), undetected, minor changes in localized water potential – eventually restricted to stomatal guard cells – could have resulted in turgor-driven partial stomatal closure in these conifers (McAdam and Brodribb 2015). Additional work examining the impact of potentially altered mesophyll anatomy, transfusion tissue area and cell size on K_{leaf} and stomatal conductance is warranted. In addition, undetected morphological changes of the stomata structure, including a greater stomatal pore depth or increases in cuticular waxes, may contribute to reduced transpiration.

We found branches of the eCO₂ seedlings to have a lower K_s and reduced K_l . This was manifested in xylem morphology, reflected in a lower conduit lumen fraction and reduced average conduit diameter in branches under eCO₂. These anatomical changes to leaf morphology and xylem structure have likely manifested during early seedling development triggered by reduced stomatal aperture and lower water demand under high CO₂. We did not find a clear signal just a tendency of increasing leaf-to-sapwood area under eCO₂ in line with a study on cottonwood trees grown under highly eCO₂ (c. 1200 ppm) (Engel et al. 2004). This suggests that trees under eCO₂ allocate comparable less resources into tree water transport but more into leaf structure. At the tree level, this resulted in a larger leaf area and increased C uptake in eCO₂ plants (Supplemental Figure S3.3b).

These anatomical responses, as depicted, should need relative long exposure times to eCO₂. For instance, in experiments on mature trees, such responses might not become apparent, as CO₂ fumigation typically spans few growing seasons and most of the woody tissue has been formed previously (e.g. Körner 2006). This indicates that particularly in diffuse-porous and conifer species, which conduct water through multiple tree rings (Maton and Gartner 2005), xylem hydraulic responses might only manifest after a large fraction of the woody tissue has been grown under eCO₂ conditions, and hence might have not been routinely observed in previous studies (Domec et al. 2017). In contrast, responses at the leaf-level should develop more quickly (e.g., Tor-ngern et al. 2015). In our study we found, albeit anatomical adjustments in leaves and xylem strongly reducing leaf-level water loss, no differences in Ψ_{leaf} and a minor response of tree-level transpiration (Supplemental Figure S3.2 and Supplemental Figure S3.3a). The reason is a pronounced increase of leaf area under eCO₂ that largely annulled leaf-level water savings (Gattmann et al. 2021). In summary, this indicates a tight coordination between anatomical adjustments and water demand in Aleppo pine seedlings grown their entire life time in a highly enriched CO₂ atmosphere.

3.4.3 Implications for drought and VPD responses under eCO₂

The rate of stomatal closure during increasing soil or atmospheric drought was not affected by eCO₂, albeit g_{c-ref} (g_c at VPD of 1 kPa) being 55 % lower in eCO₂ plants. Increasing VPD from 1 to 2 kPa resulted in a 60 % reduction of g_c in both treatments. This similar g_c behaviour was reflected in ABA levels increasing as Ψ_{leaf} declined (Figure 3.4), and supports previous findings of an unchanged physiological drought response in Aleppo pine grown under eCO₂ (Birami et al. 2020; Gattmann et al. 2021). In agreement, the hydraulic vulnerabilities reported here, indicate no differences in P_{12} , P_{50} or P_{88} values between treatments or the water potential at stomatal closure, which supports our last hypothesis. However, it is worth mentioning that the uncertainties were relatively large and a higher number of samples would have provided larger confidence in these results. Albeit hydraulic safety was not affected, we found hydraulic efficiency to decrease under eCO₂, this was not surprising as hydraulic efficiency and safety are typically weakly linked (Gleason et al. 2016). A lower hydraulic conductivity was reflected in smaller conduits (-8 %) and lower lumen fraction (-11 %) of the xylem. Decreases in xylem porosity as we found under eCO₂ are contradictory to findings in a few conifers, which apparently tend towards larger conduit diameter and less drought resistant xylem (Domec et al. 2017). But the results on CO₂ impacts on tree hydraulics and wood anatomy in conifers are generally mixed and sparse (Domec et al. 2010; Olszyk et al. 2005; Telewski et al. 1999) and no general picture emerges. Hence, it is worth noting that the CO₂ effects on wood anatomy as found in our study were moderate and became apparent only after accounting for the confounding effect of branch cross-sectional area, which might not routinely be considered in other studies. In summary, while some of the observed morphological adjustments could be interpreted as a protective measure, neither the hydraulic vulnerability curves nor the g_c response to increasing soil or atmospheric drought indicate an increased hydraulic safety of Aleppo pine seedlings grown under eCO₂.

Our study provides evidence of an unchanged metabolic and hydraulic stress response in pine seedlings grown under highly eCO₂. The water savings from reduced transpiration were largely compensated by an increased leaf area so that tree-level water loss was marginally lower in the eCO₂ treatment (Supplemental Figure S3.3a) and the drought dynamics appeared unchanged (Gattmann et al. 2021). Based on these results, we suggest that drought responses of mature trees in the field should depend on leaf area stimulations from eCO₂ (De Kauwe et al. 2021), which in turn affect tree and forest water demand. For instance, if an increase in leaf area balances CO₂-induced reductions in water loss, tree or ecosystem-level drought progression should be unchanged. In contrast, if leaf area does not respond to eCO₂, the CO₂-induced leaf-level water savings as observed here have the potential to buffer forest drought progression as soil water resources should deplete more slowly.

Funding Information

This study was supported by the German Research Foundation through its Emmy Noether Program (RU 1657/2-1), the German Research Foundation through its German-Israeli project cooperation program (SCHM 2736/2-1 and YA 274/1-1), the Alexander von Humboldt Foundation through a Fellowship to S.M., and the USDA National Institute of Food and Agriculture (Hatch project 1014908).

Acknowledgements

We are grateful to Nils Risse, Stefanie Dumberger, Johanna Schurr, and Andreas Gast for experimental support. We acknowledge the use of the Metabolite Profiling facility of the Bindley Bioscience Center, a core facility of the National Institute of Health-funded Indiana Clinical and Translational Sciences Institute, for assisting in the quantification of ABA levels.

3.5 Supplement

Supplemental Methods S1. Non-linear model fitting.

The following models were fit via Bayesian calibration as described in the main text. The number of accounted auto-correlation structures (number of seedlings measured) per model is given.

1) g_c response to increasing vapor pressure deficit (VPD)

For both treatments (aCO₂: $n = 6$ and eCO₂: $n = 6$) we assumed g_c to decline with VPD according to the following equation:

$$g_c = a_1 VPD^{b_1} \quad (S1)$$

in which g_c is the canopy conductance in mol m⁻²s⁻¹, VPD is the vapor pressure deficit in kPa, and a_1 and b_1 are the calibrated coefficients of the regression.

2) g_c response to declining midday leaf water potential (Ψ_{leaf})

For the two treatments (aCO₂ and eCO₂) we assumed a logistic decline of g_c following Ψ_{leaf} reductions, with a non-zero asymptote to represent minimum canopy conductance:

$$100 \cdot \left(\frac{g_c}{g_{c,max}} \right) = a_2 + \frac{(100 - a_2)}{1 + \left(\frac{\Psi_{leaf}}{b_2} \right)^{c_2}} \quad (S2)$$

in which $100 \cdot \left(\frac{g_c}{g_{c,max}} \right)$ is the percentage of g_c with respect to the maximum canopy conductance, and Ψ_{leaf} is the midday leaf water potential (MPa). Regarding the calibrated coefficients, a_2 is the percent of stomatal conductance relative to the maximum at the asymptote, which is the equivalent of minimum g_c . b_2 is the leaf water potential at which the percent of g_c relative to maximum g_c is $\frac{100+a_2}{2}$, and c_2 is a scaling factor.

3) ABA response to declining midday leaf water potential (Ψ_{leaf})

For the two treatments (aCO₂ and eCO₂) we assumed a potential increase of ABA concentration with declining Ψ_{leaf} as follows:

$$ABA = a_4 \cdot (-\Psi_{leaf})^{b_4} \quad (S4)$$

in which ABA is the concentration of abscisic acid in the leaves (ng g⁻¹), Ψ_{leaf} is the midday leaf water potential (MPa), and a_4 and b_4 are the calibrated coefficients for the regression.

4) Percent loss in conductance with declining xylem water potential (Ψ_{xylem})

For both treatments (aCO₂: $n = 5$ and eCO₂: $n = 6$) we fitted a cumulative probability function in form of a Weibull distribution:

$$PLC = 100 \cdot \left(1 - \exp \left(- \left(\frac{\Psi_{xylem}}{a_5} \right)^{b_5} \right) \right) \quad (S5)$$

with PLC is the percent loss of hydraulic conductance (%), Ψ_{xylem} is the xylem water potential (MPa), a_5 and b_5 are the calibrated coefficients, where a_5 is a scale parameter of reference xylem water potential value (MPa), and b_5 a shape parameter.

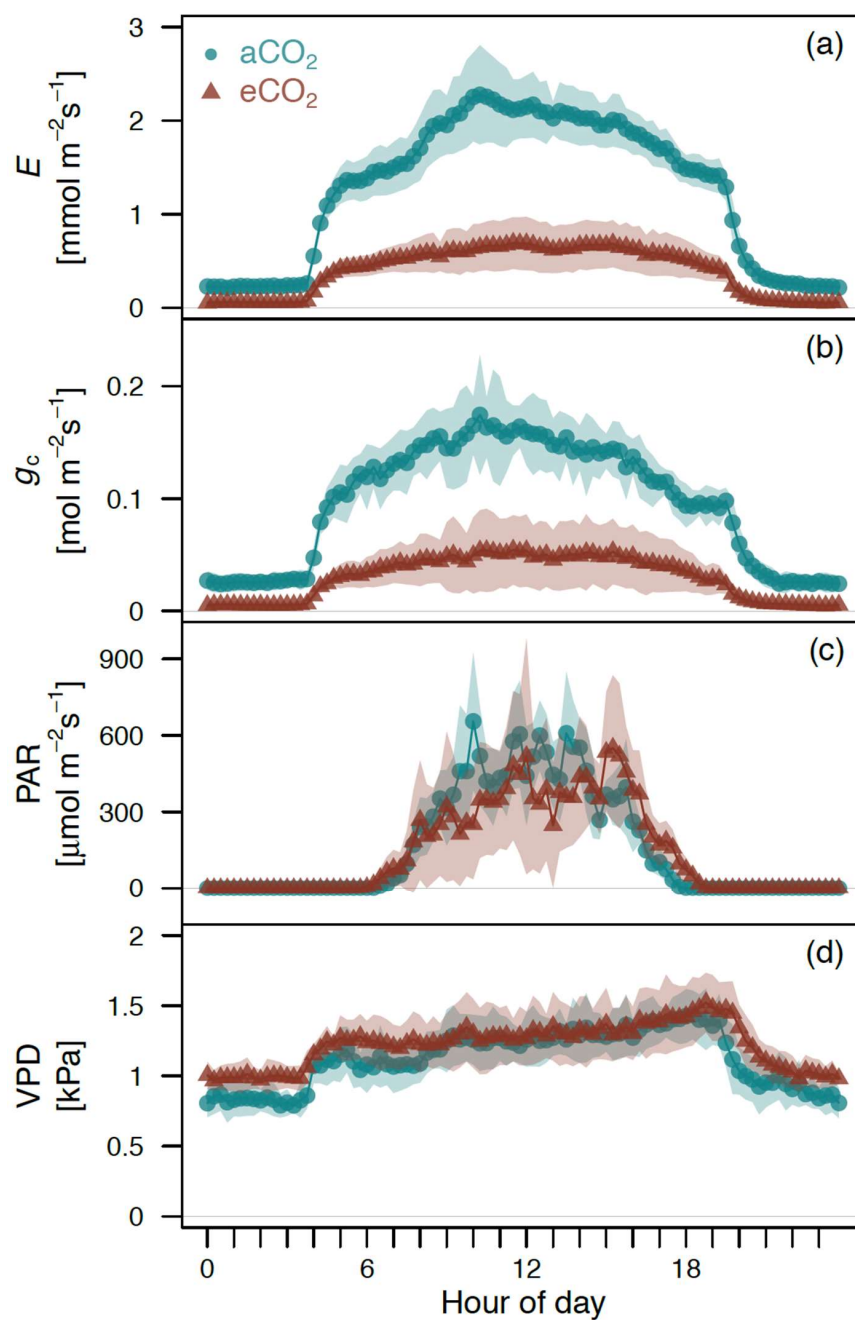
Supplemental Table S3.1: Prior distributions of the Bayesian model calibrations.

All priors are assumed to follow a uniform distribution, with minimum (min) and maximum (max) values as reported in the respective columns. ABA is abscisic acid concentration (ng g⁻¹), Ψ_{leaf} is midday leaf water potential (MPa), PLC is percent loss in xylem hydraulic conductance (%). Ψ_{xylem} is xylem water potential (MPa), g_c is canopy conductance (mol m⁻²s⁻¹), VPD is vapor pressure deficit (kPa) and g_{c-rel} is canopy conductance relative to the treatment-specific maximum canopy conductance (%).

model	parameter	distribution	min	max
ABA vs Ψ_{leaf}	<i>a</i>	uniform	50	500
	<i>b</i>	uniform	0.1	2.5
PLC vs Ψ_{xylem}	<i>a</i>	uniform	-6.5	-2.5
	<i>b</i>	uniform	1	8
g_c vs VPD	<i>a</i>	uniform	-3.5	0.5
	<i>b</i>	uniform	-4	-0.1
g_{c-rel} vs Ψ_{leaf}	<i>a</i>	uniform	1	5
	<i>b</i>	uniform	-0.5	-2
	<i>c</i>	uniform	1.5	6

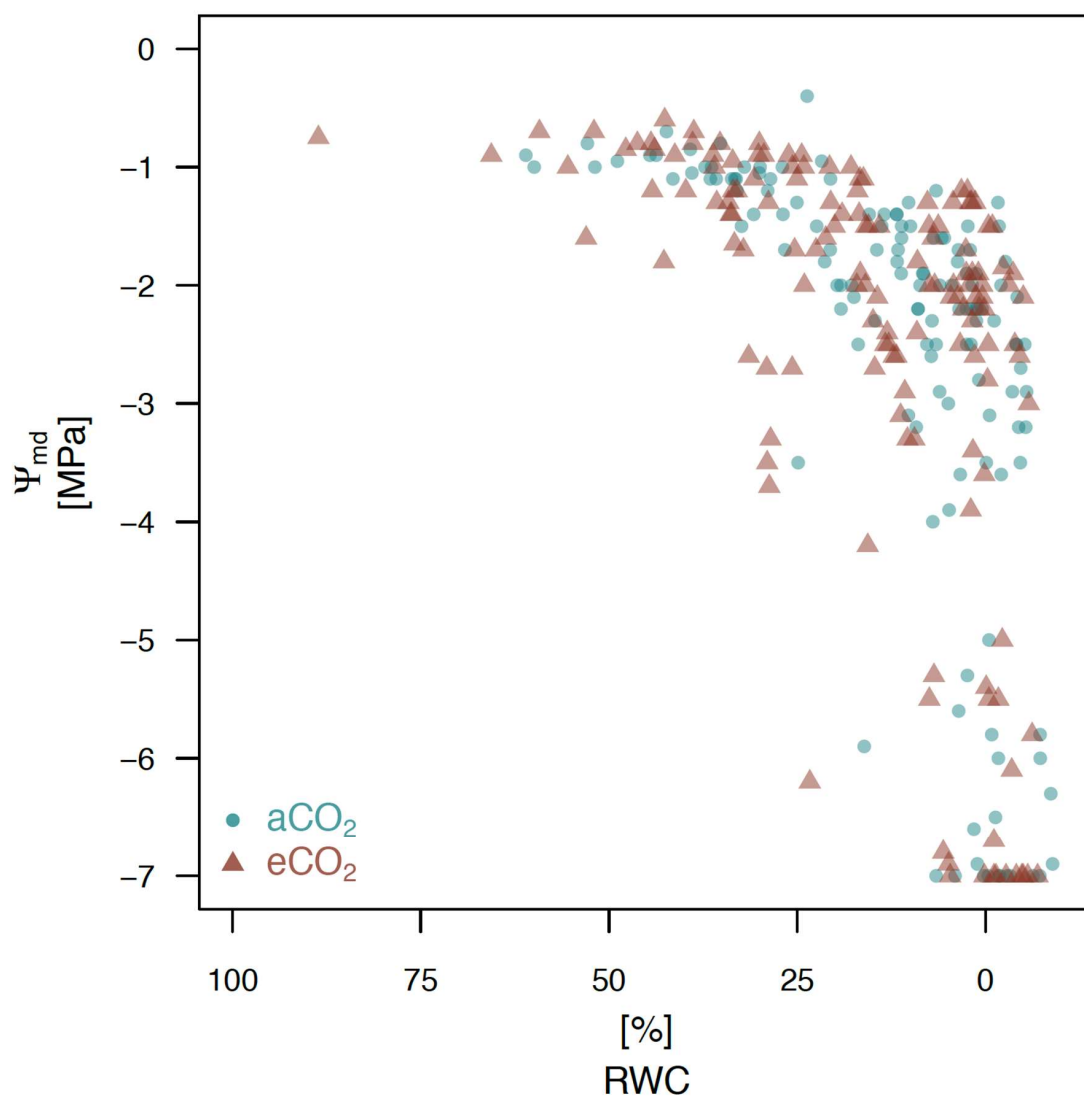
Supplemental Table S3.2: Parameter estimates of the Bayesian models.
Model coefficients are given per treatment (eCO₂ = elevated atmospheric [CO₂], aCO₂ = ambient atmospheric [CO₂]) and during decreasing CO₂ (from c. 900 to 400 to 200 ppm) in the eCO₂ seedlings. All parameter values are reported as the median and the 95 % credible intervals per treatment. Bold letters indicate nonoverlapping credible intervals between treatments for a given test. ABA is abscisic acid concentration (ng g⁻¹), Ψ_{leaf} is midday leaf water potential (MPa), PLC is percent loss in xylem hydraulic conductance (%), Ψ_{xylem} is xylem water potential (MPa), g_c is canopy conductance (mol m⁻²s⁻¹), VPD is vapor pressure deficit (kPa) and $g_{c\text{-rel}}$ is canopy conductance relative to the treatment-specific maximum canopy conductance (%).

	treatment	2.5%CI	median	97.5%CI	2.5%CI	median	97.5%CI
		coef a			coef b		
ABA vs Ψ_{leaf}	eCO ₂	62	159.6	283.4	0.99	1.37	1.93
	aCO ₂	181.3	248.9	321.9	0.85	1.02	1.21
PLC vs Ψ_{xylem}	eCO ₂	-6.48	-5.35	-4.55	2.67	4.26	5.29
	aCO ₂	-6.47	-5.38	-4.58	3.57	4.66	7.99
g_c vs VPD	eCO ₂	0.065	0.087	0.109	-2.63	-2.33	-2.05
	aCO ₂	0.173	0.202	0.405	-2.48	-1.68	-1.37
$g_{c\text{-rel}}$ vs Ψ_{leaf}	eCO ₂	2.29	2.93	3.57	-1.22	-1.2	-1.7
	aCO ₂	2.11	2.76	3.39	-1.27	-1.24	-1.21
		coef a			coef b		
					coef c		
					2.5%CI	median	97.5%CI
					4.11	4.47	4.89
					4.31	4.64	5.11



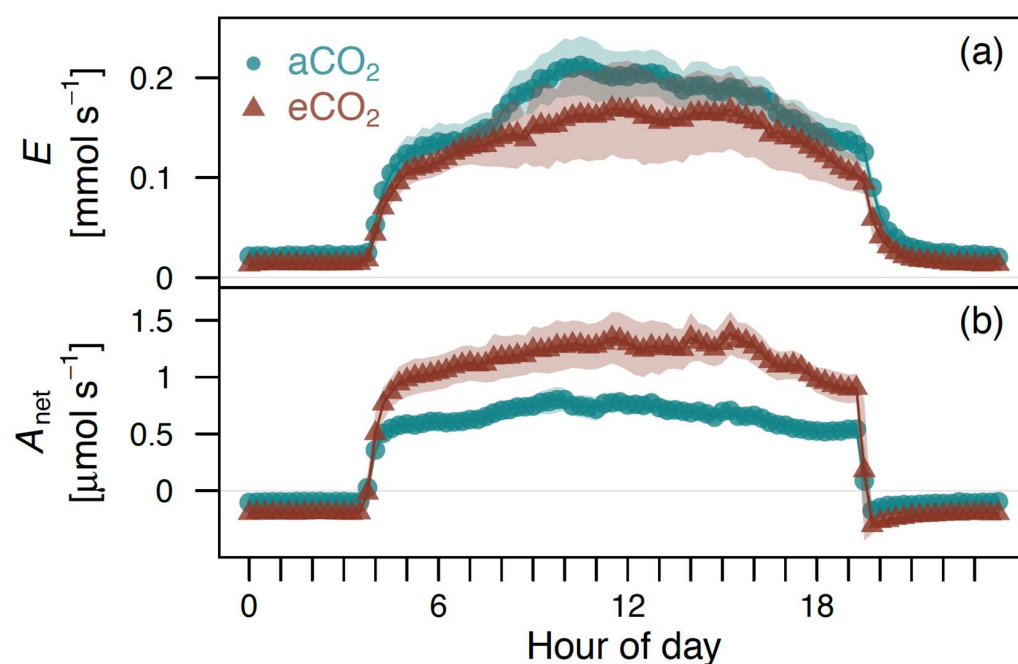
Supplemental Figure S3.1: Leaf-level gas exchange.

Diurnal course of leaf-level transpiration (E) (a) and canopy conductance (g_c) (b) as well as photosynthetic active radiation (PAR) (c) and vapor pressure deficit (VPD) (d) under ambient ($a\text{CO}_2$) and elevated ($e\text{CO}_2$) atmospheric [CO_2]. Shown are quarter-hourly treatment means over three ($a\text{CO}_2$) and four ($e\text{CO}_2$) days of acclimation with shaded areas depicting $\pm\text{SD}$ ($n = 6$ seedling per treatment). $a\text{CO}_2$ is shown in turquoise, solid points, $e\text{CO}_2$ in dark red, solid triangles.



Supplemental Figure S3.2: Midday leaf water potential during soil drought.

Midday leaf water potential (Ψ_{md}) versus daily-averaged relative soil water content (RWC) during the course of a lethal soil drought for ambient (aCO_2) and elevated (eCO_2) atmospheric [CO_2] Aleppo pine seedlings ($n = 18$ per treatment). Shown are individual Ψ_{md} measurements. aCO_2 is shown in turquoise, solid points, eCO_2 in dark red, solid triangles. See also Gattmann et al. (2021).



Supplemental Figure S3.3: Tree-level transpiration and photosynthesis.

Diurnal course of tree-level transpiration (E) (a) and tree-level net photosynthesis (A_{net}) under ambient (aCO₂) and elevated (eCO₂) atmospheric [CO₂]. Shown are quarter-hourly treatment means over three (aCO₂) and four (eCO₂) days of acclimation with shaded areas depicting \pm SD ($n = 6$ seedlings per treatment). aCO₂ is shown in turquoise, solid points, eCO₂ in dark red, solid triangles.

4 High vapor pressure deficit and soil drought impair aboveground growth before photosynthesis while shifting C allocation to roots in Scots pine

This chapter will be submitted as:

Gattmann, M. and Ruehr, N. K. "High vapor pressure deficit and soil drought impair aboveground growth before photosynthesis while shifting C allocation to roots in Scots pine".

Abstract

The development of forest C stocks as an important sink for anthropogenic CO₂ emissions has received much attention, but the dynamic responses of tree growth to climate change remain uncertain. High-resolution data on tree C balance, allocation, and growth are essential to understanding the direct influence of climatic factors, such as soil drought and vapor pressure deficit (VPD), especially as recent evidence indicates that tree growth is highly sensitive to water availability and cannot be solely predicted based on photosynthesis.

Scots pine (*Pinus sylvestris* L.) seedlings were subjected to three treatments: well-watered conditions, soil drought induced by reduced irrigation, and a combined soil drought plus elevated VPD (c. 2.9 kPa). As the drought progressed, we continuously monitored individual shoot and root gas exchange in single tree chambers including growth parameters such as stem radial increment and needle elongation. To investigate C allocation dynamics, we measured non-structural carbohydrates and performed ¹³CO₂ labeling, tracking the label through respiration and structural growth.

We found that gas exchange and stem radial growth started to decline 4–6 days earlier in the combined drought and VPD treatment compared to soil drought alone, even though midday leaf water potential remained similar between the treatments. Notably, regardless of the type of stress, stem growth stopped while photosynthesis had only declined slightly. Seedlings downregulated respiration in parallel, maintaining a positive net C balance, though at a 3–5-times lower rate than the control seedlings. The reduced C uptake under combined stress was reflected in lower ¹³CO₂ enrichment in shoot and root respiration, indicating a reduced contribution of recent assimilates to maintenance respiration under stress. This increased reliance on stored C under water shortage was further evidenced by a 70 % reduction in starch

reserves compared to control seedlings. With aboveground growth halted, recent C was preferentially allocated to root tissues where growth was largely maintained.

Our findings underscore the sensitivity of growth to water limitation (both VPD and soil drought), and suggest that C allocation shifts to belowground sinks once aboveground growth stops. This highlights the need to consider sink-driven C allocation and the role of VPD in limiting growth before photosynthesis is substantially impaired.

4.1 Introduction

Trees play a key role in the global carbon cycle (Bader et al. 2013; Friedlingstein et al. 2022; Keenan and Williams 2018; Körner 2003; Litton, Raich, and Ryan 2007; Weathers, Strayer, and Likens 2021), as they act both as carbon stocks and carbon sinks contributing to the absorption of anthropogenic CO₂ emissions (Ballantyne et al. 2012; Cole et al. 2021; Lal et al. 2018; Pan et al. 2011; Zhao and Running 2010). However, in light of climate change, the extent of mitigation remains a widely debated topic, not least because tree growth is still a factor of high uncertainty in today's vegetation models (Friend et al. 2014).

The effects of climate change are generally characterized by increased temperatures, altered precipitation regimes and greater interannual variability, which can lead to more frequent and intense climate extremes including soil and atmospheric droughts (Dai 2013; Spinoni et al. 2018). Increases in aridity, namely higher VPD of the atmosphere alongside lower soil water availability are having a major impact on tree water relations, as VPD and soil water availability are the main drivers of the water potential gradient that determines water flow through the tree (Carminati and Javaux 2020; Novick et al. 2016; Steppe et al. 2006). To limit water loss via the atmosphere-tree-soil continuum and ultimately prevent hydraulic failure, trees finely regulate stomatal aperture, with isohydric tree species showing the strictest stomatal control to VPD and soil water availability (Allen et al. 2010; Buckley et al. 2017; Cernusak et al. 2019; Choat et al. 2018; Mitchell et al. 2016; Novick et al. 2009, 2016; Novick, Konings, and Gentine 2019; Sperry et al. 2017; Starr et al. 2016). Not least because a reduction in stomatal aperture often simultaneously restricts CO₂ assimilation, high VPD and soil water scarcity are frequently associated with reduced tree growth (Babst et al. 2019; Breshears et al. 2013; Camarero et al. 2015; Castelláneta et al. 2022; Colangelo et al. 2017; Eamus et al. 2013; Gazol et al. 2018; McDowell et al. 2008; Novick et al. 2016; Restaino, Peterson, and Littell 2016; Yuan et al. 2019), resulting in lower carbon (C) uptake and biomass production (Flexas and Medrano 2002; Gruber et al. 2010; Hagedorn et al. 2016; Park Williams et al. 2013; Reddy, Chaitanya, and Vivekanandan 2004; Reichstein et al. 2013; Schimel 2018; Vieira, Carvalho, and Campelo 2020). Because of this context, linking stomatal regulation to plant hydraulics under changing climatic conditions have long been a popular trend, involving not only the degree of stomatal closure, but also the timing of subsequent impairment of key processes affecting growth.

To date, tree growth under drought is usually simulated based on the principal described above that plants reduce stomatal aperture to prevent water loss, which reduces carbon uptake (Fletcher, Sinclair, and Allen 2007; Grossiord et al. 2020; McDowell et al. 2020; Oren et al. 1999). However, this source (photosynthesis)-driven approach was considered too simplistic (Green and Keenan 2022) because there is growing evidence that tree growth is directly regulated by environmental controls and tends to stop before photosynthesis during drought (Fatichi, Leuzinger, and Körner 2014). This is partly due to the strong water dependence of the

cell expansion process, which accounts for most of the increase in cell volume during growth. In this context, water potential, and thus turgor, is thought as a key environmental control on which tissue growth depends (Hsiao 1973; Hsiao and Xu 2000; Muller et al. 2011) because lower cell turgor potentially limits cell wall and protein synthesis in addition to cell wall expansion (Hsiao 1973; Lockhart 1965; Sala, Piper, and Hoch 2010). Such a sink-driven growth limitation is missing in most vegetation models to date because high-resolution growth data are not readily available. Moreover, it is challenging to distinguish cause and effect with respect to source and sink limitations of growth (Fatichi et al. 2019), and therefore a clearer picture has yet to emerge.

In addition to the question of how soil and atmospheric drought affect growth in general, the tree's decision on how to use its less available carbohydrates when water is scarce is also of great interest. One of the first decisions to be made is whether to allocate new assimilates to respiration or to growth, with the fractionation between these two processes commonly expressed as carbon use efficiency (CUE, ratio of respiration to assimilation). However, this parameter is still under debate as reported values are highly variable (Chang et al. 2022; DeLucia et al. 2007; Rambal et al. 2014). In contrast, it is generally accepted that new assimilates are preferentially transferred to the tissues with the highest C requirement (Lambers, Chapin III, and Pons 2008), and experimental evidence suggests that drought causes a change in growth priorities (Brunner et al. 2015; Litton et al. 2007). Under mild to moderate drought stress, trees appear to distribute a greater proportion of newly photosynthesized C to the roots (Gaul et al. 2008; Poorter et al. 2012), probably as an adaptive response to maintain root functioning and access to limited soil water (Hommel et al. 2016). This favoring of the root system is often at the expense of shoot growth (Litton et al. 2007), increasing root-to-shoot ratios (Poorter et al. 2012), which should be advantageous for the plant's hydraulic status. However, such a shift in the partitioning pattern seems to be limited to the initial phase of drought or to short-term drought stress, as decreases in the transport of new assimilates belowground were observed during severe and prolonged drought periods (Brunner et al. 2015; Poorter et al. 2012; Ruehr et al. 2009). Another factor determining the impact of drought on tree growth is the availability of stored carbohydrates such as starch. When starch is hydrolyzed, it can contribute to higher concentrations of osmotically-active sugar compounds (Hartmann and Trumbore 2016). Osmotic adjustments can increase the water potential of the tissue, helping to maintain turgor in the growing regions of leaves or roots, and thus could support the continuation of growth during water limiting conditions. Additionally, the utilization of stored carbohydrates could provide the needed fuel for metabolic activity and C skeletons (e.g. McDowell, Allen, and Marshall 2010) and thus decouple growth from the reduced availability of photosynthates during drought. How the tree carbon balance is fine-tuned during drought and under which conditions sink-source processes can be sustained, has still to be resolved.

A well-established method for determining how C allocation responds to changing environmental conditions is C isotope analysis (Epron et al. 2012). Based on the natural photosynthetic C isotope discrimination, the C isotope content of the assimilated C is artificially altered so that the origin and fate of C in the tree can be traced. Stable ^{13}C is usually used for this purpose and the determination of the isotope signatures in tree compartments (Ruehr et al. 2009), non-structural and structural C (Kagawa et al. 2005; Kagawa, Sugimoto, and Maximov 2006a, 2006b) and respiratory fluxes (Rehseh et al. 2022). The ^{13}C label is typically applied either as a short pulse or over a longer period of time. A shorter pulse allows to detect the rate of C transfer from source to sinks (Epron et al. 2012), while a longer duration of the

label allows to integrate C allocation patterns over time particularly in smaller pools (Tamir Klein, Siegwolf, and Körner 2016) and/or to detect signals in pools with slower turnover (Ouyang et al. 2024), including structural compartments. While the transfer-time from source to sink organs has been shown to be delayed under drought (Barthel et al. 2011; Ruehr et al. 2009), little information exists thus far on the allocation of recent assimilates into structural biomass, particularly root growth, in response to water limitation.

This study focuses on the impacts of soil drought in combination with high VPD on carbon allocation and growth processes in Scots pine (*Pinus sylvestris* L.), which is already suffering from increasing aridity in many parts of its distribution range (Buras et al. 2018; Jaime et al. 2019). Scots pine is one of the most widespread tree species globally and can be found from boreal to Mediterranean climate, partly due to its tight stomatal control to effectively limit water loss (Ellenberg 1988; Irvine et al. 1998), a prominent feature of isohydric behavior. More specifically we aimed to determine how a moderate soil drought and high VPD affects the balance between photosynthesis and respiration, whole tree carbon allocation and above- and belowground growth. We hypothesize that i) canopy conductance responds faster than carbon uptake to atmospheric drought in isohydric Scots pine, ii) high VPD during moderate soil drought limits aboveground growth more strongly than photosynthesis, iii) belowground allocation is sustained during moderate soil drought irrespective of VPD at the expense of aboveground allocation and iv) photosynthesis declines faster than respiration, depleting NSC reserves with consequences for belowground growth.

4.2 Material and methods

4.2.1 Plant material

Bare-rooted Scots pine (*Pinus sylvestris* L., Provenance 85 115, Franconia, Germany) seedlings, that had been grown for three years in a local tree nursery were planted in individual pots (6.8 l) in March 2018. The substrate was a C-free mixture (2:2:1:2) of quartz sand (0.1 – 1.2 mm), medium-grained sand (1-2.5 mm), gravel (3-5.6 mm) and vermiculite (c. 3 mm)) enriched with 12 g slow-release fertilizer (Osmocote® Exact Standard 5–6 month fertilizer 15–9–12 + 2MgO + TE, ICL Specialty Fertilizers, Geldermalsen, The Netherlands). Additionally, immediate nutrient availability was ensured by applying liquid fertilizer monthly (Compo® Complete, 6 + 4 + 6(+2) NPK(MgO), Hornbach, Bornheim, Germany).

Until the start of the experiment at the end of July 2018, seedlings were kept in a greenhouse facility in Garmisch-Partenkirchen, Germany (732 m a.s.l., 47°28'32.8700"N, 11°30'44.0300"E) equipped with UV-transmissive glass. To ensure the experimental phase took place during active shoot development, we closely monitored needle elongation. Repotting seemed to slightly delay leaf development. Environmental drivers such as photosynthetic active radiation (PAR), relative soil water content (RWC), relative humidity and air temperature were continuously measured and controlled while seedlings were frequently relocated within the greenhouse compartment. Daily irrigation with an individual drip irrigation system (Rain Bird, Azusa, CA, USA) provided RWC near field capacity and air temperature was on average 20.7 °C (day 22.9 °C, night 17.4 °C).

4.2.2 Experimental setup

At the end of July 2018, thirteen Scot pine seedlings were randomly selected and each of these seedlings was placed into its own tree chamber within the greenhouse to continuously measure above- and belowground gas exchange separately as well as monitor $\delta^{13}\text{CO}_2$ (Birami et al. 2020; Gattmann et al. 2021, 2023; Rehschuh et al. 2022). Previously, we had randomly assigned the chambers to one of the three planned treatments: control (Cntrl), soil drought (dS) or combined air and soil drought (dSA). The light transmitting aboveground and opaque belowground compartment of each tree chamber were separated gas-tight. Chambers were constantly supplied with an air stream (aboveground $0.483 \pm 0.037 \text{ mol min}^{-1}$; belowground $0.172 \pm 0.005 \text{ mol min}^{-1}$) of predefined $[\text{H}_2\text{O}]$ ($9.66 \pm 1.94 \text{ ppt}$), $[\text{CO}_2]$ ($419.55 \pm 9.90 \text{ ppm}$) and $\delta^{13}\text{C}$ in CO_2 of $-2.28 \pm 2.65 \text{ ‰}$ before the labeling was initiated (Supplemental Figure S4.1).

Due to technical limitations, we reduced the flow rate to the aboveground compartments in dSA to $0.375 \pm 0.034 \text{ mol min}^{-1}$ on day 17 for the rest of the experiment, while flow rates in Cntrl and dS remained unchanged to avoid condensation.

Two gas analysers connected in series were used to quantify above- and belowground CO_2 and H_2O gas exchange (Cntrl: $n = 4$, dS: $n = 4$, dSA: $n = 5$). First, absolute $[\text{CO}_2]$ and $[\text{H}_2\text{O}]$ of the supply air stream (LI-840, Li-cor, Lincoln, NE) and secondly, differences between supply and sample air stream (LI-7000, Li-cor, Lincoln, NE) were measured. While automatically switching between chambers every 150 s with 70 s flushing time, the data was logged to a computer at the same intervals. Simultaneously, the associated isotopic ratios of $^{12}\text{C}/^{13}\text{C}$ in the supply and sample air stream were determined using an isotope ratio infrared spectrometer (IRIS, Delta Ray, Thermo Fisher Scientific, Bremen, Germany). A commercially available reference gas with $\delta^{13}\text{C} = -27.8 \pm 0.3 \text{ ‰}$ (141 101, Thermo Fisher Scientific) was used for hourly referencing and CO_2 -free synthetic air (N2, ALPHAGAZ 2, Air Liquide) as carrier gas.

Since all belowground C was plant related as C-free substrate has been used as potting material (see 4.2.1), CO_2 fluxes from the belowground compartment were treated as root respiration signal. To constantly monitor the system and to correct gas exchange estimates for any fluctuations in $[\text{CO}_2]$ and $[\text{H}_2\text{O}]$ not caused by changes in plant activity ($0.32 \pm 0.95 \text{ ppm CO}_2$ and $0.22 \pm 0.43 \text{ ppt H}_2\text{O}$ in the above- and $3.73 \pm 1.93 \text{ ppm CO}_2$ in the belowground compartment), two empty chambers containing the same C-free potting substrate, but without seedlings, were used as blanks. Tree net assimilation as well as root and night-time shoot respiration in $[\text{mol s}^{-1}]$ were calculated as

$$\text{CO}_2 \text{ flux} = -F_m(C_{\text{supply}} - C_{\text{sample}}) - EC_{\text{sample}} \quad (1)$$

with E $[\text{mol m}^{-2}\text{s}^{-1}]$ as tree transpiration rate, C_{supply} $[\text{mol mol}^{-1}]$ as $[\text{CO}_2]$ in supply air stream, C_{sample} $[\text{mol mol}^{-1}]$ as $[\text{CO}_2]$ in sample air stream and F_m $[\text{mol s}^{-1}]$ as molar flow. Total daily CO_2 uptake was then calculated from the sum of net assimilation minus nighttime shoot and day- and nighttime root respiration.

Canopy conductance (g_{canopy}) $[\text{mol s}^{-1}]$ was determined from daytime gas exchange data as follows

$$g_{canopy} = \frac{E \left(1000 - \frac{W_{leaf} + W_{sample}}{2} \right)}{W_{leaf} - W_{sample}} \quad (2)$$

with W_{leaf} as leaf saturated vapor pressure, W_{sample} [mol mol⁻¹] as [H₂O] in sample air stream and E [mol s⁻¹]. This approach neglects boundary layer conductance, which should be negligible under high mixing conditions inside the chamber (Birami et al. 2020). Isotopic ratios were expressed in δ notation [‰] relative to the international standard Vienna Pee Dee Belemnite (VPDB) following

$$\delta^{13}C = \left(\frac{R_{sample}}{R_{standard}} - 1 \right) * 1000 \text{ ‰} \quad (3)$$

with R_{sample} as the isotope ratio of the sample and $R_{standard}$ as the isotope ratio of the standard. The isotopic ratios in shoot and root respiration [‰] were calculated following

$$\delta^{13}CO_2 = \frac{\delta^{13}C_{sample} * C_{sample} - \delta^{13}C_{supply} * C_{supply}}{C_{sample} - C_{supply}} \quad (4)$$

with $\delta^{13}C_{sample}$ as the isotopic ratio in the sample air stream [‰] and $\delta^{13}C_{supply}$ as the isotopic ratio in the supply air stream [‰]. The ¹³C retained in each of the seedlings [g¹³C] was estimated as follows

$$^{13}C_{retained} = A_{net} * ^{13}C_{IN} - (R_{shoot\ night} * ^{13}C_S + R_{root} * ^{13}C_R) \quad (5)$$

with A_{net} as net assimilation of the seedling [gC], $^{13}C_{IN}$ as ¹³C in the aboveground compartment at daytime (PAR >100 μmol m⁻²s⁻¹) [ppm], $R_{shoot\ night}$ as the night respiration of the shoot [gC], $^{13}C_S$ as ¹³C of the shoot night respiration [ppm], R_{root} as the root respiration [gC] and $^{13}C_R$ as ¹³C of the root respiration [ppm].

Conditions in the tree chambers were kept at a daily mean air temperature (T_{air}) (5SC-TTTL-36-2 M, Newport Electronics GmbH, Deckenpfronn, Germany) of 23.64±0.37 °C (Figure 4.1a) and PAR (PQS 1, Kipp & Zonen, Delft, the Netherlands) was on average 426±93 μmol m⁻²s⁻¹ for 16 hr during daytime (Figure 4.1b) by supplementing outside light with plant growth lamps (T-agro 400 W, Philips, Hamburg, Germany). It is important to note that while we could control the water supply in the supply air stream, tree transpiration rates were also affecting the humidity conditions inside the chambers. For instance, since we omitted from increasing the supply of water vapor to the aboveground tree chambers during drought progression, VPD (Figure 4.1c) in dS and dSA increased to values of about 2.18±0.15 kPa and 2.85±0.07 kPa, respectively. Higher VPD in dSA was reached by reducing the initial supply of water vapor from 9.66±1.94 ppt to 6.18±2.00 ppt on day three followed by supplying the trees in the dSA treatment with completely dry air from day nine of the experiment onwards. Elevated VPD levels were maintained in dS and dSA during the last seven days of the experiment. VPD in the Cntrl was maintained at 0.95±0.11 kPa by adjusting the supply of water vapor to aboveground tree chambers as well as water supply to the soil to allow for higher transpiration rates. Thus, RWC (Figure 4.1d) (10HS, Decagon Devices, Inc., Pullman, WA) in Cntrl increased from 57.77±3.94 % to 83.71±0.89 %, but this had no effect on the transpiration rates. Soil drought was mimicked by gradually reducing irrigation in dS and dSA. On the fourth day of the experiment, drought was induced by reducing the water supply by half (200 ml d⁻¹ to

100 ml d⁻¹). Afterwards, irrigation was reduced further (on day 15 to 75 ml d⁻¹ and on day 19 to 50 ml d⁻¹) so that from day twenty on, daily mean RWC was about 0.60±1.24 % in dS and 2.26±0.62 % in dSA.

Until the start of the labeling, $\delta^{13}\text{CO}_2$ of the supply air stream was maintained for both shoot and root compartments at -2.28 ± 2.65 ‰ $\delta^{13}\text{C}$ (Supplemental Figure S4.1). When the seedlings had acclimatized to the desired stress conditions in the treatment groups (g_{canopy} for example at 13 % (dS) and 5 % (dSA) of the Cntrl), continuous $^{13}\text{CO}_2$ labeling began on day 21. For this, we switched the CO_2 source for the supply air stream to the shoot compartments to a $^{13}\text{CO}_2$ enriched gas, resulting in $[\text{CO}_2]$ of c. 400 ppm with a $\delta^{13}\text{CO}_2$ signature of 500 ‰, while maintaining the supply stream to the root compartments at the previous ambient CO_2 conditions (see above). Using a similar setup we have previously shown the applicability of the approach and could that no contamination of the ^{13}C label from the shoot to the root compartments occurred (Rehschuh et al. 2022).

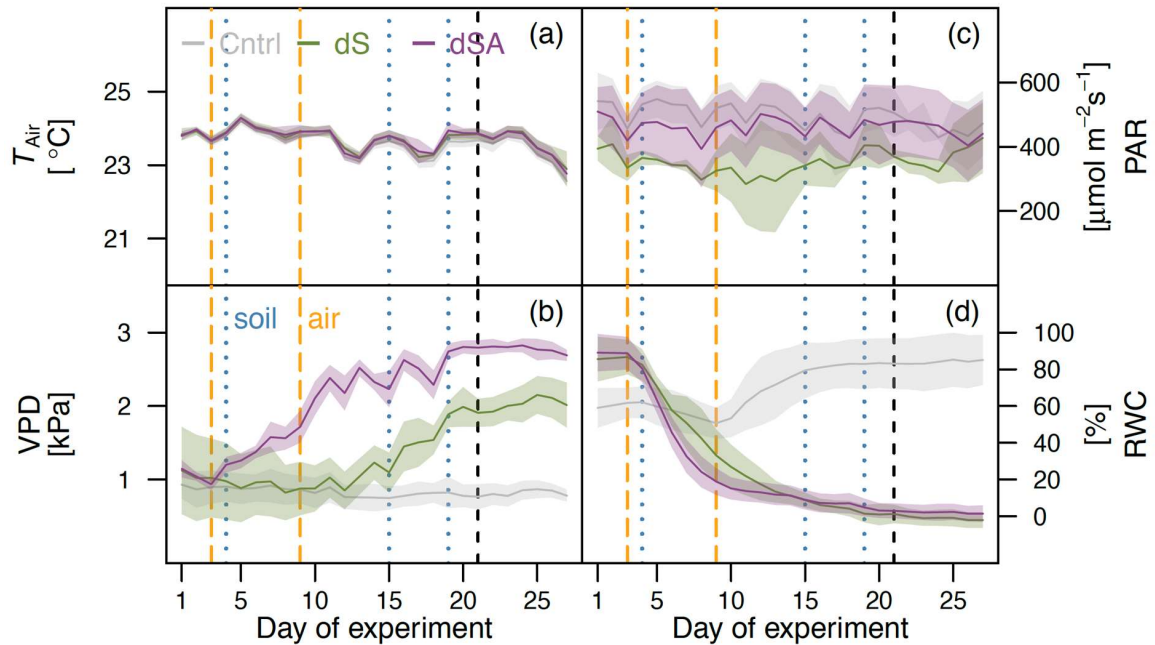


Figure 4.1: Progression of environmental drivers over the course of the experiment in Scots pine seedlings. Air temperature (T_{Air} , a), vapor pressure deficit (VPD, b), photosynthetic active radiation (PAR, c) and relative soil water content (RWC, d) in the control (Cntrl, grey), soil drought (dS, green) and combined soil and air drought (dSA, violet) treatment are shown. Lines depict daytime treatment averages ($\text{PAR} > 100 \mu\text{mol m}^{-2}\text{s}^{-1}$) and the shaded areas are $\pm\text{SD}$ (Cntrl and dS: $n = 4$, dSA: $n = 5$). Experimental reductions in air humidity in the dSA treatment are given by the dashed orange lines and reductions in irrigation in the dS and dSA treatment are shown by the dotted blue lines, with the last line on day 19 marking irrigation at 50 ml per day. The begin of the continuous $^{13}\text{CO}_2$ labeling ($\delta^{13}\text{CO}_2$ of c. 500 ‰) is highlighted by a dashed black vertical line on day 21.

4.2.3 Radial growth, sampling procedure and needle water status

In the individual tree chambers, each seedling was equipped with a point dendrometer (DD-S, Ecomatik, Dachau, Germany) at 5–10 cm stem height measuring stem diameter variations every 30 minutes throughout the experiment. At the beginning and the end of the experiment we sampled needle and fine root material for non-structural carbohydrate and stable isotope ratio analysis. The sampling was conducted between 12 p.m. and 2 p.m. Needle and root

samples were immediately frozen in liquid nitrogen and stored at -80 °C until further analysis. Tree biomass was harvested at the last day of the experiment and divided into needle, woody and root tissue and dried at 60 °C for 48 hr prior dry mass was quantified (Supplemental Table S4.1). At the same time, a few needles and fine roots were taken from each seedling and weighted before and after drying to determine the ratio of fresh to dry weight. In addition, further subsamples of needles were used to determine the specific leaf area. The leaf area was then determined by multiplying the leaf dry biomass by the specific leaf area. In addition, needle samples were taken at seven time points during the experiment, including at the beginning and the end of the experiment, to determine the needle water potential at midday (between 12 p.m. and 2 p.m.) (Ψ_{md}). Measurements were conducted using a pressure bomb (Model 1000, PMS Instrument Company, Albany, OR) on one needle fascicle per tree. Furthermore, relative needle water content (RLWC) was calculated from the needle mass (a) of the same fresh needles used for water potential analysis, (b) after 48 hr immersion in distilled water and (c) after drying at 60 °C.

4.2.4 Non-structural carbohydrate quantification

4.2.4.1 Soluble sugar

The determination of soluble sugar was conducted following Landhäusser et al. (2018) with minor modifications as described by Gattmann et al. (2021). First, 15 mg of frozen fresh plant powder was added to 0.5 ml 80 % ethanol for the extraction. After shaking, 10 min incubation at 80 °C and centrifugation (13,000 g for 3 min), the supernatant was taken and the extraction process repeated twice. While the remaining pellet swelled in 1 ml distilled water (dH₂O) at 95 °C for 2 hr before being stored at -80 °C for subsequent starch analysis (see 4.2.4.2), the supernatants were mixed and the fluids were vaporized in a vacuum concentrator. The pellet was then dissolved in 1 ml dH₂O. For sugar quantification, 200 μ l aliquots of extract (1:10 diluted in dH₂O) were mixed with 100 μ l invertase solution (300 U ml⁻¹ (Sigma-Aldrich I4504-250 mg, Merck, Darmstadt, Germany) diluted in 10 mM sodium acetate buffer (pH 4.5) and incubated for 35 min at 55 °C). Afterwards 200 μ l (5mM MgCl, 95 mM Tris-HCl, 1.7 mM ATP, 4.5 mM NAD⁺, 1.1 U ml⁻¹ G6PDH (Sigma-Aldrich G8404-2KU, Merck, Darmstadt, Germany), 10 U ml⁻¹ HK (Roche 1,142,632,001), 1.6 U ml⁻¹ phosphoglucose isomerase (Sigma-Aldrich P5381-1KU, Merck, Darmstadt, Germany) were added to 50 μ l aliquots of sugar extract in 96-well microtest plates (Brand, Wertheim, Baden-Württemberg, Germany). After 20 min of incubation at room temperature, absorbance was determined at 340 nm with a microplate absorbance reader (Epoch2, BioTek, Winooski, VT).

4.2.4.2 Starch

After thawing and shaking, 80 μ l aliquots of water diluted starch samples (see 4.2.4.1) were mixed with 20 μ l α -amylase (30 U ml⁻¹, Megazyme E-BLAAM-10 ml) and boiled at 85 °C for 1 hr. Following a quick cooling, 100 μ l amyloglucosidase (20 U ml⁻¹ amyloglucosidase (Sigma-Aldrich 10,115-1G-F, Merck, Darmstadt, Germany) dissolved in 25 mM potassium acetate buffer) were added and samples boiled at 55 °C for another hour. In preparation for the analysis, samples were cooled again and centrifuged (13,000 g for 3 min) before 50 μ l aliquots were mixed with 200 μ l buffer (5 mM MgCl, 95 mM Tris-HCl, 1.7 mM ATP, 4.5 mM NAD⁺, 1.1 U ml⁻¹ G6PDH (Sigma-Aldrich G8404-2KU, Merck, Darmstadt, Germany), 10 U ml⁻¹ HK (Roche 1,142,632,001, Roche, Mannheim, Germany), 10 U ml⁻¹ HK) in 96-well microtest plates (Brand, Wertheim, Baden-Württemberg, Germany). Absorbance at 340 nm was measured using a microplate absorbance reader (Epoch2, BioTek, Winooski, VT).

4.2.5 Sample preparation and isotope ratio mass spectrometry

In preparation for isotope ratio mass spectrometry, biomass samples (fine root, needle, stem) stored at -80°C (see 4.2.4) were freeze-dried (Alpha 24 LSC; Martin Christ Gefriertrocknungsanlagen GmbH, Osterode am Harz, Germany) and ground to fine powder (MM200; Retsch, Haan, Germany). In addition, we extracted cellulose from root and stem samples. This was done stepwise using Teflon filters using 5 % NaOH and 7 % acidified NaClO_2 at 60°C (Galiano et al. 2017) from c. 15 mg homogenized dried plant material (fine roots, stems) and then homogenized by an Ultrasonic transducer (Laumer et al. 2009) as described by Rehschuh et al. (2022). To determine isotopic composition of solid samples, c. 1 mg homogenized bulk tissue material or cellulose were weighed into tin capsules, which were combusted in an elemental analyzer (EA1110 CHN, Carlo Erba, Milan, Italy) combined with an isotope ratio mass spectrometer (Delta XL, Thermo Fisher Scientific, Bremen, Germany) (Rehschuh et al. 2022). Laboratory and international standards with known $\delta^{13}\text{C}$ were used for calibration resulting in a precision of 0.2 ‰.

4.2.6 Statistical data analyses

All data were analyzed using R 3.5.2 (R Core Team 2016). Differences were considered significant at $p < 0.05$. Treatment effects in time series data were assessed by fitting linear mixed effects models (lme) (package lme4: Bates et al. 2015) and package lmerTest: Kuznetsova et al. 2017) with time and treatment as fixed effects and tree as random factor. In addition, *post-hoc* Tukey multiple comparisons test of means (package emmeans: Lenth et al. 2019) was performed to assess daily differences. Biomass, soluble sugar, starch and isotope data were analyzed using ANOVA followed by *post-hoc* TukeyHSD.

4.3 Results

4.3.1 Responses of gas exchange and non-structural carbohydrates to drought progression

The experimental reduction in air humidity combined with a reduced soil water supply led to a steady downward trend of gas exchange rates in both drought treatments. Following an increase in VPD in the dSA treatment, daytime g_{canopy} ($\text{PAR} > 100 \mu\text{mol m}^{-2}\text{s}^{-1}$) decreased quickly (Figure 4.2a, Supplemental Figure S4.2a), followed by a later decline in E (Figure 4.2b, Supplemental Figure S4.2b) and A_{net} (Figure 4.2c, Supplemental Figure S4.2c). Compared to the Cntrl treatment, the reduction in g_{canopy} in the dSA treatment was statistically significant from the tenth day (lme: Tukey HSD, $p < 0.001$, $t = 7.45$), six days earlier than in the dS treatment (lme: Tukey HSD, $p < 0.01$, $t = 6.88$). Treatment effects on A_{net} and E were statistically significant in the dSA treatment (A_{net} : lme: Tukey HSD, $p < 0.01$, $t = 6.22$; E : lme: Tukey HSD, $p < 0.01$, $t = 7.17$) from day 16, four days earlier than in the dS treatment (A_{net} : lme: Tukey HSD, $p < 0.05$, $t = 5.19$; E : lme: Tukey HSD, $p < 0.05$, $t = 5.78$). Overall, we found that the reduction in gas exchange under combined soil and atmospheric drought in the dSA treatment occurred on average about 4–6 days earlier than under soil drought only in the dS treatment. In contrast, seedling respiration (R_{sum} , sum of daily root respiration and nighttime shoot respiration ($\text{PAR} < 100 \mu\text{mol m}^{-2}\text{s}^{-1}$)) (Figure 4.2d, Supplemental Figure S4.2d) declined somewhat later, following the second reduction in soil water supply on day 15. When all gas exchange

parameters had settled at a new stable level under the applied experimental conditions, the $^{13}\text{CO}_2$ labeling was initiated on day 21.

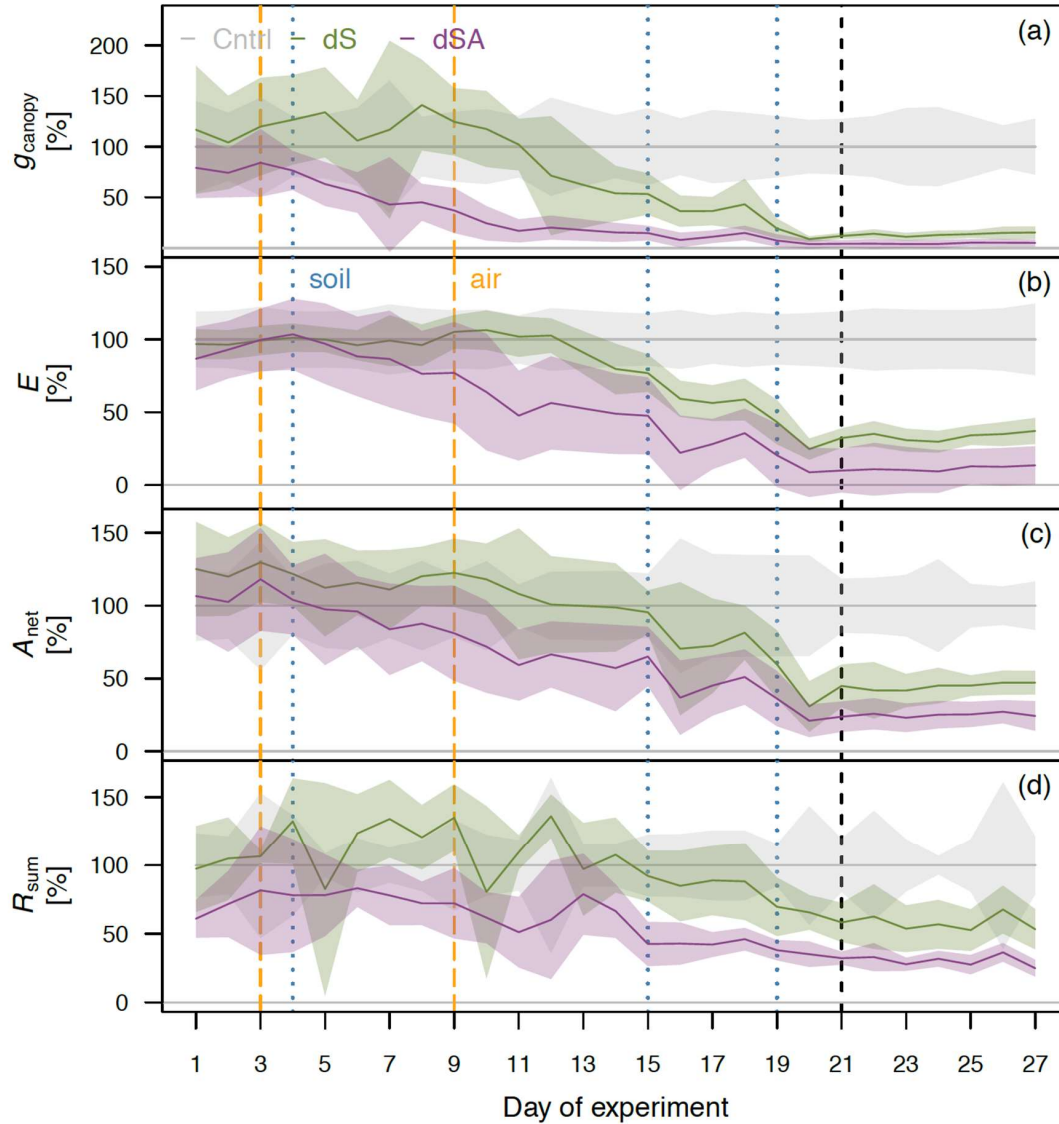


Figure 4.2: Progression of gas exchange over the course of the experiment in Scots pine seedlings. Daytime ($\text{PAR} > 100 \mu\text{mol m}^{-2}\text{s}^{-1}$) canopy conductance per leaf area (g_{canopy} , a), transpiration per leaf area (E , b), net assimilation per leaf area (A_{net} , c) and sum of daily root and nighttime ($\text{PAR} < 100 \mu\text{mol m}^{-2}\text{s}^{-1}$) shoot respiration per tree (R_{sum} , d) relative to the control (Cntrl) during the experiment in the Cntrl (grey), soil drought (dS, green) and combined soil and air drought (dSA, violet) treatment. Lines mark daily treatment averages and the shaded areas are $\pm\text{SD}$ (Cntrl and dS: $n = 4$, dSA: $n = 5$). Experimental reductions in air humidity in the dSA treatment are given by the dashed orange lines and reductions in irrigation in the dS and dSA treatment are shown by the dotted blue lines, with the last line on day 19 marking irrigation at 50 ml per day. The begin of the continuous $^{13}\text{CO}_2$ labeling ($\delta^{13}\text{CO}_2$ of 500 ‰) is highlighted by a black dashed vertical line on day 21.

Non-structural carbohydrate concentrations at the end of the experiment were affected by the drought treatments with a stronger response in the roots compared to the needle tissues (Figure 4.3, Supplemental Table S4.2). We found no responses of needle soluble sugar to the drought conditions (SS_N , Figure 4.3a). In contrast, needle starch (St_N , Figure 4.3b) was 40 %

lower in dS (anova and Tukey HSD $p > 0.05$) and 42 % lower in dSA (anova and Tukey HSD $p = 0.029$) than in the Cntrl (0.15 ± 0.04 mmol gDW⁻¹). Compared to the needles, responses in the roots were more pronounced and both root soluble sugar (SS_R, Figure 4.3c) and root starch (St_R, Figure 4.3d) were significantly lower in the dS and dSA treatments compared to the control. Root sugar concentrations were reduced by 33 % in dS (1.33 ± 0.19 mmol gDW⁻¹, anova and Tukey HSD $p = 0.026$) and by 46 % in dSA (1.07 ± 0.28 mmol gDW⁻¹, anova and Tukey HSD $p = 0.001$). This reduction was even more pronounced for starch, which was 63 % lower in the dS (anova and Tukey HSD $p < 0.001$) and 69 % lower in the dSA treatment (anova and Tukey HSD $p < 0.001$).

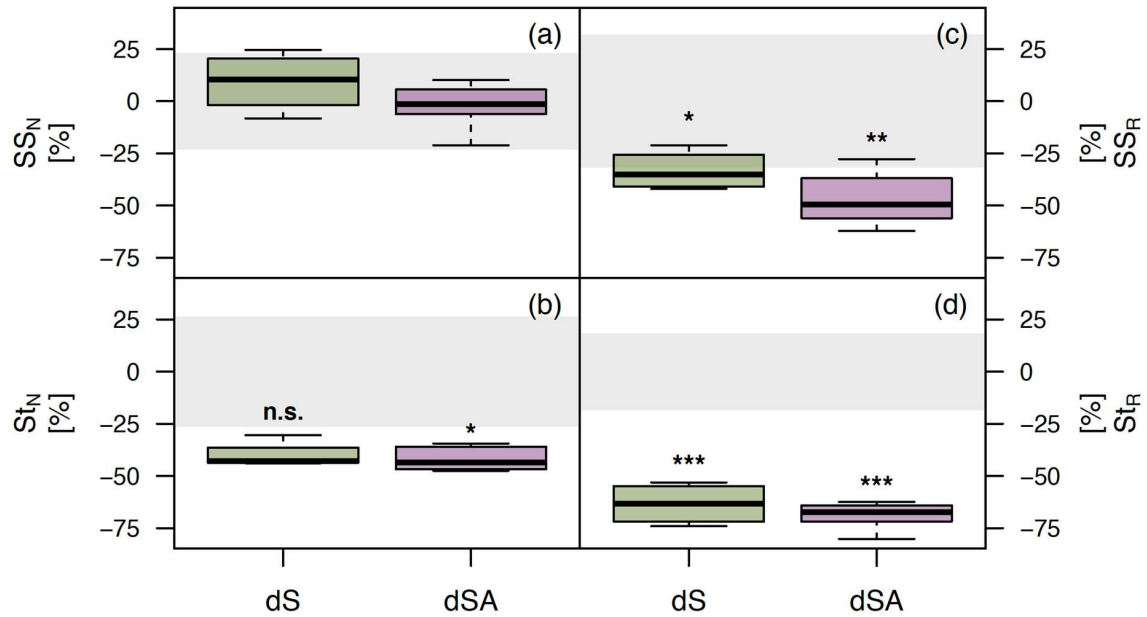


Figure 4.3: Responses of non-structural carbohydrates in Scots pine seedlings to experimental drought at the end of the experiment.

Needle soluble sugar (SS_N, a), needle starch (St_N, b), fine root soluble sugar (SS_R, c), fine root starch (St_R, d) concentrations in the control (Cntrl, $n = 4$), soil drought (dS, green, $n = 4$) and combined soil and air drought (dSA, violet, $n = 5$) treatment. Changes in soluble sugar and starch in dS and dSA are shown in percentage difference to the Cntrl treatment. Data is shown as boxplots with measurements outside 1.5 times the interquartile range above the upper quartile or below the lower quartile considered outliers. Standard deviation in the Cntrl treatment is shown as light grey area. Asterisks above dS and dSA represent statistical significance to the Cntrl treatment (anova with *post-hoc* Tukey; $p > .05$ n.s., $p < .05^*$, $p < .01^{**}$, $p < .001^{***}$). Samples were taken at the last day of the continuous ¹³CO₂ labeling experiment.

4.3.2 Needle water status, carbon uptake and growth parameters

Ψ_{md} (Figure 4.4a) apparently did not change much over the course of the experiment, but variation within each treatment was relatively large. However, as Ψ_{md} in the Cntrl tended to slightly increase from day 18 and reached -0.45 ± 0.06 MPa on day 27 while Ψ_{md} in dS and dSA remained at -1.00 ± 0.16 MPa, dS and dSA differed significantly from the Cntrl on day 21 and 27 (lme: Tukey HSD, $p < 0.01$, $t = 4.32$). RLWC (Supplemental Figure S4.3) was maintained at 70.5 ± 4.8 % in all treatments during the experiment.

The net CO₂ uptake per tree (sum of assimilation minus respiration, Figure 4.4b) tended to decrease steadily with drought progression in dS from day 14 and in dSA from day six onwards. In the dSA compared to the Cntrl treatment, the daily net CO₂ uptake was significantly lower from day 20 onwards (lme: Tukey HSD, $p = 0.034$, $t = 5.09$). The cumulative C uptake at the

end of the experiment, however, did not differ significantly between treatments. Considering that the CUE - derived from the diurnal sums of photosynthesis, root respiration and night-time shoot respiration - was unchanged between the treatments (0.36 ± 0.13 , Supplemental Figure S4.4), indicated that the trees were able to maintain a tight regulation of their C balance irrespective of the stress treatment.

Albeit a positive net C balance, aboveground growth in the stress treatments ceased. Needle elongation in dS and dSA appeared to halt under drought conditions reaching needle lengths of 3.61 ± 0.33 cm and 3.12 ± 0.14 cm at the end of the experiment, respectively (Figure 4.4c). Although needle elongation rates remained nearly constant in Cntrl and needle length was 5.23 ± 0.47 cm at the last measurement, treatment differences were not statistically significant (lme: Tukey HSD, $p > 0.05$) due to a large variation among measured needles. The responses of radial stem growth were much clearer and after the initiation of soil drought on day four, radial growth rates flattened immediately in dS and dSA trees (Figure 4.4d). The additional reduction in air humidity shortened the time between the first irrigation reduction and reaching values around zero radial growth by six days in dSA (-0.00 ± 0.03 mm d⁻¹ on average from day 10) compared to dS (-0.00 ± 0.02 mm d⁻¹ on average from day 16) while growth rates in the control remained at 0.02 ± 0.01 mm d⁻¹ on average. Accordingly, cumulative radial growth was lowest in dSA (0.11 ± 0.06 mm; lme: Tukey HSD, $p = 0.012$, $t = 6.37$) followed by dS (0.37 ± 0.16 mm; lme: Tukey HSD, $p > 0.05$) and highest in the control (0.57 ± 0.18 mm) by the end of the experiment.

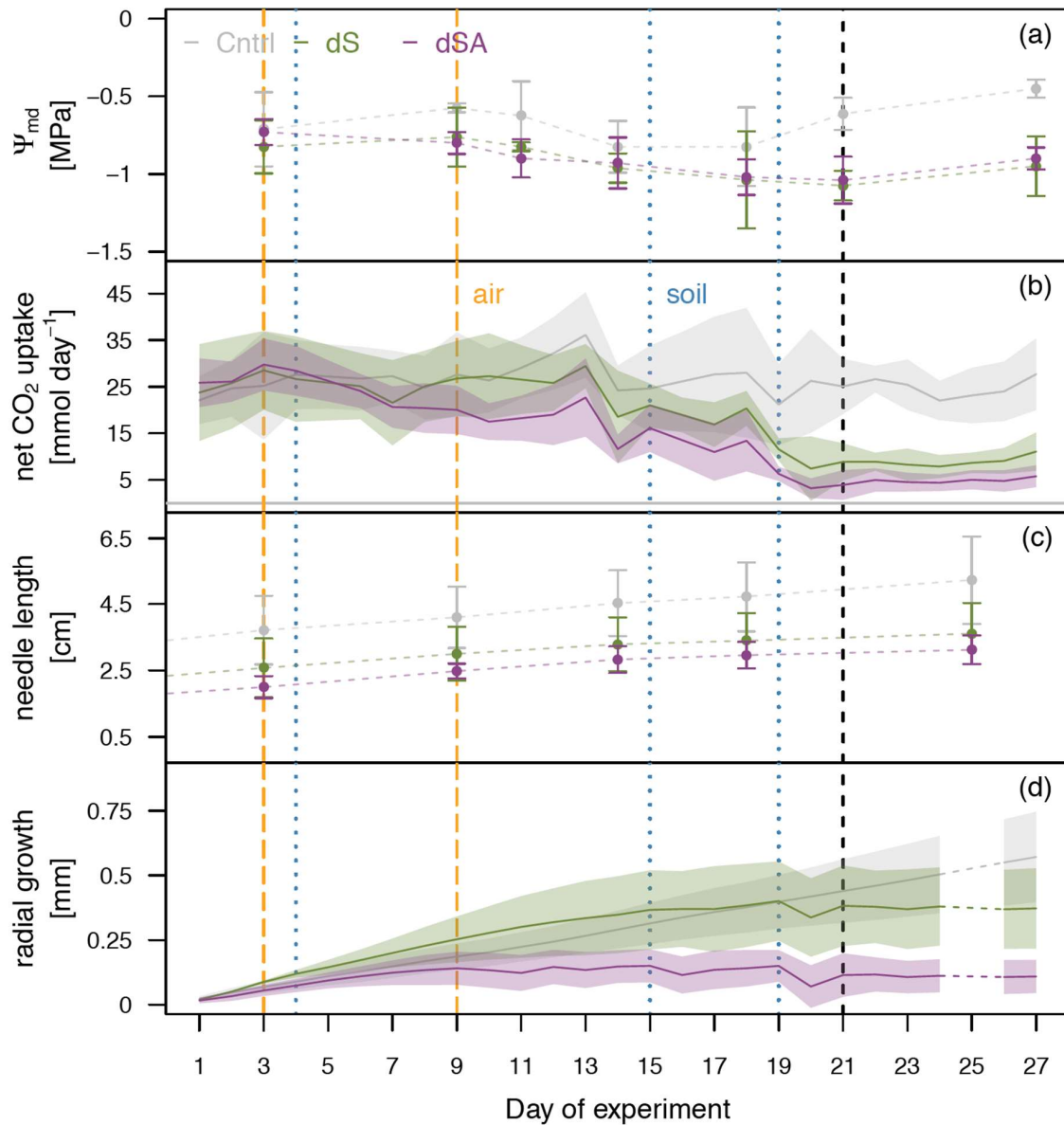


Figure 4.4: Progression of midday needle water potential and growth over the course of the experiment in Scots pine seedlings.

Midday needle water potential (Ψ_{md} , a), daily net CO_2 uptake (sum of assimilation and respiration, b), needle length (c) and cumulative radial growth (d) during the experiment in the control (Cntrl, grey), soil drought (dS, green) and combined soil and air drought (dSA, violet) treatment. Daily treatment averages \pm SD are either shown as data points and error bars (Cntrl and dS: $n = 8$, dSA: $n = 10$ in a and c) or lines and shaded areas (Cntrl and dS: $n = 4$, dSA: $n = 5$ in b and d). Data gaps are bridged by thin dashed lines. Experimental reductions in air humidity in the dSA treatment are given by the dashed orange lines and reductions in irrigation in the dS and dSA treatment are shown by the dotted blue lines, with the last line on day 19 marking irrigation at 50 ml per day. The begin of the continuous $^{13}\text{CO}_2$ labeling ($\delta^{13}\text{CO}_2$ of 500 ‰) is highlighted by a black dashed vertical line on day 21.

4.3.3 Dynamics of the ^{13}C label

Before the $^{13}\text{CO}_2$ -labeling, the isotopic signature of nighttime shoot respiration ($\delta^{13}\text{C}_S$) and root respiration ($\delta^{13}\text{C}_R$) did not differ between treatments (lme: Tukey HSD; $p > 0.05$; see Supplemental Table S4.3). Over the course of the $^{13}\text{CO}_2$ -labeling, respiration rates became enriched in $\delta^{13}\text{C}$ with the degree of the enrichment differed between the treatments. According

to their C uptake rates, highest $\delta^{13}\text{C}$ values were found in the Cntrl, followed by the dS and dSA treatment. Nighttime $\delta^{13}\text{C}_\text{S}$ (Figure 4.5a) in Cntrl trees reached a peak on day 25 at 345.37 ± 16.51 ‰, indicating that about 70 % of the respired C should have originated from the labeled C (assimilated during the first five days of the labeling). Similar dynamics were observed in dS and dSA, but $\delta^{13}\text{C}_\text{S}$ remained significantly lower than in the Cntrl (lme: Tukey HSD; dS: $p = 0.002$, $t = 9.37$; dSA: $p < 0.001$, $t = 15.55$). While $\delta^{13}\text{C}_\text{S}$ in dS peaked at 234.41 ± 33.47 ‰ on day 26, indicating that about 50 % of the respired C originated from the label, the peak value of $\delta^{13}\text{C}_\text{S}$ in dSA was with 171.25 ± 57.00 ‰ on day 25 the lowest, suggesting that the respired C originated mainly (about 65 %) from stored C assimilated prior to the labeling.

$\delta^{13}\text{C}_\text{R}$ (Figure 4.5b) followed a similar pattern, but showed a somewhat lower enrichment. Starting from $\delta^{13}\text{C}_\text{R}$ values of -12.54 ± 7.54 ‰ before labeling, $\delta^{13}\text{C}_\text{R}$ reached peak values of 302.85 ± 21.94 ‰ in Cntrl, 195.58 ± 37.24 ‰ in dS and 91.79 ± 37.24 ‰ in dSA on day 25 (lme: Tukey HSD, $p < 0.001$). This indicates a somewhat larger contribution of older C to the root respiratory efflux with treatment-specific differences. We estimated that about 40 % in the Cntrl, 60 % in the dS and 80 % in the dSA treatment originated from stored C that was assimilated prior to the labeling. The larger contribution of stored C to root respiration in the stressed seedlings agrees well with the pronounced depletion of root starch concentrations (Figure 4.3d).

The cumulative amount of ^{13}C respired (Figure 4.5c) and the amount of ^{13}C retained in the seedlings (Figure 4.5d) increased almost linearly throughout the $^{13}\text{CO}_2$ -labeling in all three treatments. The amount of ^{13}C retained compared to the ^{13}C respired was highest in the control trees with +28 %, followed by the dS: +11 % and dSA: +15 % treatments. Cntrl seedlings retained relative more of the labeled C than stressed trees, in agreement with a larger growth activity.

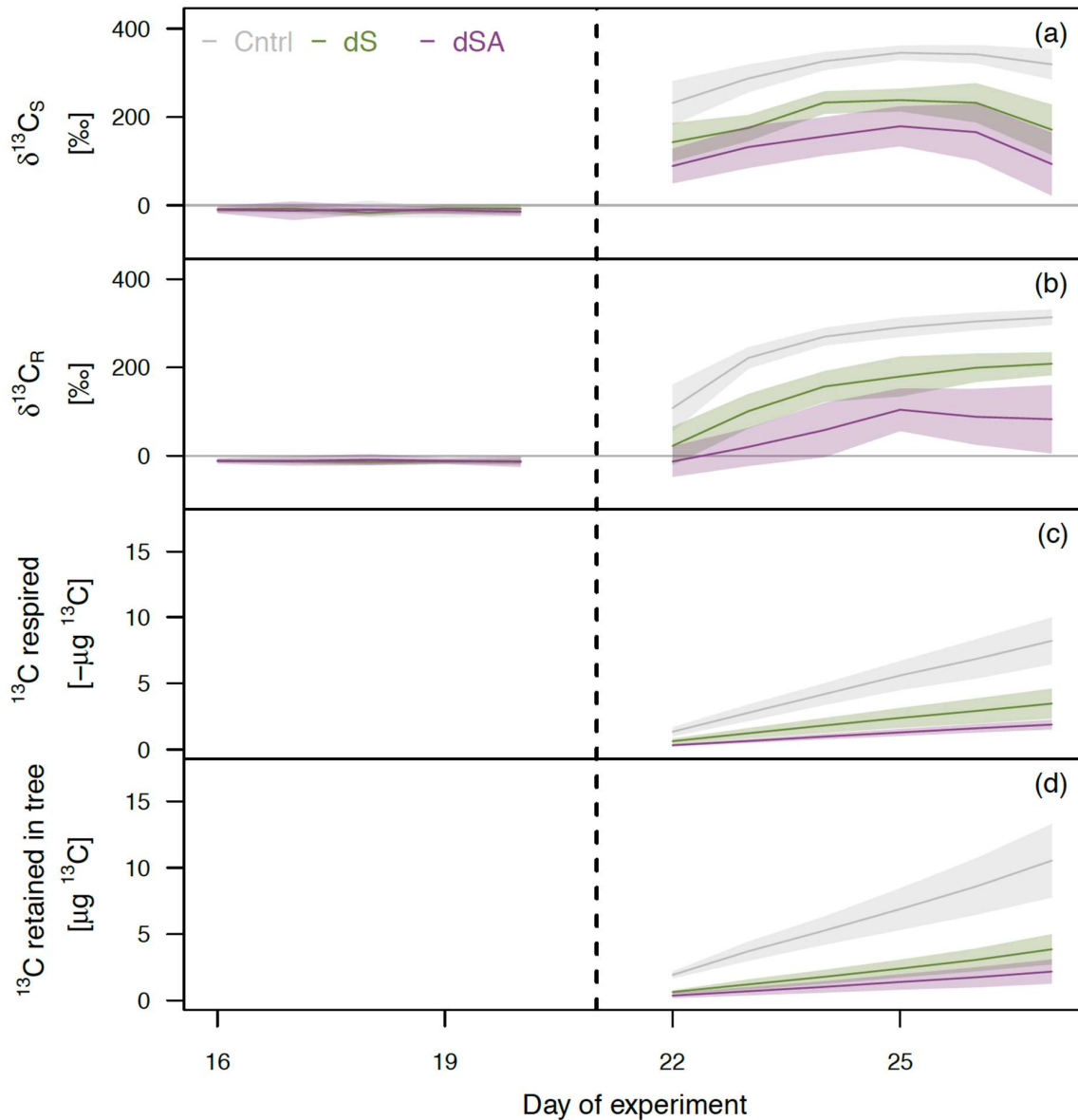


Figure 4.5: Dynamics of the isotopic signatures of nighttime shoot and root respiration before and during the $^{13}\text{CO}_2$ -labeling as well as the ^{13}C respired and retained in Scots pine seedlings.

The isotopic signature of daily-averaged shoot dark respiration ($\text{PAR} < 100 \mu\text{mol m}^{-2}\text{s}^{-1}$) ($\delta^{13}\text{C}_\text{S}$, a), root respiration ($\delta^{13}\text{C}_\text{R}$, b), cumulative sum of daily ^{13}C respired (shoot dark and root respiration) (c) and cumulative sum of daily ^{13}C retained in trees (d) are shown per treatment (control (Cntrl, grey), soil drought (dS, green) and combined soil and air drought (dSA, violet)). The shaded areas depict $\pm\text{SD}$ (Cntrl and dS: $n = 4$, dSA: $n = 5$). The begin of the labeling with ^{13}C -enriched CO_2 ($\delta^{13}\text{CO}_2$ of 500 ‰) is highlighted by the black dashed vertical line on day 21. Before the labeling, $\delta^{13}\text{CO}_2$ of the supply air stream was maintained for both shoot and root compartments at $-2.28 \pm 2.65 \text{‰}$ $\delta^{13}\text{C}$. As the switch to the ^{13}C -enriched gas interrupted the measurements on day 21, we show the results from day 22, when the measurements were reliable again. The amount of ^{13}C retained in the trees was estimated by calculating the cumulative sum of the canopy assimilation flux of ^{13}C minus the respiratory fluxes of ^{13}C .

In agreement with the ^{13}C retention, we found higher ^{13}C enrichment in the Cntrl compared to the drought-treated seedlings. Overall, a higher proportion of label in the root compared to the needle tissues indicated a more active role of roots as C sink at the end of the leaf elongation phase in Scots pine seedlings (Figure 4.6). A reduced aboveground growth activity in the droughted seedlings became further apparent as the ^{13}C label in bulk needle tissues did not

differ from before the label ($\delta^{13}\text{C}_\text{N}$, Figure 4.6a) and xylem cellulose showed only minimal enrichment in the dS treatment ($\delta^{13}\text{C}_\text{XC}$, Figure 4.6b). This was in stark contrast to the root tissues in which we found a clear signal of the label in all treatments (Figure 4.6c-d), but with a lowest enrichment in root cellulose of the dSA treatment, indicating lowest growth rates.

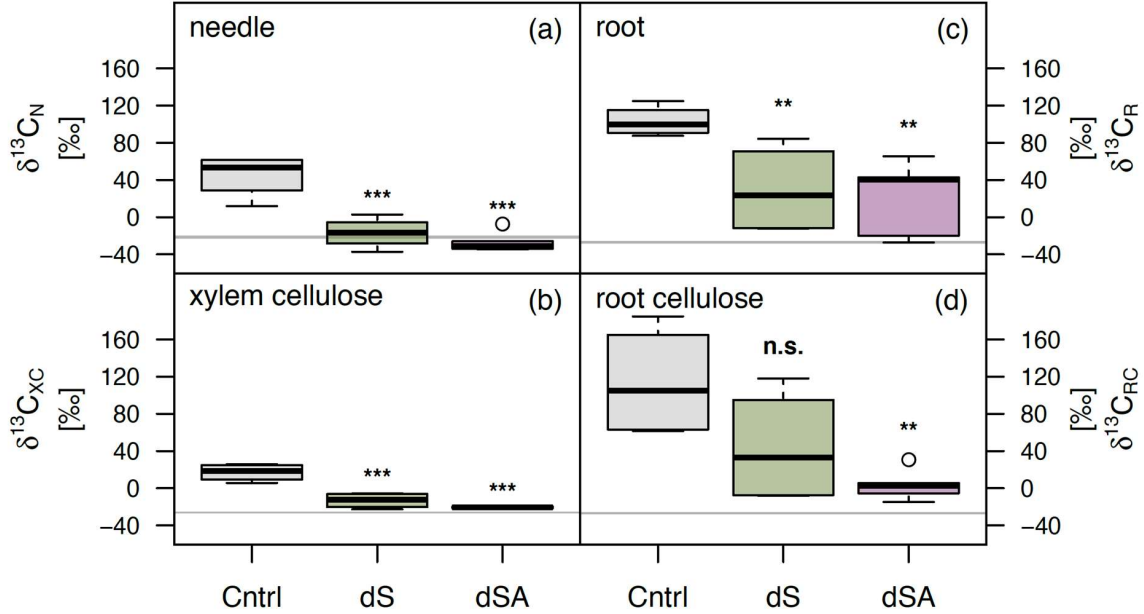


Figure 4.6: Isotopic signature of biomass and cellulose in Scots pine seedlings following six days of constant $^{13}\text{CO}_2$ -labeling ($\delta^{13}\text{CO}_2$ of 500 ‰). Changes in the isotope composition of needle biomass ($\delta^{13}\text{C}_\text{N}$, a), xylem cellulose ($\delta^{13}\text{C}_\text{XC}$, b), fine root biomass ($\delta^{13}\text{C}_\text{R}$, c) and fine root cellulose ($\delta^{13}\text{C}_\text{RC}$, d) in the control (Cntrl, grey, $n = 4$), soil drought (dS, green, $n = 4$) and combined soil and air drought (dSA, violet, $n = 5$) treatment. Data is shown as boxplots with measurements outside 1.5 times the interquartile range above the upper quartile or below the lower quartile considered as outliers. Natural abundance of needle ^{13}C is shown as light grey area (mean \pm SD). Before the labeling, $\delta^{13}\text{CO}_2$ of the supply air stream was maintained for both shoot and root compartments at -2.28 ± 2.65 ‰ $\delta^{13}\text{C}$. Asterisks above dS and dSA represent statistical significance to the Cntrl treatment (anova with *post-hoc* Tukey; $p > .05$ n.s., $p < .05^*$, $p < .01^{**}$, $p < .001^{***}$).

4.4 Discussion

The timing of the experimental drought, early during the growing season, had an influence on gas exchange and the allocation responses presented here, as growth in temperate trees is highly seasonal (Chen et al. 2022; Taeger et al. 2013; Vieira et al. 2020) and changes in allocation and C uptake might occur regardless of stress. However, the responses we observed and which deviated from the indicated constant early season allocation signal in the control seedlings can be interpreted as an early-season-specific stress signal triggered by soil and atmospheric drought.

4.4.1 Responses of canopy conductance and C uptake to VPD and soil drought

In our study we manipulated VPD in order to quantify the direct effect of increasing VPD on tree gas exchange during drought progression. We found g_canopy to respond faster than transpiration and A_net to rising VPD, confirming our first hypothesis. Depending on the degree of stomatal control, transpiration can be found to decrease (Eamus et al. 2013; Gharun et al. 2020), maintain or increase to rising VPD (Preisler et al. 2023), depending also on soil water

availability (e.g. Ruehr, Martin, and Law 2012). In addition, stomatal sensitivity to VPD varies across species (Creese et al. 2014; Cunningham 2004, 2005; Gao et al. 2015; Körner et al. 1989; McNaughton and Jarvis 1991; Whitehead, Okali, and Fasehun 1981). There is a general consensus that isohydric tree species have a greater stomatal sensitivity to VPD than anisohydric species (Buckley et al. 2017; Cernusak et al. 2019; Novick et al. 2019; Sperry et al. 2017). We found Scots pine seedlings to exhibit an immediate reduction in stomatal aperture in response to rising VPD and declining soil water content as indicated by a rapid decrease in g_{canopy} and no increase in transpiration in the combined drought-VPD treatment. This response was not observed in the drought-only treatment, where g_{canopy} declined more steadily alongside reductions in soil water content. As stomatal conductance is exponentially related to VPD, a 40 % decline in g_{canopy} has been reported for an increase in VPD from 0.5 to 1.5 kPa under non-water limiting conditions (Ruehr et al. 2016). This is further supported by the results of Poyatos et al. (2008), who found a decrease in relative sap flow in Scots pine at a VPD of 1.2 kPa. In our study, a VPD of 1.5 kPa was exceeded already one day after the first reduction in air humidity. Since there were no significant differences in RWC between the combined and the soil drought treatment, the observed reduction in g_{canopy} was sufficiently limiting transpiration. This limitation prevented increased water loss due to rising VPD throughout the experiment.

The seedling's attempt to mitigate a decline in water potential by tightly regulating leaf-level transpiration through g_{canopy} adjustments consequently affected photosynthesis. This delayed stress effect on photosynthesis is attributed to a typically lower reduction in photosynthesis at the initial decline in g_{canopy} and is mainly observed in phases when stress levels are still relatively low during conditions when photosynthesis is not affected by biochemical limitations. While this phenomenon has only recently been noted for VPD, it has been known for some time in the context of soil water deficit (Bogeat-Triboulot et al. 2007; Boyer 1970; Quick et al. 1992). The maintenance of photosynthesis under mild to moderate water stress is because mesophyll conductance to CO_2 is particularly resilient to water deficiency (Cornic 2000; Flexas and Medrano 2002; Kaiser 1987). Experiments have shown that Rubisco activity can be maintained despite a 50 % decrease in the relative water content of the leaves and a 75 % closure of the stomata (Flexas et al. 2006; Kaiser 1987). In the present study, the time between stress initiation and reduction in photosynthesis was short, as VPD increased rather rapidly alongside stomatal closure.

4.4.2 Tree growth affected by water availability and VPD

To date, tree growth in vegetation models is predominantly driven by a constant allocation from gross photosynthesis. Only recently have functions that represent direct dependencies of growth on climate parameters, such as soil water availability or VPD, found their way into the first models. This development was triggered by increasing evidence suggesting that growth processes may be more sensitive to water deficit than photosynthesis and may shut down even before assimilation is affected (Friend et al. 2019; Muller et al. 2011). This assumption is mainly based on the strong turgor dependence of the cell growth process (Cabon et al. 2020), especially cell expansion, so that a decrease in turgor during drought is likely to lead to an inhibition of tissue formation long before photosynthesis is the bottleneck process (Peters et al. 2021). In the attempt to establish such a direct relationship between drought and tree growth, the most frequently chosen method has been the analysis of radial stem growth. For example, by using a turgor-driven growth model, Peters et al. (2021) were able to successfully simulate stem radial increment of *Picea abies* (L.) Karst. and *Larix decidua* Mill. and identify a

soil water potential of -0.6 MPa as the critical value for stem growth. Similar results are reported by Eckes-Shephard et al. (2021), who simulated stem growth of trees growing in a dry temperate forest in the Swiss Alps based on soil moisture. Their results point to a crucial difference between the response of source and sink processes in trees to soil water availability, as they suggest that stem growth ceases at a soil water potential of -0.47 MPa in European larch and -0.66 MPa in Norway spruce, while photosynthesis can continue down to a soil water potential of -1.2 MPa or lower. In the present study, Scots pine radial growth also declines well before assimilation when Ψ_{md} was between -0.8 to -1.0 MPa, supporting the hypothesis that the turgor pressure in the cell-dividing tissue fell below the growth threshold before any pronounced reduction in the net photosynthesis occurred.

Despite the fact, that soil water availability seems to be a dominant factor for radial tree growth, atmospheric conditions, i.e. VPD, can also have a direct control on stem growth (Castellaneta et al. 2022; Zweifel, Zimmermann, and Newbery 2005). This can also be seen from our results since radial growth was inhibited 6 days earlier when Scots pine seedlings were additionally subjected to high VPD, while Ψ_{md} did not differ between the treatments. The importance of VPD for radial growth was also recently demonstrated by Zweifel et al. (2021), indicating that trees can grow in moderately dry soil provided that VPD is low, and that the requirement of a low VPD for radial growth of stems even leads to a temporal decoupling of stem growth (occurring at night) and photosynthesis (occurring during daylight). They identified a VPD threshold for radial growth of about 1 kPa, above that stem growth was only negligible. Our results seem to confirm such a VPD threshold, as in the high VPD treatment a VPD >1.5 kPa was maintained throughout day- and nighttime and stem increment ceased quickly, while photosynthesis continued, confirming our second hypothesis.

Since stem growth is not the only possible carbon sink, but one of several processes that can be sinks at different times, soil drought and VPD could alter primary and secondary growth processes independently. Another affected process appears to be needle elongation, as indicated by the tendency of decreasing growth rates in response to soil and air drought in the present study and no significant incorporation of the ^{13}C label in needle tissues in contrast to the control trees. This trend is consistent with other observations that water deficit affects both needle and stem growth (Irvine et al. 1998; Muller et al. 2011; Zweifel et al. 2020). For instance, Adams et al. (2015) estimated over 39 % reduction in leaf and shoot growth in response to drought and heat in piñon pine, and Dobbertin et al. (2010) found that after drought, irrigation increased needle length by 70 %, shoot length by 100 % and ring width by 120 % in Scots pine. As growth in temperate trees is highly affected by seasonality, observing stress impacts on leaf and shoot elongation is restricted to the early growing season. Therefore, we advocate for stress experiments being conducted during the leaf expansion phase to disentangle impacts of environmental stressors on tree growth.

4.4.3 Sink activity drives C allocation under drought stress

To address stress impacts on tree carbon allocation, particularly to belowground tissues, we conducted a $^{13}\text{CO}_2$ labeling. The regulation of carbon partitioning, including the export of carbon from photosynthesizing source tissues to various sink tissues, has a major impact on tree growth and development, as photoassimilates are the primary source of energy and building blocks for production and maintenance of biomass. Since carbon allocation involves the production, transport and utilization of photoassimilates and all three of these processes are highly water sensitive (DaCosta and Huang 2006; Gao et al. 2021; Lemoine et al. 2013;

McDowell 2011; Rambal et al. 2014), it is not surprising that drought affects carbon allocation at the whole tree level (Ruehr et al. 2009). In our study, we found an about 3–5-times, lower retainment of ^{13}C in the stressed trees compared to the control trees, confirming a strong downregulation of growth activities under drought conditions.

It is widely acknowledged that new assimilates are preferably transferred to the tissues with the highest C demand (Lambers et al. 2008). Some experimental evidence suggests that water scarcity shifts allocation priorities in favor of roots (DaCosta and Huang 2006; Poorter et al. 2012), possibly an adaptive mechanism to maintain the osmotic potential and cell turgor of the roots and access limited soil water (Brunner et al. 2015; Comas et al. 2013). In our experiment we found a clear ^{13}C enrichment in the root biomass and even in the root cellulose in both drought treatments, but with a lower incorporation in the dSA trees exposed to moderate soil drought and high VPD. In addition, the virtual absence of ^{13}C in the examined aboveground biomass of needles and xylem cellulose seems to confirm the cessation of stem and needle growth in response to high VPD and moderate soil drought in Scots pine seedlings while belowground growth was partially sustained, largely agreeing with our third hypothesis.

At the whole tree level, downregulation of carbon allocation to sinks before the carbon source ceases and shifting carbon allocation priorities makes physiological sense, as it could reduce the risk of a critical impact on the tree's carbon balance, which could be particularly important during prolonged or severe drought stress (Rowland et al. 2015). As both, photosynthesis and the transport system become more limited under such enhanced stress conditions, there are also reports of reduced carbon transport to the roots during drought (Brunner et al. 2015; Poorter et al. 2012; Rehschuh et al. 2022; Ruehr et al. 2009), suggesting that increased belowground carbon allocation may be restricted to the initial phase of drought and/or under mild drought conditions. In agreement we detected the lowest ^{13}C signal in root respiration and root biomass in the compound stress treatment. Additionally, our study demonstrates that not only above- and belowground growth, but also respiration rates decreased. Thus, the Scots pine seedlings maintained both a constant CUE (ratio of total respiration to net assimilation) of 0.36 ± 0.13 , which falls within the range of CUE values between 0.26 and 0.66 reported for pine forests by DeLucia et al. (2007), and a positive net carbon uptake (assimilation minus respiration) throughout the experiment, rejecting largely our fourth hypothesis. Although this could indicate that the Scots pine seedlings were not suffering from a general carbon deficiency, the low ^{13}C retainment in the stressed seedlings (about 3–5 times lower compared to the control) and the reductions in starch concentrations particularly in the roots at the end of the experiment indicate that carbon assimilation might have not longer met the belowground sink demand. This is presumably supported by the much lower contribution of the $\delta^{13}\text{C}$ label to respiration in the stressed (dS: 45 % dSA: 28 %) compared to the control seedlings (Cntrl: 65 %). Thus, instead of recent photosynthates, NSC reserves were largely utilized to meet the respiratory demand belowground. This is in agreement with previous studies showing a reduced contribution of the ^{13}C label to soil respiration during drought (Hagedorn et al. 2016). While we found that the contribution of the label to root respiration was lower than to shoot respiration, which is consistent with results from other studies on pine trees (Aaltonen et al. 2017; Chang et al. 2022; Rog, Jakoby, and Klein 2021), we detected the ^{13}C label in fine root biomass and root cellulose, but merely in the needle tissue. Such increased photosynthate allocation belowground, which presumably promotes root structural growth during drought, has been frequently suggested for pine seedlings (Aaltonen et al. 2017; Jeong, Bolan, and Kim 2021; Y. Liu et al. 2020; Solly et al. 2023). However, other labelling studies under drought have found a reduced belowground allocation as for instance shown for beech (e.g. Ruehr et al.

2009) or for Amazonian forests (Doughty et al. 2014, 2015). A likely explanation of the continuous belowground allocation and hence observed root growth in our study might have been the rather modest soil drought, as the midday leaf water potential did not decline below -1.2 MPa, due to constant night-time irrigation of 50 ml in both drought treatments. The indicated influence of the severity of the drought and possibly also the tree species illustrates the complexity of the response of C allocation to drought and makes it clear that it merits further investigation.

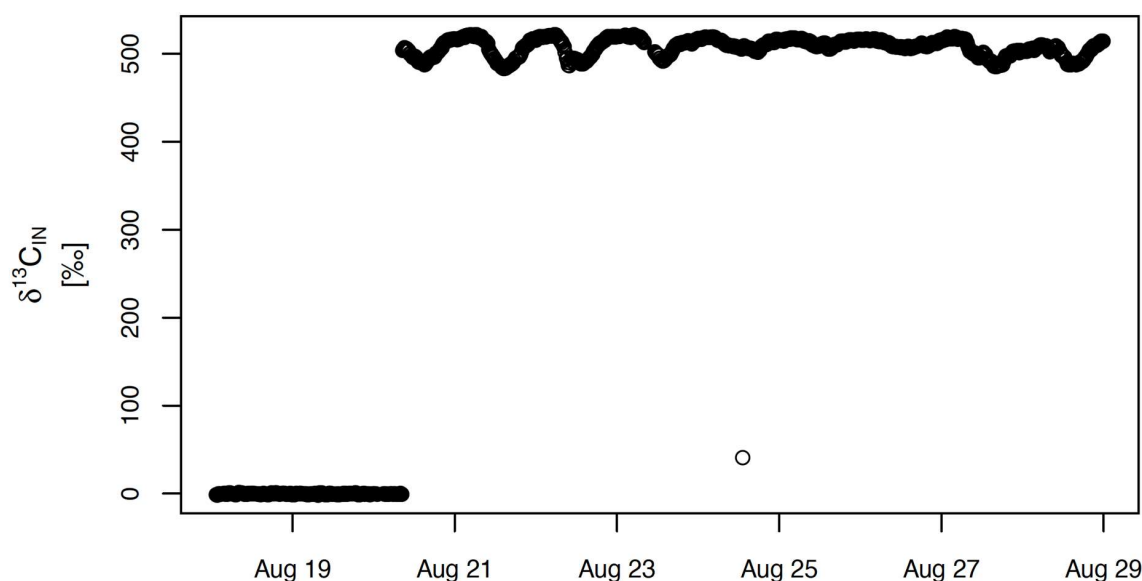
4.5 Conclusion

We studied the response of Scots pine seedlings to increased VPD under moderate soil drought based on the general hypothesis that seedlings exposed to such compound stress attempt to buffer the impact on their C balance (assimilation minus root and nighttime shoot respiration) and maintain their water uptake by tightly regulating gas exchange and shifting C allocation belowground. The C balance of the seedlings remained positive because, on the one hand, photosynthesis was less water sensitive than g_{canopy} and on the other hand, respiration decreased in parallel with photosynthesis and starch remobilization appeared to support respiration. In addition, growth processes were very sensitive to soil and atmospheric drought, as evidenced by a decline in aboveground growth that could not be linked exclusively to C limitation. At the same time, belowground sink activity was maintained, driving the allocation of recent C. Our results emphasize the need to consider sink-driven C allocation and the role of VPD in limiting growth independent of a substantial impairment of photosynthesis.

Acknowledgements

We are grateful to Rudolf Meier, Benjamin Birami and Andrea-Livia Jakab for experimental support and thank Romy Rehschuh, Manuela Oettli and Ulrike Ostler for isotopic MS analyses. This study was supported by the German Research Foundation through its Emmy Noether Program (RU 1657/2-1).

4.6 Supplement



Supplemental Figure S4.1: Isotopic signature of the supply air stream ($\delta^{13}\text{C}_{\text{IN}}$) during the last twelve days of the experiment.

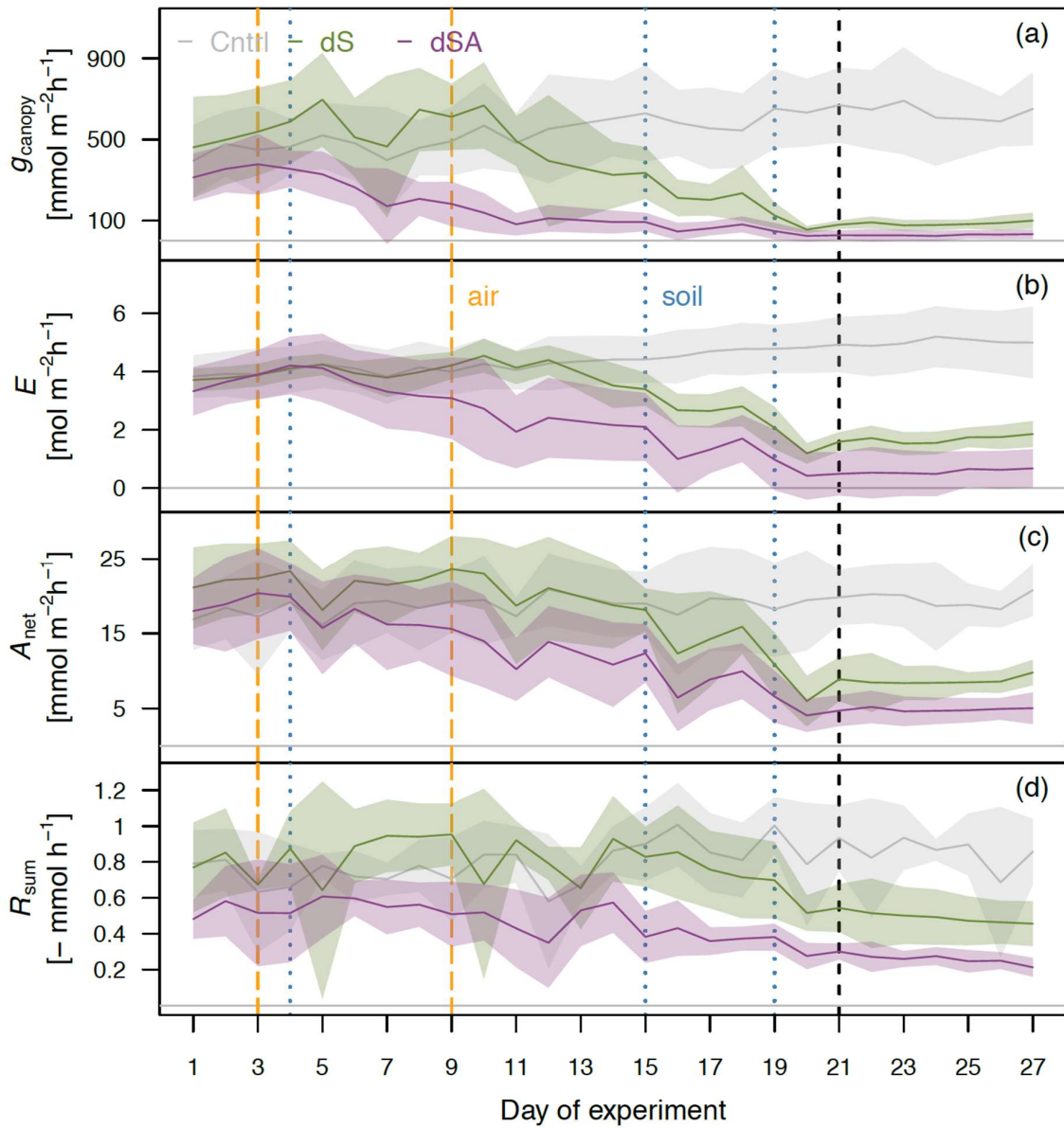
The whole-tree labeling with ^{13}C -enriched CO_2 ($\delta^{13}\text{CO}_2$ of 500 ‰) started on Aug. 20 (day 21 of the experiment). Before the labeling, $\delta^{13}\text{CO}_2$ of the supply air stream was maintained for both shoot and root compartments at -2.28 ± 2.65 ‰ $\delta^{13}\text{C}$.

Supplemental Table S4.1: Biomass of Scots pine seedlings per treatment.

Needle, woody tissue and root biomass as well as root/shoot ratio was destructively harvested end of the experiment. Shown are mean \pm SD for the Cntrl ($n = 4$), dS ($n = 4$) and dSA ($n = 5$) treatment. Values are given in dry weight (DW). Differences between treatments tested with anova and *post-hoc* Tukey were not significant ($p > 0.05$).

	biomass [gDW]			
	needle	woody tissue	root	root/shoot
Cntrl	26.92 \pm 6.92	16.16 \pm 4.10	18.97 \pm 4.14	0.45 \pm 0.04
dS	27.34 \pm 8.73	17.97 \pm 4.93	17.34 \pm 7.31	0.38 \pm 0.09
dSA	25.51 \pm 6.50	16.32 \pm 5.32	13.95 \pm 2.00	0.35 \pm 0.06

High vapor pressure deficit and soil drought impair aboveground growth before photosynthesis while shifting C allocation to roots in Scots pine



Supplemental Figure S4.2: Progression of gas exchange over the course of the experiment in Scots pine seedlings.

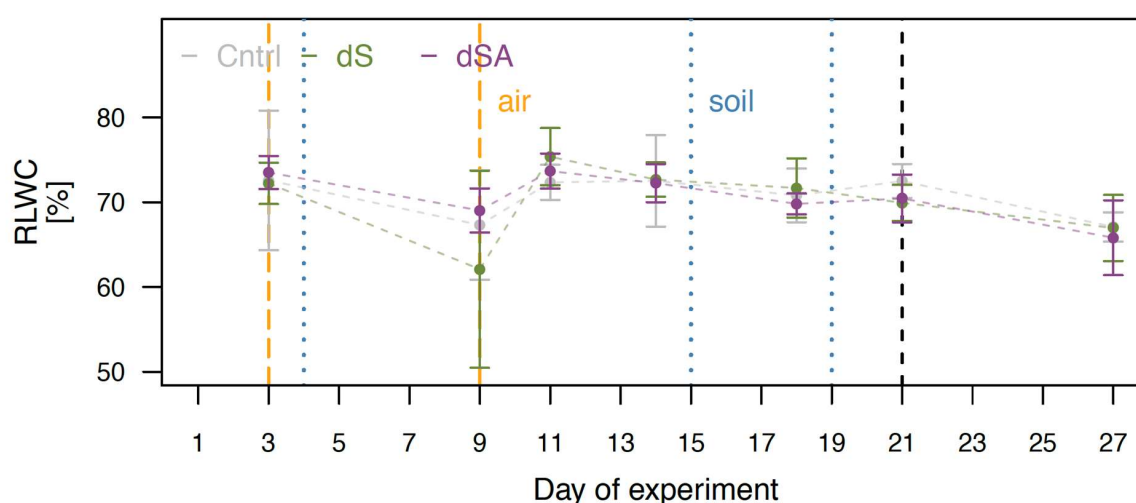
Canopy conductance per leaf area (g_{canopy} , a), transpiration per leaf area (E , b), net assimilation per leaf area (A_{net} , c) and sum of daily root and nighttime (PAR $>100 \mu\text{mol m}^{-2}\text{s}^{-1}$) shoot respiration per tree (R_{sum} , d) during the experiment in the control (Cntrl, grey), soil drought (dS, green) and combined soil and air drought (dSA, violet) treatment. Lines mark daily treatment averages and the shaded areas are \pm SD (Cntrl and dS: $n = 4$, dSA: $n = 5$). Experimental reductions in air humidity in the dSA treatment are given by the dashed orange lines and reductions in irrigation in the dS and dSA treatment are shown by the dotted blue lines, with the last line on day 19 marking irrigation at 50 ml per day. The begin of the continuous $^{13}\text{CO}_2$ labeling ($\delta^{13}\text{CO}_2$ of 500 ‰) is highlighted by a black dashed vertical line on day 21.

High vapor pressure deficit and soil drought impair aboveground growth before photosynthesis while shifting C allocation to roots in Scots pine

Supplemental Table S4.2: Non-structural carbohydrate concentration in needles and fine roots of Scots pine seedlings.

Fine root and needle biomass was sampled at the end of the experiment. Needle soluble sugar (SS_N), needle starch (St_N), fine root soluble sugar (SS_R), fine root starch (St_R) concentrations in the control (Cntrl, *n* = 4), soil drought (dS, *n* = 4) and combined soil and air drought (dSA, *n* = 5) treatment at the end of the experiment. Data is shown as mean ±SD. Lower case letters represent statistical significance between values within a column (anova with *post-hoc* Tukey; *p* < .05).

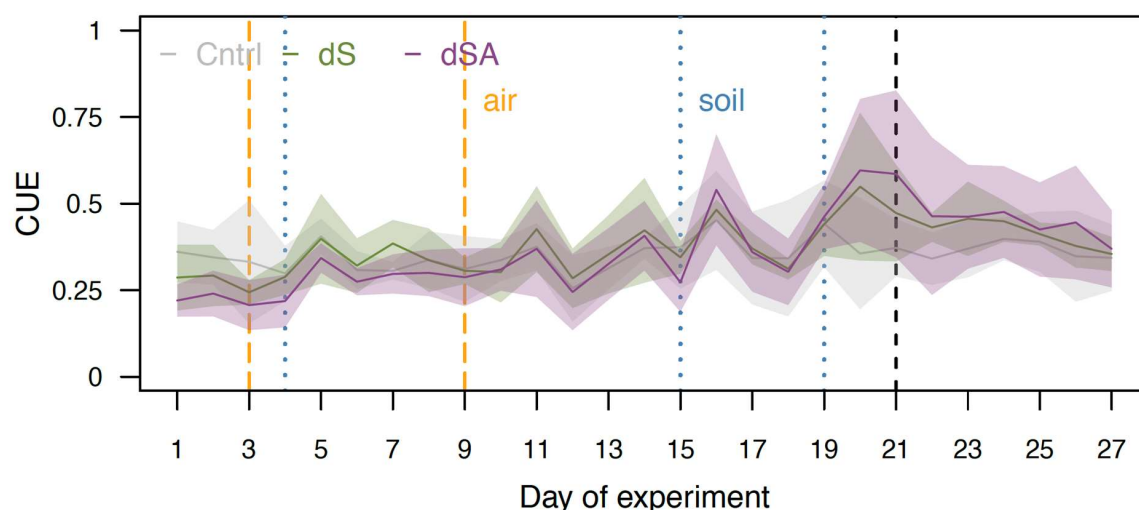
	non-structural carbohydrates [$\mu\text{mol glucose gDW}^{-1}$]					
	SS _N	St _N		SS _R	St _R	
Cntrl	476.8±109.7	150.1±39.7	a	1998.4±635.3	816.5±149.7	a
dS	520.9±68.2	90.0±9.7		1332.1±191.6	299.1±82.5	b
dSA	464.5±57.7	87.6±9.1	b	1069.5±281.0	251.8±58.1	b



Supplemental Figure S4.3: Progression of midday relative leaf water content over the course of the experiment in Scots pine seedlings.

Midday relative leaf water content (RLWC) during the experiment in the control (Cntrl, grey), soil drought (dS, green) and combined soil and air drought (dSA, violet) treatment. Daily treatment averages ±SD are shown as data points and error bars (Cntrl and dS: *n* = 8, dSA: *n* = 10). Data gaps are bridged by thin dashed lines. Experimental reductions in air humidity in the dSA treatment are given by the dashed orange lines and reductions in irrigation in the dS and dSA treatment are shown by the dotted blue lines, with the last line on day 19 marking irrigation at 50 ml per day. The begin of the continuous ¹³CO₂ labeling (δ¹³CO₂ of 500 ‰) is highlighted by a black dashed vertical line on day 21.

High vapor pressure deficit and soil drought impair aboveground growth before photosynthesis while shifting C allocation to roots in Scots pine



Supplemental Figure S4.4: Progression of the daily carbon-use efficiency (CUE) over the course of the experiment in Scots pine seedlings.

CUE ((root respiration + nighttime shoot respiration) / net assimilation) during the experiment in the control (Cntrl, grey), soil drought (dS, green) and combined soil and air drought (dSA, violet) treatment. Lines mark daily treatment averages and the shaded areas are \pm SD (Cntrl and dS: $n = 4$, dSA: $n = 5$). Experimental reductions in air humidity in the dSA treatment are given by the dashed orange lines and reductions in irrigation in the dS and dSA treatment are shown by the dotted blue lines, with the last line on day 19 marking irrigation at 50 ml per day. The begin of the continuous $^{13}\text{CO}_2$ labeling ($\delta^{13}\text{CO}_2$ of 500 ‰) is highlighted by a black dashed vertical line on day 21.

Supplemental Table S4.3: Isotopic signatures of nighttime shoot and root respiration before the $^{13}\text{CO}_2$ -labeling in Scots pine seedlings.

The isotopic signature of shoot night and root respiration are shown as daily treatment (control (Cntrl), soil drought (dS) and combined soil and air drought (dSA)) means \pm SD (Cntrl and dS: $n = 4$, dSA: $n = 5$). There was no statistically significant treatment effect before the label (lme: Tukey HSD, $p > 0.05$). The three weeks before the labeling, $\delta^{13}\text{CO}_2$ of the supply air stream was maintained for both shoot and root compartments at -2.28 ± 2.65 ‰ $\delta^{13}\text{C}$.

	$\delta^{13}\text{C}$ before label [‰]	
	shoot respiration	root respiration
Cntrl	-13.02 ± 10.98	-14.10 ± 4.42
dS	-9.20 ± 8.04	-12.23 ± 5.81
dSA	-11.41 ± 12.41	-11.47 ± 10.19

5 Synthesis

By subjecting Aleppo pine seedlings grown under elevated atmospheric $[\text{CO}_2]$ (eCO_2) to lethal soil drought events and Scots pine seedlings to combined soil and atmospheric drought using individual tree chambers in a greenhouse, this thesis aimed to determine the following:

1. The effect of eCO_2 on carbon and water relations prior to soil drought and the cause of the g_{canopy} reduction under eCO_2 in pine seedlings.
2. How eCO_2 and high VPD affect the response of pine seedlings to soil drought, particularly in terms of carbon balance, carbon allocation and growth.
3. Critical thresholds beyond which tree mortality is inevitable during severe soil drought and the effect of eCO_2 on these thresholds and hence on the mortality risk of Aleppo pine seedlings.

Carbon and water relations before drought

Growth under eCO_2 had a distinct effect on carbon-related traits in Aleppo pine seedlings, such as an increase in net C uptake (+143 %) and non-structural carbohydrates (NSC) (leaf starch +112 %), indicating excess carbon storage in leaves. In addition, needle, wood and root biomass rose equally by approximately 28 %, resulting in an unchanged root to shoot ratio (Chapter 2), confirming previous observations of unchanged C allocation patterns in pines under eCO_2 and abundant water (e.g. Curtis and Wang 1998; Dror and Klein 2022). In terms of water-related traits, observed lower leaf level canopy conductance (g_{canopy}) and transpiration rate (E) did not result in obvious water savings, as the increase in leaf area, evident in both leaf number and individual leaf size (Chapter 1), compensated for these reductions (Chapter 2). Nevertheless, in combination with the higher net C uptake, the lack of eCO_2 effect on water loss still represented an enhanced water use efficiency. Reduced g_{canopy} is a very common observation under eCO_2 and is usually a direct response via active stomatal aperture adjustment. In contrast, in Aleppo pine seedlings grown under eCO_2 , abscisic acid (ABA) levels and the insensitivity of g_{canopy} to reduced $[\text{CO}_2]$ provided evidence for an indirect g_{canopy} reduction due to anatomical changes (Chapter 1). At leaf level, the increase in radial path length (vein-to-epidermis distance +65 %) and in stomatal density (SD) (+23 %) and epidermal cell density (ED) (+25 %) probably contributed to the reduction in g_{canopy} . In addition, at the branch level, xylem porosity decreased (conduit lumen fraction -11 % and mean conduit diameter -8 %), reducing both specific conductivity (K_s) (-19 %) and leaf specific conductivity (K_i) (-34 %). (Chapter 1)

The observed anatomical changes were likely triggered by reduced stomatal aperture and reduced water demand during early seedling development under eCO_2 and consolidated during the prolonged eCO_2 exposure time of two years. Since the observed anatomical adjustments can be attributed to the prolonged exposure time, the growth reductions,

allocation shifts and reduced g_{canopy} in response to water stress events (Chapter 4) would likely also drive structural changes over time (Martínez-Vilalta et al. 2009; Poyatos et al. 2007; Sultan 2000) which could either amplify or weaken the eCO₂ effect. Evidence of such long-term acclimatization highlights the importance of considering past environmental conditions on current processes, as structural changes could, for example, alter the sensitivity of stomata and the photosynthetic apparatus to short-term environmental fluctuations. However, the structural changes did not result in obvious water savings at tree level, which challenges the assumption of an overall eCO₂ benefit during drought, as suggested by the reduced leaf-level E and increased C availability. (Figure 5.1)

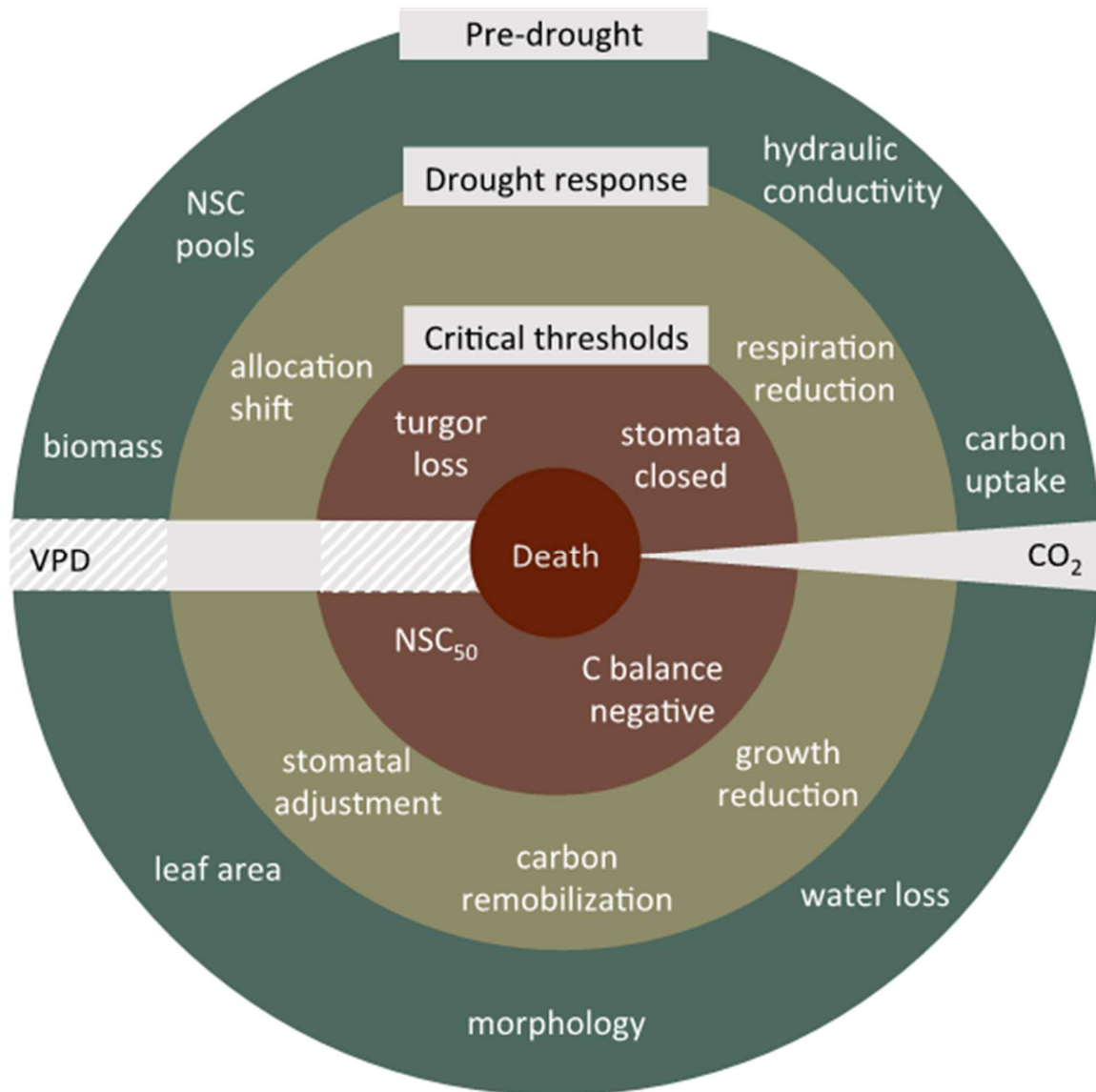


Figure 5.1: The multifaceted mortality process of pine trees during soil drought.

Representation of the progression of a lethal soil drought in pine seedlings from tree-specific pre-drought characteristics (outer ring, green) to death (center, red). In between are the drought response mechanisms (middle ring, olive) and the critical thresholds (inner ring, brown) beyond which seedling death is inevitable. Characteristic of the mortality process is the high degree of interconnectivity and interdependence of the underlying processes and mechanisms associated with hydraulic failure and carbon (C) starvation. There are also additional external factors that influence the process, such as atmospheric vapor pressure deficit (VPD) and carbon dioxide (CO₂) concentration. The effects of elevated atmospheric [CO₂] (c. 900 ppm) and high VPD (c. 2.9 kPa), as observed in the context of this thesis, are shown as gray areas. Because the effects of VPD on pre-drought characteristics and critical thresholds were not explicitly examined in this thesis, the assumed effects are shown as shaded areas. NSC, non-structural carbohydrates; NSC₅₀, 50 % loss of starch reserves.

Drought response

An important response mechanism of pine seedlings to soil drought was the gradual reduction of g_{canopy} in parallel with the reduction in soil water content (Chapter 2, Chapter 1, Chapter 4).

These short-term adjustments in g_{canopy} were facilitated by adjustments in ABA levels (Chapter 1) and served to limit water loss through transpiration and maintain the water potential gradient that determines water flow through the tree. These stomatal response mechanisms to soil drought were unaffected by $e\text{CO}_2$, as evidenced by the same leaf water potential and ABA levels in both CO_2 treatments (Chapter 2, Chapter 1). A similar observation was made for the stomatal response to high vapor pressure deficit (VPD), as g_{canopy} decreased by 60 % independent of CO_2 when VPD increased from 1 to 2 kPa, despite a reference g_{canopy} (g_{canopy} at VPD of 1 kPa) that was 55 % lower in $e\text{CO}_2$ (Chapter 1). These observations are consistent with the results of Birami et al. (2020), who found that $e\text{CO}_2$ did not alter stomatal sensitivity to heat in Aleppo pine. Given the observed g_{canopy} response to either soil drought or high VPD, it was not surprising that soil and atmospheric drought combined induced an even more rapid and pronounced g_{canopy} reduction (Chapter 4). In this way, transpiration in Scots pine seedlings was restricted to such an extent that high VPD (c. 2.9 kPa) had no effect on relative soil water content (RWC) and midday leaf water potential (Ψ_{md}) (Chapter 4).

Considering the trade-off between water loss and C uptake, the reduction in g_{canopy} in response to water stress subsequently limited photosynthesis (Chapter 2, Chapter 4) although with some delay as photosynthesis was less sensitive to soil and/or atmospheric drought than g_{canopy} (Chapter 4). In addition, respiration decreased in parallel with assimilation, which maintained a constant carbon use efficiency (CUE, ratio of respiration to assimilation) (Chapter 4) and a positive C balance (assimilation minus respiration) in pines under moderate drought stress (Chapter 2, Chapter 4). Growth processes showed high sensitivity to soil and atmospheric drought, as aboveground growth activities decreased at Ψ_{md} -0.8 MPa or when VPD exceeded 1 kPa and stopped at Ψ_{md} -1 MPa or when VPD exceeded 2 kPa, while belowground sink activity was partially maintained, driving recent C allocation (Chapter 4).

The rapid changes in leaf elongation and stem radial growth rates after abrupt changes in soil water availability or atmospheric evaporative demand in Scots pine seedlings could not be exclusively related to C, but rather to potential hydraulic limitation (Chapter 4). This would have primarily affected expansive growth, which is determined by hydromechanical processes (Pantin et al. 2011; Pantin, Simonneau, and Muller 2012). Although not explicitly investigated, this proposed hydraulic growth limitation, combined with the lack of $e\text{CO}_2$ effect on Ψ_{md} and general drought response mechanisms (Chapter 2, Chapter 1), suggests that $e\text{CO}_2$ should have no effect on the timing or magnitude of such hydraulic growth limitation. In contrast, when photosynthesis is the bottleneck process and C availability is the limiting factor for growth, $e\text{CO}_2$ should be beneficial due to sustained increased assimilation rates and NSC pools (Chapter 2), which pines draw upon to compensate for C deficits when assimilation does not meet C requirements (Chapter 2, Chapter 4).

The drought response of pine seedlings was shown to be a highly fine-tuned, interconnected process, balancing the supply and demand of carbon and water. This was characterized by different water sensitivities of key physiological processes, such as stomatal regulation and photosynthesis, and shifts in C allocation. Furthermore, $e\text{CO}_2$ -induced structural changes did not affect the metabolic and hydrological drought response of pine seedlings. In conclusion, these results suggest that, firstly, $e\text{CO}_2$ is unlikely to fully offset hydrological growth limitation and, secondly, any $e\text{CO}_2$ benefit is likely to be outweighed by the greater limitation imposed by high VPD on pine seedlings during soil drought. This effect is likely to be more pronounced if high VPD also affects soil water availability through increased soil evaporation, potentially exacerbating drought progression. (Figure 5.1)

Critical thresholds and drought mortality risk

The multifaceted nature of the mortality process during soil drought has led to the definition of critical thresholds for both hydraulic failure and carbon starvation. While leaf turgor loss (Ψ_{md} falling below the turgor loss point) is primarily associated with hydraulic failure, stomatal closure (g_{canopy} below minimum g_{canopy}) is important for both water and carbon relations, marking the point at which a tree can no longer actively reduce water loss and photosynthesis ceases. However, stomatal closure alone is not sufficient to assess the effects of water stress on the C economy of trees, as, for example, photosynthesis is significantly reduced before stomatal closure is complete (Chapter 2, Chapter 1, Chapter 4). Therefore, the transition from a positive to a negative C balance (assimilation minus shoot and root respiration) and the depletion of carbon reserves (NSC₅₀, 50 % loss of needle starch) were defined as additional thresholds mainly related to carbon deficiency. Although the underlying mechanisms are highly interrelated, the selected thresholds showed a tendency for hydraulic factors to become more important in the mortality process of Aleppo pine seedlings during severe soil drought (Chapter 2). This was particularly evident at eCO₂, as the delayed crossing of the NSC₅₀ threshold did not lead to a reduction in the overall mortality risk (all critical thresholds combined), with the risk probabilities of turgor loss and stomatal closure remaining unaffected by eCO₂ (Chapter 2; Chapter 1). Therefore, morphological changes in response to growth under eCO₂ did not improve the hydraulic safety of Aleppo pine seedlings during either a short (41 days) or a prolonged (82 days) lethal soil drought (Chapter 2; Chapter 1). This suggests that the prediction of mortality risk of pine trees may be more accurate based on hydraulic than on the C status of the tree. However, as the eCO₂ benefit of increased NSC pools was carried over into severe stress, as reflected by the delay in the NSC₅₀ threshold, and the cause of death under aCO₂ was not as clear, thresholds associated with carbon starvation should not be completely disregarded.

Overall, based on the observations presented, conditions can be defined that determine the potential benefits of eCO₂ for pines. The first critical factor relates to the stimulation of leaf area by eCO₂ and thus mainly to the observed pre-drought characteristics. If the CO₂-induced reduction in water loss at the leaf level is compensated by an increase in leaf area, then water loss at the tree level, and thus drought progression and mortality risk, should not change (Chapter 2; Chapter 1). However, if there is no compensating increase in leaf area, the CO₂-induced reduction in leaf water loss should result in water savings at the tree level and thus slow drought progression and reduce mortality risk. In controlled environments where plants do not compete for water, this conclusion may be true, but in the field, the water saving strategy would only be optimal if neighboring plants do not have access to the saved water and the saved water is not lost to the tree in other ways, such as soil evaporation. As a result, investing more in biomass at the expense of water conservation may be the more optimal approach, as an expanded root system and greater rooting depth, for example, could facilitate access to larger soil moisture pools. However, this mechanism is rarely tested because this trait is quite difficult to measure and most eCO₂ experiments take place in environments with limited soil volume, which may limit root system expansion (Arp 1991). The next factor influencing the potential eCO₂ benefit is the drought itself. If hydraulic limitations are pushed beyond their critical thresholds before C limitations exceed their respective critical thresholds, then eCO₂ should not be beneficial (Chapter 2). However, if the reverse is true, then eCO₂ should improve tree resilience to drought by delaying the crossing of critical C thresholds and potentially supporting faster or more complete recovery due to higher C availability if the drought event is not lethal. Such an eCO₂ benefit could be enhanced by high VPD if an increase in VPD further

reduces g_{canopy} and subsequently photosynthesis during soil drought, but does not affect the progression of the drought, thus promoting carbon starvation. On the other hand, if high VPD exacerbates drought progression by increasing water loss, thereby promoting hydraulic failure, then $e\text{CO}_2$ should not be beneficial. (Chapter 4)

Given the predicted increase in the frequency and severity of soil droughts and the concurrent rise in VPD (Gu et al. 2019; F. Li et al. 2023; Zheng et al. 2023), the relationships described above, combined with the observations presented, tend to argue against a general $e\text{CO}_2$ benefit in pine seedlings. Instead, they suggest that the VPD effect may offset or even exceed the $e\text{CO}_2$ effect, likely increasing the mortality risk for pine seedlings, especially in regions where water availability is already the dominant limiting factor. (Figure 5.1) This is in line with recent studies suggesting that the CO_2 fertilization effect is likely to decrease with rising CO_2 as plants approach the saturation response to $e\text{CO}_2$ while high VPD elevates the water cost of global land carbon sink attesting VPD its central role in the linking of global carbon and water cycles (Chai et al. 2024; De Kauwe et al. 2021; S. Li et al. 2023; Liu et al. 2023; Pernicová et al. 2024; Song et al. 2024). Altogether, these results point to a potential decrease in ecosystem stability and increased impacts of droughts in vulnerable ecosystems under ongoing global change.

Conclusion and outlook

The results presented in this thesis show that growth under $e\text{CO}_2$ does not reduce mortality risk for pine seedlings when drought progression promotes hydraulic failure rather than carbon starvation. This was mainly due to the lack of water savings caused by leaf-level reductions in transpiration being overridden at the canopy scale by a large proportional increase in leaf area and unaffected hydraulic safety. In addition, the observed unchanged metabolic and hydrological drought response, combined with evidence of direct sink control by soil and atmospheric drought, suggests that the potential beneficial effect of high C availability under $e\text{CO}_2$ is limited during drought stress. Although these results are based on experiments with seedlings under defined conditions in a greenhouse and therefore have limitations in terms of transferability to (adult) trees in the field, the mechanistic understanding gained in this thesis can undoubtedly improve the predictive power for quantifying the effects of soil and atmospheric drought on gas exchange, growth, production and survival of pine trees under the influence of $e\text{CO}_2$. The information provided is highly relevant for assessing future bioclimatic and growth limits of pines.

At the same time, it is clear that further research is needed to determine the extent to which the ability of not only pine but forests in general to act as carbon sinks will be limited by the projected increase in the intensity and frequency of droughts, and how the potential effect of CO_2 fertilization on tree growth and photosynthesis contributes to this. Therefore, future experiments need to investigate the role of $e\text{CO}_2$ at different levels of soil drought in combination with variable VPD and over different time scales, while measuring tree growth directly rather than via source processes to account for sink limitation.

6 References

- Aaltonen, Heidi, Aki Lindén, Jussi Heinonsalo, Christina Biasi, and Jukka Pumpanen. 2017. "Effects of Prolonged Drought Stress on Scots Pine Seedling Carbon Allocation." *Tree Physiology* 37(4):418–27.
- Adams, Henry D., Adam D. Collins, Samuel P. Briggs, Michel Vennetier, L. Turin Dickman, Sanna A. Sevanto, Núria Garcia-Forner, Heath H. Powers, and Nate G. McDowell. 2015. "Experimental Drought and Heat Can Delay Phenological Development and Reduce Foliar and Shoot Growth in Semiarid Trees." *Global Change Biology* 21(11):4210–20. doi: 10.1111/gcb.13030.
- Adams, Henry D., Maite Guardiola-Claramonte, Greg A. Barron-Gafford, Juan Camilo Villegas, David D. Breshears, Chris B. Zou, Peter A. Troch, and Travis E. Huxman. 2009. "Temperature Sensitivity of Drought-Induced Tree Mortality Portends Increased Regional Die-off under Global-Change-Type Drought." *Proceedings of the National Academy of Sciences* 106(17):7063–66.
- Adams, Henry D., Alison K. Macalady, David D. Breshears, Craig D. Allen, Nathan L. Stephenson, Scott R. Saleska, Travis E. Huxman, and Nathan G. McDowell. 2010. "Climate-Induced Tree Mortality: Earth System Consequences." *Eos, Transactions American Geophysical Union* 91(17):153. doi: 10.1029/2010EO170003.
- Adams, Henry D., Melanie J. B. Zeppel, William R. L. Anderegg, Henrik Hartmann, Simon M. Landhäusser, David T. Tissue, Travis E. Huxman, Patrick J. Hudson, Trenton E. Franz, Craig D. Allen, Leander D. L. Anderegg, Greg A. Barron-Gafford, David J. Beerling, David D. Breshears, Timothy J. Brodribb, Harald Bugmann, Richard C. Cobb, Adam D. Collins, L. Turin Dickman, Honglang Duan, Brent E. Ewers, Lucía Galiano, David A. Galvez, Núria Garcia-Forner, Monica L. Gaylord, Matthew J. Germino, Arthur Gessler, Uwe G. Hacke, Rodrigo Hakamada, Andy Hector, Michael W. Jenkins, Jeffrey M. Kane, Thomas E. Kolb, Darin J. Law, James D. Lewis, Jean-Marc Limousin, David M. Love, Alison K. Macalady, Jordi Martínez-Vilalta, Maurizio Mencuccini, Patrick J. Mitchell, Jordan D. Muss, Michael J. O'Brien, Anthony P. O'Grady, Robert E. Pangle, Elizabeth A. Pinkard, Frida I. Piper, Jennifer A. Plaut, William T. Pockman, Joe Quirk, Keith Reinhardt, Francesco Ripullone, Michael G. Ryan, Anna Sala, Sanna Sevanto, John S. Sperry, Rodrigo Vargas, Michel Vennetier, Danielle A. Way, Chonggang Xu, Enrico A. Yezpe, and Nate G. McDowell. 2017. "A Multi-Species Synthesis of Physiological Mechanisms in Drought-Induced Tree Mortality." *Nature Ecology & Evolution* 1(9):1285–91. doi: 10.1038/s41559-017-0248-x.
- Ainsworth, Elizabeth A., and Stephen P. Long. 2004. "What Have We Learned from 15 Years of Free-Air CO₂ Enrichment (FACE)? A Meta-Analytic Review of the Responses of

- Photosynthesis, Canopy Properties and Plant Production to Rising CO₂: Tansley Review." *New Phytologist* 165(2):351–72. doi: 10.1111/j.1469-8137.2004.01224.x.
- Ainsworth, Elizabeth A., and Alistair Rogers. 2007. "The Response of Photosynthesis and Stomatal Conductance to Rising [CO₂]: Mechanisms and Environmental Interactions: Photosynthesis and Stomatal Conductance Responses to Rising [CO₂]." *Plant, Cell & Environment* 30(3):258–70. doi: 10.1111/j.1365-3040.2007.01641.x.
- Allen, Craig D., David D. Breshears, and Nate G. McDowell. 2015. "On Underestimation of Global Vulnerability to Tree Mortality and Forest Die-off from Hotter Drought in the Anthropocene." *Ecosphere* 6(8):art129. doi: 10.1890/ES15-00203.1.
- Allen, Craig D., Alison K. Macalady, Haroun Chenchouni, Dominique Bachelet, Nate McDowell, Michel Vennetier, Thomas Kitzberger, Andreas Rigling, David D. Breshears, E. H. Hogg, Patrick Gonzalez, Rod Fensham, Zhen Zhang, Jorge Castro, Natalia Demidova, Jong-Hwan Lim, Gillian Allard, Steven W. Running, Akkin Semerci, and Neil Cobb. 2010. "A Global Overview of Drought and Heat-Induced Tree Mortality Reveals Emerging Climate Change Risks for Forests." *Forest Ecology and Management* 259(4):660–84. doi: 10.1016/j.foreco.2009.09.001.
- Anderegg, William R. L., Leander D. L. Anderegg, Kelly L. Kerr, and Anna T. Trugman. 2019. "Widespread Drought-induced Tree Mortality at Dry Range Edges Indicates That Climate Stress Exceeds Species' Compensating Mechanisms." *Global Change Biology* gcb.14771. doi: 10.1111/gcb.14771.
- Apple, Martha E., David M. Olszyk, Douglas P. Ormrod, James Lewis, Darlene Southworth, and David T. Tingey. 2000. "Morphology and Stomatal Function of Douglas Fir Needles Exposed to Climate Change: Elevated CO₂ and Temperature." *International Journal of Plant Sciences* 161(1):127–32. doi: 10.1086/314237.
- Arp, W. J. 1991. "Effects of Source-sink Relations on Photosynthetic Acclimation to Elevated CO₂." *Plant, Cell & Environment* 14(8):869–75.
- Atwell, B. J., M. L. Henery, and D. Whitehead. 2003. "Sapwood Development in *Pinus Radiata* Trees Grown for Three Years at Ambient and Elevated Carbon Dioxide Partial Pressures." *Tree Physiology* 23(1):13–21. doi: 10.1093/treephys/23.1.13.
- Babst, Flurin, Olivier Bouriaud, Benjamin Poulter, Valerie Trouet, Martin P. Girardin, and David C. Frank. 2019. "Twentieth Century Redistribution in Climatic Drivers of Global Tree Growth." *Science Advances* 5(1):eaat4313. doi: 10.1126/sciadv.aat4313.
- Bader, Martin K. F., Sebastian Leuzinger, Sonja G. Keel, Rolf T. W. Siegwolf, Frank Hagedorn, Patrick Schleppi, and Christian Körner. 2013. "Central European Hardwood Trees in a High-CO₂ Future: Synthesis of an 8-Year Forest Canopy CO₂ Enrichment Project." *Journal of Ecology* 101(6):1509–19. doi: 10.1111/1365-2745.12149.
- Ballantyne, A. P., C. B. Alden, J. B. Miller, P. P. Tans, and J. W. C. White. 2012. "Increase in Observed Net Carbon Dioxide Uptake by Land and Oceans during the Past 50 Years." *Nature* 488(7409):70–72. doi: 10.1038/nature11299.

- Barthel, Matthias, Albin Hammerle, Patrick Sturm, Thomas Baur, Lydia Gentsch, and Alexander Knohl. 2011. "The Diel Imprint of Leaf Metabolism on the $\delta^{13}\text{C}$ Signal of Soil Respiration under Control and Drought Conditions." *New Phytologist* 192(4):925–38. doi: 10.1111/j.1469-8137.2011.03848.x.
- Bartlett, Megan K., Tamir Klein, Steven Jansen, Brendan Choat, and Lawren Sack. 2016. "The Correlations and Sequence of Plant Stomatal, Hydraulic, and Wilting Responses to Drought." *Proceedings of the National Academy of Sciences* 113(46):13098–103. doi: 10.1073/pnas.1604088113.
- Bates, Douglas, Martin Maechler, Ben Bolker, Steven Walker, Rune Haubo Bojesen Christensen, Henrik Singmann, Bin Dai, Gabor Grothendieck, Peter Green, and M. Ben Bolker. 2015. "Package 'Lme4.'" *Convergence* 12(1):2.
- Beer, Christian, Markus Reichstein, Enrico Tomelleri, Philippe Ciais, Martin Jung, Nuno Carvalhais, Christian Rödenbeck, M. Altaf Arain, Dennis Baldocchi, and Gordon B. Bonan. 2010. "Terrestrial Gross Carbon Dioxide Uptake: Global Distribution and Covariation with Climate." *Science* 329(5993):834–38.
- Benner, P., P. Sabel, and A. Wild. 1988. "Photosynthesis and Transpiration of Healthy and Diseased Spruce Trees in the Course of Three Vegetation Periods." *Trees* 2(4). doi: 10.1007/BF00202377.
- Berg, Alexis, Kirsten Findell, Benjamin Lintner, Alessandra Giannini, Sonia I. Seneviratne, Bart Van Den Hurk, Ruth Lorenz, Andy Pitman, Stefan Hagemann, and Arndt Meier. 2016. "Land–Atmosphere Feedbacks Amplify Aridity Increase over Land under Global Warming." *Nature Climate Change* 6(9):869–74.
- Bettarini, Isabella, Francesco P. Vaccari, and Franco Miglietta. 1998. "Elevated CO_2 Concentrations and Stomatal Density: Observations from 17 Plant Species Growing in a CO_2 Spring in Central Italy." *Global Change Biology* 4(1):17–22. doi: 10.1046/j.1365-2486.1998.00098.x.
- Birami, Benjamin, Thomas Nägele, Marielle Gattmann, Yakir Preisler, Andreas Gast, Almut Arneth, and Nadine K. Ruehr. 2020. "Hot Drought Reduces the Effects of Elevated CO_2 on Tree Water-use Efficiency and Carbon Metabolism." *New Phytologist* nph.16471. doi: 10.1111/nph.16471.
- Blackman, Chris J., Danielle Creek, Chelsea Maier, Michael J. Aspinwall, John E. Drake, Sebastian Pfautsch, Anthony O'Grady, Sylvain Delzon, Belinda E. Medlyn, David T. Tissue, and Brendan Choat. 2019. "Drought Response Strategies and Hydraulic Traits Contribute to Mechanistic Understanding of Plant Dry-down to Hydraulic Failure" edited by F. Meinzer. *Tree Physiology* 39(6):910–24. doi: 10.1093/treephys/tpz016.
- Blackman, Chris J., Sebastian Pfautsch, Brendan Choat, Sylvain Delzon, Sean M. Gleason, and Remko A. Duursma. 2016. "Toward an Index of Desiccation Time to Tree Mortality under Drought: Desiccation Time to Tree Mortality." *Plant, Cell & Environment* 39(10):2342–45. doi: 10.1111/pce.12758.

- Bogeat-Triboulot, Marie-Béatrice, Mikael Brosché, Jenny Renaut, Laurent Jouve, Didier Le Thiec, Payam Fayyaz, Basia Vinocur, Erwin Witters, Kris Laukens, Thomas Teichmann, Arie Altman, Jean-François Hausman, Andrea Polle, Jaakko Kangasjärvi, and Erwin Dreyer. 2007. "Gradual Soil Water Depletion Results in Reversible Changes of Gene Expression, Protein Profiles, Ecophysiology, and Growth Performance in *Populus Euphratica*, a Poplar Growing in Arid Regions." *Plant Physiology* 143(2):876–92. doi: 10.1104/pp.106.088708.
- Bonan, Gordon B. 2008. "Forests and Climate Change: Forcings, Feedbacks, and the Climate Benefits of Forests." *Science* 320(5882):1444–49. doi: 10.1126/science.1155121.
- Boyer, J. S. 1970. "Differing Sensitivity of Photosynthesis to Low Leaf Water Potentials in Corn and Soybean." *Plant Physiology* 46(2):236–39.
- Bréda, Nathalie, Roland Huc, André Granier, and Erwin Dreyer. 2006. "Temperate Forest Trees and Stands under Severe Drought: A Review of Ecophysiological Responses, Adaptation Processes and Long-Term Consequences." *Annals of Forest Science* 63(6):625–44. doi: 10.1051/forest:2006042.
- Breshears, David D., Henry D. Adams, Derek Eamus, Nate McDowell, Darin J. Law, Rodney E. Will, A. P. Williams, and Chris B. Zou. 2013. "The Critical Amplifying Role of Increasing Atmospheric Moisture Demand on Tree Mortality and Associated Regional Die-Off." *Frontiers in Plant Science* 4. doi: 10.3389/fpls.2013.00266.
- Breshears, David D., Charles J. W. Carroll, Miranda D. Redmond, Andreas P. Wion, Craig D. Allen, Neil S. Cobb, Nashelly Meneses, Jason P. Field, Luke A. Wilson, Darin J. Law, Lindsie M. McCabe, and Olivia Newell-Bauer. 2018. "A Dirty Dozen Ways to Die: Metrics and Modifiers of Mortality Driven by Drought and Warming for a Tree Species." *Frontiers in Forests and Global Change* 1:4. doi: 10.3389/ffgc.2018.00004.
- Brodribb, Tim J., and Hervé Cochard. 2009. "Hydraulic Failure Defines the Recovery and Point of Death in Water-Stressed Conifers." *Plant Physiology* 149(1):575–84. doi: 10.1104/pp.108.129783.
- Brodribb, Tim J., Taylor S. Feild, and Gregory J. Jordan. 2007. "Leaf Maximum Photosynthetic Rate and Venation Are Linked by Hydraulics." *Plant Physiology* 144(4):1890–98.
- Brodribb, Tim J., Taylor S. Feild, and Lawren Sack. 2010. "Viewing Leaf Structure and Evolution from a Hydraulic Perspective." *Functional Plant Biology* 37(6):488–98.
- Brodribb, Timothy J., and Scott AM McAdam. 2013. "Unique Responsiveness of Angiosperm Stomata to Elevated CO₂ Explained by Calcium Signalling." *PLoS One* 8(11):e82057.
- Brodribb, Timothy J., Scott AM McAdam, Gregory J. Jordan, and Taylor S. Feild. 2009. "Evolution of Stomatal Responsiveness to CO₂ and Optimization of Water-use Efficiency among Land Plants." *New Phytologist* 183(3):839–47.
- Brodribb, Timothy J., Jennifer Powers, Hervé Cochard, and Brendan Choat. 2020. "Hanging by a Thread? Forests and Drought." *Science* 368(6488):261–66. doi: 10.1126/science.aat7631.

- Brunner, Ivano, Claude Herzog, Melissa A. Dawes, Matthias Arend, and Christoph Sperisen. 2015. "How Tree Roots Respond to Drought." *Frontiers in Plant Science* 6. doi: 10.3389/fpls.2015.00547.
- Buckley, Thomas N., Grace P. John, Christine Scoffoni, and Lawren Sack. 2017. "The Sites of Evaporation within Leaves." *Plant Physiology* 173(3):1763–82. doi: 10.1104/pp.16.01605.
- Buras, Allan, Christian Schunk, Claudia Zeiträg, Corinna Herrmann, Laura Kaiser, Hannes Lemme, Christoph Straub, Steffen Taeger, Sebastian Gößwein, Hans-Joachim Klemmt, and Annette Menzel. 2018. "Are Scots Pine Forest Edges Particularly Prone to Drought-Induced Mortality?" *Environmental Research Letters* 13. doi: 10.1088/1748-9326/aaa0b4.
- Cabon, Antoine, Laura Fernández-de-Uña, Guillermo Gea-Izquierdo, Frederick C. Meinzer, David R. Woodruff, Jordi Martínez-Vilalta, and Miquel De Cáceres. 2020. "Water Potential Control of Turgor-Driven Tracheid Enlargement in Scots Pine at Its Xeric Distribution Edge." *New Phytologist* 225(1):209–21. doi: 10.1111/nph.16146.
- Camarero, J. Julio, Antonio Gazol, Gabriel Sangüesa-Barreda, Jonàs Oliva, and Sergio M. Vicente-Serrano. 2015. "To Die or Not to Die: Early Warnings of Tree Dieback in Response to a Severe Drought." *Journal of Ecology* 103(1):44–57. doi: 10.1111/1365-2745.12295.
- Carminati, Andrea, and Mathieu Javaux. 2020. "Soil Rather than Xylem Vulnerability Controls Stomatal Response to Drought." *Trends in Plant Science* 25(9):868–80.
- Castellaneta, Maria, Angelo Rita, J. Julio Camarero, Michele Colangelo, and Francesco Ripullone. 2022. "Declines in Canopy Greenness and Tree Growth Are Caused by Combined Climate Extremes during Drought-Induced Dieback." *Science of The Total Environment* 813:152666. doi: 10.1016/j.scitotenv.2021.152666.
- Cernusak, Lucas A., Gregory R. Goldsmith, Matthias Arend, and Rolf T. W. Siegwolf. 2019. "Effect of Vapor Pressure Deficit on Gas Exchange in Wild-Type and Absciscic Acid–Insensitive Plants." *Plant Physiology* 181(4):1573–86. doi: 10.1104/pp.19.00436.
- Ceulemans, R., M. E. Jach, R. Van De Velde, J. X. Lin, and M. Stevens. 2002. "Elevated Atmospheric CO₂ Alters Wood Production, Wood Quality and Wood Strength of Scots Pine (*Pinus Sylvestris* L.) after Three Years of Enrichment." *Global Change Biology* 8(2):153–62. doi: 10.1046/j.1354-1013.2001.00461.x.
- Chai, Yuanfang, Chiyuan Miao, Wouter R. Berghuijs, Yunping Yang, Boyuan Zhu, Yong Hu, and Louise Slater. 2024. "Global Reduction in Sensitivity of Vegetation Water Use Efficiency to Increasing CO₂." *Journal of Hydrology* 641:131844. doi: 10.1016/j.jhydrol.2024.131844.
- Chang, Qing, Wenhua Xu, Bo Peng, Ping Jiang, Shanlong Li, Chao Wang, and Edith Bai. 2022. "Dynamic and Allocation of Recently Assimilated Carbon in Korean Pine (*Pinus Koraiensis*) and Birch (*Betula Platyphylla*) in a Temperate Forest." *Biogeochemistry* 160(3):395–407.
- Chater, Caspar, Kai Peng, Mahsa Movahedi, Jessica A. Dunn, Heather J. Walker, Yun-Kuan Liang, Deirdre H. McLachlan, Stuart Casson, Jean Charles Isner, Ian Wilson, Steven J. Neill, Rainer Hedrich, Julie E. Gray, and Alistair M. Hetherington. 2015. "Elevated CO₂ -Induced

- Responses in Stomata Require ABA and ABA Signaling." *Current Biology* 25(20):2709–16. doi: 10.1016/j.cub.2015.09.013.
- Chaves, Manuela M., João P. Maroco, and João S. Pereira. 2003. "Understanding Plant Responses to Drought—from Genes to the Whole Plant." *Functional Plant Biology* 30(3):239–64.
- Chen, Yizhao, Tim Rademacher, Patrick Fonti, Annemarie H. Eckes-Shephard, James M. LeMoine, Marina V. Fonti, Andrew D. Richardson, and Andrew D. Friend. 2022. "Inter-Annual and Inter-Species Tree Growth Explained by Phenology of Xylogenesis." *New Phytologist* 235(3):939–52. doi: 10.1111/nph.18195.
- Choat, Brendan, Timothy J. Brodribb, Craig R. Brodersen, Remko A. Duursma, Rosana López, and Belinda E. Medlyn. 2018. "Triggers of Tree Mortality under Drought." *Nature* 558(7711):531–39. doi: 10.1038/s41586-018-0240-x.
- Ciais, Ph, Markus Reichstein, Nicolas Viovy, André Granier, Jérôme Ogée, Vincent Allard, Marc Aubinet, Nina Buchmann, Chr Bernhofer, and Arnaud Carrara. 2005. "Europe-Wide Reduction in Primary Productivity Caused by the Heat and Drought in 2003." *Nature* 437(7058):529–33.
- Cochard, Hervé. 2006. "Cavitation in Trees." *Comptes Rendus Physique* 7(9–10):1018–26. doi: 10.1016/j.crhy.2006.10.012.
- Cochard, Hervé, Gaëlle Damour, Christian Bodet, Ibrahim Tharwat, Magalie Poirier, and Thierry Améglio. 2005. "Evaluation of a New Centrifuge Technique for Rapid Generation of Xylem Vulnerability Curves." *Physiologia Plantarum* 124(4):410–18.
- Colangelo, Michele, J. Julio Camarero, Giovanna Battipaglia, Marco Borghetti, Veronica De Micco, Tiziana Gentilesca, and Francesco Ripullone. 2017. "A Multi-Proxy Assessment of Dieback Causes in a Mediterranean Oak Species." *Tree Physiology* 37(5):617–31. doi: 10.1093/treephys/tpx002.
- Cole, Jonathan J., Oleksandra Hararuk, and Christopher T. Solomon. 2021. "Chapter 7 - The Carbon Cycle: With a Brief Introduction to Global Biogeochemistry." Pp. 131–60 in *Fundamentals of Ecosystem Science (Second Edition)*, edited by K. C. Weathers, D. L. Strayer, and G. E. Likens. Academic Press.
- Collins, Matthew, Reto Knutti, Julie Arblaster, J. L. Dufresne, Thierry Fichefet, Pierre Friedlingstein, Xuejie Gao, William J. Gutowski, Tim Johns, and Gerhard Krinner. 2013. "Chapter 12 - Long-Term Climate Change: Projections, Commitments and Irreversibility." in *Climate Change 2013: The Physical Science Basis. IPCC Working Group I Contribution to AR5*. Eds. IPCC, Cambridge: Cambridge University Press.
- Comas, Louise, Steven Becker, Von Mark V. Cruz, Patrick F. Byrne, and David A. Dierig. 2013. "Root Traits Contributing to Plant Productivity under Drought." *Frontiers in Plant Science* 4. doi: 10.3389/fpls.2013.00442.
- Conroy, J. P., P. J. Milham, M. Mazur, and E. W. R. Barlow. 1990. "Growth, Dry Weight Partitioning and Wood Properties of *Pinus Radiata* D. Don after 2 Years of CO₂ Enrichment." *Plant, Cell and Environment* 13(4):329–37. doi: 10.1111/j.1365-3040.1990.tb02136.x.

- Cornic, Gabriel. 2000. "Drought Stress Inhibits Photosynthesis by Decreasing Stomatal Aperture – Not by Affecting ATP Synthesis." *Trends in Plant Science* 5(5):187–88. doi: 10.1016/S1360-1385(00)01625-3.
- Creek, Danielle, Laurent J. Lamarque, José M. Torres-Ruiz, Camille Parise, Regis Burlett, David T. Tissue, and Sylvain Delzon. 2020. "Xylem Embolism in Leaves Does Not Occur with Open Stomata: Evidence from Direct Observations Using the Optical Visualization Technique." *Journal of Experimental Botany* 71(3):1151–59.
- Creese, Chris, Steve Oberbauer, Phil Rundel, and Lawren Sack. 2014. "Are Fern Stomatal Responses to Different Stimuli Coordinated? Testing Responses to Light, Vapor Pressure Deficit, and CO₂ for Diverse Species Grown under Contrasting Irradiances." *New Phytologist* 204(1):92–104. doi: 10.1111/nph.12922.
- Cunningham, S. C. 2005. "Photosynthetic Responses to Vapour Pressure Deficit in Temperate and Tropical Evergreen Rainforest Trees of Australia." *Oecologia* 142(4):521–28. doi: 10.1007/s00442-004-1766-1.
- Cunningham, Shaun C. 2004. "Stomatal Sensitivity to Vapour Pressure Deficit of Temperate and Tropical Evergreen Rainforest Trees of Australia." *Trees* 18(4):399–407. doi: 10.1007/s00468-004-0318-y.
- Curtis, Peter S., and Xianzhong Wang. 1998. "A Meta-Analysis of Elevated CO₂ Effects on Woody Plant Mass, Form, and Physiology." *Oecologia* 113:299–313.
- DaCosta, Michelle, and Bingru Huang. 2006. "Changes in Carbon Partitioning and Accumulation Patterns during Drought and Recovery for Colonial Bentgrass, Creeping Bentgrass, and Velvet Bentgrass." *Journal of the American Society for Horticultural Science* 131(4):484–90. doi: 10.21273/JASHS.131.4.484.
- Dai, Aiguo. 2013. "Increasing Drought under Global Warming in Observations and Models." *Nature Climate Change* 3(1):52–58. doi: 10.1038/nclimate1633.
- De Kauwe, Martin G., Belinda E. Medlyn, and David T. Tissue. 2021. "To What Extent Can Rising [CO₂] Ameliorate Plant Drought Stress?" *New Phytologist* 231(6):2118–24. doi: 10.1111/nph.17540.
- DeLucia, Evan H., John E. Drake, Richard B. Thomas, and Miquel Gonzalez-Meler. 2007. "Forest Carbon Use Efficiency: Is Respiration a Constant Fraction of Gross Primary Production?" *Global Change Biology* 13(6):1157–67.
- Dobbertin, Matthias, Britta Eilmann, Peter Bleuler, Arnaud Giuggiola, Elisabeth Graf Pannatier, Werner Landolt, Patrick Schleppi, and Andreas Rigling. 2010. "Effect of Irrigation on Needle Morphology, Shoot and Stem Growth in a Drought-Exposed Pinus Sylvestris Forest." *Tree Physiology* 30(3):346–60.
- Doi, Michio, and Ken-ichiro Shimazaki. 2008. "The Stomata of the Fern Adiantum Capillus-Veneris Do Not Respond to CO₂ in the Dark and Open by Photosynthesis in Guard Cells." *Plant Physiology* 147(2):922–30.

- Domec, J. C., K. Schafer, R. Oren, H. S. Kim, and H. R. McCarthy. 2010. "Variable Conductivity and Embolism in Roots and Branches of Four Contrasting Tree Species and Their Impacts on Whole-Plant Hydraulic Performance under Future Atmospheric CO₂ Concentration." *Tree Physiology* 30(8):1001–15. doi: 10.1093/treephys/tpq054.
- Domec, Jean-Christophe, Sari Palmroth, and Ram Oren. 2016. "Effects of *Pinus Taeda* Leaf Anatomy on Vascular and Extravascular Leaf Hydraulic Conductance as Influenced by N-Fertilization and Elevated CO₂ ." *Journal of Plant Hydraulics* 3:007. doi: 10.20870/jph.2016.e007.
- Domec, Jean-Christophe, Sari Palmroth, Eric Ward, Chris A. Maier, M. Thérézien, and Ram Oren. 2009. "Acclimation of Leaf Hydraulic Conductance and Stomatal Conductance of *Pinus Taeda* (Loblolly Pine) to Long-Term Growth in Elevated CO₂ (Free-Air CO₂ Enrichment) and N-Fertilization." *Plant, Cell & Environment* 32(11):1500–1512. doi: 10.1111/j.1365-3040.2009.02014.x.
- Domec, Jean-Christophe, Duncan D. Smith, and Kate A. McCulloh. 2017. "A Synthesis of the Effects of Atmospheric Carbon Dioxide Enrichment on Plant Hydraulics: Implications for Whole-Plant Water Use Efficiency and Resistance to Drought: CO₂ Effects on Plant Hydraulics." *Plant, Cell & Environment* 40(6):921–37. doi: 10.1111/pce.12843.
- Doughty, Christopher E., Yadvinder Malhi, Alejandro Araujo-Murakami, Daniel B. Metcalfe, Javier E. Silva-Espejo, Luzmila Arroyo, Juan P. Heredia, Erwin Pardo-Toledo, Luz M. Mendizabal, and Victor D. Rojas-Landivar. 2014. "Allocation Trade-offs Dominate the Response of Tropical Forest Growth to Seasonal and Interannual Drought." *Ecology* 95(8):2192–2201.
- Doughty, Christopher E., D. B. Metcalfe, C. A. J. Girardin, F. Farfán Amézquita, D. Galiano Cabrera, W. Huaraca Huasco, J. E. Silva-Espejo, A. Araujo-Murakami, M. C. Da Costa, and W. Rocha. 2015. "Drought Impact on Forest Carbon Dynamics and Fluxes in Amazonia." *Nature* 519(7541):78–82.
- Drake, Bert G., Miquel A. González-Meler, and Steve P. Long. 1997. "More Efficient Plants: A Consequence of Rising Atmospheric CO₂?" *Annual Review of Plant Physiology and Plant Molecular Biology* 48(1):609–39. doi: 10.1146/annurev.arplant.48.1.609.
- Dror, Dar, and Tamir Klein. 2022. "The Effect of Elevated CO₂ on Aboveground and Belowground Carbon Allocation and Eco-Physiology of Four Species of Angiosperm and Gymnosperm Forest Trees." *Tree Physiology* 42(4):831–47.
- Du, Ling, Nathaniel Mickle, Zhenhua Zou, Yuanyuan Huang, Zheng Shi, Lifan Jiang, Heather R. McCarthy, Junyi Liang, and Yiqi Luo. 2018. "Global Patterns of Extreme Drought-Induced Loss in Land Primary Production: Identifying Ecological Extremes from Rain-Use Efficiency." *Science of the Total Environment* 628:611–20.
- Duan, Honglang, Brian Chaszar, James D. Lewis, Renee A. Smith, Travis E. Huxman, and David T. Tissue. 2018. "CO₂ and Temperature Effects on Morphological and Physiological Traits Affecting Risk of Drought-Induced Mortality" edited by D. Way. *Tree Physiology* 38(8):1138–51. doi: 10.1093/treephys/tpy037.

- Duan, Honglang, Remko A. Duursma, Guomin Huang, Renee A. Smith, Brendan Choat, Anthony P. O'Grady, and David T. Tissue. 2014. "Elevated [CO₂] Does Not Ameliorate the Negative Effects of Elevated Temperature on Drought-Induced Mortality in *Eucalyptus Radiata* Seedlings: Mortality under Rising [CO₂] and Temperature." *Plant, Cell & Environment* 37(7):1598–1613. doi: 10.1111/pce.12260.
- Duan, Honglang, Anthony P. O'Grady, Remko A. Duursma, Brendan Choat, Guomin Huang, Renee A. Smith, Yanan Jiang, and David T. Tissue. 2015. "Drought Responses of Two Gymnosperm Species with Contrasting Stomatal Regulation Strategies under Elevated [CO₂] and Temperature" edited by F. Meinzer. *Tree Physiology* 35(7):756–70. doi: 10.1093/treephys/tpv047.
- Dubbe, Dean R., Graham D. Farquhar, and Klaus Raschke. 1978. "Effect of Abscissic Acid on the Gain of the Feedback Loop Involving Carbon Dioxide and Stomata." *Plant Physiology* 62(3):413–17.
- Dubeaux, Guillaume, Po-Kai Hsu, Paulo HO Ceciliato, Kelsey J. Swink, Wouter-Jan Rappel, and Julian I. Schroeder. 2021. "Deep Dive into CO₂-Dependent Molecular Mechanisms Driving Stomatal Responses in Plants." *Plant Physiology* 187(4):2032–42.
- Dusenge, Mirindi Eric, André Galvao Duarte, and Danielle A. Way. 2019. "Plant Carbon Metabolism and Climate Change: Elevated CO₂ and Temperature Impacts on Photosynthesis, Photorespiration and Respiration." *New Phytologist* 221(1):32–49. doi: 10.1111/nph.15283.
- Eamus, Derek, Nicolas Boulain, James Cleverly, and David D. Breshears. 2013. "Global Change-Type Drought-Induced Tree Mortality: Vapor Pressure Deficit Is More Important than Temperature per Se in Causing Decline in Tree Health." *Ecology and Evolution* 3(8):2711–29. doi: 10.1002/ece3.664.
- Eckes-Shephard, Annemarie H., Egor Tiavlovsky, Yizhao Chen, Patrick Fonti, and Andrew D. Friend. 2021. "Direct Response of Tree Growth to Soil Water and Its Implications for Terrestrial Carbon Cycle Modelling." *Global Change Biology* 27(1):121–35. doi: 10.1111/gcb.15397.
- Eguchi, N., E. Fukatsu, R. Funada, H. Tobita, M. Kitao, Y. Maruyama, and T. Koike. 2004. "Changes in Morphology, Anatomy, and Photosynthetic Capacity of Needles of Japanese Larch (*Larix Kaempferi*) Seedlings Grown in High CO₂ Concentrations." *Photosynthetica* 42(2):173–78. doi: 10.1023/B:PHOT.0000040587.99518.a8.
- Ellenberg, Heinz. 1988. *Vegetation Ecology of Central Europe*. Cambridge University Press.
- Engel, Victor C., Kevin L. Griffin, Ramesh Murthy, Lane Patterson, Christie Klimas, and Mark Potosnak. 2004. "Growth CO₂ Concentration Modifies the Transpiration Response of *Populus Deltoides* to Drought and Vapor Pressure Deficit." *Tree Physiology* 24(10):1137–45. doi: 10.1093/treephys/24.10.1137.
- Epron, Daniel, Michael Bahn, Delphine Derrien, Fernando Alfredo Lattanzi, Jukka Pumpanen, Arthur Gessler, Peter Höglberg, Pascale Maillard, Masako Dannoura, Dominique Gérant, and Nina Buchmann. 2012. "Pulse-Labeling Trees to Study Carbon Allocation Dynamics: A Review of Methods, Current Knowledge and Future Prospects." *Tree Physiology* 32(6):776–98. doi: 10.1093/treephys/tps057.

- Fatichi, Simone, Sebastian Leuzinger, and Christian Körner. 2014. "Moving beyond Photosynthesis: From Carbon Source to Sink-Driven Vegetation Modeling." *New Phytologist* 201(4):1086–95. doi: 10.1111/nph.12614.
- Fatichi, Simone, Christoforos Pappas, Jakob Zscheischler, and Sebastian Leuzinger. 2019. "Modelling Carbon Sources and Sinks in Terrestrial Vegetation." *New Phytologist* 221(2):652–68. doi: 10.1111/nph.15451.
- Fensham, R. J., and J. E. Holman. 1999. "Temporal and Spatial Patterns in Drought-Related Tree Dieback in Australian Savanna." *Journal of Applied Ecology* 36(6):1035–50. doi: 10.1046/j.1365-2664.1999.00460.x.
- Ferris, R. 1996. "Elevated CO₂ and Temperature Have Different Effects on Leaf Anatomy of Perennial Ryegrass in Spring and Summer." *Annals of Botany* 78(4):489–97. doi: 10.1006/anbo.1996.0146.
- Field, Christopher B., Robert B. Jackson, and Harold A. Mooney. 1995. "Stomatal Responses to Increased CO₂: Implications from the Plant to the Global Scale." *Plant, Cell & Environment* 18(10):1214–25.
- Fletcher, Andrew L., Thomas R. Sinclair, and L. Hartwell Allen. 2007. "Transpiration Responses to Vapor Pressure Deficit in Well Watered 'Slow-Wilting' and Commercial Soybean." *Environmental and Experimental Botany* 61(2):145–51. doi: 10.1016/j.envexpbot.2007.05.004.
- Flexas, J., and H. Medrano. 2002. "Drought-Inhibition of Photosynthesis in C₃ Plants: Stomatal and Non-Stomatal Limitations Revisited." *Annals of Botany* 89(2):183–89. doi: 10.1093/aob/mcf027.
- Flexas, J., M. Ribas-Carbó, J. Bota, J. Galmés, M. Henkle, S. Martínez-Cañellas, and H. Medrano. 2006. "Decreased Rubisco Activity during Water Stress Is Not Induced by Decreased Relative Water Content but Related to Conditions of Low Stomatal Conductance and Chloroplast CO₂ Concentration." *The New Phytologist* 172(1):73–82. doi: 10.1111/j.1469-8137.2006.01794.x.
- Franks, Peter J., and Zoe J. Britton-Harper. 2016. "No Evidence of General CO₂ Insensitivity in Ferns: One Stomatal Control Mechanism for All Land Plants?" *New Phytologist* 211(3):819–27.
- Friedlingstein, Pierre, Matthew W. Jones, Michael O'Sullivan, Robbie M. Andrew, Dorothee C. E. Bakker, Judith Hauck, Corinne Le Quéré, Glen P. Peters, Wouter Peters, Julia Pongratz, Stephen Sitch, Josep G. Canadell, Philippe Ciais, Rob B. Jackson, Simone R. Alin, Peter Anthoni, Nicholas R. Bates, Meike Becker, Nicolas Bellouin, Laurent Bopp, Thi Tuyet Trang Chau, Frédéric Chevallier, Louise P. Chini, Margot Cronin, Kim I. Currie, Bertrand Decharme, Laique M. Djeutchouang, Xinyu Dou, Wiley Evans, Richard A. Feely, Liang Feng, Thomas Gasser, Dennis Gilfillan, Thanos Gkritzalis, Giacomo Grassi, Luke Gregor, Nicolas Gruber, Özgür Gürses, Ian Harris, Richard A. Houghton, George C. Hurtt, Yosuke Iida, Tatiana Ilyina, Ingrid T. Luijkx, Atul Jain, Steve D. Jones, Etsushi Kato, Daniel Kennedy, Kees Klein Goldewijk, Jürgen Knauer, Jan Ivar Korsbakken, Arne Körtzinger, Peter Landschützer, Siv K. Lauvset, Nathalie Lefèvre, Sebastian Lienert, Junjie Liu, Gregg Marland, Patrick C. McGuire, Joe R. Melton, David R. Munro, Julia E. M. S. Nabel, Shin-Ichiro Nakaoka, Yosuke Niwa, Tsuneo Ono,

- Denis Pierrot, Benjamin Poulter, Gregor Rehder, Laure Resplandy, Eddy Robertson, Christian Rödenbeck, Thais M. Rosan, Jörg Schwinger, Clemens Schwingshackl, Roland Séférian, Adrienne J. Sutton, Colm Sweeney, Toste Tanhua, Pieter P. Tans, Hanqin Tian, Bronte Tilbrook, Francesco Tubiello, Guido R. van der Werf, Nicolas Vuichard, Chisato Wada, Rik Wanninkhof, Andrew J. Watson, David Willis, Andrew J. Wiltshire, Wenping Yuan, Chao Yue, Xu Yue, Sönke Zaehle, and Jiye Zeng. 2022. "Global Carbon Budget 2021." *Earth System Science Data* 14(4):1917–2005. doi: 10.5194/essd-14-1917-2022.
- Friend, Andrew D., Annemarie H. Eckes-Shephard, Patrick Fonti, Tim T. Rademacher, Cyrille B. K. Rathgeber, Andrew D. Richardson, and Rachael H. Turton. 2019. "On the Need to Consider Wood Formation Processes in Global Vegetation Models and a Suggested Approach." *Annals of Forest Science* 76(2):1–13. doi: 10.1007/s13595-019-0819-x.
- Friend, Andrew D., Wolfgang Lucht, Tim T. Rademacher, Rozenn Keribin, Richard Betts, Patricia Cadule, Philippe Ciais, Douglas B. Clark, Rutger Dankers, Pete D. Falloon, Akihiko Ito, Ron Kahana, Axel Kleidon, Mark R. Lomas, Kazuya Nishina, Sebastian Ostberg, Ryan Pavlick, Philippe Peylin, Sibyll Schaphoff, Nicolas Vuichard, Lila Warszawski, Andy Wiltshire, and F. Ian Woodward. 2014. "Carbon Residence Time Dominates Uncertainty in Terrestrial Vegetation Responses to Future Climate and Atmospheric CO₂." *Proceedings of the National Academy of Sciences* 111(9):3280–85. doi: 10.1073/pnas.1222477110.
- Fu, Zheng, Philippe Ciais, I. Colin Prentice, Pierre Gentine, David Makowski, Ana Bastos, Xiangzhong Luo, Julia K. Green, Paul C. Stoy, and Hui Yang. 2022. "Atmospheric Dryness Reduces Photosynthesis along a Large Range of Soil Water Deficits." *Nature Communications* 13(1):989.
- Fuhrer, J., Martin Beniston, Andreas Fischlin, Ch Frei, Stéphane Goyette, K. Jasper, and Ch Pfister. 2006. "Climate Risks and Their Impact on Agriculture and Forests in Switzerland." *Climate Variability, Predictability and Climate Risks: A European Perspective* 79–102.
- Galiano, L., J. Martínez-Vilalta, and F. Lloret. 2011. "Carbon Reserves and Canopy Defoliation Determine the Recovery of Scots Pine 4 Yr after a Drought Episode." *New Phytologist* 190(3):750–59. doi: 10.1111/j.1469-8137.2010.03628.x.
- Galiano, Lucía, Galina Timofeeva, Matthias Saurer, Rolf Siegwolf, Jordi Martínez-Vilalta, Robert Hommel, and Arthur Gessler. 2017. "The Fate of Recently Fixed Carbon after Drought Release: Towards Unravelling C Storage Regulation in And." *Plant, Cell & Environment* 40(9):1711–24. doi: 10.1111/pce.12972.
- Gamage, Dananjali, Michael Thompson, Mark Sutherland, Naoki Hirotsu, Amane Makino, and Saman Seneweera. 2018. "New Insights into the Cellular Mechanisms of Plant Growth at Elevated Atmospheric Carbon Dioxide Concentrations: Elevated CO₂ Effect on Plant Growth and Development." *Plant, Cell & Environment* 41(6):1233–46. doi: 10.1111/pce.13206.
- Gao, Decai, Jobin Joseph, Roland A. Werner, Ivano Brunner, Alois Zürcher, Christian Hug, Ao Wang, Chunhong Zhao, Edith Bai, Katrin Meusburger, Arthur Gessler, and Frank Hagedorn. 2021. "Drought Alters the Carbon Footprint of Trees in Soils-Tracking the Spatio-Temporal Fate of ¹³C-Labelled Assimilates in the Soil of an Old-Growth Pine Forest." *Global Change Biology* 27(11):2491–2506. doi: 10.1111/gcb.15557.

- Gao, Jianguo, Ping Zhao, Weijun Shen, Junfeng Niu, Liwei Zhu, and Guangyan Ni. 2015. "Biophysical Limits to Responses of Water Flux to Vapor Pressure Deficit in Seven Tree Species with Contrasting Land Use Regimes." *Agricultural and Forest Meteorology* 200:258–69. doi: 10.1016/j.agrformet.2014.10.007.
- Garcia-Forner, Núria, Anna Sala, Carme Biel, Robert Savé, and Jordi Martínez-Vilalta. 2016. "Individual Traits as Determinants of Time to Death under Extreme Drought in *Pinus Sylvestris* L." edited by D. Whitehead. *Tree Physiology* 36(10):1196–1209. doi: 10.1093/treephys/tpw040.
- Gattmann, Marielle, Benjamin Birami, Daniel Nadal Sala, and Nadine Katrin Ruehr. 2021. "Dying by Drying: Timing of Physiological Stress Thresholds Related to Tree Death Is Not Significantly Altered by Highly Elevated CO₂." *Plant, Cell & Environment* 44(2):356–70. doi: 10.1111/pce.13937.
- Gattmann, Marielle, Scott A. M. McAdam, Benjamin Birami, Roman Link, Daniel Nadal-Sala, Bernhard Schuldt, Dan Yakir, and Nadine K. Ruehr. 2023. "Anatomical Adjustments of the Tree Hydraulic Pathway Decrease Canopy Conductance under Long-Term Elevated CO₂." *Plant Physiology* 191(1):252–64. doi: 10.1093/plphys/kiac482.
- Gaul, Dirk, Dietrich Hertel, Werner Borken, Egbert Matzner, and Christoph Leuschner. 2008. "Effects of Experimental Drought on the Fine Root System of Mature Norway Spruce." *Forest Ecology and Management* 256(5):1151–59. doi: 10.1016/j.foreco.2008.06.016.
- Gazol, Antonio, J. Julio Camarero, Gabriel Sangüesa-Barreda, and Sergio M. Vicente-Serrano. 2018. "Post-Drought Resilience After Forest Die-Off: Shifts in Regeneration, Composition, Growth and Productivity." *Frontiers in Plant Science* 9. doi: 10.3389/fpls.2018.01546.
- Gelman, Andrew, and Donald B. Rubin. 1992. "Inference from Iterative Simulation Using Multiple Sequences." *Statistical Science* 7(4):457–72.
- Gharun, Mana, Lukas Hörtnagl, Eugénie Paul-Limoges, Shiva Ghiasi, Iris Feigenwinter, Susanne Burri, Kristiina Marquardt, Sophia Etzold, Roman Zweifel, Werner Eugster, and Nina Buchmann. 2020. "Physiological Response of Swiss Ecosystems to 2018 Drought across Plant Types and Elevation." *Philosophical Transactions of the Royal Society B: Biological Sciences* 375(1810):20190521. doi: 10.1098/rstb.2019.0521.
- Giday, Habtamu, Dimitrios Fanourakis, Katrine H. Kjaer, Inge S. Fomsgaard, and Carl-Otto Ottosen. 2014. "Threshold Response of Stomatal Closing Ability to Leaf Abscissic Acid Concentration during Growth." *Journal of Experimental Botany* 65(15):4361–70. doi: 10.1093/jxb/eru216.
- Giorgi, Filippo, and Piero Lionello. 2008. "Climate Change Projections for the Mediterranean Region." *Global and Planetary Change* 63(2–3):90–104.
- Gleason, Sean M., Mark Westoby, Steven Jansen, Brendan Choat, Uwe G. Hacke, Robert B. Pratt, Radika Bhaskar, Tim J. Brodribb, Sandra J. Bucci, Kun-Fang Cao, Hervé Cochard, Sylvain Delzon, Jean-Christophe Domec, Ze-Xin Fan, Taylor S. Feild, Anna L. Jacobsen, Daniel M. Johnson, Frederic Lens, Hafiz Maherali, Jordi Martínez-Vilalta, Stefan Mayr, Katherine A. McCulloh, Maurizio Mencuccini, Patrick J. Mitchell, Hugh Morris, Andrea Nardini, Jarmila Pittermann, Lenka Plavcová, Stefan G. Schreiber, John S. Sperry, Ian J. Wright, and

- Amy E. Zanne. 2016. "Weak Tradeoff between Xylem Safety and Xylem-Specific Hydraulic Efficiency across the World's Woody Plant Species." *New Phytologist* 209(1):123–36. doi: 10.1111/nph.13646.
- Green, Julia K., and Trevor F. Keenan. 2022. "The Limits of Forest Carbon Sequestration." *Science* 376(6594):692–93. doi: 10.1126/science.abo6547.
- Greer, D. H. 2019. "Limitations to Photosynthesis of Leaves of Apple (*Malus Domestica*) Trees across the Growing Season Prior to and after Harvest." *Photosynthetica* 57(2):483–90. doi: 10.32615/ps.2019.063.
- Grossiord, Charlotte, Thomas N. Buckley, Lucas A. Cernusak, Kimberly A. Novick, Benjamin Poulter, Rolf T. W. Siegwolf, John S. Sperry, and Nate G. McDowell. 2020. "Plant Responses to Rising Vapor Pressure Deficit." *New Phytologist* 226(6):1550–66. doi: 10.1111/nph.16485.
- Gruber, Andreas, Stefan Strobl, Barbara Veit, and Walter Oberhuber. 2010. "Impact of Drought on the Temporal Dynamics of Wood Formation in *Pinus Sylvestris*." *Tree Physiology* 30(4):490–501. doi: 10.1093/treephys/tpq003.
- Grünzweig, J. M., T. Lin, E. Rotenberg, A. Schwartz, and D. Yakir. 2003. "Carbon Sequestration in Arid-Land Forest." *Global Change Biology* 9(5):791–99. doi: 10.1046/j.1365-2486.2003.00612.x.
- Gu, Xihui, Qiang Zhang, Jianfeng Li, Vijay P. Singh, Jianyu Liu, Peng Sun, and Changxiu Cheng. 2019. "Attribution of Global Soil Moisture Drying to Human Activities: A Quantitative Viewpoint." *Geophysical Research Letters* 46(5):2573–82.
- Hagedorn, Frank, Jobin Joseph, Martina Peter, Jörg Luster, Karin Pritsch, Uwe Geppert, Rene Kerner, Virginie Molinier, Simon Egli, Marcus Schaub, Jian-Feng Liu, Maihe Li, Krunoslav Sever, Markus Weiler, Rolf T. W. Siegwolf, Arthur Gessler, and Matthias Arend. 2016. "Recovery of Trees from Drought Depends on Belowground Sink Control." *Nature Plants* 2(8):1–5. doi: 10.1038/nplants.2016.111.
- Hammond, William M., and Henry D. Adams. 2019. "Dying on Time: Traits Influencing the Dynamics of Tree Mortality Risk from Drought" edited by S. Sevanto. *Tree Physiology* 39(6):906–9. doi: 10.1093/treephys/tpz050.
- Hammond, William M., A. Park Williams, John T. Abatzoglou, Henry D. Adams, Tamir Klein, Rosana López, Cuauhtémoc Sáenz-Romero, Henrik Hartmann, David D. Breshears, and Craig D. Allen. 2022. "Global Field Observations of Tree Die-off Reveal Hotter-Drought Fingerprint for Earth's Forests." *Nature Communications* 13(1):1761.
- Hammond, William M., Kailiang Yu, Luke A. Wilson, Rodney E. Will, William R. L. Anderegg, and Henry D. Adams. 2019. "Dead or Dying? Quantifying the Point of No Return from Hydraulic Failure in Drought-induced Tree Mortality." *New Phytologist* 223(4):1834–43. doi: 10.1111/nph.15922.
- Hartig, Florian, Francesco Minunno, Stefan Paul, D. Cameron, and T. Ott. 2019. "BayesianTools: General-Purpose MCMC and SMC Samplers and Tools for Bayesian Statistics." *R Package Version 0.1 6*.

- Hartmann, Henrik. 2015. "Carbon Starvation during Drought-Induced Tree Mortality – Are We Chasing a Myth?" *Journal of Plant Hydraulics* 2:005. doi: 10.20870/jph.2015.e005.
- Hartmann, Henrik, Catarina F. Moura, William R. L. Anderegg, Nadine K. Ruehr, Yann Salmon, Craig D. Allen, Stefan K. Arndt, David D. Breshears, Hendrik Davi, David Galbraith, Katinka X. Ruthrof, Jan Wunder, Henry D. Adams, Jasper Bloemen, Maxime Cailleret, Richard Cobb, Arthur Gessler, Thorsten E. E. Grams, Steven Jansen, Markus Kautz, Francisco Lloret, and Michael O'Brien. 2018. "Research Frontiers for Improving Our Understanding of Drought-Induced Tree and Forest Mortality." *New Phytologist* 218(1):15–28. doi: 10.1111/nph.15048.
- Hartmann, Henrik, and Susan Trumbore. 2016. "Understanding the Roles of Nonstructural Carbohydrates in Forest Trees – from What We Can Measure to What We Want to Know." *New Phytologist* 211(2):386–403. doi: 10.1111/nph.13955.
- Hausfather, Zeke, and Glen P. Peters. 2020. "Emissions – the 'Business as Usual' Story Is Misleading." *Nature* 577(7792):618–20. doi: 10.1038/d41586-020-00177-3.
- Haworth, Matthew, Caroline Elliott-Kingston, and Jennifer C. McElwain. 2011. "The Stomatal CO₂ Proxy Does Not Saturate at High Atmospheric CO₂ Concentrations: Evidence from Stomatal Index Responses of *Araucariaceae* Conifers." *Oecologia* 167(1):11–19. doi: 10.1007/s00442-011-1969-1.
- Haworth, Matthew, Caroline Elliott-Kingston, and Jennifer C. McElwain. 2013. "Co-Ordination of Physiological and Morphological Responses of Stomata to Elevated [CO₂] in Vascular Plants." *Oecologia* 171:71–82.
- Haworth, Matthew, James Heath, and Jennifer C. McElwain. 2010. "Differences in the Response Sensitivity of Stomatal Index to Atmospheric CO₂ among Four Genera of *Cupressaceae* Conifers." *Annals of Botany* 105(3):411–18. doi: 10.1093/aob/mcp309.
- Hereş, Ana-Maria, Jesús Julio Camarero, Bernat C. López, and Jordi Martínez-Vilalta. 2014. "Declining Hydraulic Performances and Low Carbon Investments in Tree Rings Predate Scots Pine Drought-Induced Mortality." *Trees* 28:1737–50.
- Hereş, Ana-Maria, Jordi Voltas, Bernat Claramunt López, and Jordi Martínez-Vilalta. 2013. "Drought-Induced Mortality Selectively Affects Scots Pine Trees That Show Limited Intrinsic Water-Use Efficiency Responsiveness to Raising Atmospheric CO₂." *Functional Plant Biology* 41(3):244–56.
- Hlásny, Tomáš, Jiří Trombik, Michal Bošela, Ján Merganič, Róbert Marušák, Vladimír Šebeň, Petr Štěpánek, Jaroslav Kubišta, and Miroslav Trnka. 2017. "Climatic Drivers of Forest Productivity in Central Europe." *Agricultural and Forest Meteorology* 234–235:258–73. doi: 10.1016/j.agrformet.2016.12.024.
- Hommel, R., R. Siegwolf, S. Zavadlav, M. Arend, M. Schaub, L. Galiano, M. Haeni, Z. E. Kayler, and A. Gessler. 2016. "Impact of Interspecific Competition and Drought on the Allocation of New Assimilates in Trees." *Plant Biology (Stuttgart, Germany)* 18(5):785–96. doi: 10.1111/plb.12461.

- Hsiao, Theodore C. 1973. "Plant Responses to Water Stress." *Annual Review of Plant Physiology* 24(1):519–70. doi: 10.1146/annurev.pp.24.060173.002511.
- Hsiao, Theodore C., and Liu-Kang Xu. 2000. "Sensitivity of Growth of Roots versus Leaves to Water Stress: Biophysical Analysis and Relation to Water Transport." *Journal of Experimental Botany* 51(350):1595–1616. doi: 10.1093/jexbot/51.350.1595.
- Huang, Bingru, and Yi Xu. 2015. "Cellular and Molecular Mechanisms for Elevated CO₂ - Regulation of Plant Growth and Stress Adaptation." *Crop Science* 55(4):1405–24. doi: 10.2135/cropsci2014.07.0508.
- Huang, Jianping, Haipeng Yu, Xiaodan Guan, Guoyin Wang, and Ruixia Guo. 2016. "Accelerated Dryland Expansion under Climate Change." *Nature Climate Change* 6(2):166–71. doi: 10.1038/nclimate2837.
- Hui, Dafeng, Qi Deng, Hanqin Tian, and Yiqi Luo. 2017. "Climate Change and Carbon Sequestration in Forest Ecosystems." *Handbook of Climate Change Mitigation and Adaptation* 555:594.
- IPCC. 2014. "Climate Change 2014: Synthesis Report. Contribution of Working Groups I, II and III to the Fifth Assessment Report of the Intergovernmental Panel on Climate Change [Core Writing Team, R. K. Pachauri and L. A. Meyer (Eds.)]. Geneva, Switzerland: IPCC."
- IPCC. 2021. "IPCC, 2021: Climate Change 2021 - the Physical Science Basis, Contribution of Working Group I to the Sixth Assessment Report of the Intergovernmental Panel on Climate Change [Masson-Delmotte, V., P. Zhai, A. Pirani, S.L. Connors, C. Péan, S. Berger, N. Caud, Y. Chen, L. Goldfarb, M.I. Gomis, M. Huang, K. Leitzell, E. Lonnoy, J.B.R. Matthews, T.K. Maycock, T. Waterfield, O. Yelekçi, R. Yu, and B. Zhou (Eds.)]. Cambridge University Press, In Press, Published: 9 August 2021."
- Irvine, J., M. P. Perks, F. Magnani, and J. Grace. 1998. "The Response of *Pinus Sylvestris* to Drought: Stomatal Control of Transpiration and Hydraulic Conductance." *Tree Physiology* 18(6):393–402. doi: 10.1093/treephys/18.6.393.
- Jaime, Luciana, Enric Batllori, Jordi Margalef-Marrase, María Ángeles Pérez Navarro, and Francisco Lloret. 2019. "Scots Pine (*Pinus Sylvestris* L.) Mortality Is Explained by the Climatic Suitability of Both Host Tree and Bark Beetle Populations." *Forest Ecology and Management* 448:119–29. doi: 10.1016/j.foreco.2019.05.070.
- Jasechko, Scott, Zachary D. Sharp, John J. Gibson, S. Jean Birks, Yi Yi, and Peter J. Fawcett. 2013. "Terrestrial Water Fluxes Dominated by Transpiration." *Nature* 496(7445):347–50. doi: 10.1038/nature11983.
- Je, Sun-Mi, Su Young Woo, Seong Han Lee, Myung Ja Kwak, Tae Yoon Lee, and Sun Hee Kim. 2018. "Combined Effect of Elevated CO₂ Concentration and Drought on the Photosynthetic Apparatus and Leaf Morphology Traits in Seedlings of Yellow Poplar." *Ecological Research* 33(2):403–12. doi: 10.1007/s11284-017-1495-7.

- Jeong, J., N. S. Bolan, and C. Kim. 2021. "Allocation of Photoassimilated Carbon of Radiata Pine (*Pinus Radiata*) Seedlings as Affected by Soil Water Stress." *Australian Forestry* 84(1):4–12.
- Jin, Zhenong, Elizabeth A. Ainsworth, Andrew D. B. Leakey, and David B. Lobell. 2018. "Increasing Drought and Diminishing Benefits of Elevated Carbon Dioxide for Soybean Yields across the US Midwest." *Global Change Biology* 24(2):e522–33. doi: 10.1111/gcb.13946.
- Kagawa, Akira, Atsuko Sugimoto, and Trofim C. Maximov. 2006a. "¹³CO₂ Pulse-Labeling of Photoassimilates Reveals Carbon Allocation within and between Tree Rings." *Plant, Cell & Environment* 29(8):1571–84. doi: 10.1111/j.1365-3040.2006.01533.x.
- Kagawa, Akira, Atsuko Sugimoto, and Trofim C. Maximov. 2006b. "Seasonal Course of Translocation, Storage and Remobilization of ¹³C Pulse-Labeled Photoassimilate in Naturally Growing *Larix Gmelinii* Saplings." *The New Phytologist* 171(4):793–803. doi: 10.1111/j.1469-8137.2006.01780.x.
- Kagawa, Akira, Atsuko Sugimoto, Kana Yamashita, and Hisashi Abe. 2005. "Temporal Photosynthetic Carbon Isotope Signatures Revealed in a Tree Ring through ¹³CO₂ Pulse-Labeling." *Plant, Cell & Environment* 28(7):906–15. doi: 10.1111/j.1365-3040.2005.01343.x.
- Kaiser, Werner M. 1987. "Effects of Water Deficit on Photosynthetic Capacity." *Physiologia Plantarum* 71(1):142–49. doi: 10.1111/j.1399-3054.1987.tb04631.x.
- Keenan, T. F., and C. A. Williams. 2018. "The Terrestrial Carbon Sink." *Annual Review of Environment and Resources* 43(Volume 43, 2018):219–43. doi: 10.1146/annurev-environ-102017-030204.
- Kilpelainen, A., A. Z. Gerendai, K. Luostarinen, H. Peltola, and S. Kellomäki. 2007. "Elevated Temperature and CO₂ Concentration Effects on Xylem Anatomy of Scots Pine." *Tree Physiology* 27(9):1329–38. doi: 10.1093/treephys/27.9.1329.
- Klein, T., S. Cohen, I. Paudel, Y. Preisler, E. Rotenberg, and D. Yakir. 2016. "Diurnal Dynamics of Water Transport, Storage and Hydraulic Conductivity in Pine Trees under Seasonal Drought." *iForest - Biogeosciences and Forestry* 9(5):710–19. doi: 10.3832/for2046-009.
- Klein, T., S. Cohen, and D. Yakir. 2011. "Hydraulic Adjustments Underlying Drought Resistance of *Pinus Halepensis*." *Tree Physiology* 31(6):637–48. doi: 10.1093/treephys/tpr047.
- Klein, Tamir, and Uri Ramon. 2019. "Stomatal Sensitivity to CO₂ Diverges between Angiosperm and Gymnosperm Tree Species" edited by K. McCulloh. *Functional Ecology* 33(8):1411–24. doi: 10.1111/1365-2435.13379.
- Klein, Tamir, Rolf T. W. Siegwolf, and Christian Körner. 2016. "Belowground Carbon Trade among Tall Trees in a Temperate Forest." *Science* 352(6283):342–44. doi: 10.1126/science.aad6188.
- Knauer, Jürgen, Sönke Zaehle, Markus Reichstein, Belinda E. Medlyn, Matthias Forkel, Stefan Hagemann, and Christiane Werner. 2017. "The Response of Ecosystem Water-use Efficiency to Rising Atmospheric CO₂ Concentrations: Sensitivity and Large-scale Biogeochemical Implications." *New Phytologist* 213(4):1654–66. doi: 10.1111/nph.14288.

- Knipfer, Thorsten, Nicolas Bambach, M. Isabel Hernandez, Megan K. Bartlett, Gabriela Sinclair, Fiona Duong, Daniel A. Kluepfel, and Andrew J. McElrone. 2020. "Predicting Stomatal Closure and Turgor Loss in Woody Plants Using Predawn and Midday Water Potential." *Plant Physiology* 184(2):881–94.
- Körner, Christian. 2003. "Carbon Limitation in Trees." *Journal of Ecology* 91(1):4–17. doi: 10.1046/j.1365-2745.2003.00742.x.
- Körner, Christian. 2006. "Plant CO₂ Responses: An Issue of Definition, Time and Resource Supply." *New Phytologist* 172(3):393–411.
- Körner, Christian. 2019. "No Need for Pipes When the Well Is Dry—a Comment on Hydraulic Failure in Trees." *Tree Physiology* 39(5):695–700. doi: 10.1093/treephys/tpz030.
- Körner, Christian, Monika Neumayer, Susanna Pelaez Menendez-Riedl, and Angelika Smeets-Scheel. 1989. "Functional Morphology of Mountain Plants." *Flora* 182(5):353–83. doi: 10.1016/S0367-2530(17)30426-7.
- Kouwenberg, L. L. R., J. C. McElwain, W. M. Kurschner, F. Wagner, D. J. Beerling, F. E. Mayle, and H. Visscher. 2003. "Stomatal Frequency Adjustment of Four Conifer Species to Historical Changes in Atmospheric CO₂." *American Journal of Botany* 90(4):610–19. doi: 10.3732/ajb.90.4.610.
- Kubásek, Jiří, Tomáš Hájek, Jeffrey Duckett, Silvia Pressel, and Jiří Šantrůček. 2021. "Moss Stomata Do Not Respond to Light and CO₂ Concentration but Facilitate Carbon Uptake by Sporophytes: A Gas Exchange, Stomatal Aperture, and ¹³C-labelling Study." *New Phytologist* 230(5):1815–28.
- Kurepin, Leonid V., Zsolt R. Stangl, Alexander G. Ivanov, Vi Bui, Marin Mema, Norman P. A. Hüner, Gunnar Öquist, Danielle Way, and Vaughan Hurry. 2018. "Contrasting Acclimation Abilities of Two Dominant Boreal Conifers to Elevated CO₂ and Temperature: CO₂ and Warming Effects on Spruce and Pine." *Plant, Cell & Environment* 41(6):1331–45. doi: 10.1111/pce.13158.
- Kuznetsova, Alexandra, Per B. Brockhoff, and Rune Haubo Bojesen Christensen. 2017. "lmerTest Package: Tests in Linear Mixed Effects Models." *Journal of Statistical Software* 82(13).
- Lal, Rattan, Pete Smith, Hermann F. Jungkunst, William J. Mitsch, Johannes Lehmann, P. K. Ramachandran Nair, Alex B. McBratney, João Carlos de Moraes Sá, Julia Schneider, Yuri L. Zinn, Alba L. A. Skorupa, Hai-Lin Zhang, Budiman Minasny, Cherukumalli Srinivasrao, and Nijavalli H. Ravindranath. 2018. "The Carbon Sequestration Potential of Terrestrial Ecosystems." *Journal of Soil and Water Conservation* 73(6):145A–152A. doi: 10.2489/jswc.73.6.145A.
- Lambers, Hans, F. Stuart Chapin III, and Thijs L. Pons. 2008. *Plant Physiological Ecology*. Springer Science & Business Media.
- Landhäusser, Simon M., Pak S. Chow, L. Turin Dickman, Morgan E. Furze, Iris Kuhlman, Sandra Schmid, Julia Wiesenbauer, Birgit Wild, Gerd Gleixner, Henrik Hartmann, Günter Hoch,

Nate G. McDowell, Andrew D. Richardson, Andreas Richter, and Henry D. Adams. 2018. "Standardized Protocols and Procedures Can Precisely and Accurately Quantify Non-Structural Carbohydrates." *Tree Physiology* 38(12):1764–78. doi: 10.1093/treephys/tpy118.

Lange, Oo L., R. Lösch, E. D. Schulze, and L. Kappen. 1971. "Responses of Stomata to Changes in Humidity." *Planta* 100:76–86.

Laumer, W., L. Andreu, G. Helle, G. H. Schleser, T. Wieloch, and H. Wissel. 2009. "A Novel Approach for the Homogenization of Cellulose to Use Micro-Amounts for Stable Isotope Analyses." *Rapid Communications in Mass Spectrometry: RCM* 23(13):1934–40. doi: 10.1002/rcm.4105.

Lavergne, Aliénor, Heather Graven, Martin G. De Kauwe, Trevor F. Keenan, Belinda E. Medlyn, and Iain Colin Prentice. 2019. "Observed and Modelled Historical Trends in the Water-use Efficiency of Plants and Ecosystems." *Global Change Biology* gcb.14634. doi: 10.1111/gcb.14634.

Lemoine, Remi, Sylvain La Camera, Rossitza Atanassova, Fabienne Dédaldéchamp, Thierry Allario, Nathalie Pourtau, Jean-Louis Bonnemain, Maryse Laloi, Pierre Coutos-Thévenot, Laurence Maurousset, Mireille Faucher, Christine Girousse, Pauline Lemonnier, Jonathan Parrilla, and Mickael Durand. 2013. "Source-to-Sink Transport of Sugar and Regulation by Environmental Factors." *Frontiers in Plant Science* 4. doi: 10.3389/fpls.2013.00272.

Lenth, Russell, H. Singmann, J. Love, P. Buerkner, and M. Herve. 2019. "Emmeans: Estimated Marginal Means, Aka Least-Squares Means (Version 1.3.4)." *Emmeans Estim Marg Means Aka Least-Sq Means*.

Li, Fei, Jingfeng Xiao, Jiquan Chen, Ashley Ballantyne, Ke Jin, Bing Li, Michael Abraha, and Ranjeet John. 2023. "Global Water Use Efficiency Saturation Due to Increased Vapor Pressure Deficit." *Science* 381(6658):672–77.

Li, Shijie, Guojie Wang, Chenxia Zhu, Jiao Lu, Waheed Ullah, Daniel Fiifi Tawia Hagan, Giri Kattel, Yi Liu, Zhenyu Zhang, Yang Song, Shanlei Sun, Yi Zheng, and Jian Peng. 2023. "Vegetation Growth Due to CO₂ Fertilization Is Threatened by Increasing Vapor Pressure Deficit." *Journal of Hydrology* 619:129292. doi: 10.1016/j.jhydrol.2023.129292.

Li, Weibin, Henrik Hartmann, Henry D. Adams, Hongxia Zhang, Changjie Jin, Chuanyan Zhao, Dexin Guan, Anzhi Wang, Fenghui Yuan, and Jiabing Wu. 2018. "The Sweet Side of Global Change—Dynamic Responses of Non-Structural Carbohydrates to Drought, Elevated CO₂ and Nitrogen Fertilization in Tree Species." *Tree Physiology*. doi: 10.1093/treephys/tpy059.

Lin, Jinxing, M. E. Jach, and R. Ceulemans. 2001. "Stomatal Density and Needle Anatomy of Scots Pine (*Pinus Sylvestris*) Are Affected by Elevated CO₂." *New Phytologist* 150(3):665–74. doi: 10.1046/j.1469-8137.2001.00124.x.

Lindquist, Erik J., ed. 2012. *Global Forest Land-Use Change 1990 - 2005*. Rome: Food and Agriculture Organization of the United Nations.

- Linton, M. J., J. S. Sperry, and D. G. Williams. 1998. "Limits to Water Transport in *Juniperus Osteosperma* and *Pinus Edulis*: Implications for Drought Tolerance and Regulation of Transpiration." *Functional Ecology* 12(6):906–11.
- Litton, Creighton M., James W. Raich, and Michael G. Ryan. 2007. "Carbon Allocation in Forest Ecosystems." *Global Change Biology* 13(10):2089–2109. doi: 10.1111/j.1365-2486.2007.01420.x.
- Liu, Hongyan, A. Park Williams, Craig D. Allen, Dali Guo, Xiuchen Wu, Oleg A. Anenkhonov, Eryuan Liang, Denis V. Sandanov, Yi Yin, and Zhaohuan Qi. 2013. "Rapid Warming Accelerates Tree Growth Decline in Semi-arid Forests of Inner Asia." *Global Change Biology* 19(8):2500–2510.
- Liu, Laibao, Lukas Gudmundsson, Mathias Hauser, Dahe Qin, Shuangcheng Li, and Sonia I. Seneviratne. 2020. "Soil Moisture Dominates Dryness Stress on Ecosystem Production Globally." *Nature Communications* 11(1):4892.
- Liu, Shuguang, Ben Bond-Lamberty, Lena R. Boysen, James D. Ford, Andrew Fox, Kevin Gallo, Jerry Hatfield, Geoffrey M. Henebry, Thomas G. Huntington, Zhihua Liu, Thomas R. Loveland, Richard J. Norby, Terry Sohl, Allison L. Steiner, Wenping Yuan, Zhao Zhang, and Shuqing Zhao. 2017. "Grand Challenges in Understanding the Interplay of Climate and Land Changes." *Earth Interactions* 21(2):1–43. doi: 10.1175/EI-D-16-0012.1.
- Liu, Xianfeng, Gaopeng Sun, Zheng Fu, Philippe Ciais, Xiaoming Feng, Jing Li, and Bojie Fu. 2023. "Compound Droughts Slow down the Greening of the Earth." *Global Change Biology* 29(11):3072–84. doi: 10.1111/gcb.16657.
- Liu, Ying, Peng Li, Lie Xiao, Wen Wang, Kunxia Yu, and Peng Shi. 2020. "Heterogeneity in Short-Term Allocation of Carbon to Roots of *Pinus Tabuliformis* Seedlings and Root Respiration under Drought Stress." *Plant and Soil* 452:359–78.
- Lockhart, James A. 1965. "An Analysis of Irreversible Plant Cell Elongation." *Journal of Theoretical Biology* 8(2):264–75. doi: 10.1016/0022-5193(65)90077-9.
- Luomala, Eeva-Maria, Kaisa Laitinen, Sirkka Sutinen, Seppo Kellomaki, and Elina Vapaavuori. 2005. "Stomatal Density, Anatomy and Nutrient Concentrations of Scots Pine Needles Are Affected by Elevated CO₂ and Temperature." *Plant, Cell and Environment* 28(6):733–49. doi: 10.1111/j.1365-3040.2005.01319.x.
- Mackay, D. Scott, David E. Roberts, Brent E. Ewers, John S. Sperry, Nathan G. McDowell, and William T. Pockman. 2015. "Interdependence of Chronic Hydraulic Dysfunction and Canopy Processes Can Improve Integrated Models of Tree Response to Drought: Modeling Chronic Hydraulic Dysfunction and Canopy Processes." *Water Resources Research* 51(8):6156–76. doi: 10.1002/2015WR017244.
- Maherali, Hafiz, and Evan H. DeLucia. 2000. "Interactive Effects of Elevated CO₂ and Temperature on Water Transport Inponderosa Pine." *American Journal of Botany* 87(2):243–49. doi: 10.2307/2656912.

- Martínez-Vilalta, Jordi, Hervé Cochard, Maurizia Mencuccini, Frank Sterck, Asier Herrero, J. F. J. Korhonen, Pilar Llorens, Eero Nikinmaa, Angelo Nole, and Rafael Poyatos. 2009. "Hydraulic Adjustment of Scots Pine across Europe." *New Phytologist* 184(2):353–64.
- Martínez-Vilalta, Jordi, Anna Sala, Dolores Asensio, Lucía Galiano, Günter Hoch, Sara Palacio, Frida I. Piper, and Francisco Lloret. 2016. "Dynamics of Non-Structural Carbohydrates in Terrestrial Plants: A Global Synthesis." *Ecological Monographs* 86(4):495–516. doi: 10.1002/ecm.1231.
- Martin-StPaul, Nicolas, Sylvain Delzon, and Hervé Cochard. 2017. "Plant Resistance to Drought Depends on Timely Stomatal Closure" edited by H. Maherali. *Ecology Letters* 20(11):1437–47. doi: 10.1111/ele.12851.
- Maruyama, Yutaka, Shozo Nakamura, Ricardo Antonio Marengo, Gil Vieira, and Akira Sato. 2005. "Photosynthetic Traits of Seedlings of Several Tree Species in an Amazonian Forest." *Tropics* 14(3):211–19. doi: 10.3759/tropics.14.211.
- Maton, Clarisse, and Barbara L. Gartner. 2005. "Do Gymnosperm Needles Pull Water through the Xylem Produced in the Same Year as the Needle?" *American Journal of Botany* 92(1):123–31.
- McAdam, Scott A. M., and Timothy J. Brodribb. 2015. "The Evolution of Mechanisms Driving the Stomatal Response to Vapor Pressure Deficit." *Plant Physiology* 167(3):833–43. doi: 10.1104/pp.114.252940.
- McAdam, Scott AM, Timothy J. Brodribb, John J. Ross, and Gregory J. Jordan. 2011. "Augmentation of Abscissic Acid (ABA) Levels by Drought Does Not Induce Short-Term Stomatal Sensitivity to CO₂ in Two Divergent Conifer Species." *Journal of Experimental Botany* 62(1):195–203.
- McDowell, Nate G., Craig D. Allen, Kristina Anderson-Teixeira, Brian H. Aukema, Ben Bond-Lamberty, Louise Chini, James S. Clark, Michael Dietze, Charlotte Grossiord, Adam Hanbury-Brown, George C. Hurtt, Robert B. Jackson, Daniel J. Johnson, Lara Kueppers, Jeremy W. Lichstein, Kiona Ogle, Benjamin Poulter, Thomas A. M. Pugh, Rupert Seidl, Monica G. Turner, Maria Uriarte, Anthony P. Walker, and Chonggang Xu. 2020. "Pervasive Shifts in Forest Dynamics in a Changing World." *Science* 368(6494):eaaz9463. doi: 10.1126/science.aaz9463.
- McDowell, Nate G., Craig D. Allen, and Laura Marshall. 2010. "Growth, Carbon-Isotope Discrimination, and Drought-Associated Mortality across a *Pinus Ponderosa* Elevational Transect." *Global Change Biology* 16(1):399–415. doi: 10.1111/j.1365-2486.2009.01994.x.
- McDowell, Nate G., Rosie A. Fisher, Chonggang Xu, J. C. Domec, Teemu Hölttä, D. Scott Mackay, John S. Sperry, Amanda Boutz, Lee Dickman, Nathan Gehres, Jean Marc Limousin, Alison Macalady, Jordi Martínez-Vilalta, Maurizio Mencuccini, Jennifer A. Plaut, Jérôme Ogée, Robert E. Pangle, Daniel P. Rasse, Michael G. Ryan, Sanna Sevanto, Richard H. Waring, A. Park Williams, Enrico A. Yezpez, and William T. Pockman. 2013. "Evaluating Theories of Drought-Induced Vegetation Mortality Using a Multimodel-Experiment Framework." *New Phytologist* 200(2):304–21. doi: 10.1111/nph.12465.

McDowell, Nate G., Gerard Sapes, Alexandria Pivovarovoff, Henry D. Adams, Craig D. Allen, William R. L. Anderegg, Matthias Arend, David D. Breshears, Tim Brodribb, Brendan Choat, Hervé Cochard, Miquel De Cáceres, Martin G. De Kauwe, Charlotte Grossiord, William M. Hammond, Henrik Hartmann, Günter Hoch, Ansgar Kahmen, Tamir Klein, D. Scott Mackay, Marylou Mantova, Jordi Martínez-Vilalta, Belinda E. Medlyn, Maurizio Mencuccini, Andrea Nardini, Rafael S. Oliveira, Anna Sala, David T. Tissue, José M. Torres-Ruiz, Amy M. Trowbridge, Anna T. Trugman, Erin Wiley, and Chonggang Xu. 2022. “Mechanisms of Woody-Plant Mortality under Rising Drought, CO₂ and Vapour Pressure Deficit.” *Nature Reviews Earth & Environment* 3(5):294–308. doi: 10.1038/s43017-022-00272-1.

McDowell, Nate, William T. Pockman, Craig D. Allen, David D. Breshears, Neil Cobb, Thomas Kolb, Jennifer Plaut, John Sperry, Adam West, David G. Williams, and Enrico A. Yezpez. 2008. “Mechanisms of Plant Survival and Mortality during Drought: Why Do Some Plants Survive While Others Succumb to Drought?” *New Phytologist* 178(4):719–39. doi: 10.1111/j.1469-8137.2008.02436.x.

McDowell, Nathan G. 2011. “Mechanisms Linking Drought, Hydraulics, Carbon Metabolism, and Vegetation Mortality.” *Plant Physiology* 155(3):1051–59. doi: 10.1104/pp.110.170704.

McNaughton, K. G., and P. G. Jarvis. 1991. “Effects of Spatial Scale on Stomatal Control of Transpiration.” *Agricultural and Forest Meteorology* 54(2):279–302. doi: 10.1016/0168-1923(91)90010-N.

Medlyn, B. E., C. V. M. Barton, M. S. J. Broadmeadow, R. Ceulemans, P. De Angelis, M. Forstreuter, M. Freeman, S. B. Jackson, S. Kellomäki, E. Laitat, A. Rey, P. Roberntz, B. D. Sigurdsson, J. Strassemeier, K. Wang, P. S. Curtis, and P. G. Jarvis. 2001. “Stomatal Conductance of Forest Species after Long-term Exposure to Elevated CO₂ Concentration: A Synthesis.” *New Phytologist* 149(2):247–64. doi: 10.1046/j.1469-8137.2001.00028.x.

Meinzer, F. C., and D. A. Grantz. 1990. “Stomatal and Hydraulic Conductance in Growing Sugarcane: Stomatal Adjustment to Water Transport Capacity.” *Plant, Cell and Environment* 13(4):383–88. doi: 10.1111/j.1365-3040.1990.tb02142.x.

Meir, Patrick, Maurizio Mencuccini, and Roderick C. Dewar. 2015. “Drought-Related Tree Mortality: Addressing the Gaps in Understanding and Prediction.” *New Phytologist* 207(1):28–33. doi: 10.1111/nph.13382.

Mendonca, Caren C., Lisa J. Samuelson, Tom A. Stokes, Michael R. Ramirez, Carlos Gonzalez-Benecke, and Michael J. Aspinwall. 2023. “Soil Moisture and Vapor Pressure Deficit Controls of Longleaf Pine Physiology: Results from a Throughfall Reduction Study.” *Trees* 37(4):1249–65. doi: 10.1007/s00468-023-02423-3.

Mitchell, P. J., A. P. O’Grady, D. T. Tissue, D. Worledge, and E. A. Pinkard. 2014. “Co-Ordination of Growth, Gas Exchange and Hydraulics Define the Carbon Safety Margin in Tree Species with Contrasting Drought Strategies.” *Tree Physiology* 34(5):443–58. doi: 10.1093/treephys/tpu014.

Mitchell, Patrick J., Anthony P. O’Grady, Elizabeth A. Pinkard, Timothy J. Brodribb, Stefan K. Arndt, Chris J. Blackman, Remko A. Duursma, Rod J. Fensham, David W. Hilbert, Craig R. Nitschke, Jaymie Norris, Stephen H. Roxburgh, Katinka X. Ruthrof, and David T. Tissue. 2016.

- “An Ecoclimatic Framework for Evaluating the Resilience of Vegetation to Water Deficit.” *Global Change Biology* 22(5):1677–89. doi: 10.1111/gcb.13177.
- Mitchell, Patrick J., Anthony P. O’Grady, David T. Tissue, Donald A. White, Maria L. Ottenschlaeger, and Elizabeth A. Pinkard. 2013. “Drought Response Strategies Define the Relative Contributions of Hydraulic Dysfunction and Carbohydrate Depletion during Tree Mortality.” *New Phytologist* 197(3):862–72. doi: 10.1111/nph.12064.
- Morison, James IL. 1985. “Sensitivity of Stomata and Water Use Efficiency to High CO₂.” *Plant, Cell & Environment* 8(6):467–74.
- Morison, James IL. 1987. “Intercellular CO₂ Concentration and Stomatal Response to CO₂.” *See Ref* 113:229–51.
- Mott, Keith A., Erik D. Sibbersen, and Joseph C. Shope. 2008. “The Role of the Mesophyll in Stomatal Responses to Light and CO₂.” *Plant, Cell & Environment* 31(9):1299–1306.
- Mount, John, and Nina Zumel. 2019. *Practical Data Science with R*. Simon and Schuster.
- Muller, Bertrand, Florent Pantin, Michel Génard, Olivier Turc, Sandra Freixes, Maria Piques, and Yves Gibon. 2011. “Water Deficits Uncouple Growth from Photosynthesis, Increase C Content, and Modify the Relationships between C and Growth in Sink Organs.” *Journal of Experimental Botany* 62(6):1715–29. doi: 10.1093/jxb/erq438.
- Nabuurs, G. J., G. M. Hengeveld, D. C. van der Werf, and A. H. Heidema. 2010. “European Forest Carbon Balance Assessed with Inventory Based Methods—An Introduction to a Special Section.” *Forest Ecology and Management* 260(3):239–40. doi: 10.1016/j.foreco.2009.11.024.
- Nadal-Sala, Daniel, Rüdiger Grote, Benjamin Birami, Timo Knüver, Romy Rehschuh, Selina Schwarz, and Nadine K. Ruehr. 2021. “Leaf Shedding and Non-Stomatal Limitations of Photosynthesis Mitigate Hydraulic Conductance Losses in Scots Pine Saplings during Severe Drought Stress.” *Frontiers in Plant Science* 12:715127.
- Nardini, Andrea, Marta Battistuzzo, and Tadeja Savi. 2013. “Shoot Desiccation and Hydraulic Failure in Temperate Woody Angiosperms during an Extreme Summer Drought.” *New Phytologist* 200(2):322–29. doi: 10.1111/nph.12288.
- Niu, Shuli, Yiqi Luo, Dejun Li, Shuanghe Cao, Jianyang Xia, Jianwei Li, and Melinda D. Smith. 2014. “Plant Growth and Mortality under Climatic Extremes: An Overview.” *Environmental and Experimental Botany* 98:13–19. doi: 10.1016/j.envexpbot.2013.10.004.
- Novick, Kimberly A., Darren L. Ficklin, Charlotte Grossiord, Alexandra G. Konings, Jordi Martínez-Vilalta, Walid Sadok, Anna T. Trugman, A. Park Williams, Alexandra J. Wright, John T. Abatzoglou, Matthew P. Dannenberg, Pierre Gentine, Kaiyu Guan, Miriam R. Johnston, Lauren E. L. Lowman, David J. P. Moore, and Nate G. McDowell. 2024. “The Impacts of Rising Vapour Pressure Deficit in Natural and Managed Ecosystems.” *Plant, Cell & Environment* 47(9):3561–89. doi: 10.1111/pce.14846.
- Novick, Kimberly A., Darren L. Ficklin, Paul C. Stoy, Christopher A. Williams, Gil Bohrer, A. Christopher Oishi, Shirley A. Papuga, Peter D. Blanken, Asko Noormets, Benjamin N. Sulman, Russell L. Scott, Lixin Wang, and Richard P. Phillips. 2016. “The Increasing Importance of

Atmospheric Demand for Ecosystem Water and Carbon Fluxes.” *Nature Climate Change* 6(11):1023–27. doi: 10.1038/nclimate3114.

Novick, Kimberly A., Alexandra G. Konings, and Pierre Gentine. 2019. “Beyond Soil Water Potential: An Expanded View on Isohydrlicity Including Land–Atmosphere Interactions and Phenology.” *Plant, Cell & Environment* 42(6):1802–15. doi: 10.1111/pce.13517.

Novick, Kimberly, Ram Oren, Paul Stoy, Jehn-Yih Juang, Mario Siqueira, and Gabriel Katul. 2009. “The Relationship between Reference Canopy Conductance and Simplified Hydraulic Architecture.” *Advances in Water Resources* 32(6):809–19. doi: 10.1016/j.advwatres.2009.02.004.

O’Brien, Michael J., Bettina M. J. Engelbrecht, Julia Joswig, Gabriela Pereyra, Bernhard Schuldt, Steven Jansen, Jens Kattge, Simon M. Landhäusser, Shaun R. Levick, Yakir Preisler, Päivi Väänänen, and Cate Macinnis-Ng. 2017. “A Synthesis of Tree Functional Traits Related to Drought-Induced Mortality in Forests across Climatic Zones” edited by J. Firn. *Journal of Applied Ecology* 54(6):1669–86. doi: 10.1111/1365-2664.12874.

O’Brien, Michael J., Sebastian Leuzinger, Christopher D. Philipson, John Tay, and Andy Hector. 2014. “Drought Survival of Tropical Tree Seedlings Enhanced by Non-Structural Carbohydrate Levels.” *Nature Climate Change* 4(8):710–14. doi: 10.1038/nclimate2281.

Olszyk, David, Martha Apple, Barbara Gartner, Rachel Spicer, Claudia Wise, Erica Buckner, Annick Benson-Scott, and David Tingey. 2005. “Xeromorphy Increases in Shoots of *Pseudotsuga Menziesii* (Mirb.) Franco Seedlings with Exposure to Elevated Temperature but Not Elevated CO₂.” *Trees* 19(5):552–63. doi: 10.1007/s00468-005-0414-7.

Oren, R., J. S. Sperry, G. G. Katul, D. E. Pataki, B. E. Ewers, N. Phillips, and K. V. R. Schäfer. 1999. “Survey and Synthesis of Intra- and Interspecific Variation in Stomatal Sensitivity to Vapour Pressure Deficit.” *Plant, Cell & Environment* 22(12):1515–26. doi: 10.1046/j.1365-3040.1999.00513.x.

Ouyang, Shengnan, Liehua Tie, Matthias Saurer, Arun K. Bose, Honglang Duan, Maihe Li, Xingliang Xu, Weijun Shen, and Arthur Gessler. 2024. “Divergent Role of Nutrient Availability in Determining Drought Responses of Sessile Oak and Scots Pine Seedlings: Evidence from ¹³C and ¹⁵N Dual Labeling.” *Tree Physiology* 44(1):tpad105. doi: 10.1093/treephys/tpad105.

Pan, Yude, Richard A. Birdsey, Jingyun Fang, Richard Houghton, Pekka E. Kauppi, Werner A. Kurz, Oliver L. Phillips, Anatoly Shvidenko, Simon L. Lewis, Josep G. Canadell, Philippe Ciais, Robert B. Jackson, Stephen W. Pacala, A. David McGuire, Shilong Piao, Aapo Rautiainen, Stephen Sitch, and Daniel Hayes. 2011. “A Large and Persistent Carbon Sink in the World’s Forests.” *Science* 333(6045):988–93. doi: 10.1126/science.1201609.

Pan, Yude, Richard A. Birdsey, Oliver L. Phillips, Richard A. Houghton, Jingyun Fang, Pekka E. Kauppi, Heather Keith, Werner A. Kurz, Akihiko Ito, and Simon L. Lewis. 2024. “The Enduring World Forest Carbon Sink.” *Nature* 631(8021):563–69.

Pantin, Florent, Thierry Simonneau, and Bertrand Muller. 2012. “Coming of Leaf Age: Control of Growth by Hydraulics and Metabolics during Leaf Ontogeny.” *New Phytologist* 196(2):349–66.

Pantin, Florent, Thierry Simonneau, Gaëlle Rolland, Myriam Dauzat, and Bertrand Muller. 2011. "Control of Leaf Expansion: A Developmental Switch from Metabolics to Hydraulics." *Plant Physiology* 156(2):803–15.

Park Williams, A., Craig D. Allen, Alison K. Macalady, Daniel Griffin, Connie A. Woodhouse, David M. Meko, Thomas W. Swetnam, Sara A. Rauscher, Richard Seager, Henri D. Grissino-Mayer, Jeffrey S. Dean, Edward R. Cook, Chandana Gangodagamage, Michael Cai, and Nate G. McDowell. 2013. "Temperature as a Potent Driver of Regional Forest Drought Stress and Tree Mortality." *Nature Climate Change* 3(3):292–97. doi: 10.1038/nclimate1693.

Passioura, J. B. 1982. "Water in the Soil-Plant-Atmosphere Continuum." Pp. 5–33 in *Physiological plant ecology II: Water relations and carbon assimilation*. Springer.

Pernicová, Natálie, Otmar Urban, Josef Čáslavský, Tomáš Kolář, Michal Rybníček, Irena Sochová, Josep Peñuelas, Michal Bošela, and Miroslav Trnka. 2024. "Impacts of Elevated CO₂ Levels and Temperature on Photosynthesis and Stomatal Closure along an Altitudinal Gradient Are Counteracted by the Rising Atmospheric Vapor Pressure Deficit." *Science of The Total Environment* 921:171173. doi: 10.1016/j.scitotenv.2024.171173.

Peters, Richard L., Kathy Steppe, Henri E. Cuny, Dirk J. W. De Pauw, David C. Frank, Marcus Schaub, Cyrille B. K. Rathgeber, Antoine Cabon, and Patrick Fonti. 2021. "Turgor – a Limiting Factor for Radial Growth in Mature Conifers along an Elevational Gradient." *New Phytologist* 229(1):213–29. doi: 10.1111/nph.16872.

Phillips, Oliver L., Geertje van der Heijden, Simon L. Lewis, Gabriela López-González, Luiz E. O. C. Aragão, Jon Lloyd, Yadvinder Malhi, Abel Monteagudo, Samuel Almeida, Esteban Alvarez Dávila, Iêda Amaral, Sandy Andelman, Ana Andrade, Luzmila Arroyo, Gerardo Aymard, Tim R. Baker, Lilian Blanc, Damien Bonal, Átila Cristina Alves de Oliveira, Kuo-Jung Chao, Nallaret Dávila Cardozo, Lola da Costa, Ted R. Feldpausch, Joshua B. Fisher, Nikolaos M. Fyllas, Maria Aparecida Freitas, David Galbraith, Emanuel Gloor, Niro Higuchi, Eurídice Honorio, Eliana Jiménez, Helen Keeling, Tim J. Killeen, Jon C. Lovett, Patrick Meir, Casimiro Mendoza, Alexandra Morel, Percy Núñez Vargas, Sandra Patiño, Kelvin S. H. Peh, Antonio Peña Cruz, Adriana Prieto, Carlos A. Quesada, Fredy Ramírez, Hirma Ramírez, Agustín Rudas, Rafael Salamão, Michael Schwarz, Javier Silva, Marcos Silveira, J. W. Ferry Slik, Bonaventure Sonké, Anne Sota Thomas, Juliana Stropp, James R. D. Taplin, Rodolfo Vásquez, and Emilio Vilanova. 2010. "Drought-Mortality Relationships for Tropical Forests." *New Phytologist* 187(3):631–46. doi: 10.1111/j.1469-8137.2010.03359.x.

Pinheiro, Jose, Douglas Bates, Saikat DebRoy, Deepayan Sarkar, and R. Core Team. 2007. "Linear and Nonlinear Mixed Effects Models." *R Package Version* 3(57):1–89.

Piñol, J., and A. Sala. 2000. "Ecological Implications of Xylem Cavitation for Several *Pinaceae* in the Pacific Northern USA." *Functional Ecology* 14(5):538–45.

Poorter, H., Y. Van Berkel, R. Baxter, J. Den Hertog, P. Dijkstra, R. M. Gifford, K. L. Griffin, C. Roumet, J. Roy, and S. C. Wong. 1997. "The Effect of Elevated CO₂ on the Chemical Composition and Construction Costs of Leaves of 27 C3 Species." *Plant, Cell and Environment* 20(4):472–82. doi: 10.1046/j.1365-3040.1997.d01-84.x.

- Poorter, Hendrik, Oliver Knopf, Ian J. Wright, Andries A. Temme, Sander W. Hogewoning, Alexander Graf, Lucas A. Cernusak, and Thijs L. Pons. 2022. "A Meta-analysis of Responses of C3 Plants to Atmospheric CO₂: Dose–Response Curves for 85 Traits Ranging from the Molecular to the Whole-plant Level." *New Phytologist* 233(4):1560–96.
- Poorter, Hendrik, Karl J. Niklas, Peter B. Reich, Jacek Oleksyn, Pieter Poot, and Liesje Mommer. 2012. "Biomass Allocation to Leaves, Stems and Roots: Meta-Analyses of Interspecific Variation and Environmental Control." *New Phytologist* 193(1):30–50. doi: 10.1111/j.1469-8137.2011.03952.x.
- Poyatos, R., J. Martínez-Vilalta, J. Čermák, R. Ceulemans, A. Granier, J. Irvine, B. Köstner, Fredrik Lagergren, Linda Meiresonne, and N. Nadezhdina. 2007. "Plasticity in Hydraulic Architecture of Scots Pine across Eurasia." *Oecologia* 153:245–59.
- Poyatos, Rafael, Pilar Llorens, Josep Piñol, and Carles Rubio. 2008. "Response of Scots Pine (*Pinus Sylvestris* L.) and Pubescent Oak (*Quercus Pubescens* Willd.) to Soil and Atmospheric Water Deficits under Mediterranean Mountain Climate." *Annals of Forest Science* 65(3):306–306. doi: 10.1051/forest:2008003.
- Preisler, Yakir, José M. Grünzweig, Ori Ahiman, Madi Amer, Itai Oz, Xue Feng, Jonathan D. Muller, Nadine Ruehr, Eyal Rotenberg, Benjamin Birami, and Dan Yakir. 2023. "Vapour Pressure Deficit Was Not a Primary Limiting Factor for Gas Exchange in an Irrigated, Mature Dryland Aleppo Pine Forest." *Plant, Cell & Environment* 46(12):3775–90. doi: 10.1111/pce.14712.
- Preisler, Yakir, Fyodor Tatarinov, José M. Grünzweig, Didier Bert, Jérôme Ogée, Lisa Wingate, Eyal Rotenberg, Shani Rohatyn, Nir Her, and Itzhak Moshe. 2019. "Mortality versus Survival in Drought-affected Aleppo Pine Forest Depends on the Extent of Rock Cover and Soil Stoniness." *Functional Ecology* 33(5):901–12.
- Pritchard, Seth. G., Hugo. H. Rogers, Stephen A. Prior, and Curt. M. Peterson. 1999. "Elevated CO₂ and Plant Structure: A Review." *Global Change Biology* 5(7):807–37. doi: 10.1046/j.1365-2486.1999.00268.x.
- Purcell, C., S. P. Batke, Charilaos Yiotis, Rodrigo Caballero, W. K. Soh, Michelle Murray, and Jennifer C. McElwain. 2018. "Increasing Stomatal Conductance in Response to Rising Atmospheric CO₂." *Annals of Botany* 121(6):1137–49.
- Pushnik, James C., Richard S. Demaree, James L. J. Houppis, William B. Flory, Scott M. Bauer, and Paul D. Anderson. 1995. "The Effect of Elevated Carbon Dioxide on a Sierra-Nevadan Dominant Species: *Pinus Ponderosa*." *Journal of Biogeography* 22(2/3):249. doi: 10.2307/2845918.
- Quick, W. P., M. M. Chaves, R. Wendler, M. David, M. L. Rodrigues, J. A. Passaharinho, J. S. Pereira, M. d. Adcock, R. C. Leegood, and M. Stitt. 1992. "The Effect of Water Stress on Photosynthetic Carbon Metabolism in Four Species Grown under Field Conditions." *Plant, Cell & Environment* 15(1):25–35. doi: 10.1111/j.1365-3040.1992.tb01455.x.
- Rambal, S., M. Lempereur, J. M. Limousin, N. K. Martin-StPaul, J. M. Ourcival, and J. Rodríguez-Calcerrada. 2014. "How Drought Severity Constrains Gross Primary Production

- (GPP) and Its Partitioning among Carbon Pools in a *Quercus Ilex* Coppice?" *Biogeosciences* 11(23):6855–69. doi: 10.5194/bg-11-6855-2014.
- Ranasinghe, Sanathanie, and Gail Taylor. 1996. "Mechanism for Increased Leaf Growth in Elevated CO₂." *Journal of Experimental Botany* 47(3):349–58.
- Raschke, Klaus. 1975. "Simultaneous Requirement of Carbon Dioxide and Abscissic Acid for Stomatal Closing in *Xanthium Strumarium* L." *Planta* 125:243–59.
- Reddy, Attipalli Ramachandra, Kolluru Viswanatha Chaitanya, and Munusamy Vivekanandan. 2004. "Drought-Induced Responses of Photosynthesis and Antioxidant Metabolism in Higher Plants." *Journal of Plant Physiology* 161(11):1189–1202. doi: 10.1016/j.jplph.2004.01.013.
- Rehsehuh, Romy, Stephanie Rehsehuh, Andreas Gast, Andrea-Livia Jakab, Marco M. Lehmann, Matthias Saurer, Arthur Gessler, and Nadine K. Ruehr. 2022. "Tree Allocation Dynamics beyond Heat and Hot Drought Stress Reveal Changes in Carbon Storage, Belowground Translocation and Growth." *New Phytologist* 233(2):687–704. doi: 10.1111/nph.17815.
- Reichstein, Markus, Michael Bahn, Philippe Ciais, Dorothea Frank, Miguel D. Mahecha, Sonia I. Seneviratne, Jakob Zscheischler, Christian Beer, Nina Buchmann, David C. Frank, Dario Papale, Anja Rammig, Pete Smith, Kirsten Thonicke, Marijn van der Velde, Sara Vicca, Ariane Walz, and Martin Wattenbach. 2013. "Climate Extremes and the Carbon Cycle." *Nature* 500(7462):287–95. doi: 10.1038/nature12350.
- Reid, Chantal D. 2003. "On the Relationship between Stomatal Characters and Atmospheric CO₂." *Geophysical Research Letters* 30(19):1983. doi: 10.1029/2003GL017775.
- Rennenberg, H., F. Loreto, A. Polle, F. Brilli, S. Fares, R. S. Beniwal, and A. Gessler. 2006. "Physiological Responses of Forest Trees to Heat and Drought." *Plant Biology* 8(5):556–71. doi: 10.1055/s-2006-924084.
- Resco, Víctor, Brent E. Ewers, Wei Sun, Travis E. Huxman, Jake F. Weltzin, and David G. Williams. 2009. "Drought-Induced Hydraulic Limitations Constrain Leaf Gas Exchange Recovery after Precipitation Pulses in the C3 Woody Legume, *Prosopis Velutina*." *New Phytologist* 181(3):672–82. doi: 10.1111/j.1469-8137.2008.02687.x.
- Restaino, Christina M., David L. Peterson, and Jeremy Littell. 2016. "Increased Water Deficit Decreases Douglas Fir Growth throughout Western US Forests." *Proceedings of the National Academy of Sciences* 113(34):9557–62. doi: 10.1073/pnas.1602384113.
- Rigden, Angela J., and Guido D. Salvucci. 2017. "Stomatal Response to Humidity and CO₂ Implicated in Recent Decline in US Evaporation." *Global Change Biology* 23(3):1140–51.
- Roberntz, P., and J. Stockfors. 1998. "Effects of Elevated CO₂ Concentration and Nutrition on Net Photosynthesis, Stomatal Conductance and Needle Respiration of Field-Grown Norway Spruce Trees." *Tree Physiology* 18(4):233–41. doi: 10.1093/treephys/18.4.233.
- Robredo, A., U. Pérez-López, M. Lacuesta, A. Mena-Petite, and A. Muñoz-Rueda. 2010. "Influence of Water Stress on Photosynthetic Characteristics in Barley Plants under Ambient

and Elevated CO₂ Concentrations." *Biologia Plantarum* 54(2):285–92. doi: 10.1007/s10535-010-0050-y.

Rog, Ido, Gilad Jakoby, and Tamir Klein. 2021. "Carbon Allocation Dynamics in Conifers and Broadleaved Tree Species Revealed by Pulse Labeling and Mass Balance." *Forest Ecology and Management* 493:119258.

Rowland, L., A. C. L. da Costa, D. R. Galbraith, R. S. Oliveira, O. J. Binks, A. a. R. Oliveira, A. M. Pullen, C. E. Doughty, D. B. Metcalfe, S. S. Vasconcelos, L. V. Ferreira, Y. Malhi, J. Grace, M. Mencuccini, and P. Meir. 2015. "Death from Drought in Tropical Forests Is Triggered by Hydraulics Not Carbon Starvation." *Nature* 528(7580):119–22. doi: 10.1038/nature15539.

Royo, Antonio, Luis Gil, and José A. Pardos. 2001. "Effect of Water Stress Conditioning on Morphology, Physiology and Field Performance of Pinus Halepensis Mill. Seedlings." *New Forests* 21:14.

Ruehr, Nadine K., Andreas Gast, Christina Weber, Baerbel Daub, and Almut Arneth. 2016. "Water Availability as Dominant Control of Heat Stress Responses in Two Contrasting Tree Species." *Tree Physiology* 36(2):164–78. doi: 10.1093/treephys/tpv102.

Ruehr, Nadine K., Rüdiger Grote, Stefan Mayr, and Almut Arneth. 2019. "Beyond the Extreme: Recovery of Carbon and Water Relations in Woody Plants Following Heat and Drought Stress." *Tree Physiology* 39(8):1285–99. doi: 10.1093/treephys/tpz032.

Ruehr, Nadine K., Jonathan G. Martin, and Beverly E. Law. 2012. "Effects of Water Availability on Carbon and Water Exchange in a Young Ponderosa Pine Forest: Above- and Belowground Responses." *Agricultural and Forest Meteorology* 164:136–48. doi: 10.1016/j.agrformet.2012.05.015.

Ruehr, Nadine K., Christine A. Offermann, Arthur Gessler, Jana Barbro Winkler, Juan Pedro Ferrio, Nina Buchmann, and Romain L. Barnard. 2009. "Drought Effects on Allocation of Recent Carbon: From Beech Leaves to Soil CO₂ Efflux." *The New Phytologist* 184(4):950–61. doi: 10.1111/j.1469-8137.2009.03044.x.

Ryan, M. G. 2011. "Tree Responses to Drought." *Tree Physiology* 31(3):237–39. doi: 10.1093/treephys/tpv022.

Sáenz-Romero, Cuauhtémoc, Maximilien Larter, Noelia González-Muñoz, Christian Wehenkel, Arnulfo Blanco-Garcia, Dante Castellanos-Acuña, Regis Burlett, and Sylvain Delzon. 2017. "Mexican Conifers Differ in Their Capacity to Face Climate Change." *Journal of Plant Hydraulics* 4:003. doi: 10.20870/jph.2017.e003.

Sala, Anna, Frida Piper, and Günter Hoch. 2010. "Physiological Mechanisms of Drought-Induced Tree Mortality Are Far from Being Resolved." *New Phytologist* 186(2):274–81. doi: 10.1111/j.1469-8137.2009.03167.x.

Santiago, L. S., G. Goldstein, F. C. Meinzer, J. B. Fisher, K. Machado, D. Woodruff, and T. Jones. 2004. "Leaf Photosynthetic Traits Scale with Hydraulic Conductivity and Wood Density in Panamanian Forest Canopy Trees." *Oecologia* 140(4):543–50. doi: 10.1007/s00442-004-1624-1.

- Saurer, Matthias, Rolf T. W. Siegwolf, and Fritz H. Schweingruber. 2004. "Carbon Isotope Discrimination Indicates Improving Water-Use Efficiency of Trees in Northern Eurasia over the Last 100 Years." *Global Change Biology* 10(12):2109–20. doi: 10.1111/j.1365-2486.2004.00869.x.
- Schimel, Joshua P. 2018. "Life in Dry Soils: Effects of Drought on Soil Microbial Communities and Processes." *Annual Review of Ecology, Evolution, and Systematics* 49(Volume 49, 2018):409–32. doi: 10.1146/annurev-ecolsys-110617-062614.
- Schneider, Caroline A., Wayne S. Rasband, and Kevin W. Eliceiri. 2012. "NIH Image to ImageJ: 25 Years of Image Analysis." *Nature Methods* 9(7):671–75.
- Seneviratne, Sonia I., Xuebin Zhang, Muhammad Adnan, Wafae Badi, Claudine Dereczynski, A. Di Luca, Subimal Ghosh, Iskhaq Iskandar, James Kossin, and Sophie Lewis. 2021. "Weather and Climate Extreme Events in a Changing Climate."
- Sevanto, Sanna. 2018. "Drought Impacts on Phloem Transport." *Current Opinion in Plant Biology* 43:76–81. doi: 10.1016/j.pbi.2018.01.002.
- Sevanto, Sanna, Nate G. McDowell, L. Turin Dickman, Robert Pangle, and William T. Pockman. 2014. "How Do Trees Die? A Test of the Hydraulic Failure and Carbon Starvation Hypotheses." *Plant, Cell & Environment* 37(1):153–61. doi: 10.1111/pce.12141.
- Solly, Emily F., Astrid CH Jaeger, Matti Barthel, Roland A. Werner, Alois Zürcher, Frank Hagedorn, Johan Six, and Martin Hartmann. 2023. "Water Limitation Intensity Shifts Carbon Allocation Dynamics in Scots Pine Mesocosms." *Plant and Soil* 490(1):499–519.
- Song, Jiaxi, Sha Zhou, Bofu Yu, Yan Li, Yanxu Liu, Ying Yao, Shuai Wang, and Bojie Fu. 2024. "Serious Underestimation of Reduced Carbon Uptake Due to Vegetation Compound Droughts." *Npj Climate and Atmospheric Science* 7(1):1–11. doi: 10.1038/s41612-024-00571-y.
- Sperlich, D., C. T. Chang, J. Penuelas, C. Gracia, and S. Sabate. 2015. "Seasonal Variability of Foliar Photosynthetic and Morphological Traits and Drought Impacts in a Mediterranean Mixed Forest." *Tree Physiology* 35(5):501–20. doi: 10.1093/treephys/tpv017.
- Sperry, J. S., and N. Z. Saliendra. 1994. "Intra-and Inter-plant Variation in Xylem Cavitation in *Betula Occidentalis*." *Plant, Cell & Environment* 17(11):1233–41.
- Sperry, John S., F. R. Adler, G. S. Campbell, and J. P. Comstock. 1998. "Limitation of Plant Water Use by Rhizosphere and Xylem Conductance: Results from a Model." *Plant, Cell & Environment* 21(4):347–59.
- Sperry, John S., Martin D. Venturas, William R. L. Anderegg, Maurizio Mencuccini, D. Scott Mackay, Yujie Wang, and David M. Love. 2017. "Predicting Stomatal Responses to the Environment from the Optimization of Photosynthetic Gain and Hydraulic Cost." *Plant, Cell & Environment* 40(6):816–30. doi: 10.1111/pce.12852.
- Spinoni, Jonathan, Jürgen V. Vogt, Gustavo Naumann, Paulo Barbosa, and Alessandro Dosio. 2018. "Will Drought Events Become More Frequent and Severe in Europe?" *International Journal of Climatology* 38(4):1718–36. doi: 10.1002/joc.5291.

- Starr, Gregory, Christina L. Staudhammer, Susanne Wiesner, Sujit Kunwor, Henry W. Loescher, Andres F. Baron, Andrew Whelan, Robert J. Mitchell, and Lindsay Boring. 2016. "Carbon Dynamics of *Pinus Palustris* Ecosystems Following Drought." *Forests* 7(5):98. doi: 10.3390/f7050098.
- Steppe, Kathy, Dirk J. W. De Pauw, Raoul Lemeur, and Peter A. Vanrolleghem. 2006. "A Mathematical Model Linking Tree Sap Flow Dynamics to Daily Stem Diameter Fluctuations and Radial Stem Growth." *Tree Physiology* 26(3):257–73. doi: 10.1093/treephys/26.3.257.
- Sulman, Benjamin N., D. Tyler Roman, Koong Yi, Lixin Wang, Richard P. Phillips, and Kimberly A. Novick. 2016. "High Atmospheric Demand for Water Can Limit Forest Carbon Uptake and Transpiration as Severely as Dry Soil." *Geophysical Research Letters* 43(18):9686–95.
- Sultan, Sonia E. 2000. "Phenotypic Plasticity for Plant Development, Function and Life History." *Trends in Plant Science* 5(12):537–42.
- Taeger, Steffen, Christian Zang, Mirko Liesebach, Volker Schneck, and Annette Menzel. 2013. "Impact of Climate and Drought Events on the Growth of Scots Pine (*Pinus Sylvestris* L.) Provenances." *Forest Ecology and Management* 307:30–42. doi: 10.1016/j.foreco.2013.06.053.
- Taïbi, Khaled, Antonio D. del Campo, Alberto Vilagrosa, José M. Bellés, María Pilar López-Gresa, Davinia Pla, Juan J. Calvete, José M. López-Nicolás, and José M. Mulet. 2017. "Drought Tolerance in *Pinus Halepensis* Seed Sources As Identified by Distinctive Physiological and Molecular Markers." *Frontiers in Plant Science* 8:1202. doi: 10.3389/fpls.2017.01202.
- Tardieu, F., and W. J. Davies. 1993. "Integration of Hydraulic and Chemical Signalling in the Control of Stomatal Conductance and Water Status of Droughted Plants." *Plant, Cell & Environment* 16(4):341–49.
- Tardieu, François, and Thierry Simonneau. 1998. "Variability among Species of Stomatal Control under Fluctuating Soil Water Status and Evaporative Demand: Modelling Isohydic and Anisohydic Behaviours." *Journal of Experimental Botany* 419–32.
- Tatarinov, Fedor, Eyal Rotenberg, Kadmiel Maseyk, Jérôme Ogée, Tamir Klein, and Dan Yakir. 2016. "Resilience to Seasonal Heat Wave Episodes in a Mediterranean Pine Forest." *New Phytologist* 210(2):485–96. doi: 10.1111/nph.13791.
- Telewski, F. W., R. T. Swanson, B. R. Strain, and J. M. Burns. 1999. "Wood Properties and Ring Width Responses to Long-Term Atmospheric CO₂ Enrichment in Field-Grown Loblolly Pine (*Pinus Taeda* L.)." *Plant, Cell and Environment* 22(2):213–19. doi: 10.1046/j.1365-3040.1999.00392.x.
- Ter Braak, Cajo JF, and Jasper A. Vrugt. 2008. "Differential Evolution Markov Chain with Snooker Updater and Fewer Chains." *Statistics and Computing* 18:435–46.
- Tor-ngern, Pantana, Ram Oren, Eric J. Ward, Sari Palmroth, Heather R. McCarthy, and Jean-Christophe Domec. 2015. "Increases in Atmospheric CO₂ Have Little Influence on

- Transpiration of a Temperate Forest Canopy." *New Phytologist* 205(2):518–25. doi: 10.1111/nph.13148.
- Torres-Ruiz, José M., Hervé Cochard, Sylvain Delzon, Thomas Boivin, Regis Burlett, Maxime Cailleret, Déborah Corso, Chloé EL Delmas, Miquel De Caceres, and Antonio Diaz-Espejo. 2024. "Plant Hydraulics at the Heart of Plant, Crops and Ecosystem Functions in the Face of Climate Change." *New Phytologist* 241(3):984–99.
- Trueba, Santiago, Guillaume Thérout-Rancourt, J. Mason Earles, Thomas N. Buckley, David Love, Daniel M. Johnson, and Craig Brodersen. 2022. "The Three-dimensional Construction of Leaves Is Coordinated with Water Use Efficiency in Conifers." *New Phytologist* 233(2):851–61.
- Trugman, Anna T., Leander DL Anderegg, Brett T. Wolfe, Benjamin Birami, Nadine K. Ruehr, Matteo Detto, Megan K. Bartlett, and William RL Anderegg. 2019. "Climate and Plant Trait Strategies Determine Tree Carbon Allocation to Leaves and Mediate Future Forest Productivity." *Global Change Biology* 25(10):3395–3405.
- Trumbore, Susan, Paulo Brando, and Henrik Hartmann. 2015. "Forest Health and Global Change." *Science* 349(6250):814–18.
- Vicente-Serrano, Sergio M., Diego G. Miralles, Nate McDowell, Tim Brodribb, Fernando Domínguez-Castro, Ruby Leung, and Akash Koppa. 2022. "The Uncertain Role of Rising Atmospheric CO₂ on Global Plant Transpiration." *Earth-Science Reviews* 230:104055.
- Vieira, Joana, Ana Carvalho, and Filipe Campelo. 2020. "Tree Growth Under Climate Change: Evidence From Xylogenesis Timings and Kinetics." *Frontiers in Plant Science* 11. doi: 10.3389/fpls.2020.00090.
- Villar-Salvador, Pedro, Luís Ocaña, Juan Peñuelas, and Inmaculada Carrasco. 1999. "Effect of Water Stress Conditioning on the Water Relations, Root Growth Capacity, and the Nitrogen and Non-Structural Carbohydrate Concentration of Pinus Halepensis Mill. (Aleppo Pine) Seedlings." *ANNALS OF FOREST SCIENCE* 56(6):459–65. doi: 10.1051/forest:19990602.
- Wang, Licheng, Yi Li, Xincheng Zhang, Ke Chen, and Kadambot H. M. Siddique. 2024. "Soil Water Content and Vapor Pressure Deficit Affect Ecosystem Water Use Efficiency through Different Pathways." *Journal of Hydrology* 640:131732. doi: 10.1016/j.jhydrol.2024.131732.
- Weathers, Strayer, and Likens. 2021. *Fundamentals of Ecosystem Science*. 2nd edition. London: Academic Press.
- Whitehead, D., D. U. U. Okali, and F. E. Fasehun. 1981. "Stomatal Response to Environmental Variables in Two Tropical Forest Species During the Dry Season in Nigeria." *Journal of Applied Ecology* 18(2):571–87. doi: 10.2307/2402418.
- Williams, A. Park, Edward R. Cook, Jason E. Smerdon, Benjamin I. Cook, John T. Abatzoglou, Kasey Bolles, Seung H. Baek, Andrew M. Badger, and Ben Livneh. 2020. "Large Contribution from Anthropogenic Warming to an Emerging North American Megadrought." *Science* 368(6488):314–18.

- Woodward, F. I., and C. K. Kelly. 1995. "The Influence of CO₂ Concentration on Stomatal Density." *New Phytologist* 131(3):311–27. doi: 10.1111/j.1469-8137.1995.tb03067.x.
- Wullschlegel, S. D., T. J. Tschaplinski, and R. J. Norby. 2002. "Plant Water Relations at Elevated CO₂ - Implications for Water-Limited Environments." *Plant, Cell and Environment* 25(2):319–31. doi: 10.1046/j.1365-3040.2002.00796.x.
- Xu, Z., and G. Zhou. 2008. "Responses of Leaf Stomatal Density to Water Status and Its Relationship with Photosynthesis in a Grass." *Journal of Experimental Botany* 59(12):3317–25. doi: 10.1093/jxb/ern185.
- Xu, Zhenzhu, Yanling Jiang, Bingrui Jia, and Guangsheng Zhou. 2016. "Elevated CO₂ Response of Stomata and Its Dependence on Environmental Factors." *Frontiers in Plant Science* 7. doi: 10.3389/fpls.2016.00657.
- Xu, Zhenzhu, Hideyuki Shimizu, Shoko Ito, Yasumi Yagasaki, Chunjing Zou, Guangsheng Zhou, and Yuanrun Zheng. 2014. "Effects of Elevated CO₂, Warming and Precipitation Change on Plant Growth, Photosynthesis and Peroxidation in Dominant Species from North China Grassland." *Planta* 239(2):421–35. doi: 10.1007/s00425-013-1987-9.
- Yu, Xiaojing, Lixia Zhang, Tianjun Zhou, Jianghua Zheng, and Jingyun Guan. 2024. "Higher Atmospheric Aridity-Dominated Drought Stress Contributes to Aggravating Dryland Productivity Loss under Global Warming." *Weather and Climate Extremes* 44:100692. doi: 10.1016/j.wace.2024.100692.
- Yuan, Wenping, Yi Zheng, Shilong Piao, Philippe Ciais, Danica Lombardozzi, Yingping Wang, Youngryel Ryu, Guixing Chen, Wenjie Dong, Zhongming Hu, Atul K. Jain, Chongya Jiang, Etsushi Kato, Shihua Li, Sebastian Lienert, Shuguang Liu, Julia E. M. S. Nabel, Zhangcai Qin, Timothy Quine, Stephen Sitch, William K. Smith, Fan Wang, Chaoyang Wu, Zhiqiang Xiao, and Song Yang. 2019. "Increased Atmospheric Vapor Pressure Deficit Reduces Global Vegetation Growth." *Science Advances* 5(8):eaax1396. doi: 10.1126/sciadv.aax1396.
- Zhang, Wenqiang, Geping Luo, Rafiq Hamdi, Xiumei Ma, Piet Termonia, and Philippe De Maeyer. 2024. "Drought Changes the Dominant Water Stress on the Grassland and Forest Production in the Northern Hemisphere." *Agricultural and Forest Meteorology* 345:109831. doi: 10.1016/j.agrformet.2023.109831.
- Zhao, Maosheng, and Steven W. Running. 2010. "Drought-Induced Reduction in Global Terrestrial Net Primary Production from 2000 through 2009." *Science (New York, N.Y.)* 329(5994):940–43. doi: 10.1126/science.1192666.
- Zhao, Shoudong, Yuan Jiang, Manyu Dong, Hui Xu, Rubén Delgado Manzanedo, and Neil Pederson. 2018. "Early Monsoon Failure and Mid-Summer Dryness Induces Growth Cessation of Lower Range Margin *Picea Crassifolia*." *Trees* 32:1401–13.
- Zheng, Chen, Shaoqiang Wang, Jinghua Chen, Ning Xiang, Leigang Sun, Bin Chen, Zheng Fu, Kai Zhu, and Xinlei He. 2023. "Divergent Impacts of VPD and SWC on Ecosystem Carbon-Water Coupling under Different Dryness Conditions." *Science of The Total Environment* 905:167007. doi: 10.1016/j.scitotenv.2023.167007.

- Zhou, Yumei, Xiaojie Jiang, Marcus Schaub, Xuejuan Wang, Jianqiu Han, Shi-jie Han, and Mai-He Li. 2013. "Ten-Year Exposure to Elevated CO₂ Increases Stomatal Number of *Pinus Koraiensis* and *P. Sylvestriformis* Needles." *European Journal of Forest Research* 132:899–908.
- Zhu, Shi-Dan, Ya-Jun Chen, Qing Ye, Peng-Cheng He, Hui Liu, Rong-Hua Li, Pei-Li Fu, Guo-Feng Jiang, and Kun-Fang Cao. 2018. "Leaf Turgor Loss Point Is Correlated with Drought Tolerance and Leaf Carbon Economics Traits." *Tree Physiology* 38(5):658–63. doi: 10.1093/treephys/tpy013.
- Zweifel, R., L. Zimmermann, and D. M. Newbery. 2005. "Modeling Tree Water Deficit from Microclimate: An Approach to Quantifying Drought Stress." *Tree Physiology* 25(2):147–56. doi: 10.1093/treephys/25.2.147.
- Zweifel, Roman, Sophia Etzold, Frank Sterck, Arthur Gessler, Tommaso Anfodillo, Maurizio Mencuccini, Georg von Arx, Martina Lazzarin, Matthias Haeni, and Linda Feichtinger. 2020. "Determinants of Legacy Effects in Pine Trees – Implications from an Irrigation-stop Experiment." *New Phytologist* 227(4):1081–96.
- Zweifel, Roman, Frank Sterck, Sabine Braun, Nina Buchmann, Werner Eugster, Arthur Gessler, Matthias Häni, Richard L. Peters, Lorenz Walthert, Micah Wilhelm, Kasia Ziemińska, and Sophia Etzold. 2021. "Why Trees Grow at Night." *New Phytologist* 231(6):2174–85. doi: 10.1111/nph.17552.
- Zwieniecki, Maciej A., Timothy J. Brodribb, and N. Michele Holbrook. 2007. "Hydraulic Design of Leaves: Insights from Rehydration Kinetics." *Plant, Cell & Environment* 30(8):910–21.

Acknowledgements

In some ways, this is the most difficult part of my thesis to write, because words can only say so much. Looking at the acknowledgements of others, I realize that it is customary to reserve one's purest prose for the acknowledgements. I'm afraid this is the best I can do:

THANK YOU to all who have made this work possible!

Dear Nadine, "thank you" seems so embarrassingly simple and completely inadequate to convey the depth of my gratitude towards you. When I first met you on 3 August 2015 at the start of my internship, I had no idea how significant that moment would be. With your positive, warm and open manner, you created an atmosphere that made me feel at home and kept me coming back. Your relentless enthusiasm has been inspiring and has helped me get through my recent 'I-hate-every-word' days. This thesis would not have been possible without your mentoring and unwavering support over the years. Thank you for everything you have done to make me the person I am today!

Dear Benni, thank you for always letting me barge into your office when I had problems in the lab or wanted to pick your brain, and for simply saying "I'll be right there". I can't begin to describe how kind and supportive you were without expecting anything in return. The memories of our many lively and funny discussions about structuring and analyzing data will always stay with me. I am very happy to count you as a friend!

Dear Andi, I have to laugh when I remember certain moments of inner melodrama tinged with fatigue, usually after yet another 'Error' had appeared on my screen and I wondered how on earth I was going to complete the experiments. However, it was very reassuring to know that you had my back by always working with me to find a technical solution. I am very grateful to you for that!

Liebe Mama, lieber Papa, liebe Joline, liebe Oma, danke, dass ich immer auf eure Unterstützung, Ermutigung und euer Verständnis zählen kann und ihr immer für mich da seid. Ich habe großes Glück, euch zu haben!

Und auch wenn diese Worte für dich keine Bedeutung haben: Ich danke dir, Fiete, dass du gute Zeiten besser machst, mich die schlechten vergessen lässt und ich sagen kann:

„Mir reicht's! Wir geh'n Gassi!“